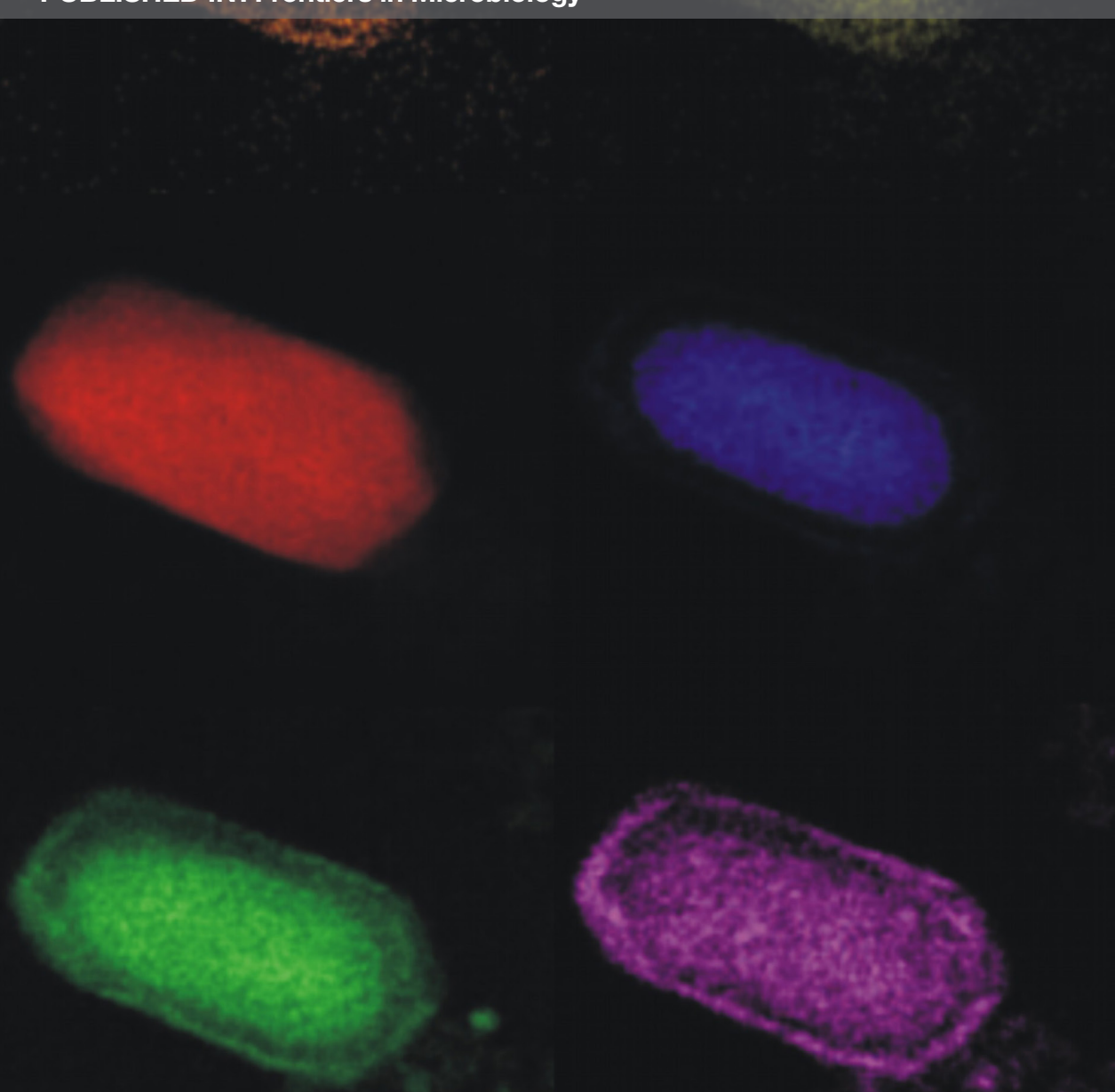


SPORES AND SPORE FORMERS

EDITED BY: Imrich Barák, Simon M. Cutting, Ezio Ricca, Neil Fairweather
and Ivan Mijakovic

PUBLISHED IN: *Frontiers in Microbiology*





frontiers

Frontiers Copyright Statement

© Copyright 2007-2017 Frontiers Media SA. All rights reserved.

All content included on this site, such as text, graphics, logos, button icons, images, video/audio clips, downloads, data compilations and software, is the property of or is licensed to Frontiers Media SA ("Frontiers") or its licensees and/or subcontractors. The copyright in the text of individual articles is the property of their respective authors, subject to a license granted to Frontiers.

The compilation of articles constituting this e-book, wherever published, as well as the compilation of all other content on this site, is the exclusive property of Frontiers. For the conditions for downloading and copying of e-books from Frontiers' website, please see the Terms for Website Use. If purchasing Frontiers e-books from other websites or sources, the conditions of the website concerned apply.

Images and graphics not forming part of user-contributed materials may not be downloaded or copied without permission.

Individual articles may be downloaded and reproduced in accordance with the principles of the CC-BY licence subject to any copyright or other notices. They may not be re-sold as an e-book.

As author or other contributor you grant a CC-BY licence to others to reproduce your articles, including any graphics and third-party materials supplied by you, in accordance with the Conditions for Website Use and subject to any copyright notices which you include in connection with your articles and materials.

All copyright, and all rights therein, are protected by national and international copyright laws.

The above represents a summary only. For the full conditions see the Conditions for Authors and the Conditions for Website Use.

ISSN 1664-8714

ISBN 978-2-88945-238-5

DOI 10.3389/978-2-88945-238-5

About Frontiers

Frontiers is more than just an open-access publisher of scholarly articles: it is a pioneering approach to the world of academia, radically improving the way scholarly research is managed. The grand vision of Frontiers is a world where all people have an equal opportunity to seek, share and generate knowledge. Frontiers provides immediate and permanent online open access to all its publications, but this alone is not enough to realize our grand goals.

Frontiers Journal Series

The Frontiers Journal Series is a multi-tier and interdisciplinary set of open-access, online journals, promising a paradigm shift from the current review, selection and dissemination processes in academic publishing. All Frontiers journals are driven by researchers for researchers; therefore, they constitute a service to the scholarly community. At the same time, the Frontiers Journal Series operates on a revolutionary invention, the tiered publishing system, initially addressing specific communities of scholars, and gradually climbing up to broader public understanding, thus serving the interests of the lay society, too.

Dedication to Quality

Each Frontiers article is a landmark of the highest quality, thanks to genuinely collaborative interactions between authors and review editors, who include some of the world's best academicians. Research must be certified by peers before entering a stream of knowledge that may eventually reach the public - and shape society; therefore, Frontiers only applies the most rigorous and unbiased reviews.

Frontiers revolutionizes research publishing by freely delivering the most outstanding research, evaluated with no bias from both the academic and social point of view.

By applying the most advanced information technologies, Frontiers is catapulting scholarly publishing into a new generation.

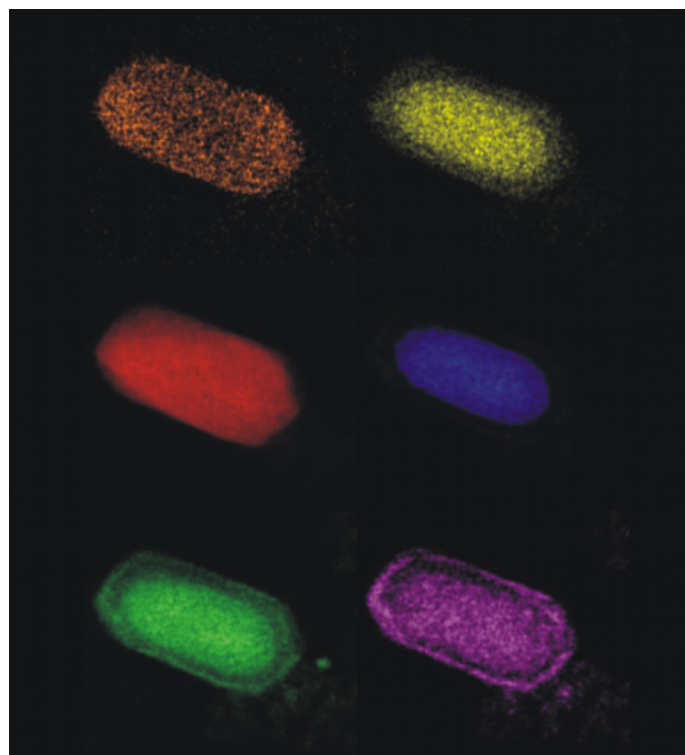
What are Frontiers Research Topics?

Frontiers Research Topics are very popular trademarks of the Frontiers Journals Series: they are collections of at least ten articles, all centered on a particular subject. With their unique mix of varied contributions from Original Research to Review Articles, Frontiers Research Topics unify the most influential researchers, the latest key findings and historical advances in a hot research area! Find out more on how to host your own Frontiers Research Topic or contribute to one as an author by contacting the Frontiers Editorial Office: researchtopics@frontiersin.org

SPORES AND SPORE FORMERS

Topic Editors:

Imrich Barák, Institute of Molecular Biology, Slovak Academy of Sciences Bratislava, Slovakia
Simon M. Cutting, Royal Holloway, University of London, United Kingdom
Ezio Ricca, University of Naples Federico II, Italy
Neil Fairweather, Imperial College London, London, United Kingdom
Ivan Mijakovic, Chalmers University of Technology, Göteborg, Sweden



STEM/EDS (Scanning Transmission Electron Microscopy coupled to Energy Dispersive Spectroscopy) imaging of *Bacillus subtilis* spores showing the core and cortex/coat. Spatial distribution of elements: Cl, S, C, Ca, O and P are shown in different colors. Details about the method are in this Research Topic (<https://doi.org/10.3389/fmicb.2016.01791>).

Bacterial spore formers have been the focus of intense study for almost half a century centered primarily on *Bacillus subtilis*. This research has given us a detailed picture of the genetic, physiological and biochemical mechanisms that allow bacteria to survive harsh environmental conditions by forming highly robust spores. Although, many basic aspects of this process are

now understood in great detail, bacterial sporulation still continues to be a highly attractive model for studying various cell processes at a molecular level. There are several reasons for such scientific interest. First, some of the complex steps in sporulation are not fully understood and/or only are only described by ‘controversial’ models. Second, intensive research on unicellular development of a single microorganism, *B. subtilis*, left us largely unaware of the multitude of diverse sporulation mechanisms in many other Gram-positive endospore and exospore formers. This diversity would likely increase if we were to include sporulation processes in the Gram-negative spore formers. In addition, spore formers have great potential in applied research. Spore forming bacteria are becoming increasingly important in the areas of probiotics, vaccine technology and biotechnology. This Research Topic in Frontiers in Microbiology details the most recent advances in basic science of spore research and cover also emerging areas of scientific importance involving the use of spores.

Citation: Barák, I., Cutting, S. M., Ricca, E., Fairweather, N., Mijakovic, I., eds. (2017). Spores and Spore Formers. Lausanne: Frontiers Media. doi: 10.3389/978-2-88945-238-5

Table of Contents

06 Editorial: Spores and Spore Formers

Imrich Barák

Sporulation Initiation and Regulation

08 Time Series Analysis of the *Bacillus subtilis* Sporulation Network Reveals Low Dimensional Chaotic Dynamics

Paola Lecca, Ivan Mura, Angela Re, Gary C. Barker and Adaoha E. C. Ihekweaba

25 Impact of Serine/Threonine Protein Kinases on the Regulation of Sporulation in *Bacillus subtilis*

Frédérique Pompeo, Elodie Foulquier and Anne Galinier

32 SpoVT: From Fine-Tuning Regulator in *Bacillus subtilis* to Essential Sporulation Protein in *Bacillus cereus*

Robyn T. Eijlander, Siger Holsappel, Anne de Jong, Abhinaba Ghosh, Graham Christie and Oscar P. Kuipers

Resistance of Spores and Spore Coat

43 Variability in DPA and Calcium Content in the Spores of Clostridium Species

Jan Jamroskovic, Zuzana Chromikova, Cornelia List, Barbora Bartova, Imrich Barak and Rizlan Bernier-Latmani

54 Chemical and Stress Resistances of *Clostridium difficile* Spores and Vegetative Cells

Adrienne N. Edwards, Samiha T. Karim, Ricardo A. Pascual, Lina M. Jowhar, Sarah E. Anderson and Shonna M. McBride

67 The Influence of Sporulation Conditions on the Spore Coat Protein Composition of *Bacillus subtilis* Spores

Wishwas R. Abhyankar, Kiki Kamphorst, Bhagyashree N. Swarge, Henk van Veen, Nicole N. van der Wel, Stanley Brul, Chris G. de Koster and Leo J. de Koning

77 The Exosporium of *Bacillus megaterium* QM B1551 Is Permeable to the Red Fluorescence Protein of the Coral *Discosoma* sp.

Mariamichela Lanzilli, Giuliana Donadio, Roberta Addevico, Anella Saggese, Giuseppina Cangiano, Loredana Baccigalupi, Graham Christie, Ezio Ricca and Rachele Istitato

Germination

85 Diversity of the Germination Apparatus in *Clostridium botulinum* Groups I, II, III, and IV

Jason Brunt, Arnoud H. M. van Vliet, Féodor van den Bos, Andrew T. Carter and Michael W. Peck

98 Identification of Differentially Expressed Genes during *Bacillus subtilis* Spore Outgrowth in High-Salinity Environments Using RNA Sequencing

Katja Nagler, Antonina O. Krawczyk, Anne De Jong, Kazimierz Madela, Tamara Hoffmann, Michael Laue, Oscar P. Kuipers, Erhard Bremer and Ralf Moeller

113 *FlhF* Is Required for Swarming Motility and Full Pathogenicity of *Bacillus cereus*

Diletta Mazzantini, Francesco Celandroni, Sara Salvetti, Sokhna A. Gueye, Antonella Lupetti, Sonia Senesi and Emilia Ghelardi



Editorial: Spores and Spore Formers

Imrich Barák *

Department of Microbial Genetics, Institute of Molecular Biology, Slovak Academy of Sciences, Bratislava, Slovakia

Keywords: bacterial spores, *Bacillus subtilis*, Clostridia, initiation of sporulation, germination and dormancy, regulation of sporulation

Editorial on the Research Topic

Spores and Spore Formers

Bacterial spore formers have been the focus of intense study for almost half a century. The most heavily studied of these is *Bacillus subtilis*, an internationally recognized model organism, whose physiology, biochemistry, and genetics have been studied for many years. Under nutrient rich conditions, *B. subtilis* grows and multiplies by a process of cell expansion followed by division at mid-cell to generate identical daughter cells; however, *B. subtilis* also has the ability to form spores, dormant cells which are resistant to many of the chemical and physical challenges that normally kill bacteria. Although many of the basic aspects of this process are now well-understood, bacterial sporulation still remains a highly attractive model for studying various cell processes at a molecular level. There are several reasons for this interest. First, some of the more complex sporulation steps are not fully understood or are only described using “controversial” models. Second, the extensive attention lavished on the unicellular development of *B. subtilis*, a single microorganism, has left us largely ignorant of the multitude of different sporulation mechanisms present in many other Gram-positive endospore and exospore formers; this diversity would likely increase if the sporulation processes of the Gram-negative spore formers were also included. The ability of spores to lie dormant and then germinate presents both threats and potential benefits to human health and welfare. Botulism and tetanus are infectious diseases transmitted by spores, while the spores of *Clostridium difficile* are responsible for hospital-acquired infections, which are harmful to patients and expensive to treat and eradicate. *Bacillus cereus* spores cause food poisoning and present a challenge to the food industry, while the spores of *B. anthracis*, the cause of anthrax, are a concern because of their potential use as bioterrorism and biowarfare agents. On the other hand, spore formers also have great potential in applied research. Spore forming bacteria are becoming increasingly important in the areas of probiotics, vaccine technology, and biotechnology. This Research Topic in *Frontiers in Microbiology* details the most recent advances in spore research basic science, covers emerging areas of scientific importance involving the use of spores, including their use as probiotics in humans and animals, and examines the use of spores as tools for nanobiotechnology where the spore surface can be used to efficiently display heterologous proteins. In addition, this Topic covers the ecological roles of spores, the taxonomy and systematics of spore forming bacteria, and the architecture and assembly of spores. This Research Topic was partially but not exclusively linked to the 7th European Spores Conference, held in Egham (UK) on 18–20 April 2016 (<http://sporesconference.org/>).

Generally, the sporulation process can be thought of as the last opportunity for the bacterial cell to endure when all other attempts to grow, compete, and survive have been exhausted. Sporulation initiation is a complex process in which different types of input, including nutritional, population density, and cell cycle signals, are integrated by the cell before the decision to sporulate is made. Sophisticated and sensitive signal transduction pathways are essential for accurately monitoring all these signals. In *B. subtilis* and most endospore-forming bacteria, sporulation initiation is under the control of a phosphorelay, an expanded two-component sensory signaling system, and the key

OPEN ACCESS

Edited by:

Michael Sauer,

University of Natural Resources and Life Sciences, Vienna, Austria

Reviewed by:

Michael Sauer,

University of Natural Resources and Life Sciences, Vienna, Austria

Paola Branduardi,

University of Milano-Bicocca, Italy

***Correspondence:**

Imrich Barák

imrich.barak@savba.sk

Specialty section:

This article was submitted to
Microbial Physiology and Metabolism,
a section of the journal
Frontiers in Microbiology

Received: 11 January 2017

Accepted: 24 May 2017

Published: 08 June 2017

Citation:

Barák I (2017) Editorial: Spores and Spore Formers. *Front. Microbiol.* 8:1046. doi: 10.3389/fmicb.2017.01046

molecule in transducing signals into the activation of those genes required for sporulation is the response regulator Spo0A. In this Research Topic, Lecca et al. analyse numerical simulations of a model of the gene network which regulates sporulation initiation in *Bacillus subtilis* to find that the non-linearity underlying the time series data is due to low-dimensional chaos. Pompeo et al. review the importance of serine/threonine protein kinases in sporulation regulation in *B. subtilis*.

The sporulation process is controlled at the gene expression level by a complex regulatory cascade composed of different compartment-specific sigma factors and additional regulator proteins, which are highly conserved among various spore formers. Despite this conservation, both regulatory and phenotypic differences are observed between different species of spore forming bacteria. Eijlander et al., demonstrate that deletion of the regulatory sporulation protein SpoVT results in a severe sporulation defect in *B. cereus*, but not in *B. subtilis*.

The resistance of spores to environmental attacks is attributable to the unique morphology of the spore, which is formed by several layers: the core, the cortex, the coat, the crust, and, in some cases, the exosporium. Dipicolinic acid (DPA), with its ability to bind Ca^{2+} ions, plays a key role in the dehydration and mineralization of the spore core. Dehydration of the spore core is the main factor underlying the resistance of spores to wet heat. The work of Jamroskovic et al. cataloged the heterogeneity in the heat resistance capacity and the overall DPA/calcium content in the spores of several *Clostridium* species. Edwards et al. characterized the chemical and stress resistances of *C. difficile* spores. Abhyankar et al. determined the influence of sporulation conditions on spore coat composition in *B. subtilis*. The spores of some *Bacillus* species are surrounded by the exosporium, an outermost surface layer. Lanzilli et al. clarified the *B. megaterium* exosporium permeability.

Under favorable conditions, spores germinate to produce vegetative cells that multiply. Brunt et al. characterized the

diversity of germination apparatuses in different *C. botulinum* groups. Nagler et al. identified genes which are differentially expressed during *B. subtilis* germination in high-salinity environments. Besides sporulation, *B. cereus* can also undergo a differentiation process in which short swimmer cells become elongated and hyperflagellated swarmer cells which favor the migration of the bacterial community on a surface. Mazzantini et al. showed that the flagellar FlhF protein is required for the swarming motility and full pathogenicity of this bacterium.

AUTHOR CONTRIBUTIONS

The author confirms being the sole contributor of this work and approved it for publication.

ACKNOWLEDGMENTS

The author receives support from the Slovak Academy of Sciences (Grant 2/0007/17), from the Slovak Research and Development Agency under contract APVV-14-0181, and from FNSNF (SCOPES IZ 73Z0_152527/1). The author thanks to Research Topic editors and organizers of 7th European Spores Conference—Simon Cutting, Ezio Ricca, Neil Fairweather, and Ivan Mijakovic. He also thanks to Jacob Bauer for helpful comments.

Conflict of Interest Statement: The author declares that the research was conducted in the absence of any commercial or financial relationships that could be construed as a potential conflict of interest.

Copyright © 2017 Barák. This is an open-access article distributed under the terms of the Creative Commons Attribution License (CC BY). The use, distribution or reproduction in other forums is permitted, provided the original author(s) or licensor are credited and that the original publication in this journal is cited, in accordance with accepted academic practice. No use, distribution or reproduction is permitted which does not comply with these terms.



Time Series Analysis of the *Bacillus subtilis* Sporulation Network Reveals Low Dimensional Chaotic Dynamics

Paola Lecca^{1*}, Ivan Mura², Angela Re³, Gary C. Barker⁴ and Adaoha E. C. Ihewkaba^{4*}

¹ Department of Mathematics, University of Trento, Trento, Italy, ² Department of Industrial Engineering, Universidad de los Andes, Bogotá, Colombia, ³ Laboratory of Translational Genomics, Centre for Integrative Biology, University of Trento, Trento, Italy, ⁴ Gut Health and Food Safety, Institute of Food Research, Norwich, UK

OPEN ACCESS

Edited by:

Imrich Barak,
Slovak Academy of Sciences, Slovakia

Reviewed by:

Anthony Joseph Wilkinson,
University of York, UK

Andreas Kremling,
Technische Universität München,
Germany

*Correspondence:

Paola Lecca
paola.lecca@unitn.it
Adaoha E. C. Ihewkaba
Adaoha.Ihekwa@ifr.ac.uk

Specialty section:

This article was submitted to
Microbial Physiology and Metabolism,
a section of the journal
Frontiers in Microbiology

Received: 21 July 2016

Accepted: 19 October 2016

Published: 07 November 2016

Citation:

Lecca P, Mura I, Re A, Barker GC and Ihewkaba AEC (2016) Time Series Analysis of the *Bacillus subtilis* Sporulation Network Reveals Low Dimensional Chaotic Dynamics. *Front. Microbiol.* 7:1760.
doi: 10.3389/fmicb.2016.01760

Chaotic behavior refers to a behavior which, albeit irregular, is generated by an underlying deterministic process. Therefore, a chaotic behavior is potentially controllable. This possibility becomes practically amenable especially when chaos is shown to be low-dimensional, i.e., to be attributable to a small fraction of the total systems components. In this case, indeed, including the major drivers of chaos in a system into the modeling approach allows us to improve predictability of the systems dynamics. Here, we analyzed the numerical simulations of an accurate ordinary differential equation model of the gene network regulating sporulation initiation in *Bacillus subtilis* to explore whether the non-linearity underlying time series data is due to low-dimensional chaos. Low-dimensional chaos is expectedly common in systems with few degrees of freedom, but rare in systems with many degrees of freedom such as the *B. subtilis* sporulation network. The estimation of a number of indices, which reflect the chaotic nature of a system, indicates that the dynamics of this network is affected by deterministic chaos. The neat separation between the indices obtained from the time series simulated from the model and those obtained from time series generated by Gaussian white and colored noise confirmed that the *B. subtilis* sporulation network dynamics is affected by low dimensional chaos rather than by noise. Furthermore, our analysis identifies the principal driver of the networks chaotic dynamics to be sporulation initiation phosphotransferase B (SpoOB). We then analyzed the parameters and the phase space of the system to characterize the instability points of the network dynamics, and, in turn, to identify the ranges of values of SpoOB and of the other drivers of the chaotic dynamics, for which the whole system is highly sensitive to minimal perturbation. In summary, we described an unappreciated source of complexity in the *B. subtilis* sporulation network by gathering evidence for the chaotic behavior of the system, and by suggesting candidate molecules driving chaos in the system. The results of our chaos analysis can increase our understanding of the intricacies of the regulatory network under analysis, and suggest experimental work to refine our behavior of the mechanisms underlying *B. subtilis* sporulation initiation control.

Keywords: systems biology, computational modeling, sensitivity analysis, low dimensional chaos, signal transduction, sporulation, *Bacillus subtilis*

1. INTRODUCTION

Bacterial spores are important contaminants in food, and the spore forming bacteria are often implicated in food safety and food quality considerations (Carlin, 2011). Most microbial spore forming bacteria respond to stress (e.g., nutrient deprivation) by inducing the expression of an appropriate suit of adaptive (stress-response) genes to help them cope with adverse environmental circumstances; an extreme example is endospore formation (Ihekweaba et al., 2014).

Since sporulation is an energy consuming process that requires a significant reorganization of cellular activity, the decision to commit to spore formation is subject to the result of integration of multiple signals by a complex gene regulation network.

The initiation of sporulation is one of the decisive moments in spore formation, as exemplified by the bacterium *Bacillus subtilis*. The changes in gene expression and morphology induced by sporulation are regulated in *B. subtilis* by a complex network involving more than 120 genes (Stragier and Losick, 1996; Fawcett et al., 2000).

The DNA-binding protein Spo0A is the master regulator for entry into sporulation in *B. subtilis*. The concentration level and the phosphorylation state determine the ability of Spo0A to alter transcription. Upon phosphorylation, Spo0A undergoes an allosteric change that re-orientates a phenylalanine residue and allows the molecule to bind DNA (Muchová et al., 2004) and activate key genes that drive the positive regulation of sporulation, particularly the *spoIIA*, *spoIIE*, and *spoIIG* genes involved in establishing compartment-specific transcription under the control of σ F (*spoIIA* operon and the *spoIIE* gene) and σ E (*spoIIG* operon) (Satola et al., 1991, 1992; York et al., 1992). Phosphorylated Spo0A also acts as a repressor, blocking the expression of the *abrB* gene. This repression has the consequence of setting up a self-reinforcing cycle that contributes to the further accumulation of Spo0A at the start of sporulation (Fujita and Losick, 2005; Tojo et al., 2013). Indeed, the inhibition that phosphorylated Spo0A exerts on *abrB* gene expression leads to the depletion of the AbrB protein from the cell and to the accumulation of σ H, with the net result of enhancing the expression of KinA, Spo0F and of the Spo0A gene itself (Strauch et al., 1993; Tojo et al., 2013).

Spo0A activation is under the control of a complex network capable of integrating diverse physiological and environmental signals, and relaying signals through a three-level phosphorelay down to the response regulator Spo0A. Various mathematical models of *B. subtilis* sporulation mechanisms can be found in the literature, among the most recent ones we mention (Kuchina et al., 2011; Sen et al., 2011; Narula et al., 2012; Kothamachu et al., 2013; Vishnoi et al., 2013; Ihekweaba et al., 2014).

This paper is based on the model proposed in Ihekweaba et al. (2014), which integrates most of previous mathematical modeling works on *B. subtilis* sporulation initiation. The model we consider encodes the relationships among the time-dependent concentrations of sporulation signals, histidine kinases, phosphorelay proteins and sporulation initiation proteins in the form of a deterministic differential model

having 27 variables. Simulation of the differential equations via numerical integration provides predictions about the evolution of the *B. subtilis* sporulation initiation regulation network, given the initial state of variables. Ihekweaba et al. (2014) also performed a sensitivity analysis of the model to explore the set of possible behaviors with varying the values of its parameters (i.e., the kinetic rate constants).

In this paper, we continue the analysis of model behavior, with the aim of investigating whether the time series of the variables, as predicted by the differential equations model, are affected by deterministic chaos, or simply *chaos*. A chaotic system is a system that is predictable up until a given time, after which it becomes unpredictable (i.e., long term unpredictability) due to its sensitivity to initial conditions (Kellert, 1993). Even if the initial state is known at a very accurate level of detail, any imprecision in its quantification, no matter how small, grows quickly (exponentially) with time, rendering long-term prediction impossible.

Identifying chaos and its drivers in a biological system provides useful information (i) to understand the origins of the observed dynamics (Weiss et al., 1994; Lecca et al., 2016), and (ii) to shed light into the control mechanisms that a biological system may have implemented to maintain a stable activity even when subject to perturbations of its initial conditions (Sinha, 1997). Both chaotic dynamics and stochastic dynamics exhibit a complex phase space structure and are not predictable, but chaos is not stochastic noise (Lecca et al., 2016). Indeed, a chaotic dynamics is governed by deterministic laws in which no randomness is involved, whereas a stochastic dynamics is governed by rules involving random variables. As a consequence, if the laws and the drivers of the dynamics of a chaotic system are known, its unpredictability can potentially be controlled (Sinha, 1997; Lai, 2014).

Low-dimensional chaos occurs when a reduced number of contributing species are responsible for the complex dynamics. Such a low-dimensional chaos is of particular interest in biology (Skinner, 1994; Kaneko, 2006; Vasseur, 2015). Since in a biological system affected by low-dimensional chaos the variables governing the spatial and temporal dynamics are few in number, a low-energy control of unpredictability of the system dynamics can be implemented and a simpler model of a complex dynamics can be provided. Low-dimensional chaos is expected to be common in systems with few degrees of freedom (Skinner, 1994), but is expected to be rare in systems with many degree of freedom such as the sporulation network of *B. subtilis*. The results of our analysis show that only few molecular species are contributing to the appearance of deterministic chaos in the dynamics of the modeled network.

2. THE MODEL

In Ihekweaba et al. (2014), a mathematical model of the network regulating *Bacillus subtilis* sporulation initiation was proposed. The model represents at the molecular level the sequence of events that lead to the activation of the early genes under control of the master regulator molecule Spo0A, distilling and extending the results obtained in various modeling studies focused on

systems where sporulation is induced by an artificial inducer, the Isopropyl-D-1-thiogalactopyranoside (IPTG) (see for instance Narula et al., 2012), and modeling as well the induction of sporulation that occurs in wild-type cells.

A high-level diagrammatic description of the molecular network governing sporulation initiation in *B. subtilis* is provided in **Figure 1**, where pointed arrows represent activation and blunt arrows indicate repression.

The *B. subtilis* sporulation network model considered in this study is the published model by Lecca et al. (2016) and Ihekweaba et al. (2014). It follows the topology of the network shown in **Figure 1**, thereby encompassing three distinct sub-models:

1. input signal, representing the sporulation initiation processes induced by the signals on the histidine kinases;
2. phosphorelay, encoding the signal transduction along the phosphorelay components, from histidine kinases downwards to the master regulator Spo0A;
3. gene expression, modeling the target gene expression activation operated by the activated effector Spo0A.

In the following section, we explain the structure of each sub-model, and use a graphical notation to represent activation/repression (arrows with non-solid ends) which is introduced in **Figure 1**. In our modeling, we consider both transcription and translation of proteins. For each species involved in a synthesis process (i.e., transcripts and proteins), the model includes a degradation reaction, not shown in the model diagrams for clarity.

2.1. Input Signal Sub-model

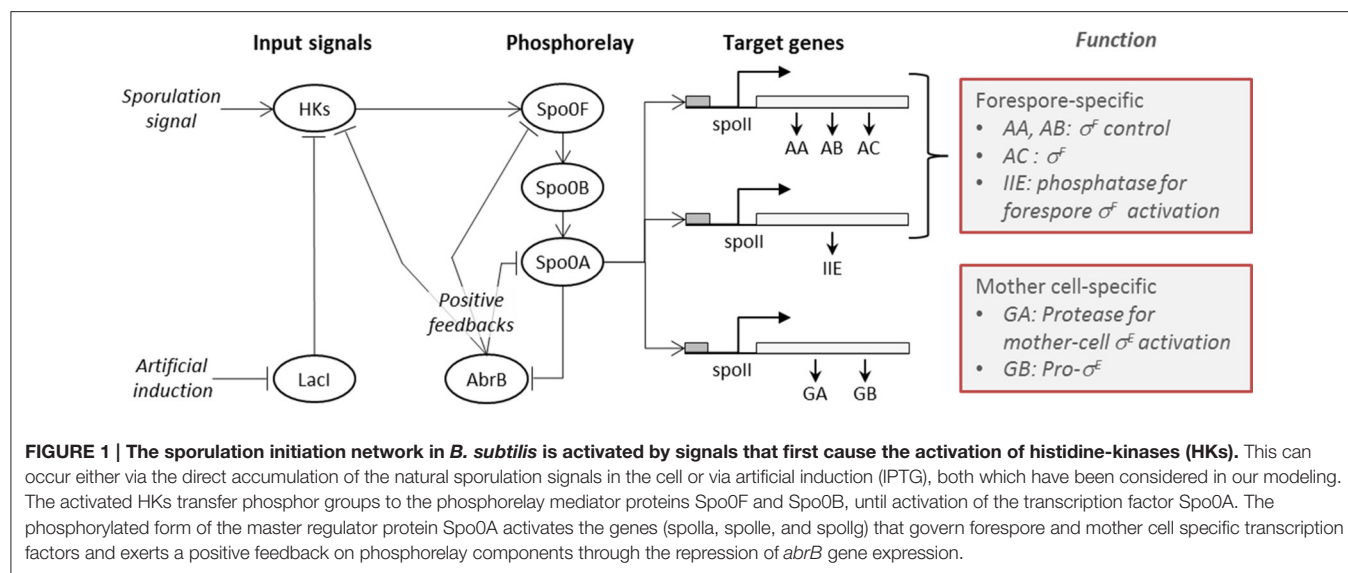
The input signal sub-model, shown in **Figure 2**, represents the regulation effects that artificial inducers (in this case IPTG) and cell produced sporulation signals (modeled by species SS) have on the HKs. In the model, reactions are consecutively numbered. In our model, of the five known kinases that have been identified

as being capable of initiating sporulation in *B. subtilis* (Jiang et al., 2000), we only considered the histidine kinase KinA. This is the major kinase responsible for initiation of sporulation and its overexpression during exponential growth is sufficient to induce entry into sporulation (Fujita and Losick, 2005).

The IPTG regulation of sporulation is rendered by the indirect release of inhibition for the transcription initiation of KinA (Eswaramoorthy et al., 2009; Narula et al., 2012), exerted by the lactose repressor (LacI) on the binding site incorporated into the promoter. The addition of IPTG causes a conformational change in the LacI protein, bringing it (reaction r_{17}) to an inactive form (LacI_d) that has very low affinity for the KinA promoter. The consequence of the inhibition release is an increased level of KinA transcription (reaction r_{11}). In the diagrammatic representation, we use a “droplet” notation for species that are not explicitly represented, such as genes in transcription reactions. The LacI conformational change is however reversible (see reaction r_{18}). Molecules of KinA transcript are translated into protein molecules (reaction r_{12}), which can reversibly bind (reactions r_{13} and r_{14}) to form dimers. KinA dimers have the ability to autophosphorylate (reaction r_{15}), producing the active species that initiates the phosphorelay signaling (Wang et al., 2001; Eswaramoorthy et al., 2009). We model the dephosphorylation and the unbinding of the KinA dimer as a single reaction (r_{16}). The model also considers the activation of the histidine kinase caused by the naturally occurring sporulation signals (SS), which accelerate the KinA autophosphorylation reaction and can lead *B. subtilis* into sporulation alone. Last, the model includes the positive effect that active Spo0A has on the transcription of KinA, via the double repression feedback loop that links phosphorylated Spo0A with AbrB, and AbrB with KinA.

2.2. Phosphorelay Sub-model

The phosphorelay sub-model depicted in **Figure 3** is based on phosphorylation, dephosphorylation and phosphotransfer



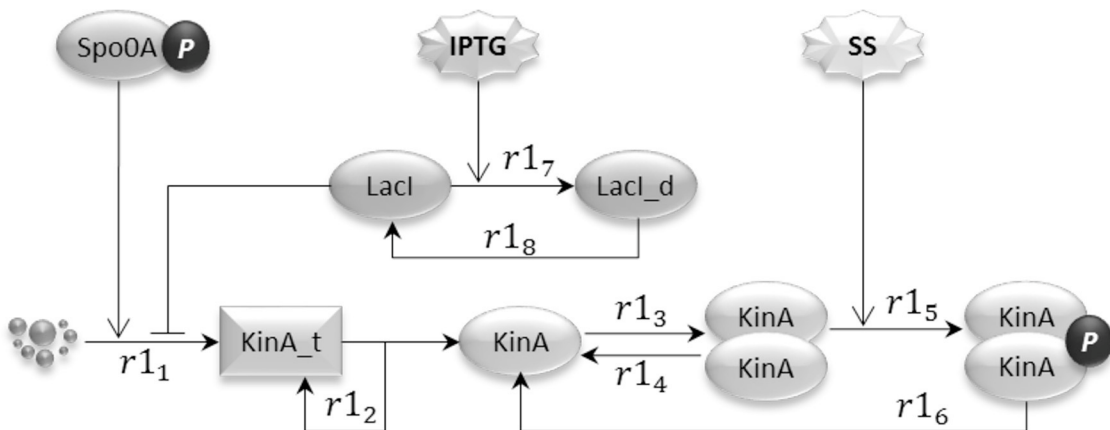


FIGURE 2 | The input signal model represents the artificial sporulation initiation induced by IPTG through the effect on KinA, as well as the activation of KinA dimers by unknown sporulation signals (SS) generated under unfavorable environmental conditions.

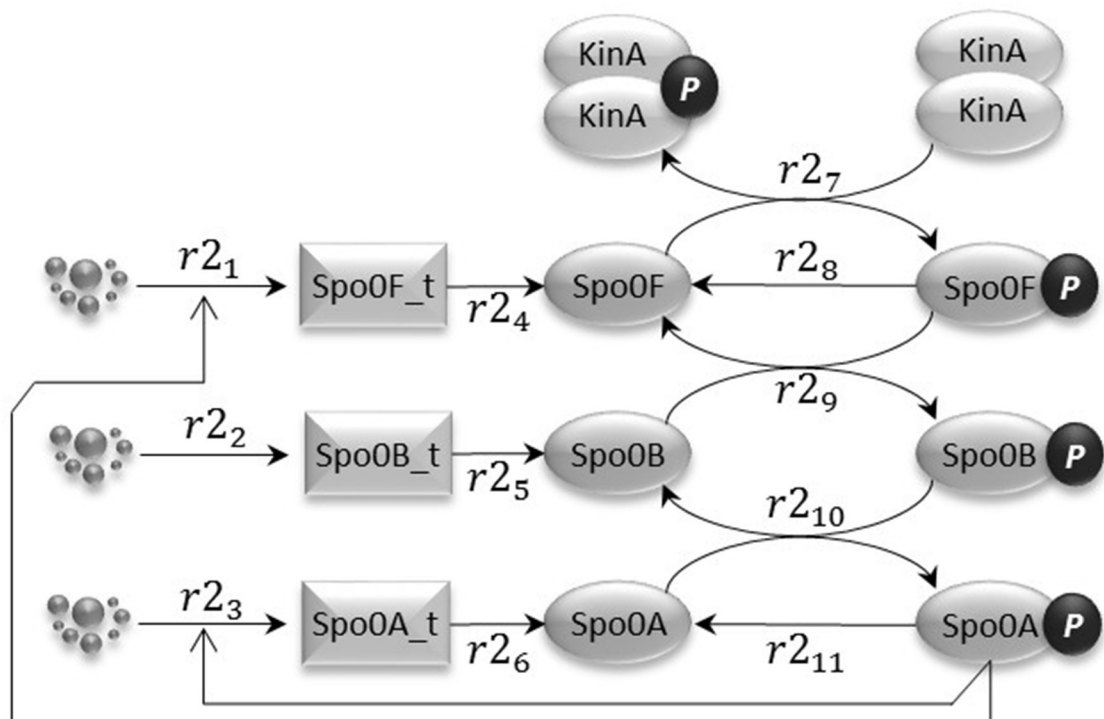


FIGURE 3 | The phosphorelay sub-model encodes the transfer of phospho groups from activated KinA to SpoOF, which then leads to SpoOA phosphorylation via the phosphotransferase SpoOB. Dephosphorylation of SpoOF and SpoOA is modeled by abstracting the phosphatase species.

reactions. Our model includes the main phosphorelay species SpoOF, SpoOB, and SpoOA, which together form a cascading phosphotransfer (de Jong et al., 2010; Sen et al., 2011). For each of these proteins, the model includes a gene transcription reaction (r_{2_1} , r_{2_2} , and r_{2_3}), and a translation reaction (r_{2_4} , r_{2_5} , and r_{2_6}). The phosphorylated KinA dimer transfers the phosphate group to SpoOF (reaction r_{2_7}), phosphorylated SpoOF transfers the phosphate group to SpoOB (reaction r_{2_9}),

and finally phosphorylated SpoOB transfers the phosphate group to SpoOA (reaction $r_{2_{10}}$). In the model, phosphorylated SpoOF and phosphorylated SpoOA spontaneously lose the phosphate group (reactions r_{2_8} and $r_{2_{11}}$). Finally, we include in the model the phosphorelay self-activation loop induced by phosphorylated SpoOA, which as already described positively affects the transcription of both SpoOF and SpoOA species.

2.3. Gene Expression Sub-model

Phosphorylated Spo0A up-regulates transcription from spoIIA, spoIIE, and spoIIG promoters. The gene expression sub-model shown in **Figure 4** encodes the activation of transcription exerted by Spo0A, and includes transcription reactions (r_{31} , r_{32} , and r_{33}) and translation reactions for AA, AB, and AC proteins (r_{34} , r_{35} , and r_{36}), IIE protein (r_{37}) and GA and GB protein molecules (r_{38} and r_{39}). Notice that AA, AB, and AC, and also GA and GB, are transcribed polycistronically from the spoIIA and spoIIG operons, respectively (Narula et al., 2012).

In the rest of the paper and in the Supplementary Material, we adopt the following notation to indicate the variables corresponding with the molecular species of the model: the name of the protein is written in lowercase (e.g., Spo0A, *spo0a*), the transcript of the gene is denoted by the suffix “_t” (e.g., the transcript of gene Spo0A is denoted by *spo0a_t*), and the phosphorylated form of the protein is indicated by the suffix “p” (e.g., the phosphorylated form of protein Spo0A is *spo0ap*). The mathematical specification of the model and its parameters are given in Tables S1–S4. The time is measured in seconds (s), and the molecular species concentration in nM.

3. DETECTING CHAOS IN *B. SUBTILIS* SPORULATION NETWORK DYNAMICS

A system is affected by deterministic chaos if its dynamics is governed by deterministic rules and any change in the initial state, no matter how small, grows quickly with time, rendering long-term prediction of the system behavior impossible. A system is affected by *low-dimensional* chaos if only a small number of variables exhibits a chaotic dynamics, i.e., an aperiodic irregular time-behavior (Tél and Gruiz, 2005; Layek, 2015).

The presence of low-dimensional chaos in biological systems is of particular interest, because it indicates that the variables governing the spatial and temporal behavior of the system may be few in number. This means that the dynamics of the system might

be controlled by only a few crucial variables. The complexity of control inherent in chaotic systems may be important in the dynamics of gene expression regulation. Therefore, it is of particular interest to assess the presence of low-dimensional chaos in a complex system such as the *B. subtilis* sporulation network, as this analysis allows the identification of the variables (few in numbers) that control the predictability of the dynamics of the whole system.

There are two-established methods to explore chaotic behavior of a dynamical biological system. The first one is a direct analysis of the experimental time series, combined with the development of algorithms for computing relevant indices quantifying the features of the system dynamics. The second is the implementation of a model developed directly from the experimental observations that aims to account for the essential mechanisms at work in the real system and explain the dominant behavior. Then, a subsequent analysis focuses on the simulated time series obtained by model solution and its phase space in order (i) to evaluate the control parameters, (ii) to detect the system components (e.g., genes, proteins, chemical species, etc.) that exhibit a chaotic dynamics, and (iii) to investigate the robustness of the dynamics against perturbations. We implemented the second approach, because the inclusion in the analysis of a model of the systems dynamics affords not only the identification of the drivers of chaotic dynamics, but also the conceptualization of their role and of their effects within the mechanisms of interaction with other molecular species. In the next section, we provide a detailed explanation of this analysis.

3.1. Sensitivity Analysis

We undertook local sensitivity analysis to assess the sensitivity of the solutions of the system's equations to the variation of individual parameter in the system. We discussed the feasibility of global sensitivity analysis of the system to variation in parameters in the Supplementary Information.

We randomly sampled N_p values from a uniform distribution for each parameter (i.e., kinetic rate constant). The uniform

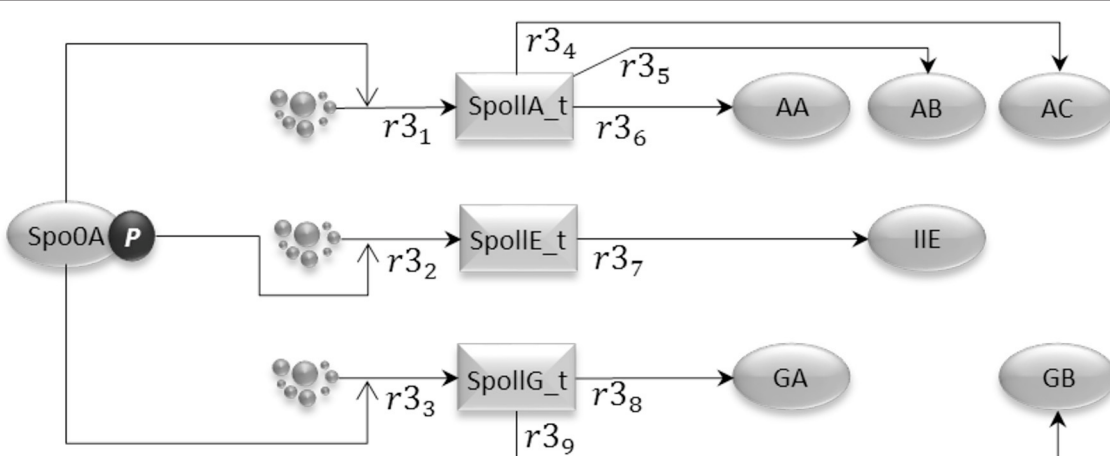


FIGURE 4 | The gene expression model represents the transcriptional activity of phosphorylated Spo0A, which binds to the *SpoII* promoters and promotes transcription initiation for the important sporulation initiation proteins, AA, AB, AC, IIE, GA, and GB.

distributions were positively defined on the maximal range of parameter variability in which the system of ordinary differential equations has a unique solution (i.e., it is not underdetermined). We determined this range $I_{q^*}(p_h)$ by attempting to solve the system of equations for different sets of parameters $P(q) = \{p_h\}$, $h = 1, 2, \dots, N_p$, obtained by varying the value of $q \in \mathbb{N}^+$ in the interval [2, 30] in the following expression

$$I_q(p_h) = \left[\frac{p_h}{q}, q \times p_h \right], \quad h = 1, 2, \dots, N_p \quad (1)$$

The maximal interval of parameter variation is defined by the maximal value of q for which the system of differential equations has a unique solution.

The parameters were changed one at a time while keeping the values of the others fixed. Since for each parameter p_h we sampled N_p values, we performed N_p model simulations, i.e., one simulation for each sampled value in the range of parameter variability $I_q(p_h)$. The index of sensitivity of the time series $x_s(t)$, ($s = 1, 2, \dots, d$, where d is the number of molecular species in the system), with respect to the change of the h -th parameter from the value p_h to the value p'_h is calculated as the mean of the standard deviations of the distributions of the simulated values of the variable over the range of parameter variability and over time, i.e.:

$$SI_{s,h} = \frac{1}{N} \sum_{k=1}^N \left(\frac{1}{N_p - 1} \sum_{r=1}^{N_p} (x_s^{(r)}(t_k | p_h \leftarrow p'_h) - \bar{x}_s^{(r)}(p_h \leftarrow p'_h))^2 \right)^{\frac{1}{2}} \quad (2)$$

where N is the length of the time series, and

$$\bar{x}_s(p_h \leftarrow p'_h) = \frac{1}{N_p} \sum_{k=1}^{N_p} x_s(t_k | p_h \leftarrow p'_h). \quad (3)$$

With the expression $p_h \leftarrow p'_h$, we denote the replacement of value p_h with the value p'_h .

3.2. Complexity Indices

In order to detect the presence of chaos in *B. subtilis* network dynamics, for the time series of each molecular species we calculated a set of indices that capture different aspects of the complexity. This set of indices includes:

- Lyapunov exponents (λ):** they measure the rate of separation of infinitesimally close trajectories in the phase space generated by slightly different values in the initial state of the system. The largest Lyapunov exponent is usually considered important in the determination of chaotic behavior. A positive value for the largest Lyapunov exponent indicate orbital instability and chaos (Kaneko and Tsuda, 2001; Sprott, 2003; Kalitin, 2004).
- fractal dimension (D_F):** a statistical index for pairwise distances of the points of a time series; it indicates how a set of points fills its space and thus quantifies the complexity of the behavior of a trajectory;

- sample entropy (S_E):** a measure of data regularity; a smaller value of sample entropy indicates more self-similarity in the data of the time series and a less noise (less disorder);
- time lag (T_L):** the time after which the auto-correlation of the time series is negligible;
- embedding dimension (D_E):** similarly to the fractal dimension, it measures topological complexity of a time series. A set of points has embedding dimension D_E if D_E is the smallest integer for which it can be embedded into \mathbf{R}^{D_E} without intersecting itself. So, D_E is the minimum dimension of a space in which a trajectory in the phase space reconstructed from the observed time series does not cross itself (in this case the dynamics is deterministic) (Abarbanel, 1996; Tammaro and Khubchandani, 2016).

In chaotic systems, small differences in the initial condition result in strongly different solutions. Therefore, a chaotic system is unpredictable in the sense that the variability of the prediction induced by small changes in the initial conditions is unacceptably high in comparison to the difference of the initial states.

In deterministic systems, complete knowledge of the rules of the dynamics and of the initial state (i.e., values for the abundance of the system's components at initial time t_0 —sometimes called *initial conditions*) $\mathbf{x}(t_0)$, is sufficient to determine $\mathbf{x}(t)$ at each $t > t_0$. In chaotic deterministic systems, if the initial state is changed by a small value ϵ , two trajectories that were initially close, will exponentially separate. Formally, if $\mathbf{x}(t)$ and $\mathbf{x}'(t)$ are the two trajectories generated by the initial states $\mathbf{x}(t_0)$ and $\mathbf{x}'(t_0)$, and if $|\mathbf{x}(t_0) - \mathbf{x}'(t_0)| < \epsilon$, we have that

$$|\mathbf{x}(t) - \mathbf{x}'(t)| \sim \epsilon e^{\lambda t} \quad (4)$$

where λ is the angular coefficient of the straight line defining $\ln |\mathbf{x}(t) - \mathbf{x}'(t)|$ as a function of time t :

$$\ln |\mathbf{x}(t) - \mathbf{x}'(t)| = \lambda t + \ln \epsilon.$$

Using Equation (4) it is possible to predict the time t^* after which the predicted trajectory is too imprecise. Indeed, if δ is the tolerance on the precision of the prediction, then from Equation (4) $\epsilon e^{\lambda t^*} \sim \delta$, and therefore

$$t^* \sim \frac{1}{\lambda} \ln \frac{\delta}{\epsilon}. \quad (5)$$

The expression in Equation (5) suggests that t^* can be arbitrarily increased by decreasing ϵ . However, de facto, it is not possible to obtain a value of t^* much greater than $\frac{1}{\lambda}$. For instance, if we want to increase t^* by one order of magnitude, we have to decrease ϵ by a factor $e^{10} \sim 10^4$. This example points out that the dependence of t^* on the ratio $\frac{\delta}{\epsilon}$ is so weak that in Equation (5), the only term that strongly influences t^* is λ (Vulpiani, 2004; Cencini et al., 2009; Lecca et al., 2016).

The system of differential equations describing the dynamics of the *B. subtilis* sporulation network is a d -dimensional system, where d is the number of molecular species involved in the system. At each instant of time t the system is contained in a d -dimensional sphere in the phase-space. In particular, this d -dimensional sphere is centered at $\mathbf{x}(0)$ ($\mathbf{x}(0)$ belonging to the

attractor) and has radius ϵ . The time evolution of the system dictated by the equations deforms the sphere into an ellipse. If $l_i(t)$ denotes the length of the i -th semi-axis of the ellipse at time t , the characteristic *Lyapunov exponents* ($\lambda_1 \geq \lambda_2 \geq \dots \geq \lambda_d$) are defined as follows:

$$\lambda_i = \frac{1}{t} \ln \frac{l_i(t)}{\epsilon}, \quad i = 1, 2, \dots, d. \quad (6)$$

If $\lambda_i > 0$, the i -th semi-axis grows with time; in contrast, if $\lambda_i < 0$ the i -th semi-axis shrinks with time. In a system extremely sensitive to the initial conditions, at least one of the Lyapunov exponents is greater than zero.

For each molecular species i in the *B. subtilis* network we have calculated the maximal Lyapunov exponent from the corresponding simulated time series, i.e., the Lyapunov exponent at the maximum observed time, formally defined as follows

$$\lambda_i^{\max} = \lim_{t \rightarrow \infty} \lim_{\epsilon \rightarrow 0} \lambda_i \quad (7)$$

The greater a positive maximal Lyapunov exponent, the faster the rate of divergence of the two trajectories $\mathbf{x}(t)$ and $\mathbf{x}'(t)$. Thus, the Lyapunov coefficients were used to measure the contribution of each molecular species to the system's dynamics. In this study, we used the Rosenstein et al. (1993) algorithm to estimate the maximal Lyapunov exponent.

The Lyapunov exponents capture the unpredictability in a system's evolution which can be generated by slightly different initial states. However, unpredictability could depend also on an irregular aperiodic behavior of the abundance of some molecular species in the system.

To capture this aspect of a chaotic dynamical system, and, most importantly to distinguish it from noise, we have estimated the *fractal* and the *embedding* dimensions of the time series of each gene and protein in the system. Both fractal and embedding dimensions are generalizations of the topological dimension and measure the dimensionality of the space occupied by the set of points of the time series. The more complex and irregular the distribution of the points in space is, the higher the fractal and embedding dimensions of the system.

We estimate the fractal dimension as a *correlation dimension* (Theiler, 1990; Ding et al., 1993), defined in terms of the correlation integral $C(\epsilon)$:

$$C(\epsilon) = \lim_{N \rightarrow \infty} \frac{g_\epsilon}{N^2} \quad (8)$$

where N is the number of points in the time series, and g is the total number of pairs of points that dist from each other is less than ϵ (a graphical representation of such close pairs is the *recurrence plot* (Marwan et al., 2016). The correlation integral estimates the probability that a pair of points of the time series is separated by a distance less than ϵ . For $\epsilon \ll 1$ it can be shown (Theiler, 1990) that

$$C(\epsilon) \sim \epsilon^{D_F} \quad (9)$$

where D_F is the correlation dimension. For a sufficiently large, and evenly distributed, number of points in a time series, a log-log graph of the correlation integral vs. ϵ can be used to estimate

D_F (Kantz, 2004). The more complex and irregular a time series is, the higher its correlation dimension, as the number of ways for points to be close to each other is greater (Higuchi, 1988). Indeed the fractal dimension corresponds to the number of the degrees of freedom of the time series (Mera and Morán, 2002).

Unlike topological dimension, the fractal dimension can take non-integer values, indicating that a set of points of a trajectory can fill its space qualitatively, and quantitatively, in a different way from an ordinary geometrical set. For instance, a curve with fractal dimension very near to 1, behaves quite like an ordinary line, but a curve with fractal dimension greater than 2 winds convolutedly through space very nearly like a surface or a volume. As a consequence, if a time series of a gene or protein has a fractal dimension significantly greater than 1, the dynamics of that gene or protein is more likely affected by chaos than by noise.

The sample entropy S_E adds further information to that provided by the Lyapunov exponents and the fractal dimension, as it is a direct measure of the unpredictability of a time series (Mao, 2011). Indeed, S_E estimates how much a given data point depends on the values of a number m of preceding data points, averaged over the whole time series. S_E is computed as the negative logarithm of the conditional probability that two similar samples from the time series remain similar at the next point (Richman and Moorman, 2000; Azar and Vaidyanathan, 2016). To calculate the sample entropy, points matching within a tolerance ϵ are computed until there is no match according to this condition. Formally, if

$$X(t) = \{x(t_1), x(t_2), \dots, x(t_N)\} \equiv \{x_1, x_2, \dots, x_N\}$$

is a time series of length N , the sample entropy is defined as in the following by Azar and Vaidyanathan (2016), Sokunbi (2014), and Richman and Moorman (2000).

$$S_E(m, r, N, \tau) = -\ln \frac{U^{(m+1)}(\epsilon)}{U^{(m)}(r)} \quad (10)$$

where B_i is the number of j where $|X(i) - X(j)| \leq r$, and

$$U^{(m)}(\epsilon) = \frac{1}{N - m\tau} \sum_{i=1}^{N-m\tau} \frac{B_i}{N - (m+1)\tau}$$

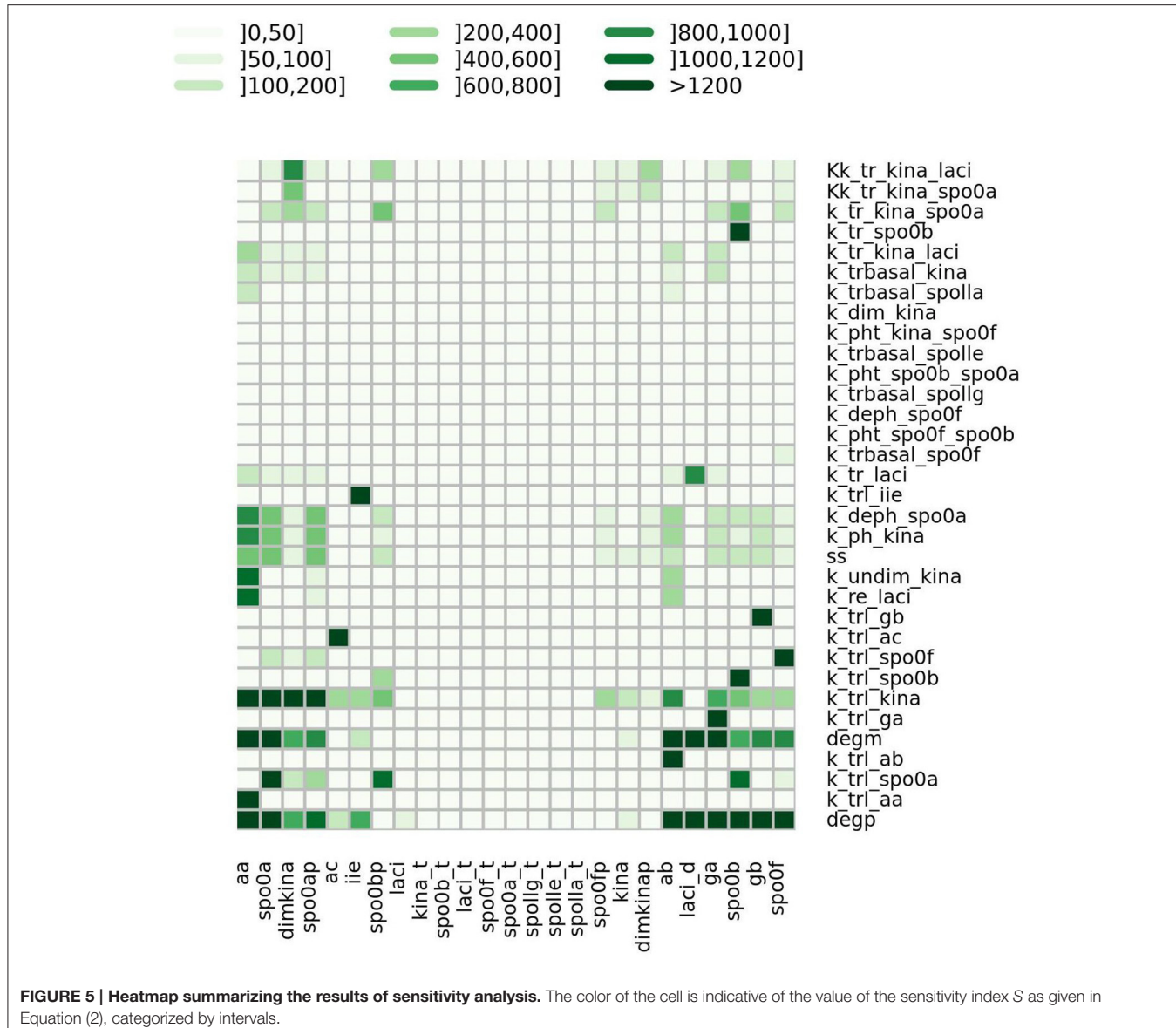
$$X_m(i) = \{x_i, x_{i+\tau}, \dots, x_{i+(m-1)\tau}\}$$

$$X_m(j) = \{x_j, x_{j+\tau}, \dots, x_{j+(m-1)\tau}\}$$

$$1 \leq j \leq N - m\tau, \quad j \neq i.$$

$X_m(i)$ is called *template vector* of length m of the time series $X(t)$, and an instance where a vector $X_m(j)$ is within ϵ of $X_m(i)$ is called a template *match*. The quantity $\frac{B_i}{N - (m+1)\tau}$ is the probability that any vector $X_m(j)$ is within r of $X_m(i)$. Finally, τ is called *time delay*, and in our analysis it has been set equal to the time lag T_L^* , that is an estimate of the time at which the time series behavior becomes unpredictable. It can be computed using the auto-correlation function method (Zeraoulia, 2011) and is taken as the lag time T_L^* at which the auto-correlation function

$$r_{T_L} = \frac{\sum_{i=1}^{N-T_L} (x_i - \bar{x})(x_{i+T_L} - \bar{x})}{\sum_{i=1}^N (x_i - \bar{x})^2}. \quad (11)$$



first crosses zero. This choice of τ in the estimation of sample entropy is motivated by the need to capture also non-linear autocorrelation properties of the time series (Kaffashia et al., 2008). For instance, it has been proved that with a unity time delay (Kaffashia et al., 2008), the sample entropy measures only the linear autocorrelation properties of the time series. A lower value of S_E (and a higher value of T_L^*) indicates higher predictability of the time series, while a higher value of S_E (and a lower value of T_L^*) indicates lower predictability.

Finally, we also considered the embedding dimension as a measure of time series complexity. The embedding dimension of a time series is the smallest dimension required to embed it, and it can be estimated by the Cao's algorithm (Cao, 1997). In our analysis, the parameter m in the definition of sample entropy has been set equal to the embedding dimension.

3.2.1. Distinguishing Noise from Chaos

Since both the presence of chaos and the presence of noise are manifested as topological and statistical complexity of a time series, our analysis aims to distinguish chaos from noise. In the past decade many methods in a different application domains have been proposed to make this distinction, the most recent are reported in Skiadas and Skiadas (2016), Ravetti et al. (2014), Rohde (2008), Gao et al. (2006), and Rosso et al. (2007).

We adopted a simple well established method based on the comparison of the complexity indices identified above and obtained from the time series simulated by the model with those obtained from Gaussian white noise, colored noise and power-law noise (Skiadas and Skiadas, 2016). The expectation is that sample entropy, time lag, and embedding dimension for the non-noisy candidate chaotic times series are significantly different from those estimated for the white and colored noise time

TABLE 1 | Molecular species and the parameters mostly controlling their dynamics.

Molecular species	Parameters
aa	degp, k_trl_aa
spo0a	degp, k_trl_spo0a
dimkina	k_trl_kina, Kk_tr_kina_laci
spo0ap	k_trl_kina, degp
ac	k_trl_ac, k_trl_kina
ie	k_trl_ie, degp
spo0bp	k_trl_spo0a, k_trl_kina
ab	degp, k_trl_ab
laci_d	degp, degm
ga	degp, k_trl_ga
spo0b	degp, k_trl_spo0b
gb	degp, k_trl_gb
spo0f	degp, k_trl_spo0f

series. Moreover, the time behavior of the Lyapunov exponents is expected to be non-linear for the noise and at least linear for chaotic non-noisy time series (Gao and Zheng, 1994).

3.3. Analysis of the Jacobian Matrix: The Time Evolution of the Phase Space

In order to explore the phase space of the systems and calculate its equilibria and its time evolution we analyzed the Jacobian matrix J of the system of ordinary differential equations describing the dynamics.

$$J = \begin{bmatrix} \frac{\partial f_1}{\partial s_1} & \frac{\partial f_1}{\partial s_2} & \cdots & \frac{\partial f_1}{\partial s_d} \\ \frac{\partial f_2}{\partial s_1} & \frac{\partial f_2}{\partial s_2} & \cdots & \frac{\partial f_2}{\partial s_d} \\ \vdots & \vdots & \ddots & \vdots \\ \frac{\partial f_d}{\partial s_1} & \frac{\partial f_d}{\partial s_2} & \cdots & \frac{\partial f_d}{\partial s_d} \end{bmatrix} \quad (12)$$

where $f_i = \frac{ds_i}{dt}$, and s_i is the abundance of the i -th molecular species in the system ($i = 1, 2, \dots, d$).

A steady state point $s_{eq} = \{s_i^{eq}\}$, $i = 1, 2, \dots, d$, of the systems is defined by a solution of the system of algebraic equations as in the follows:

$$\frac{ds_i}{dt} = 0, \quad i = 1, 2, \dots, d.$$

The stability of a steady state point is determined by the sign of the real part of the eigenvalues of the Jacobian matrix. In particular, if the real parts of all eigenvalues are negative, the steady state point is stable. It's termed *sink*, because, there is a basin around it, and any initial condition in that basin will result in a trajectory falling in toward the steady state point.

If the real parts of all the eigenvalues are positive, the steady state point is *unstable*. It is termed *source*, because, starting from an initial point close to it, the trajectory will move away from it. If the real parts of the eigenvalues are of different signs, the steady state point is called a *saddle point*. It is *unstable*, attracting along some axes and repelling along others. If there are also complex components, the nature of the fixed point doesn't change (it's still

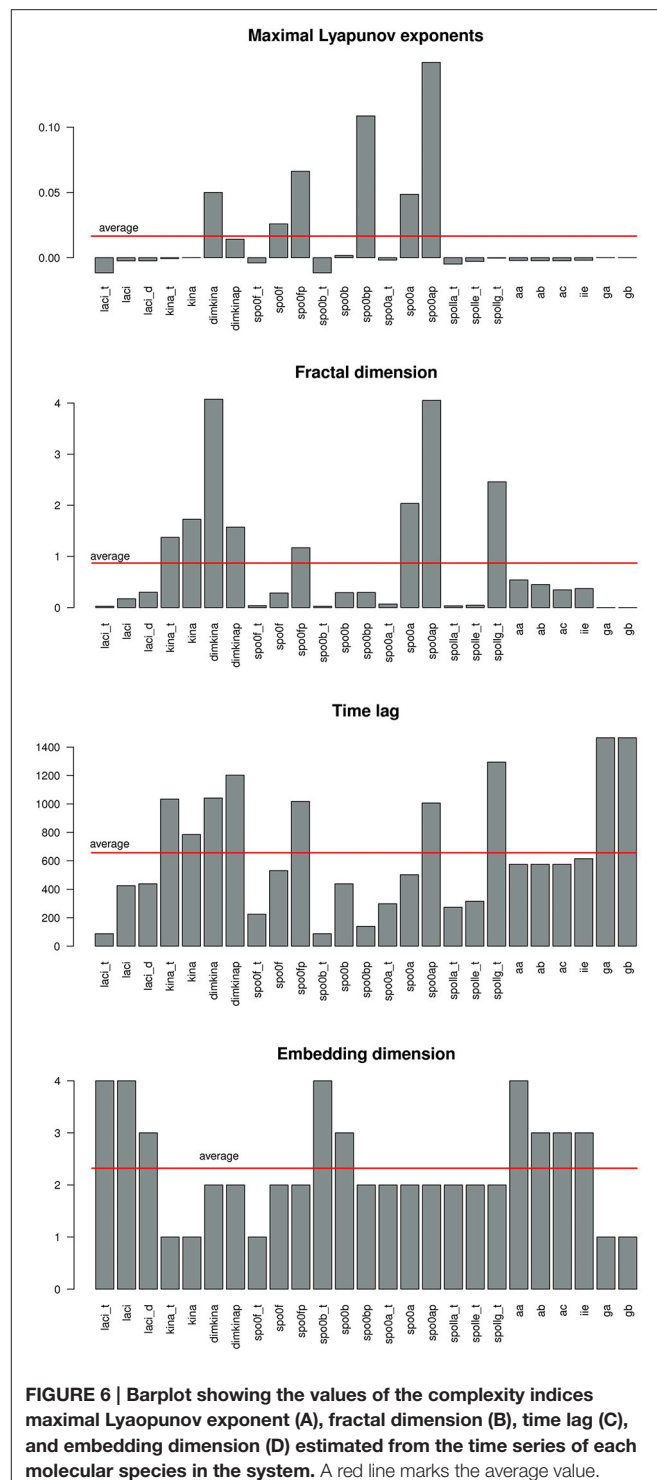
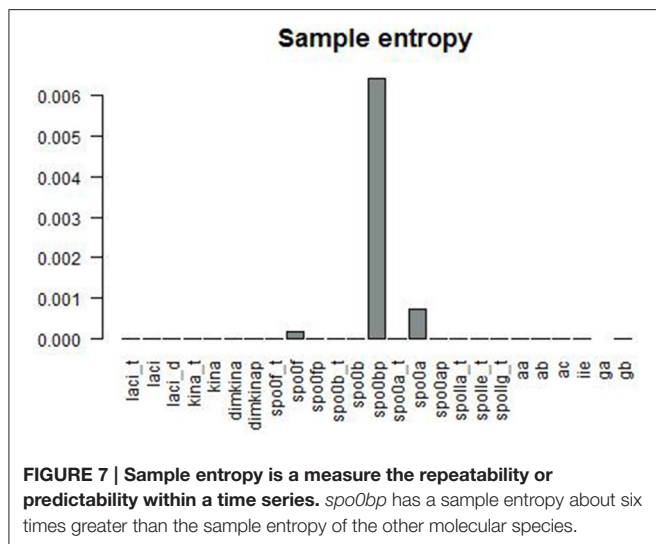


FIGURE 6 | Barplot showing the values of the complexity indices maximal Lyapunov exponent (A), fractal dimension (B), time lag (C), and embedding dimension (D) estimated from the time series of each molecular species in the system. A red line marks the average value.

a sink, source, or saddle point) but with a twist. If the eigenvalues are purely complex, then there are closed orbits around the fixed point.

The eigenvectors of the Jacobian matrix give the axes along which the behaviors indicated by the eigenvalues are centered. So, the eigenvector associated with a negative eigenvalue is a vector along which the fixed point attracts. The eigenvector associated



with a positive eigenvalue is an axis along which the fixed point repels.

4. RESULTS

In this section we collect the results of three different analyses: (i) the parameter sensitivity analysis, (ii) the model time series analysis, and (iii) the phase space analysis. The first two analyses capture different aspects and manifestations of the presence of chaos and their outputs are sets of molecular species whose behavior is a likely candidate for chaotic dynamics. The final result is an intersecting set of molecular species that represents the consensus set of molecular species whose dynamics is affected by chaos. The third analysis aims at determining how the topology and the parameters of the network of interactions among the molecular species evolves with time. This last analysis allows the determination of the time variation of the active degrees of freedom in the system (Hilborn, 2000).

4.1. Kinetic Rate Constants Controlling the Dynamics

We explored the parameters' space in which the systems of ordinary differential equations that represent the model has a solution. We found that the largest range of variation for the parameters at which the systems still admits a unique solution is defined by

$$I(p_h) = \left[\frac{p_h}{10}, 10 \times p_h \right], \quad h = 1, 2, \dots, N_p \quad (13)$$

where p_h is the value of the h -th parameter assigned from experimental data. For each parameter we randomly sampled 50 values from a uniform distribution positively defined in $I(p_h)$. In turn these were used in simulations to give sensitivity indices according to Equation (2). In Figure 5 a heatmap shows the value of the sensitivity index collapsed into intervals. Moreover, Table 1 lists the variables and the parameters which affect them most.

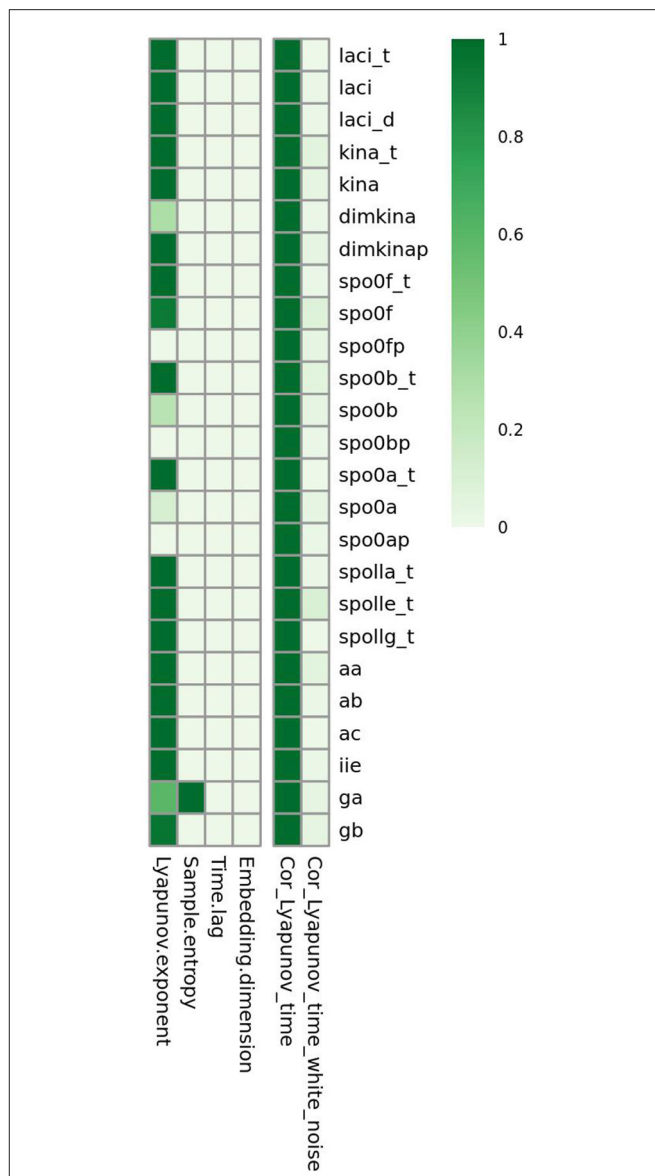


FIGURE 8 | Complexity detected in the *B. subtilis* sporulation network dynamics is due to low dimensional chaos and not to noise. For the time series of molecular species *spo0a*, *spo0b*, *spo0ap*, *spo0bp*, *spo0f*, and *spo0fp*, all the indices of complexity are significantly greater than those for the time series of Gaussian white noise.

Appreciable parameter sensitivity is only apparent in an interval ranging from a tenth to ten times the parameter value obtained from data. The dynamics of the majority of the molecular species is robust with respect to the variations of the parameters' values on smaller intervals (see Figure S2). The molecular species *spo0a*, *spo0b*, *spo0ap*, and *spo0bp* are the most sensitive to perturbation of parameters even on small intervals.

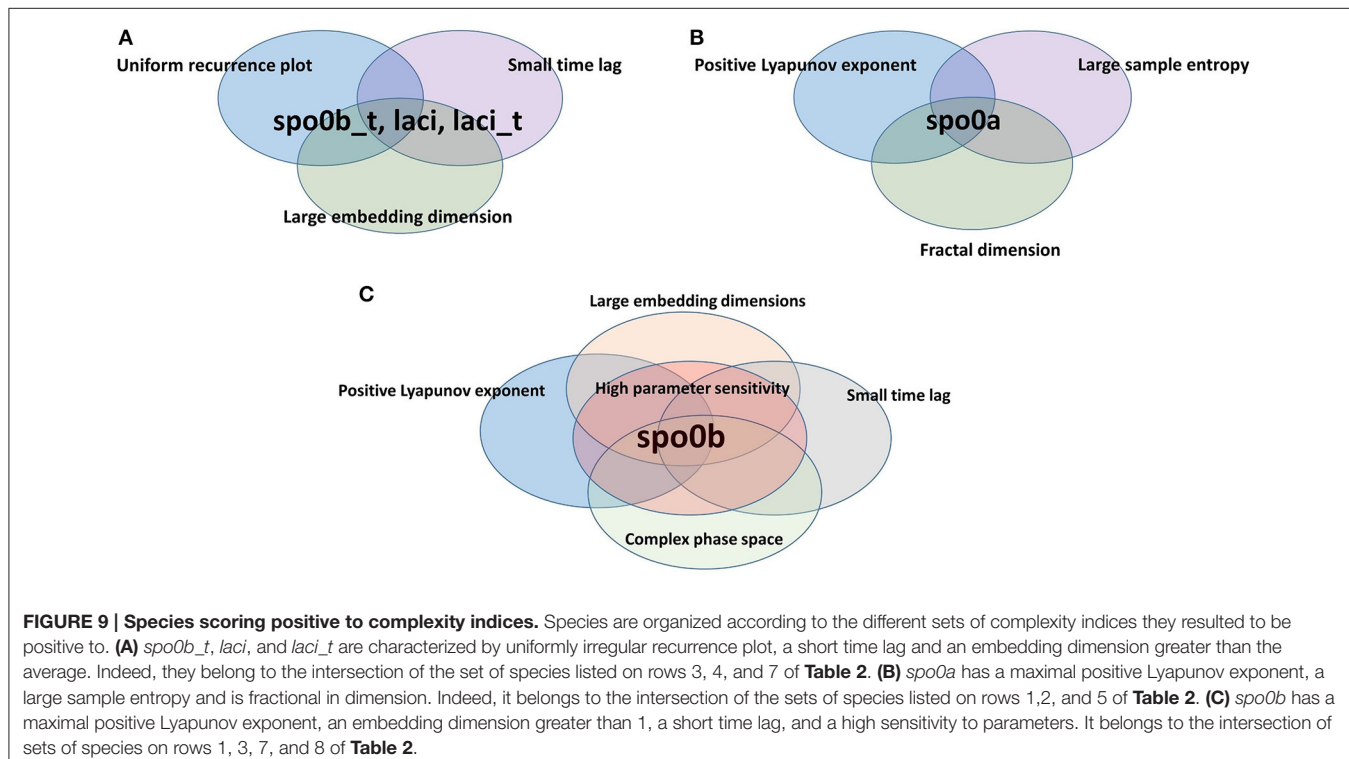
4.2. Complexity Indices Identify the Drivers of Chaotic Dynamics

Figure 6 gives a graphical summary of the complexity indices estimated for the time series of each molecular species. The

TABLE 2 | Sets of molecular species with values of the complexity indices indicative of presence of chaos.

Index	Variables	% of total nr. of variables
Positive Lyapunov exponent	dimkina, dimkinap, spo0f, spo0fp, spo0b, spo0bp, spo0a, spo0ap	32
Fractal dimension (above the average)	kina_t, kina, dimkina, dimkinap, spo0fp, spo0a, spo0ap, spollg_t	32
Embedding dimension (above the average)	kina_t, kina, dimkina, dimkinap, spo0fp, spo0a, spo0ap, spollg_t	36
Time lag (below the average)	laci_t, laci, laci_d, spo0f_t, spo0f, spo0b_t, spo0b, spo0bp, spo0a_t	64
	spo0a, spolla_t, spolle_t, aa, ab, ac, iie	
Sample entropy (above the average)	spo0f, spo0bp, spo0a	12
Complex trajectory in phase space	ga, gb, spo0a, spo0a_t, spo0b, spo0f_t, spollg_t	28
Recurrence plot reveals chaos	spo0b, spo0bp, spo0a, spo0ap, aa, ab	24
High parameter sensitivity	aa, spo0a, dimkina, spo0ap, ac, iie, spo0bp, ab, laci_d,	52
(ordered by sensitivity)	ga, spo0b, gb, spo0f	

The third column reports the percentage of species scoring positive to the test of chaos according to a set of indices.



majority of the molecular species have positive Lyapunov exponents, fractional dimension, time lag between 0 and 400 (that is the about 3% of the time range used in the simulation), and embedding dimension greater than 1. **Figure 7** shows the sample entropy values and reports that the highest vale of sample entropy is assumed by spo0bp.

To distinguish chaotic from noisy dynamics, we compared the complexity indices of the time series of each variable with the mean and the standard deviation of the complexity indices estimated from 50 time series of white Gaussian noise of mean $\mu = 0$, variance $\sigma^2 = 1$ generated for each variable and having amplitude equal to the range of variability of the

variable. The heatmap in **Figure 8** shows, on the left side, the frequency at which the noisy time series has an index value higher than that observed for the time series from the real model. Comparison of indices under chaotic and noisy conditions is performed for each index (shown by column) and each variable (shown by row). The heatmap on the right side shows correlation between Lyapunov index and time points in the time series. Column “Cor_Lyapunov_time” displays statistical significance for Pearson’s correlation relating Lyapunov exponent and time. Column “Cor_Lyapunov_time_white_noise” displays similar information for the time series of white Gaussian noise generated for each variable. We found that sample entropy,

TABLE 3 | Coordinates of the stable steady state point of the model solved with initial conditions $s_i(t = 0) = 0 \forall i = 1, 2, \dots, 25$.

Molecular species	Coordinate (nM)
<i>laci_t</i>	17.24
<i>laci</i>	18.27
<i>laci_d</i>	2855.29
<i>kina_t</i>	77.89
<i>kina</i>	674.32
<i>dimkina</i>	1719.72
<i>dimkinap</i>	81.81
<i>spo0f_t</i>	20.68
<i>spo0f</i>	1219.14
<i>spo0fp</i>	26.7
<i>spo0b_t</i>	41.1
<i>spo0b</i>	3683.52
<i>spo0bp</i>	2.09
<i>spo0a_t</i>	23.92
<i>spo0a</i>	2350.24
<i>spo0ap</i>	1921.15
<i>spolla_t</i>	76.6
<i>spolle_t</i>	57.45
<i>spollg_t</i>	81.74
<i>aa</i>	7979.31
<i>ab</i>	3542.82
<i>ac</i>	880.92
<i>iie</i>	660.73
<i>ga</i>	2316.09
<i>gb</i>	940.06

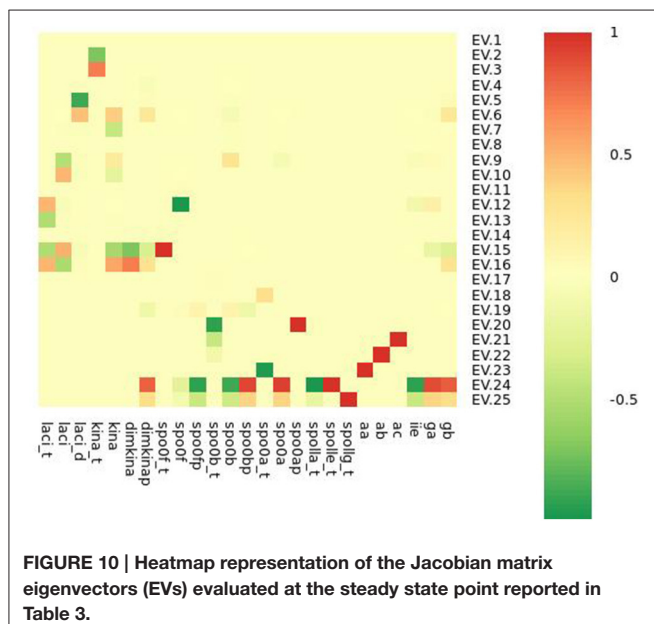


FIGURE 10 | Heatmap representation of the Jacobian matrix eigenvectors (EVs) evaluated at the steady state point reported in Table 3.

time lag and embedding dimension are significantly higher in the model time series than in the white noise time series. The Lyapunov exponents are significantly greater for the white noise time series compared with the model's time series, except for

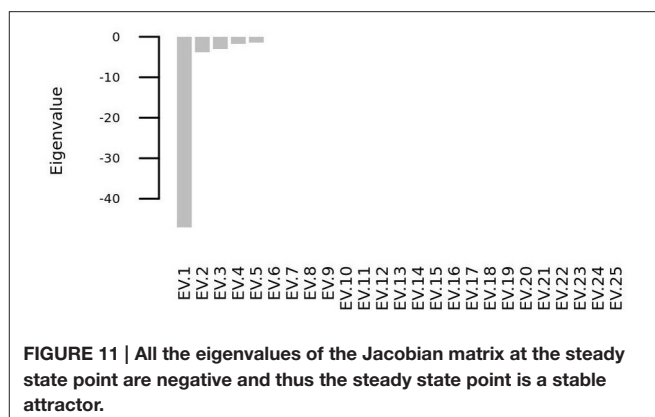


FIGURE 11 | All the eigenvalues of the Jacobian matrix at the steady state point are negative and thus the steady state point is a stable attractor.

spo0a, *spo0ap*, *spo0bp*, *spo0f*, and *spo0fp*. This result suggests that these molecular species exhibit remarkable chaotic dynamics. The left part of the heatmap confirms a non linear time behavior of the Lyapunov exponents of the white noise time series, and suggests a linear time behavior of the Lyapunov exponents of the model's time series. Again, this result distinguishes between chaotic dynamics and random noisy dynamics (Gao and Zheng, 1994). In the Supplementary Material (Figures S4–S6), we report similar results obtained in the comparison of the complexity indices of the model's time series with the ones for the colored and power law noise.

For each index of complexity, **Table 2** (and a graphical summary of it in **Figure 9**) reports the set of molecular species where results indicate the presence of chaos. In this Table, we also included two qualitative indicators of the presence of chaos, such as a complex phase space (i.e., convoluted trajectories) and recurrence plot. These plots are provided in Supplementary Material (Figure S7), and visualize a square matrix, whose elements are the times at which a state of a dynamical system recurs (columns and rows correspond then to a certain pair of times) (Marwan et al., 2016, 2007). We refer the reader to the Supplementary Material for a comprehensive description of the recurrence plots analysis.

The variable *spo0b* is the one with the largest set of complexity indices whose values point to the presence of chaos.

4.3. Phase Space Analysis

We solved the systems of differential equations setting to zero the initial concentration of all the molecular species (i.e. $s_i(t = 0) = 0 \forall i = 1, 2, \dots, 25$), and we found that the system has one steady state point, whose coordinates are shown in **Table 3**. This point is a stable equilibrium, as the eigenvalues of the Jacobian matrix (**Figure 10**) of the system are all negative (**Figure 11**).

We also calculated the value of the elements of the Jacobian matrix at different time points to determine its time evolution. Since the entries of the Jacobian matrix are the partial derivatives of the rate equations with respect to the variables [i.e., $J_{ij} = \frac{\partial f_i}{\partial s_j}$ (Equation 12)], the Jacobian matrix can be represented by a weighted graph, where the nodes represent the variables (i.e., the molecular species) and the edge weights are the elements of the matrix J_{ij} . We introduced the estimate of the error on

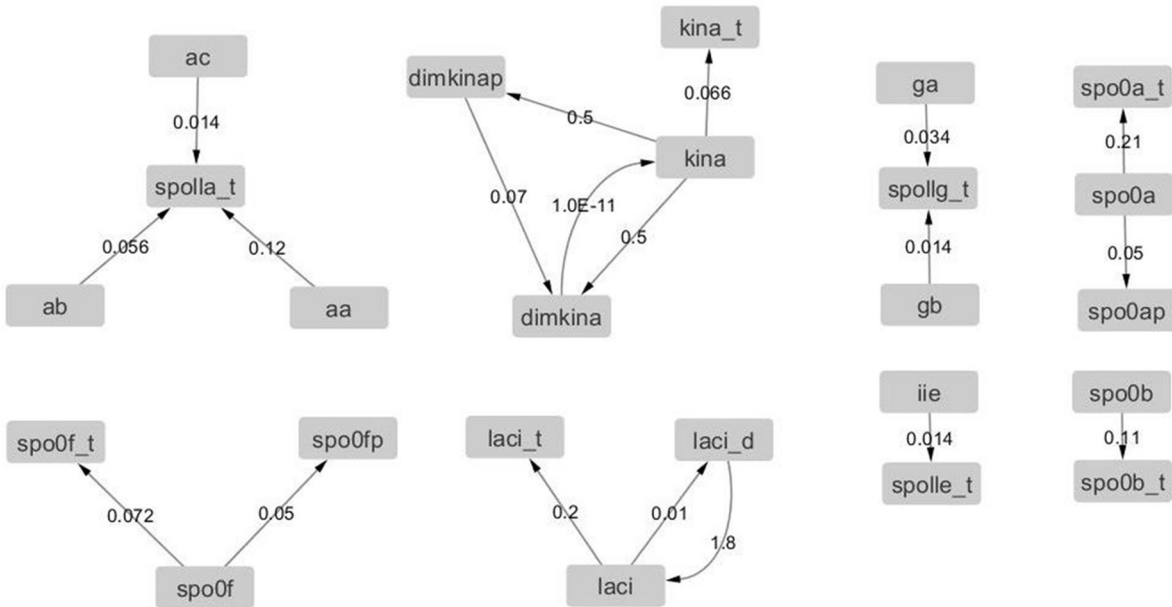


FIGURE 12 | Graph with adjacency matrix equal to the Jacobian matrix at time $t = 0$ s. The graphs shows the basal reactions, i.e., those that initiate the time evolution for the network.

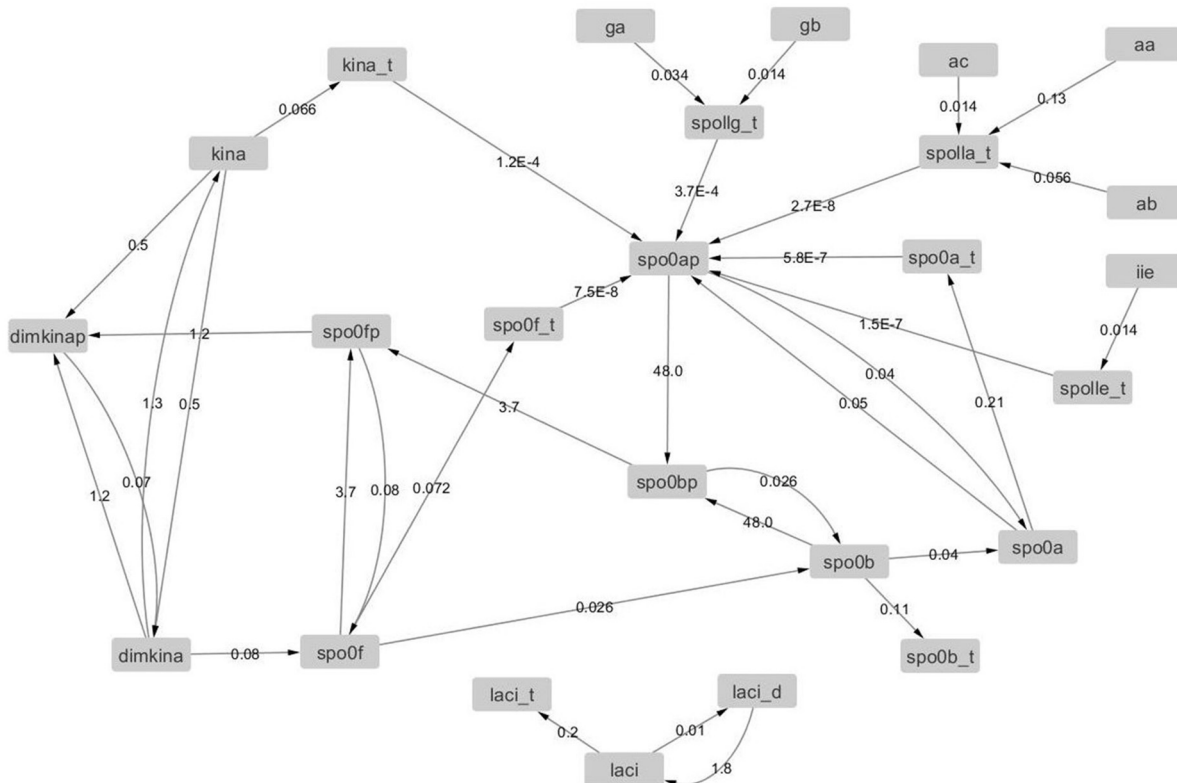


FIGURE 13 | Graph with adjacency matrix equal to the Jacobian matrix at time $t = 500$.

J_{ij} defined as $\Delta J_{ij} = \text{prec} \times \frac{\partial^2 f_i}{\partial S_j^2}$, where $\text{prec} = 10^{-8}$ is the precision of the numerical solution of the model, and set the threshold of 20% on the relative error $ER = \frac{\Delta J_{ij}}{J_{ij}}$. Edges with $ER < 20\%$ were retained and allowed for the estimation of the number of active degrees of freedom in the system, i.e., the number of variables involved in active interactions (Hilborn, 2000). Hence, the graphs derived from the Jacobian matrices estimated at different time points are temporal snapshots of the molecular interaction network.

TABLE 4 | Minimum, first quartile, median, mean, third quartile, and maximum of the distributions of the Jacobian matrix values (i.e., edge weights of the networks) at times $t = \{0, 500, 1000, \dots, 7500\}$.

Time (sec)	Min.	1st Qu.	Median	Mean	3rd Qu.	Max.
0	0.00	0.02	0.07	0.20	0.16	1.80
500	0.00	0.01	0.07	3.09	0.50	48.00
1000	0.00	0.01	0.07	3.09	0.50	48.00
1500	0.00	0.01	0.07	3.04	0.50	47.00
2000	0.00	0.01	0.07	3.04	0.50	47.00
2500	0.00	0.01	0.07	3.03	0.50	47.00
3000	0.00	0.01	0.07	3.04	0.50	47.00
3500	0.00	0.01	0.07	3.04	0.50	47.00
4000	0.00	0.01	0.05	0.90	0.46	11.00
4500	0.00	0.01	0.05	2.76	0.50	43.00
5000	0.00	0.01	0.06	3.30	0.50	52.00
5500	0.00	0.01	0.07	3.36	0.50	53.00
6000	0.00	0.01	0.07	3.25	0.50	51.00
6500	0.00	0.01	0.07	3.20	0.50	50.00
7000	0.00	0.01	0.07	3.14	0.50	49.00
7500	0.00	0.01	0.07	3.09	0.50	48.00

Steep changes of the values of the quartiles reveal an irregular behavior of the dynamics, and reflect the presence of chaos.

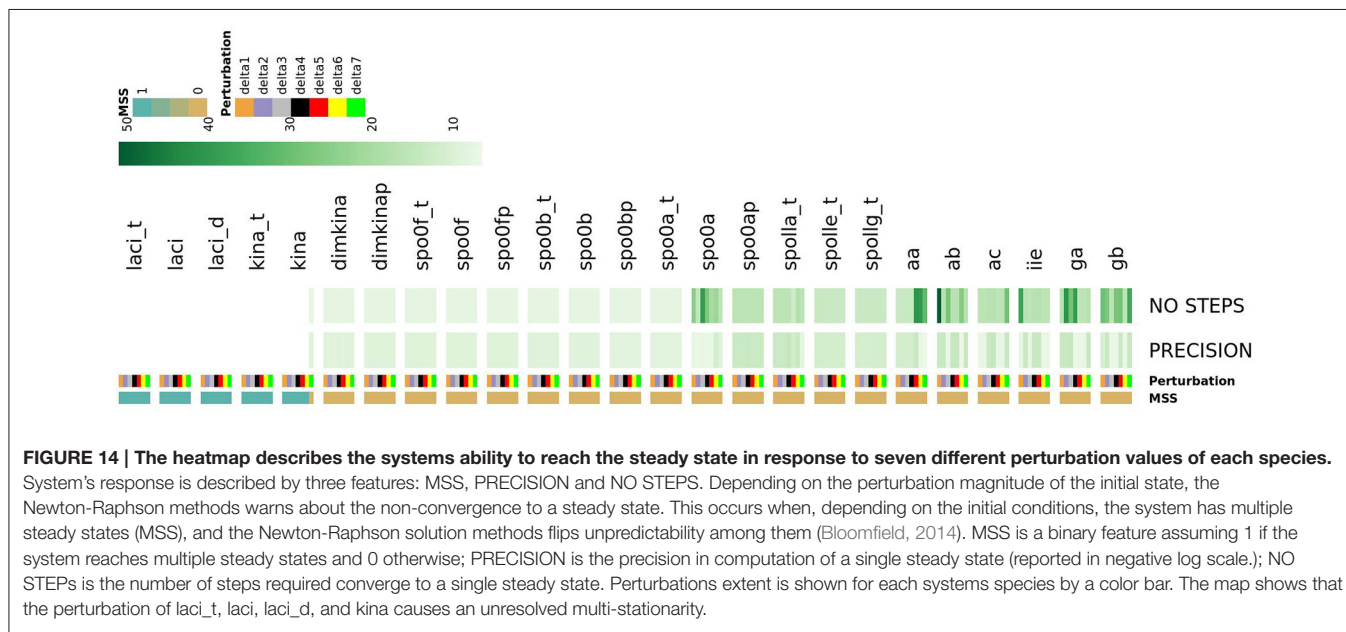
The graphs derived from the Jacobian matrix estimated at different time points are time snapshots of the interaction network of the molecular species. These graphs visualize the interactions that are active (i.e., with an edge that has a weight significantly different from zero) at a given time, and thus provide an approximate estimation and representation of the number of active degree of freedom of the system. We report in **Figures 12, 13**, the graphs obtained from the Jacobian matrices evaluated at times $t = \{0, 500\}$ s. For $t > 500$ s the variations of the Jacobian matrix are minimal and thus not shown here (in the Supplementary Material we provide the graphs for $t > 500$ s in GraphML format).

In **Table 4**, we observe a rapid increment of the edge weights from $t = 0$ to $t = 500$, than a plateau till $t = 4,000$, and then a decrement at $t = 4,000$ s. These changes reflect the changes of the topology of the network of *B. subtilis* sporulation initiation. These steep decrements and increments are expressions of a stiff and highly non linear dynamics, and in turn confirms the presence of chaos (unpredictability) in (of) it.

Sensitivity to Initial Conditions

In order to assess the existence and, eventually, the sensitivity of the steady state point in response to perturbations of the initial conditions, we introduced a set Δ of perturbations of different magnitudes: $\Delta = \{\Delta_h, h = 1, 2, \dots, 7\}$, where $\Delta_1 = 10^{-5}$ and $\Delta_{i+1} = 10\Delta_i, i = 1, 2, \dots, 6$. We perturbed the initial state of one variable at a time by Δ_h ($h = 1, 2, \dots, 7$), and calculated the steady state point with the Newton-Raphson method (Deuflhard, 2004; Bressoud, 2007), which is one of the most consolidated and efficient algorithms for finding the zeros of a function (Hoppensteadt, 1993; Ortega and Rheinboldt, 2000).

As shown in **Figure 14**, this analysis allowed detecting a number of species which, once perturbed, can cause different types of complex evolutionary trajectories from the initial state of the system. Perturbing the initial state of the



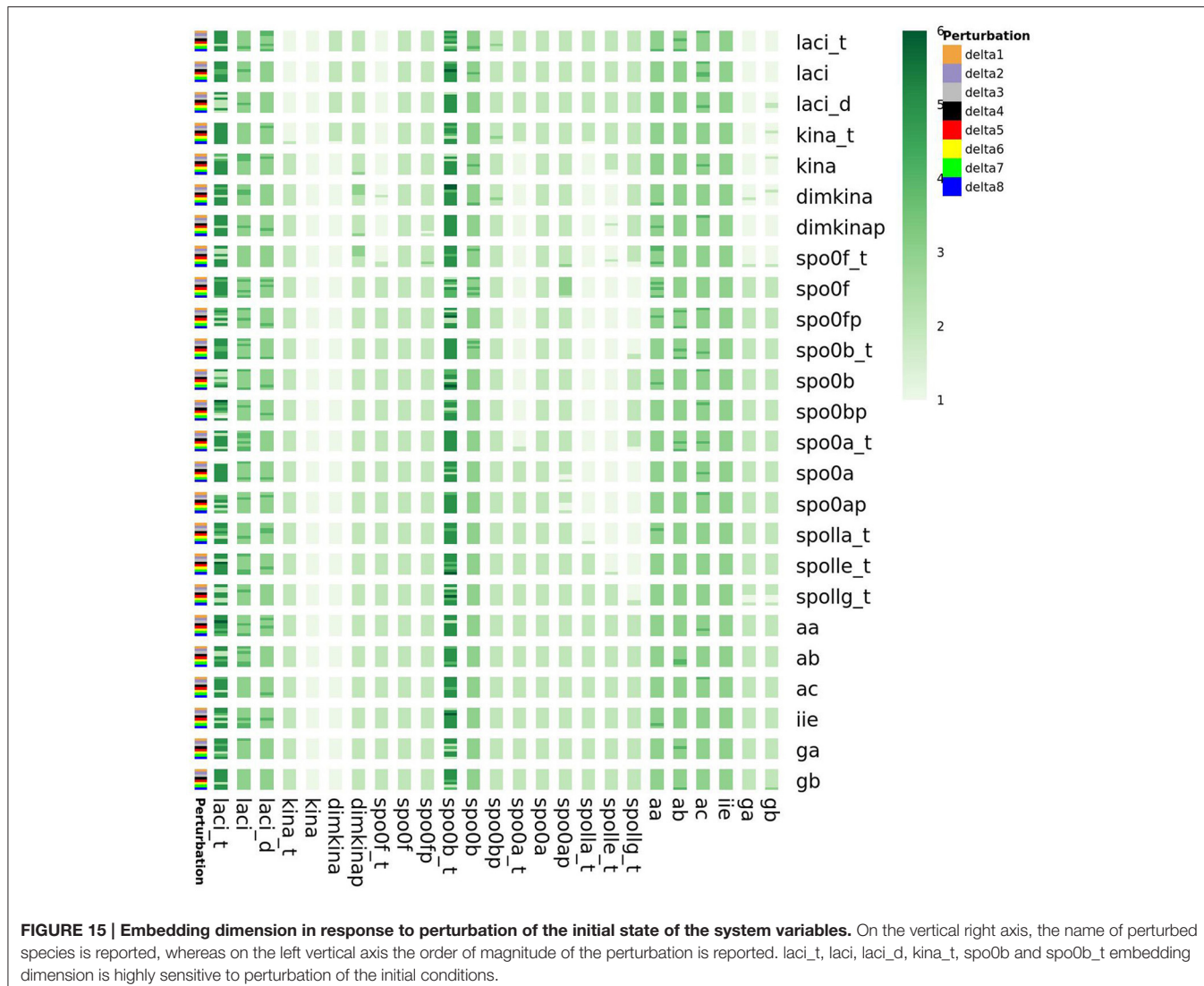


FIGURE 15 | Embedding dimension in response to perturbation of the initial state of the system variables. On the vertical right axis, the name of perturbed species is reported, whereas on the left vertical axis the order of magnitude of the perturbation is reported. *laci_t*, *laci*, *laci_d*, *kina_t*, *spo0b* and *spo0b_t* embedding dimension is highly sensitive to perturbation of the initial conditions.

laci_t, *laci*, *laci_d*, *kina_t* and *kina* species caused the most noticeable consequence, preventing the system from reaching the steady state, irrespectively of the applied perturbation extent. This finding reflects the role of the species as starters of sporulation dynamics. For another subset of species, such as *spo0a*, *aa*, *ab*, *ga*, and *gb*, perturbing the initial state caused an increase in the number of iterative steps required by the Newton-Raphson method to reach the steady state, compared to the majority of the species in the system. This effect is indicative of increased complexity in the evolving system.

Furthermore, as shown in the Supplementary Material, we also found that the perturbations of the initial state of all the species cause variations in the minimum embedding dimension of *spo0b*, and *spo0b_t*, as well as of *laci_t*, *laci*, *laci_d*, *kina_t* (**Figure 15**). Quantification of the increase in minimum embedding dimension upon perturbation of the initial state is a further indication of the high sensitivity to perturbations, for the species highlighted by the initial analysis of complexity indices,

such as *spo0b*, *spo0b_t*, and for the species emerging from the previous characterization of perturbation experiments.

Perturbations of initial conditions also cause variations of the Kaplan-Yorke ratio (i.e., $(\sum_{i=1}^j \lambda_i)/\lambda_{i+j}$, where j is the largest integer such that $\sum_{i=1}^j \lambda_i > 0$) of *spo0b_t*, *kina_t*, and *gb* and of the Kolmogorov-Sinai entropy (i.e., the sum of positive Lyapunov exponents) of *kina_t* (Figures S8–S10). Hence, by multiple analyses the system showed a highly unpredictable behavior to perturbation of the initial state, as reflected by exponentially growing separation of the trajectories as well as by the topological complexity of the time series.

CONCLUSIONS

We have presented a detailed, and original analysis of the *B. subtilis* sporulation initiation network dynamics. This analysis aimed to detect the presence of low-dimensional chaos in the dynamics of the system. Unlike more common approaches to chaos detection, this analysis includes and, is based on,

a mathematical model of the *B. subtilis* sporulation initiation dynamics. This approach allows a comprehensive explanation of the mechanisms through which those molecular species with chaotic dynamics interact with the others and propagate the effects of chaos throughout the system.

Our analysis has: (i) assessed sensitivity of the dynamics by varying the kinetic parameters and the initial state of the model to determine the dynamic control parameters and identify the most crucial molecular species; (ii) calculated the complexity indices of the time series obtained from the model, and used these to identify the drivers of chaotic dynamics, and finally, (iii) calculated the Jacobian matrix of the system of equations as a function of time to find the steady state points and their nature to give an estimate of the number of active degrees of freedom of system as function of time.

We found that the dynamics of the *B. subtilis* sporulation initiation network is affected by low-dimensional chaos and identified Spo0B as the principal driver of the chaotic dynamics in this system. Spo0B scored positive for the majority of the chaos indices. This result suggests a new role for this molecular species, which so far has received little attention, and highlights the importance of its dynamics and interactions within the network model structure. Our analysis also indicates additional experimental work that could be conducted to improve our understanding of the sporulation network and to determine the role of Spo0B. On one hand, it would be important to conduct phosphoproteomics experiments to measure the amount of phosphorylated species, for which no experimental data is yet available. On the other hand, the study of Spo0B mutated (overexpressed/silenced) strains would refine our knowledge about the dynamics of the 3-level *B. subtilis* phosphorelay and the so far elusive mechanisms that could be regulating its expression. Other molecular species that also showed positive results for the test of chaos were *spo0a*, *spo0b_t*, *laci*, and *laci_t*. These molecular species also represent the degrees of freedom that are active during most of the range of the simulated time. These species have been identified as the drivers of the chaotic dynamics of

B. subtilis sporulation initiation network model, and have an active role in determining its predictability.

One of the most challenging goal of studying a complex biological system is to control it. In this vein, our work proposes a method to identify the drivers in our *B. subtilis* sporulation initiation network on which such methods of chaos control might be applied. At the same time, our work highlights the need to investigate on these drivers and their mechanism of interaction in order to successfully implement chaos control.

AUTHOR CONTRIBUTIONS

All authors have equally contributed to the design and implementation of the mathematical analytical procedure, the discussion of the results and the writing of this paper.

FUNDING

This work was partially supported by the Biotechnology and Biological Sciences Research Council (BBSRC) Institute Strategic Programme [BB/J004529/1]: The Gut Health and Food Safety ISP.

ACKNOWLEDGMENTS

The authors gratefully acknowledge the support of the Biotechnology and Biological Sciences Research Council (BBSRC). We thank everyone at quantitative microbial risk assessment group and the Clostridium botulinum bacterial pathogens group at the IFR.

SUPPLEMENTARY MATERIAL

The Supplementary Material for this article can be found online at: <http://journal.frontiersin.org/article/10.3389/fmicb.2016.01760/full#supplementary-material>

REFERENCES

- Abarbanel, H. D. (1996). *Analysis of Observed Chaotic Data*. New York, NY: Springer-Verlag. doi: 10.1007/978-1-4612-0763-4
- Azar, A. T., and Vaidyanathan, S. (2016). *Advances in Chaos Theory and Intelligent Control*. Springer International Publishing. doi: 10.1007/978-3-319-30340-6
- Bloomfield, V. A. (2014). *Using R for Numerical Analysis in Science and Engineering*. Boca Raton, FL: CRC Press, Taylor and Francis Group.
- Bressoud, D. M. (2007). *A Radical Approach to Real Analysis*. Washington, DC: The Mathematical Association of America.
- Cao, L. (1997). Practical method for determining the minimum embedding dimension of a scalar time series. *Physica D* 110, 43–50. doi: 10.1016/S0167-2789(97)00118-8
- Carlin, F. (2011). Origin of bacterial spores contaminating foods. *Food Microbiol.* 28, 177–182. doi: 10.1016/j.fm.2010.07.008
- Cencini, M., Cecconi, F., and Vulpiani, A. (2009). *Chaos. From Simple Models to Complex Systems*. Singapore: World Scientific. doi: 10.1142/7351
- de Jong, I. G., Veening, J. W., and Kuipers, O. P. (2010). Heterochronic phosphorelay gene expression as a source of heterogeneity in *Bacillus subtilis* spore formation. *J. Bacteriol.* 192, 2053–2067. doi: 10.1128/JB.01484-09
- Deuflhard, P. (2004). *Newton Methods for Nonlinear Problems. Affine Invariance and Adaptive Algorithms*. Springer Series in Computational Mathematics. Berlin: Springer.
- Ding, M., Grebogi, C., Ott, E., Sauer, T., and Yorke, J. A. (1993). Estimating correlation dimension from a chaotic time series: when does plateau onset occur? *Physica D* 69, 404–424. doi: 10.1016/0167-2789(93)90103-8
- Eswaramoorthy, P., Guo, T., and Fujita, M. (2009). *In vivo* domain-based functional analysis of the major sporulation sensor kinase, KinA, in *Bacillus subtilis*. *J. Bacteriol.* 191, 5358–5368. doi: 10.1128/JB.00503-09
- Fawcett, P., Eichenberger, P., Losick, R., and Youngman, P. (2000). The transcriptional profile of early to middle sporulation in *Bacillus subtilis*. *Proc. Natl. Acad. Sci. U.S.A.* 97, 8063–8068. doi: 10.1073/pnas.140209597
- Fujita, M., and Losick, R. (2005). Evidence that entry into sporulation in *Bacillus subtilis* is governed by a gradual increase in the level and activity of the master regulator Spo0A. *Genes Dev.* 19, 2236–2244. doi: 10.1101/gad.1335705
- Gao, J., and Zheng, Z. (1994). Direct dynamical test for deterministic chaos. *Europhys. Lett.* 25:485. doi: 10.1209/0295-5075/25/7/002
- Gao, J. B., Hu, J., Tung, W. W., and Cao, Y. H. (2006). Distinguishing chaos from noise by scale-dependent Lyapunov exponent. *Phys. Rev. E* 74:066204. doi: 10.1103/PhysRevE.74.066204

- Higuchi, T. (1988). Approach to an irregular time series on basis of fractal dimension. *Physica D* 21, 277–283. doi: 10.1016/0167-2789(88)90081-4
- Hilborn, R. (2000). *Chaos and Nonlinear Dynamics, An Introduction for Scientists and Engineers*. Oxford: Oxford University Press.
- Hoppensteadt, F. C. (1993). *Analysis and Simulation of Chaotic Systems*. New York, NY: Springer-Verlag.
- Ihekwebe, A., Mura, I., and Barker, G. C. (2014). Computational modelling and analysis of the molecular network regulating sporulation initiation in *Bacillus subtilis*. *BMC Syst. Biol.* 8:119. doi: 10.1186/s12918-014-0119-x
- Jiang, M., Shao, W., Perego, M., and Hoch, J. A. (2000). Multiple histidine kinases regulate entry into stationary phase and sporulation in *Bacillus subtilis*. *Mol. Microbiol.* 38, 535–542. doi: 10.1046/j.1365-2958.2000.002148.x
- Kaffashia, F., Foglyanob, R., Wilsonb, C. G., and Loparao, K. A. (2008). The effect of time delay on approximate & sample entropy calculations. *Physica D* 237, 3069–3074. doi: 10.1016/j.physd.2008.06.005
- Kalitin, B. S. (2004). Lyapunov stability and orbital stability of dynamical systems. *Diff. Equat.* 40, 1096–1105. doi: 10.1023/B:DIEQ.0000049826.73745.c1
- Kaneko, K. (2006). *Life: An Introduction to Complex Systems Biology*. Berlin, Heidelberg: Springer-Verlag.
- Kaneko, K., and Tsuda, I. (2001). *Complex Systems: Chaos and Beyond. A Constructive Approach with Applications in Life Sciences*. Berlin; Heidelberg: Springer-Verlag.
- Kantz, H. (2004). *Nonlinear Time Series Analysis*. Cambridge: Cambridge University Press.
- Kellert, S. H. (1993). *In the Wake of Chaos: Unpredictable Order in Dynamical Systems*. Chicago, IL: University of Chicago Press.
- Kothamachu, V. B., Feliu, E., Wiuf, C., Cardelli, L., and Soyer, O. S. (2013). Phosphorelays provide tunable signal processing capabilities for the cell. *PLoS Comput. Biol.* 9:e1003322. doi: 10.1371/journal.pcbi.1003322
- Kuchina, A., Espinar, L., Garcia-Ojalvo, J., and Süel, G. M. (2011). Reversible and noisy progression towards a commitment point enables adaptable and reliable cellular decision-making. *PLoS Comput. Biol.* 7:e1002273. doi: 10.1371/journal.pcbi.1002273
- Lai, Y.-C. (2014). Controlling complex, non-linear dynamical networks. *Nat. Sci. Rev.* 1, 339–341. doi: 10.1093/nsr/nwu023
- Layek, G. C. (2015). *An Introduction to Dynamical Systems and Chaos*. Springer.
- Lecca, P., Re, A., Ihekwebe, A., Mura, I., and Nguyen, T.-P. (2016). *Computational Systems Biology. Inference and Modelling*. Oxford: Elsevier.
- Mao, D. (2011). *Biological Time Series Classification Via Reproducing Kernels and Sample Entropy*. Oxford: Proquest, Umi Dissertation Publishing.
- Marwan, N., Romano, M., and Thiel, M. (2016). *Recurrence Plots and Cross Recurrence Plots*. Available online at: <http://www.recurrence-plot.tk/>
- Marwan, N., Romano, M. C., Thiel, M., and Kurths, J. (2007). Recurrence plots for the analysis of complex systems. *Phys. Rep.* 438, 237–329. doi: 10.1016/j.physrep.2006.11.001
- Mera, M. E., and Morán, M. (2002). Degrees of freedom of a time series. *J. Stat. Phys.* 106, 125–145. doi: 10.1023/A:1013172129075
- Muchová, K., Lewis, R. J., Perecko, D., Brannigan, J. A., Ladds, J. C., Leech, A., et al. (2004). Dimer-induced signal propagation in Spo0A. *Mol. Microbiol.* 53, 829–842. doi: 10.1111/j.1365-2958.2004.04171.x
- Narula, J., Devi, S. N., Fujita, M., and Igoshin, O. A. (2012). Ultrasensitivity of the *Bacillus subtilis* sporulation decision. *Proc. Natl. Acad. Sci. U.S.A.* 109, E3513–E3522. doi: 10.1073/pnas.1213974109
- Ortega, J. M., and Rheinboldt, W. C. (2000). *Iterative Solution of Nonlinear Equations in Several Variables*. Philadelphia, PA: Society for Industrial and Applied Mathematics.
- Ravetti, M. G., Carpi, L. C., Goncalves, B. A., Frery, A. C., and Rosso, O. A. (2014). Distinguishing noise from chaos: objective versus subjective criteria using horizontal visibility graph. *PLoS ONE* 9:e108004. doi: 10.1371/journal.pone.0108004
- Richman, J. S., and Moorman, J. R. (2000). Physiological time-series analysis using approximate entropy and sample entropy. *Am. J. Physiol.* 278, H2039–H2049.
- Rohde, G. K. (2008). Chaotic signal detection and estimation based on attractor sets: applications to secure communications. *Chaos* 18:013114. doi: 10.1063/1.2838853
- Rosenstein, M. T., Collins, J. J., and Luca, C. J. D. (1993). A practical method for calculating largest Lyapunov exponents from small data sets. *Physica D* 65, 117–134. doi: 10.1016/0167-2789(93)90009-P
- Rosso, O. A., Larrondo, H. A., Martin, M. T., Plastino, A., and Fuentes, M. A. (2007). Distinguishing noise from chaos. *Phys. Rev. Lett.* 99:154102. doi: 10.1103/PhysRevLett.99.154102
- Satola, S., Kirchman, P. A., and Moran, C. P. (1991). Spo0A binds to a promoter used by sigma A RNA polymerase during sporulation in *Bacillus subtilis*. *Proc. Natl. Acad. Sci. U.S.A.* 88, 4533–4537. doi: 10.1073/pnas.88.10.4533
- Satola, S. W., Baldus, J. M., and Moran, C. P. (1992). Binding of Spo0A stimulates spoIIIG promoter activity in *Bacillus subtilis*. *J. Bacteriol.* 174, 1448–1453.
- Sen, S., Garcia-Ojalvo, J., and Elowitz, M. B. (2011). Dynamical consequences of bandpass feedback loops in a bacterial phosphorelay. *PLoS ONE* 6:e25102. doi: 10.1371/journal.pone.0025102
- Sinha, S. (1997). Controlling chaos in biology. *Curr. Sci. Biol.* 75, 977–983.
- Skiadas, C. H., and Skiadas, C. (2016). *Handbook of Applications of Chaos Theory*. Boca Raton, FL: Taylor and Francis Group, CRC Press.
- Skinner, J. E. (1994). Low-dimensional chaos in biological systems. *Biotechnology* 12, 596–600. doi: 10.1038/nbt0694-596
- Sokunbi, M. O. (2014). Sample entropy reveals high discriminative power between young and elderly adults in short fMRI data sets. *Front. Neuroinformatics* 8:69. doi: 10.3389/fninf.2014.00069
- Sprott, J. C. (2003). *Chaos and Time-Series Analysis*. Oxford: Oxford University Press.
- Stragier, P., and Losick, R. (1996). Molecular genetics of sporulation in *Bacillus subtilis*. *Ann. Rev. Genet.* 30, 297–241. doi: 10.1146/annurev.genet.30.1.297
- Strauch, M. A., Wu, J. J., Jonas, R. H., and Hoch, J. A. (1993). A positive feedback loop controls transcription of the spoO β gene, a component of the sporulation phosphorelay in *Bacillus subtilis*. *Mol. Microbiol.* 7, 967–974. doi: 10.1111/j.1365-2958.1993.tb01188.x
- Tamma, A., and Khubchandani, B. L. (2016). Accurate determination of time delay and embedding dimension for state space reconstruction from a scalar time series. *Chaotic Dyn.* arxiv:1605.01571v1.
- Tél, T., and Gruiz, M. (2005). *Chaotic Dynamics: An Introduction Based on Classical Mechanics*. Cambridge: Cambridge University Press.
- Theiler, J. (1990). Estimating the fractal dimension of chaotic time series. *Lincoln Lab. J.* 3, 63–86.
- Tojo, S., Hirooka, K., and Fujita, Y. (2013). Expression of kinA and kinB of *Bacillus subtilis*, necessary for sporulation initiation, is under positive stringent transcription control. *J. Bacteriol.* 195, 1656–1665. doi: 10.1128/JB.02131-12
- Vasseur, D. A. (2015). *Biological Chaos and Complex Dynamics*. Available online at: www.oxfordbibliographies.com/document/obo-9780199830060/obo-9780199830060-0024.xml
- Vishnoi, M., Narula, J., Devi, S. N., Dao, H.-A., Igoshin, O. A., and Fujita, M. (2013). Triggering sporulation in *Bacillus subtilis* with artificial two-component systems reveals the importance of proper Spo0A activation dynamics. *Mol. Microbiol.* 90, 181–194. doi: 10.1111/mmi.12357
- Vulpiani, A. (2004). *Determinismo e caos*. Roma: Carocci.
- Wang, L., Fabret, C., Kanamaru, K., Stephenson, K., Dartois, V., Perego, M., et al. (2001). Dissection of the functional and structural domains of phosphorelay histidine kinase a of *Bacillus subtilis*. *J. Bacteriol.* 183, 2795–2802.
- Weiss, J. N., Garfinkel, A., Spano, M. L., and Ditto, W. L. (1994). Chaos and chaos control in biology. *J. Clin. Invest.* 93, 1355–1360. doi: 10.1172/JCI17111
- York, K., Kenney, T. J., Satola, S., Moran, C. P., Poth, H., and Youngman, P. (1992). Spo0A controls the sigma A-dependent activation of *Bacillus subtilis* sporulation-specific transcription unit spoIIE. *J. Bacteriol.* 174, 2648–2658.
- Zeraoulia, E. (2011). *Models and Application of Chaos Theory in Modern Science*. St. Helier: Science Publisher, CRC Press.

Conflict of Interest Statement: The authors declare that the research was conducted in the absence of any commercial or financial relationships that could be construed as a potential conflict of interest.

Copyright © 2016 Lecca, Mura, Re, Barker and Ihekwebe. This is an open-access article distributed under the terms of the Creative Commons Attribution License (CC BY). The use, distribution or reproduction in other forums is permitted, provided the original author(s) or licensor are credited and that the original publication in this journal is cited, in accordance with accepted academic practice. No use, distribution or reproduction is permitted which does not comply with these terms.



Impact of Serine/Threonine Protein Kinases on the Regulation of Sporulation in *Bacillus subtilis*

Frédérique Pompeo*, Elodie Foulquier and Anne Galinier

Laboratoire de Chimie Bactérienne, CNRS, UMR 7283, Institut de Microbiologie de la Méditerranée, Aix-Marseille Université, Marseille, France

OPEN ACCESS

Edited by:

Imrich Barak,
Slovak Academy of Sciences,
Slovakia

Reviewed by:

Wiep Klaas Smits,
Leiden University Medical Center,
Netherlands
Jörg Stülke,
Georg-August-Universität Göttingen,
Germany

***Correspondence:**

Frédérique Pompeo
fpompeo@imm.cnrs.fr

Specialty section:

This article was submitted to
Microbial Physiology and Metabolism,
a section of the journal
Frontiers in Microbiology

Received: 02 March 2016

Accepted: 05 April 2016

Published: 20 April 2016

Citation:

Pompeo F, Foulquier E and Galinier A (2016) Impact of Serine/Threonine Protein Kinases on the Regulation of Sporulation in *Bacillus subtilis*. *Front. Microbiol.* 7:568.
doi: 10.3389/fmicb.2016.00568

Bacteria possess many kinases that catalyze phosphorylation of proteins on diverse amino acids including arginine, cysteine, histidine, aspartate, serine, threonine, and tyrosine. These protein kinases regulate different physiological processes in response to environmental modifications. For example, in response to nutritional stresses, the Gram-positive bacterium *Bacillus subtilis* can differentiate into an endospore; the initiation of sporulation is controlled by the master regulator SpoOA, which is activated by phosphorylation. SpoOA phosphorylation is carried out by a multi-component phosphorelay system. These phosphorylation events on histidine and aspartate residues are labile, highly dynamic and permit a temporal control of the sporulation initiation decision. More recently, another kind of phosphorylation, more stable yet still dynamic, on serine or threonine residues, was proposed to play a role in spore maintenance and spore revival. Kinases that perform these phosphorylation events mainly belong to the Hanks family and could regulate spore dormancy and spore germination. The aim of this mini review is to focus on the regulation of sporulation in *B. subtilis* by these serine and threonine phosphorylation events and the kinases catalyzing them.

Keywords: Ser/Thr protein kinases, phosphorylation, regulation, sporulation, *Bacillus subtilis*

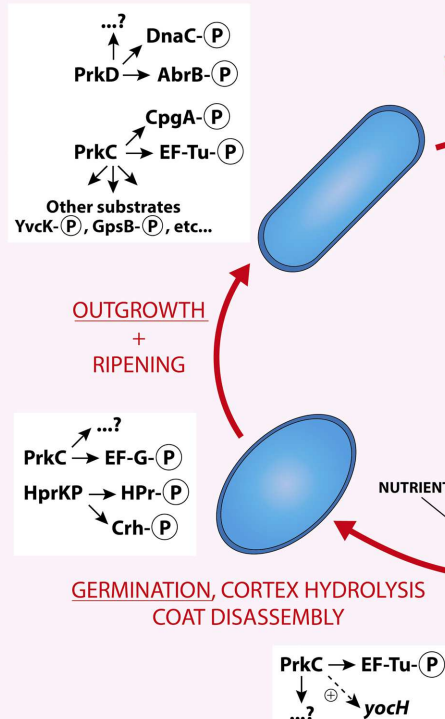
INTRODUCTION

Many Gram-positive bacteria form endospores in response to stress or nutrient limitation (Stragier and Losick, 1996; Higgins and Dworkin, 2012). Spores are morphologically distinct cells that are highly resistant to heat, chemicals, and radiation (Nicholson et al., 2000; Setlow, 2003, 2006, 2008). These dormant cells are able to reinitiate growth rapidly in response to environmental signals like amino acids or cell-wall muropeptides released by growing cells (Setlow, 2003, 2008). These processes are well regulated and orchestrated by a series of protein phosphorylation events and changes in gene expressions controlled by sigma factors (σ^E , σ^F , σ^G and σ^K). In *Bacillus subtilis*, a landmark of the initiation of sporulation is the activation of the transcriptional master regulator SpoOA. It is activated by phosphorylation through a remarkable multi-component phosphorelay system of autophosphorylating histidine kinases (KinA-KinE) (Burbulys et al., 1991; LeDeaux et al., 1995; Tan and Ramamurthi, 2014). These phosphorylations are labile and highly dynamic, thus permitting a temporal regulation of the sporulation initiation decision (De Jong et al., 2010). More recently, another kind of phosphorylation, more stable yet still dynamic, on serine or threonine residues of protein substrates, has been proposed to play a role in sporulation (Cousin et al., 2013). These phosphorylation reactions are generally catalyzed by Ser/Thr protein kinases (STPKs)

of the Hanks family (Hanks and Hunter, 1995). They seem to regulate entry into sporulation, dormancy, and spore revival. These kinases share a common fold for their cytosolic catalytic domain typically composed of 12 subdomains organized in two lobes surrounding the active site (Kornev and Taylor, 2010). In some STPKs, the kinase domain is attached to a transmembrane helix connected to an extracellular ligand binding domain responsible for kinase activation. In some, the kinase domain is connected to a transmembrane helix without any extracellular domain. In others, the kinase domain is soluble. They are themselves activated by autophosphorylation on Ser or Thr residues of their activation loop (Pereira et al., 2011). In addition, each kinase is able to phosphorylate various substrates on Ser and/or Thr residues. In *B. subtilis*, four Ser/Thr kinases of the Hanks family have been characterized to date: PrkA, PrkC, PrkD, and YabT. All of them, except PrkD, are implicated at different levels of the sporulation process: onset, dormancy, germination, and outgrowth (Figure 1) (Shah et al., 2008; Bidnenko et al., 2013; Yan et al., 2015). Several phosphoproteome studies have been performed during the last 10 years and

thanks to technical progress especially in mass spectrometry, more and more phosphorylated proteins have been identified in *B. subtilis* (Eymann et al., 2007; Macek et al., 2007; Soufi et al., 2010; Kobir et al., 2011; Ravikumar et al., 2014; Rosenberg et al., 2015). In early studies, only one experimental condition was probed. Nowadays, dynamic phosphoproteomes can be analyzed, and allow to explore several growth conditions for the same bacterial population. Furthermore, it has recently been proposed that cross-talks exist between two-component systems and STPKs as well as cross-phosphorylations among STPKs (Pereira et al., 2011; Shi et al., 2014a). This network of regulations may also be complicated by cross-talk with bacterial tyrosine kinases (BY-kinases) (Cousin et al., 2013). Such a complex regulatory network could allow quick and efficient regulation of bacterial physiology in response to the environmental variations. Broadly, the role of phosphorylation in several bacterial processes like DNA-related mechanisms, cell division and morphogenesis have been discussed recently (Garcia-Garcia et al., 2016; Manuse et al., 2016). In this review, we will specially focus on regulations mediated by STPKs during

SPORE REVIVAL



VEGETATIVE GROWTH

KinA,B,C,D → SpoOA~(P)

STARVATION

GERMINANTS

MUROPEPTIDES

NUTRIENTS

...

...

...

...

...

...

...

...

...

...

...

...

...

...

...

...

...

...

...

...

...

...

...

...

...

...

...

...

...

...

...

...

...

...

...

...

...

...

...

...

...

...

...

...

...

...

...

...

...

...

...

...

...

...

...

...

...

...

...

...

...

...

...

...

...

...

...

...

...

...

...

...

...

...

...

...

...

...

...

...

...

...

...

...

...

...

...

...

...

...

...

...

...

...

...

...

...

...

...

...

...

...

...

...

...

...

...

...

...

...

...

...

...

...

...

...

...

...

...

...

...

...

...

...

...

...

...

...

...

...

...

...

...

...

...

...

...

...

...

...

...

...

...

...

...

...

...

...

...

...

...

...

...

...

...

...

...

...

...

...

...

...

...

...

...

...

...

...

...

...

...

...

...

...

...

...

...

...

...

...

...

...

...

...

...

...

...

...

...

...

...

...

...

...

...

...

...

...

...

...

...

...

...

...

...

...

...

...

...

...

...

...

...

...

...

...

...

...

...

...

...

...

...

...

...

...

...

...

...

...

...

...

...

...

...

...

...

...

...

...

...

...

...

...

...

...

...

...

...

...

...

...

...

...

...

...

...

...

...

...

...

...

...

...

...

...

...

...

...

...

...

...

...

...

...

...

...

...

...

...

...

...

the different stages of sporulation in the model bacterium *B. subtilis*.

SPORULATION

Sporulation is a morphological differentiation event that is initiated by an asymmetric division yielding a smaller forespore and a larger mother cell (Stragier and Losick, 1996; Higgins and Dworkin, 2012). Several steps are necessary from the formation of a forespore to the release of a mature spore after lysis of the mother cell. These include engulfment, cortex synthesis and coat formation (Figure 1) in order to confer to the spore the resistance properties required to survive extreme conditions of temperature, desiccation and ionization (Setlow, 2006). This robustness is the result of several factors like dehydration, DNA compaction, and dormant metabolism (Nicholson et al., 2000; Setlow, 2007; Camp and Losick, 2009; Doan et al., 2009). As mentioned before, initiation of sporulation is controlled by a cascade of phosphorylation events catalyzed by two-component systems and eventually leading to the activation of Spo0A. When the level of Spo0A-P is sufficient (Vishnoi et al., 2013), the compartment-specific transcription factor σ^F is activated, definitely engaging the sporulating cell into a specific program of genes expression (Tan and Ramamurthi, 2014). In addition, the expression of two genes encoding the STPKs PrkA and YabT increases strongly during sporulation under the control of the spore-specific sigma factors, σ^E and σ^F , respectively (Figure 2). These two kinases have been indeed shown to participate in the regulation of several mechanisms occurring during the initiation of sporulation (Fischer et al., 1996; Bidnenko et al., 2013; Yan et al., 2015). PrkA is a STPK that only possesses a catalytical

domain and localizes in the coat of the forespore (Eichenberger et al., 2003). This protein also shows a distant homology to eukaryotic cAMP-dependent protein kinases and several essential residues of their active site are apparently conserved in PrkA. Using a *B. subtilis* crude extract, it has been proposed that PrkA phosphorylates an unidentified 60-kDa protein on Ser residue(s) (Fischer et al., 1996). However, no PrkA autophosphorylation was detected. That is surprising since STPKs generally need to be autophosphorylated to be active. However, even if the enzymatic properties of PrkA are poorly characterized, the role of this protein in sporulation seems clearly established. Actually, deletion of *prkA* gene leads to a sporulation defect corresponding to a delay in the entry into sporulation and a decrease in the number of spores. It has recently been shown that PrkA was involved in the synthesis of the σ^K transcription factor (Yan et al., 2015). Indeed, PrkA increases the expression of σ^K and its downstream target genes, by inhibiting the negative transcriptional regulator ScoC (Hpr) (Figure 1). However, the complete mechanism of regulation, potentially via the kinase activity of PrkA, is not known: how does PrkA act on ScoC? Is it a direct or indirect regulation of ScoC and does PrkA phosphorylate ScoC on Ser/Thr residue(s)? What are the exact targets of PrkA phosphorylation? Though it appears that PrkA is a key player in the regulation of sporulation in *B. subtilis*, more work needs to be done in order to completely understand the role of this putative STPK. The second regulatory protein YabT is a STPK containing three domains: a transmembrane region, a kinase domain and a DNA-binding domain. YabT kinase activity has been clearly established and targets of YabT have been identified. Binding of YabT to DNA activates its kinase activity; YabT is then able to autophosphorylate and to phosphorylate exogenous substrates (Bidnenko et al., 2013). It colocalizes with

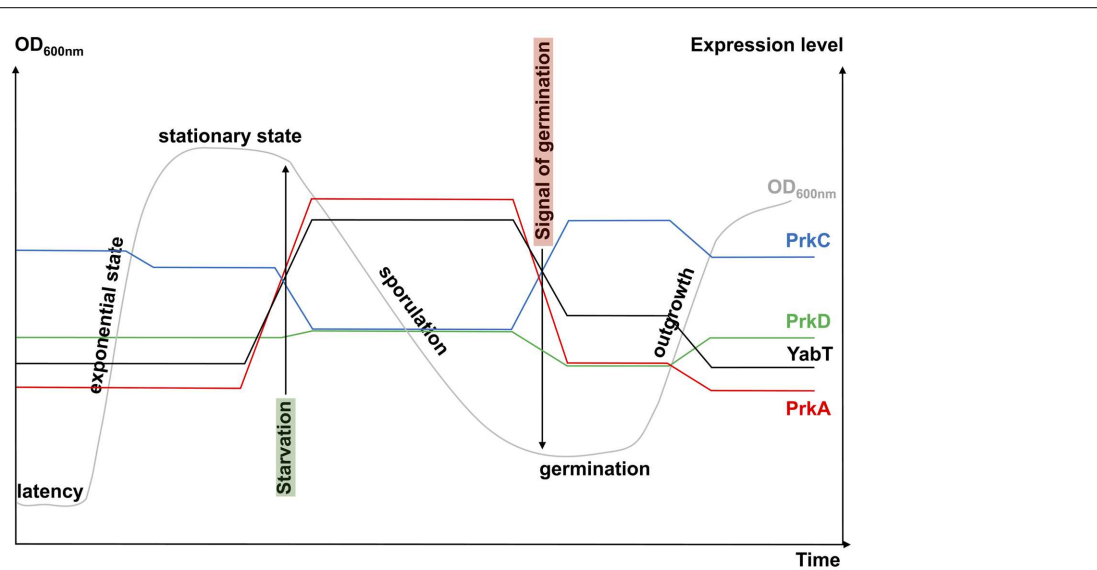


FIGURE 2 | Schematic view of STPK gene expression during growth. The growth curve of a *B. subtilis* cell culture in rich medium is presented in gray ($OD_{600\text{ nm}}$). The levels of kinase gene expression are obtained from <http://subtiwiki.uni-goettingen.de/> (Michna et al., 2016) and from Nicolas et al. (2012). They are presented in color: blue for *prkC*, green for *prkD*, red for *prkA*, and black for *yabT*. Signals for starvation (highlighted in green) and germination (highlighted in red) are indicated by arrows.

the septal inner membrane separating the forespore from the mother cell. As for *prkA*, deletion of the *yabT* gene leads to a sporulation delay. Furthermore, resistance to DNA damages decreases in the *yabT* mutant spores. Both phenotypes were also observed in a *recA* mutant (Shafikhani et al., 2004; Bidnenko et al., 2013). The recombinase RecA is actually a YabT substrate *in vitro* (phosphorylation on Ser2) and consistently, RecA was previously identified in a phosphoproteome study revealing the same phosphorylated residue (Soufi et al., 2010). It is, therefore, likely that YabT regulates RecA activity in the forespore in order to allow DNA damage repair before nucleoid compaction in the spore (Sciochetti et al., 2001). Similarities between the bacterial STPK YabT and the eukaryotic STPKs C-Abl and Mec1 have been found: all these kinases are activated by DNA and phosphorylate proteins involved in DNA damage repair mechanisms (Bidnenko et al., 2013). *In vitro*, YabT is able to phosphorylate RacA, another DNA-related protein involved in DNA anchoring to the cell pole (Ben-Yehuda et al., 2003; Shi et al., 2014b). RacA can be dephosphorylated *in vitro* by SpoIIE, a serine protein phosphatase known to modulate the phosphorylation state of the anti-anti α^F factor SpoIIAA (Arigoni et al., 1996). Interestingly, YabT and SpoIIE have been found associated to the same protein partners in a recent yeast two-hybrid screen suggesting that they function as a kinase/phosphatase couple during sporulation (Shi et al., 2014b). Another potential substrate of YabT is the global transcriptional regulator AbrB which is phosphorylated on Ser86 *in vivo* (Figure 1) (Soufi et al., 2010) as well as *in vitro* by YabT, PrkC and PrkD (Kobir et al., 2014). AbrB is a global gene regulator involved in transition phases (i.e., from exponential to stationary growth phase) that also antagonizes sporulation by repressing the expression of Spo0A (Phillips and Strauch, 2002). It has been proposed that AbrB phosphorylation serves as an additional input for a subtle control of AbrB activity. Indeed, AbrB phosphorylation inhibits its ability to bind its DNA targets (Kobir et al., 2014). In addition, a strain expressing phosphomimetic AbrB produces fewer spores and sporulates much slower. Because the YabT kinase is produced just after the onset of sporulation, it is the best candidate for AbrB phosphorylation in sporulation conditions.

DORMANCY

It is commonly accepted that when the mature spore is released by the mother cell, it is metabolically dormant and environmentally resistant. The spore is protected by thick layers: the cortex and the coat, and contains a high level of dipicolinic acid (DPA) and a low amount of water. However, it has been recently shown that the spore RNA profile is highly dynamic a few days following sporulation (Segev et al., 2012). During this short period, spores are responsive to environmental changes and can adapt their RNA content consequently. Furthermore, some enzymatic activities necessary for full maturation of coat proteins have been described in spores (Zilhão et al., 2005; Sanchez-Salas et al., 2011). Taking these observations into account, it is possible to consider that regulation of enzymatic activities or protein synthesis by phosphorylation reactions exist in spore

during this adaptive period. For example, the overall metabolism is down regulated, in particular protein synthesis, which is an energy-intensive cellular process. This regulation is mediated by phosphorylation of the elongation factor Tu (EF-Tu). Indeed, phosphorylated EF-Tu is unable to hydrolyze GTP and remains bound to the ribosome which leads to a dominant-negative effect in elongation, thus inhibiting protein synthesis (Pereira et al., 2015). It has been proposed that the kinase involved in this phosphorylation is YabT because it is present in the spore during dormancy and it is able to phosphorylate EF-Tu *in vitro* on Thr63. *In vivo* experiments confirmed that YabT is responsible of EF-Tu phosphorylation in the spore since no phosphorylated EF-Tu was found in a *yabT* mutant (Figure 1) (Pereira et al., 2015). Moreover, *in vitro* phosphorylation of EF-Tu by PrkC was previously reported on Thr384 but the *in vivo* regulatory function of this phosphorylation has not been accounted for so far (Absalon et al., 2009).

GERMINATION AND OUTGROWTH

Spores of *B. subtilis* can remain dormant for years but return to life quickly after exposure to nutrients or muropeptides (Setlow, 2003, 2008, 2014). Specific receptors (including GerA, GerB, and GerK) that detect nutrients have been known for years (Atluri et al., 2006; Ramirez-Peralta et al., 2013). More recently, in the inner spore membrane, the STPK PrkC has been shown to bind muropeptides released by growing cells thus inducing germination (Shah et al., 2008). Spores can also reinitiate growth stochastically at a low frequency due to phenotypic variations in individual spore (Sturm and Dworkin, 2015). The revival process (Figure 1) can be divided into three consecutive phases: (i) germination with spore rehydration, release of DPA, cortex hydrolysis, and coat disassembly, then (ii) a ripening period with no morphological changes but a molecular reorganization of the cell, and finally (iii) outgrowth with synthesis of macromolecules, membrane elongation, and cell division (Sinai et al., 2015). However, it seems that synthesis of proteins might start earlier, as early as 30 min after the initiation of germination. Up to 650 new proteins are synthesized during the three steps described above (Sinai et al., 2015). A dynamic phosphoproteome of reviving spores established a functional connection between Ser/Thr/Tyr-phosphorylation and progression of this process (Rosenberg et al., 2015). Though it was proposed that the STPK PrkC, and, therefore, phosphorylation of PrkC protein substrates, stimulates germination only in the presence of muropeptides as germinant (Shah et al., 2008), this phosphoproteome analysis was only done in the presence of L-Ala as germinant. It will be interesting to perform the same study using muropeptides as germinant to compare the profile of phosphorylated proteins identified. Nevertheless, the high number of new phosphoproteins already characterized (Rosenberg et al., 2015) suggests an important modulation of protein activity during this cellular transition to vegetative growth. The phosphoproteins identified are involved in spore-specific functions, transcription, metabolism, and stress response, some of which are probably phosphorylated by STPKs. YabT and PrkA are highly synthesized during sporulation

whereas PrkC is more expressed during germination (**Figure 2**). However, these three kinases and possibly other still unknown protein kinases (with weak homology to classical STPK) could contribute to these regulatory mechanisms. PrkC is a transmembrane protein composed of an intracellular catalytic domain and an extracellular regulatory C-terminal region containing several beta-lactam-binding domains. These PASTA domains (for penicillin-binding protein and serine/threonine kinase-associated domains) are predicted to interact with the peptidoglycan (PG) (Yeats et al., 2002). Biochemical studies of PrkC homologues confirmed the *in vitro* interaction between PG fragments and PrkC (Mir et al., 2011; Ruggiero et al., 2011; Squeglia et al., 2011). Thus, binding of PG fragments released from growing cells to the extracellular domain of PrkC could stimulate PrkC kinase activity to induce the germination of the spore (**Figure 1**) (Shah et al., 2008). The *prkC* gene expression is low during sporulation and stimulated during germination but its expression level during vegetative growth and especially during stationary phase is not negligible (**Figure 2**). Hence, PrkC can phosphorylate several substrates produced during vegetative growth or sporulation and, up to now, more than 10 substrates of PrkC have been identified *in vitro*. These targets include proteins of carbon metabolism (Pietack et al., 2010) or proteins involved in protein synthesis like CpgA, a GTPase involved in a late stage of ribosome assembly, and the elongation factors EF-G and EF-Tu (Shah et al., 2008; Absalon et al., 2009; Pompeo et al., 2012). It has been proposed that PrkC phosphorylates EF-G in the spore to allow re-initiation of protein synthesis. But, it is unlikely that this phosphorylation is the only cause of germination. PrkC also promotes the expression of *yocH*, a muralytic enzyme encoding gene. YocH is exported and digests the PG of other growing bacteria, thus producing more muropeptides that in turn stimulate germination (Shah and Dworkin, 2010; Libby et al., 2015). Moreover, the phosphorylation of several proteins has been shown to be important for germination. These include the spore specific proteins SspA et SspB involved in DNA protection, the ribosomal protein RpsJ, the elongation factors EF-Tu and EF-G, and the phosphocarrier protein HPr (Rosenberg et al., 2015). But, for many of them, the kinase that catalyzes their phosphorylation is still unknown. In the particular case of HPr, which is a component of the phosphoenolpyruvate-dependent sugar system (PTS) and a key player of carbon catabolite regulation in *B. subtilis*, phosphorylation is catalyzed by HprK/P, an atypical ATP-dependent kinase/phosphorylase. This enzyme does not share homology with eukaryotic STPKs and does not belong to the Hanks kinase family. Instead, it shares limited homology with the phosphoenolpyruvate carboxykinase (Galinier et al., 2002). It does not autophosphorylate but phosphorylates two protein substrates, HPr and its homologue Crh, on the Ser46 residue (Galinier et al., 1997, 1998). HprK/P is stimulated by phosphorylated sugars like glucose 6-phosphate or fructose 1,6-bisphosphate (Jault et al., 2000) for the regulation of carbohydrate utilization (Galinier et al., 1998; Martin-Verstraete et al., 1999). However, during spore revival, it may be activated in the presence of alternative PTS sugars (Rosenberg et al., 2015). In addition, strains producing some HPr mutant proteins on the Ser46 phosphorylation site (both phosphoablati-

and phosphomimetic mutants) exhibited reduced sporulation efficiency (Rosenberg et al., 2015). These results indicate that the phosphorylation level of HPr is important for spore revival. This is not surprising since optimal carbon utilization needs to take place rapidly upon revival. Therefore, the regulation of spore revival by phosphorylation on Ser and Thr residues is an important mechanism that can be mediated by several types of kinases like STPKs and HprK/P, or even other atypical protein kinases not yet identified. This network of regulations may also be complicated by cross-talk with other phosphorylation systems like BY-kinases (Cousin et al., 2013), two-component systems, or recently identified Arg phosphorylations (Elsholz et al., 2012; Schmidt et al., 2014).

CONCLUSION

It is now widely accepted that regulatory Ser/Thr phosphorylation is as present in prokaryotes as in eukaryotes and that enzymes responsible for these modifications are mainly eukaryotic-like Ser/Thr kinases. To date, four of these proteins have been characterized in *B. subtilis* (PrkA, PrkC, PrkD, and YabT) and several examples highlight their regulatory role in cellular physiology during vegetative growth as well as during sporulation. In this mini review, we focused on their regulatory functions in spores and showed that STPKs have relaxed substrate selectivity that confers to the cell a quick way to adapt to the physiological conditions. Taking into account that cross-phosphorylation events occur among STPKs, BY-kinases, and two-component systems, the regulatory network controlling a spore life is highly dynamic and sophisticated. Given the role of spores in many diseases, understanding mechanisms and regulation of spore formation and spore germination has long been a researcher's interest in order to find a way to get rid of them more efficiently. However, a new interest has now emerged with the use of spores as a tool in biotechnology (Isticato and Ricca, 2014).

AUTHOR CONTRIBUTIONS

All authors listed, have made substantial, direct and intellectual contribution to the work, and approved it for publication.

FUNDING

This research was supported by the CNRS, the ANR (ANR-12-BSV3-0008-01), and Aix-Marseille University.

ACKNOWLEDGMENTS

We thank J.R. Fantino for drawings with Adobe Illustrator and T. Doan for critical reading of the manuscript. We thank B. Khadaroo and the reviewers for English proofreading.

REFERENCES

- Absalon, C., Obuchowski, M., Madec, E., Delattre, D., Holland, I. B., and Seror, S. J. (2009). CpgA, EF-Tu and the stressosome protein YezB are substrates of the Ser/Thr kinase/phosphatase couple, PrkC/PrpC, in *Bacillus subtilis*. *Microbiology* 155, 932–943. doi: 10.1099/mic.0.022475-0
- Arigoni, F., Duncan, L., Alper, S., Losick, R., and Stragier, P. (1996). SpoIIIE governs the phosphorylation state of a protein regulating transcription factor sigma F during sporulation in *Bacillus subtilis*. *Proc. Natl. Acad. Sci. U.S.A.* 93, 3238–3242. doi: 10.1073/pnas.93.8.3238
- Atluri, S., Ragkousi, K., Cortezzo, D. E., and Setlow, P. (2006). Cooperativity between different nutrient receptors in germination of spores of *Bacillus subtilis* and reduction of this cooperativity by alterations in the GerB receptor. *J. Bacteriol.* 188, 28–36. doi: 10.1128/JB.188.1.28-36.2006
- Ben-Yehuda, S., Rudner, D. Z., and Losick, R. (2003). RacA, a bacterial protein that anchors chromosomes to the cell poles. *Science* 299, 532–536. doi: 10.1126/science.1079914
- Bidnenko, V., Shi, L., Kobir, A., Ventroux, M., Pigeonneau, N., Henry, C., et al. (2013). *Bacillus subtilis* serine/threonine protein kinase YabT is involved in spore development via phosphorylation of a bacterial recombinase. *Mol. Microbiol.* 88, 921–935. doi: 10.1111/mmi.12233
- Burbulya, D., Trach, K. A., and Hoch, J. A. (1991). Initiation of sporulation in *B. subtilis* is controlled by a multicomponent phosphorelay. *Cell* 64, 545–552. doi: 10.1016/0092-8674(91)90238-T
- Camp, A. H., and Losick, R. (2009). A feeding tube model for activation of a cell-specific transcription factor during sporulation in *Bacillus subtilis*. *Genes Dev.* 23, 1014–1024. doi: 10.1101/gad.1781709
- Cousin, C., Derouiche, A., Shi, L., Pagot, Y., Poncet, S., and Mijakovic, I. (2013). Protein-serine/threonine/tyrosine kinases in bacterial signaling and regulation. *FEMS Microbiol. Lett.* 346, 11–19. doi: 10.1111/1574-6968.12189
- De Jong, I. G., Veening, J. W., and Kuipers, O. P. (2010). Heterochronic phosphorelay gene expression as a source of heterogeneity in *Bacillus subtilis* spore formation. *J. Bacteriol.* 192, 2053–2067. doi: 10.1128/JB.01484-09
- Doan, T., Morlot, C., Meisner, J., Serrano, M., Henriques, A. O., Moran, C. P., et al. (2009). Novel secretion apparatus maintains spore integrity and developmental gene expression in *Bacillus subtilis*. *PLoS Genet.* 5:e1000566. doi: 10.1371/journal.pgen.1000566
- Eichenberger, P., Jensen, S. T., Conlon, E. M., Van Ooi, C., Silvaggi, J., González-Pastor, J. E., et al. (2003). The sigmaE regulon and the identification of additional sporulation genes in *Bacillus subtilis*. *J. Mol. Biol.* 327, 945–972. doi: 10.1016/S0022-2836(03)00205-5
- Elsholz, A. K., Turgay, K., Michalik, S., Hessling, B., Gronau, K., Oertel, D., et al. (2012). Global impact of protein arginine phosphorylation on the physiology of *Bacillus subtilis*. *Proc. Natl. Acad. Sci. U.S.A.* 109, 7451–7456. doi: 10.1073/pnas.1117483109
- Eymann, C., Becher, D., Bernhardt, J., Gronau, K., Klutzy, A., and Hecker, M. (2007). Dynamics of protein phosphorylation on Ser/Thr/Tyr in *Bacillus subtilis*. *Proteomics* 7, 3509–3526. doi: 10.1002/pmic.200700232
- Fischer, C., Geourjon, C., Bourson, C., and Deutscher, J. (1996). Cloning and characterization of the *Bacillus subtilis* prkA gene encoding a novel serine protein kinase. *Gene* 168, 55–60. doi: 10.1016/0378-1119(95)00758-X
- Foulquier, E., Pompeo, F., Freton, C., Cordier, B., Grangeasse, C., and Galinier, A. (2014). PrkC-mediated phosphorylation of overexpressed YvcK protein regulates PBP1 protein localization in *Bacillus subtilis* mreB mutant cells. *J. Biol. Chem.* 289, 23662–23669. doi: 10.1074/jbc.M114.562496
- Galinier, A., Haiech, J., Kilhoffer, M. C., Jaquinod, M., Stulke, J., Deutscher, J., et al. (1997). The *Bacillus subtilis* crh gene encodes a HPr-like protein involved in carbon catabolite repression. *Proc. Natl. Acad. Sci. U.S.A.* 94, 8439–8444. doi: 10.1073/pnas.94.16.8439
- Galinier, A., Kravanja, M., Engelmann, R., Hengstenberg, W., Kilhoffer, M. C., Deutscher, J., et al. (1998). New protein kinase and protein phosphatase families mediate signal transduction in bacterial catabolite repression. *Proc. Natl. Acad. Sci. U.S.A.* 95, 1823–1828. doi: 10.1073/pnas.95.4.1823
- Galinier, A., Lavergne, J. P., Geourjon, C., Fieulaine, S., Nessler, S., and Jault, J. M. (2002). A new family of phosphotransferases with a P-loop motif. *J. Biol. Chem.* 277, 11362–11367. doi: 10.1074/jbc.M109527200
- Garcia-Garcia, T., Poncet, S., Derouiche, A., Shi, L., Mijakovic, I., and Noirot-Gros, M. F. (2016). Role of protein phosphorylation in the regulation of cell cycle and DNA-related processes in bacteria. *Front. Microbiol.* 7:184. doi: 10.3389/fmicb.2016.00184
- Hanks, S. K., and Hunter, T. (1995). Protein kinases 6. The eukaryotic protein kinase superfamily: kinase (catalytic) domain structure and classification. *FASEB J.* 9, 576–596. doi: 10.1016/B978-012324719-3/50003-0
- Higgins, D., and Dworkin, J. (2012). Recent progress in *Bacillus subtilis* sporulation. *FEMS Microbiol. Rev.* 36, 131–148. doi: 10.1111/j.1574-6976.2011.00310.x
- Isticato, R., and Ricca, E. (2014). Spore surface display. *Microbiol. Spectr.* 2, 1–15. doi: 10.1128/microbiolspec.TBS-0011-2012
- Jault, J. M., Fieulaine, S., Nessler, S., Gonzalo, P., Di Pietro, A., Deutscher, J., et al. (2000). The HPr kinase from *Bacillus subtilis* is a homo-oligomeric enzyme which exhibits strong positive cooperativity for nucleotide and fructose 1,6-bisphosphate binding. *J. Biol. Chem.* 275, 1773–1780. doi: 10.1074/jbc.275.3.1773
- Kobir, A., Poncet, S., Bidnenko, V., Delumeau, O., Jers, C., Zouhir, S., et al. (2014). Phosphorylation of *Bacillus subtilis* gene regulator AbrB modulates its DNA-binding properties. *Mol. Microbiol.* 92, 1129–1141. doi: 10.1111/mmi.12617
- Kobir, A., Shi, L., Boskovic, A., Grangeasse, C., Franjevic, D., and Mijakovic, I. (2011). Protein phosphorylation in bacterial signal transduction. *Biochim. Biophys. Acta* 1810, 989–994. doi: 10.1016/j.bbagen.2011.01.006
- Kornev, A. P., and Taylor, S. S. (2010). Defining the conserved internal architecture of a protein kinase. *Biochim. Biophys. Acta* 1804, 440–444. doi: 10.1016/j.bbapap.2009.10.017
- LeDeaux, J. R., Yu, N., and Grossman, A. D. (1995). Different roles for KinA, KinB, and KinC in the initiation of sporulation in *Bacillus subtilis*. *J. Bacteriol.* 177, 861–863.
- Libby, E. A., Goss, L. A., and Dworkin, J. (2015). The eukaryotic-like Ser/Thr Kinase PrkC regulates the essential WalRK two-component system in *Bacillus subtilis*. *PLoS Genet.* 11:e1005275. doi: 10.1371/journal.pgen.1005275
- Macek, B., Mijakovic, I., Olsen, J. V., Gnäd, F., Kumar, C., Jensen, P. R., et al. (2007). The serine/threonine/tyrosine phosphoproteome of the model bacterium *Bacillus subtilis*. *Mol. Cell Proteomics* 6, 697–707. doi: 10.1074/mcp.M600464-MCP200
- Manuse, S., Fleurie, A., Zucchini, L., Lesterlin, C., and Grangeasse, C. (2016). Role of eukaryotic-like serine/threonine kinases in bacterial cell division and morphogenesis. *FEMS Microbiol. Rev.* 40, 41–56. doi: 10.1093/femsre/fuv041
- Martin-Verstraete, I., Deutscher, J., and Galinier, A. (1999). Phosphorylation of HPr and Crh by HprK, early steps in the catabolite repression signalling pathway for the *Bacillus subtilis* levanase operon. *J. Bacteriol.* 181, 2966–2969.
- Michna, R. H., Zhu, B., Mäder, U., and Stölke, J. (2016). SubtiWiki 2.0—an integrated database for the model organism *Bacillus subtilis*. *Nucleic Acids Res.* 44, D654–D662. doi: 10.1093/nar/gkv1006
- Mir, M., Asong, J., Li, X., Cardot, J., Boons, G. J., and Husson, R. N. (2011). The extracytoplasmic domain of the *Mycobacterium tuberculosis* Ser/Thr kinase PknB binds specific muropeptides and is required for PknB localization. *PLoS Pathog.* 7:e1002182. doi: 10.1371/journal.ppat.1002182
- Nicholson, W. L., Munakata, N., Horneck, G., Melosh, H. J., and Setlow, P. (2000). Resistance of *Bacillus endospores* to extreme terrestrial and extraterrestrial environments. *Microbiol. Mol. Biol. Rev.* 64, 548–572. doi: 10.1128/MMBR.64.3.548-572.2000
- Nicolas, P., Mäder, U., Dervyn, E., Rochat, T., Leduc, A., Pigeonneau, N., et al. (2012). Condition-dependent transcriptome reveals high-level regulatory architecture in *Bacillus subtilis*. *Science* 335, 1103–1106. doi: 10.1126/science.1206848
- Pereira, S. F., Gonzalez, R. L., and Dworkin, J. (2015). Protein synthesis during cellular quiescence is inhibited by phosphorylation of a translational elongation factor. *Proc. Natl. Acad. Sci. U.S.A.* 112, E3274–E3281. doi: 10.1073/pnas.1505297112
- Pereira, S. F., Goss, L., and Dworkin, J. (2011). Eukaryote-like serine/threonine kinases and phosphatases in bacteria. *Microbiol. Mol. Biol. Rev.* 75, 192–212. doi: 10.1128/MMBR.00042-10
- Phillips, Z. E., and Strauch, M. A. (2002). *Bacillus subtilis* sporulation and stationary phase gene expression. *Cell Mol. Life Sci.* 59, 392–402. doi: 10.1007/s00018-002-8431-9
- Pietack, N., Becher, D., Schmidl, S. R., Saier, M. H., Hecker, M., Commichau, F. M., et al. (2010). In vitro phosphorylation of key metabolic enzymes from *Bacillus subtilis*: PrkC phosphorylates enzymes from different branches of basic metabolism. *J. Mol. Microbiol. Biotechnol.* 18, 129–140. doi: 10.1159/000308512

- Pompeo, F., Foulquier, E., Serrano, B., Grangeasse, C., and Galinier, A. (2015). Phosphorylation of the cell division protein GpsB regulates PrkC kinase activity through a negative feedback loop in *Bacillus subtilis*. *Mol. Microbiol.* 97, 139–150. doi: 10.1111/mmi.13015
- Pompeo, F., Freton, C., Wicker-Planquart, C., Grangeasse, C., Jault, J. M., and Galinier, A. (2012). Phosphorylation of CpgA protein enhances both its GTPase activity and its affinity for ribosome and is crucial for *Bacillus subtilis* growth and morphology. *J. Biol. Chem.* 287, 20830–20838. doi: 10.1074/jbc.M112.340331
- Ramirez-Peralta, A., Gupta, S., Butzin, X. Y., Setlow, B., Korza, G., Leyva-Vazquez, M. A., et al. (2013). Identification of new proteins that modulate the germination of spores of *Bacillus* species. *J. Bacteriol.* 195, 3009–3021. doi: 10.1128/JB.00257-13
- Ravikumar, V., Shi, L., Krug, K., Derouiche, A., Jers, C., Cousin, C., et al. (2014). Quantitative phosphoproteome analysis of *Bacillus subtilis* reveals novel substrates of the kinase PrkC and phosphatase PppC. *Mol. Cell Proteomics* 13, 1965–1978. doi: 10.1074/mcp.M113.035949
- Rosenberg, A., Soufi, B., Ravikumar, V., Soares, N. C., Krug, K., Smith, Y., et al. (2015). Phosphoproteome dynamics mediate revival of bacterial spores. *BMC Biol.* 13:76. doi: 10.1186/s12915-015-0184-7
- Ruggiero, A., Squeglia, F., Marasco, D., Marchetti, R., Molinaro, A., and Berisio, R. (2011). X-ray structural studies of the entire extracellular region of the serine/threonine kinase PrkC from *Staphylococcus aureus*. *Biochem. J.* 435, 33–41. doi: 10.1042/BJ20101643
- Sanchez-Salas, J. L., Setlow, B., Zhang, P., Li, Y. Q., and Setlow, P. (2011). Maturation of released spores is necessary for acquisition of full spore heat resistance during *Bacillus subtilis* sporulation. *Appl. Environ. Microbiol.* 77, 6746–6754. doi: 10.1128/AEM.05031-11
- Schmidt, A., Trentini, D. B., Spiess, S., Fuhrmann, J., Ammerer, G., Mechtler, K., et al. (2014). Quantitative phosphoproteomics reveals the role of protein arginine phosphorylation in the bacterial stress response. *Mol. Cell Proteomics* 13, 537–550. doi: 10.1074/mcp.M113.032292
- Sciochetti, S. A., Blakely, G. W., and Piggot, P. J. (2001). Growth phase variation in cell and nucleoid morphology in a *Bacillus subtilis* recA mutant. *J. Bacteriol.* 183, 2963–2968. doi: 10.1128/JB.183.9.2963-2968.2001
- Segev, E., Smith, Y., and Ben-Yehuda, S. (2012). RNA dynamics in aging bacterial spores. *Cell* 148, 139–149. doi: 10.1016/j.cell.2011.11.059
- Setlow, P. (2003). Spore germination. *Curr. Opin. Microbiol.* 6, 550–556. doi: 10.1016/j.mib.2003.10.001
- Setlow, P. (2006). Spores of *Bacillus subtilis*: their resistance to and killing by radiation, heat and chemicals. *J. Appl. Microbiol.* 101, 514–525. doi: 10.1111/j.1365-2672.2005.02736.x
- Setlow, P. (2007). I will survive: DNA protection in bacterial spores. *Trends Microbiol.* 15, 172–180. doi: 10.1016/j.tim.2007.02.004
- Setlow, P. (2008). Dormant spores receive an unexpected wake-up call. *Cell* 135, 410–412. doi: 10.1016/j.cell.2008.10.006
- Setlow, P. (2014). Germination of spores of *Bacillus* species: what we know and do not know. *J. Bacteriol.* 196, 1297–1305. doi: 10.1128/JB.01455-13
- Shafikhani, S. H., Núñez, E., and Leighton, T. (2004). Hpr (ScoC) and the phosphorelay couple cell cycle and sporulation in *Bacillus subtilis*. *FEMS Microbiol. Lett.* 231, 99–110. doi: 10.1016/S0378-1097(03)00936-4
- Shah, I. M., and Dworkin, J. (2010). Induction and regulation of a secreted peptidoglycan hydrolase by a membrane Ser/Thr kinase that detects muropeptides. *Mol. Microbiol.* 75, 1232–1243. doi: 10.1111/j.1365-2958.2010.07046.x
- Shah, I. M., Laaberki, M. H., Popham, D. L., and Dworkin, J. (2008). A eukaryotic-like Ser/Thr kinase signals bacteria to exit dormancy in response to peptidoglycan fragments. *Cell* 135, 486–496. doi: 10.1016/j.cell.2008.08.039
- Shi, L., Pigeonneau, N., Ravikumar, V., Dobrinic, P., Macek, B., Franjevic, D., et al. (2014a). Cross-phosphorylation of bacterial serine/threonine and tyrosine protein kinases on key regulatory residues. *Front. Microbiol.* 5:495. doi: 10.3389/fmicb.2014.00495
- Shi, L., Pigeonneau, N., Ventroux, M., Derouiche, A., Bidnenko, V., Mijakovic, I., et al. (2014b). Protein-tyrosine phosphorylation interaction network in *Bacillus subtilis* reveals new substrates, kinase activators and kinase cross-talk. *Front. Microbiol.* 5:538. doi: 10.3389/fmicb.2014.00538
- Sinai, L., Rosenberg, A., Smith, Y., Segev, E., and Ben-Yehuda, S. (2015). The molecular timeline of a reviving bacterial spore. *Mol. Cell* 57, 695–707. doi: 10.1016/j.molcel.2014.12.019
- Soufi, B., Kumar, C., Gnad, F., Mann, M., Mijakovic, I., and Macek, B. (2010). Stable isotope labeling by amino acids in cell culture (SILAC) applied to quantitative proteomics of *Bacillus subtilis*. *J. Proteome Res.* 9, 3638–3646. doi: 10.1021/pr100150w
- Squeglia, F., Marchetti, R., Ruggiero, A., Lanzetta, R., Marasco, D., Dworkin, J., et al. (2011). Chemical basis of peptidoglycan discrimination by PrkC, a key kinase involved in bacterial resuscitation from dormancy. *J. Am. Chem. Soc.* 133, 20676–20679. doi: 10.1021/ja208080r
- Stragier, P., and Losick, R. (1996). Molecular genetics of sporulation in *Bacillus subtilis*. *Annu. Rev. Genet.* 30, 297–341. doi: 10.1146/annurev.genet.30.1.297
- Sturm, A., and Dworkin, J. (2015). Phenotypic diversity as a mechanism to exit cellular dormancy. *Curr. Biol.* 25, 2272–2277. doi: 10.1016/j.cub.2015.07.018
- Tan, I. S., and Ramamurthi, K. S. (2014). Spore formation in *Bacillus subtilis*. *Environ. Microbiol. Rep.* 6, 212–225. doi: 10.1111/1758-2229.12130
- Vishnoi, M., Narula, J., Devi, S. N., Dao, H. A., Igoshin, O. A., and Fujita, M. (2013). Triggering sporulation in *Bacillus subtilis* with artificial two-component systems reveals the importance of proper Spo0A activation dynamics. *Mol. Microbiol.* 90, 181–194. doi: 10.1111/mmi.12357
- Yan, J., Zou, W., Fang, J., Huang, X., Gao, F., He, Z., et al. (2015). Eukaryote-like Ser/Thr protein kinase PrkA modulates sporulation via regulating the transcriptional factor σ(K) in *Bacillus subtilis*. *Front. Microbiol.* 6:382. doi: 10.3389/fmicb.2015.00382
- Yeats, C., Finn, R. D., and Bateman, A. (2002). The PASTA domain: a beta-lactam-binding domain. *Trends Biochem. Sci.* 27:438. doi: 10.1016/S0968-004(02)02164-3
- Zilhão, R., Iстикато, R., Martins, L. O., Steil, L., Völler, U., Ricca, E., et al. (2005). Assembly and function of a spore coat-associated transglutaminase of *Bacillus subtilis*. *J. Bacteriol.* 187, 7753–7764. doi: 10.1128/JB.187.22.7753-7764.2005

Conflict of Interest Statement: The authors declare that the research was conducted in the absence of any commercial or financial relationships that could be construed as a potential conflict of interest.

Copyright © 2016 Pompeo, Foulquier and Galinier. This is an open-access article distributed under the terms of the Creative Commons Attribution License (CC BY). The use, distribution or reproduction in other forums is permitted, provided the original author(s) or licensor are credited and that the original publication in this journal is cited, in accordance with accepted academic practice. No use, distribution or reproduction is permitted which does not comply with these terms.



SpoVT: From Fine-Tuning Regulator in *Bacillus subtilis* to Essential Sporulation Protein in *Bacillus cereus*

Robyn T. Eijlander^{1,2†}, Siger Holsappel², Anne de Jong^{1,2}, Abhinaba Ghosh³,
Graham Christie³ and Oscar P. Kuipers^{1,2*}

¹ Top Institute Food and Nutrition, Wageningen, Netherlands, ² Department of Molecular Genetics, Groningen Biomolecular Sciences and Biotechnology Institute, University of Groningen, Groningen, Netherlands, ³ Department of Chemical Engineering and Biotechnology, Institute of Biotechnology, University of Cambridge, Cambridge, UK

OPEN ACCESS

Edited by:

Imrich Barak,
Slovak Academy of Sciences, Slovakia

Reviewed by:

Daniel Paredes-Sabja,
Universidad Andres Bello, Chile
Christophe Nguyen-The,
Institut National de la Recherche
Agronomique, France

*Correspondence:

Oscar P. Kuipers
O.P.Kuipers@rug.nl

†Present Address:

Robyn T. Eijlander,
NIZO Food Research, Ede,
Netherlands

Specialty section:

This article was submitted to
Microbial Physiology and Metabolism,
a section of the journal
Frontiers in Microbiology

Received: 12 August 2016

Accepted: 26 September 2016

Published: 13 October 2016

Citation:

Eijlander RT, Holsappel S, de Jong A,
Ghosh A, Christie G and Kuipers OP
(2016) SpoVT: From Fine-Tuning
Regulator in *Bacillus subtilis* to
Essential Sporulation Protein in
Bacillus cereus.
Front. Microbiol. 7:1607.
doi: 10.3389/fmicb.2016.01607

Sporulation is a highly sophisticated developmental process adopted by most Bacilli as a survival strategy to withstand extreme conditions that normally do not support microbial growth. A complicated regulatory cascade, divided into various stages and taking place in two different compartments of the cell, involves a number of primary and secondary regulator proteins that drive gene expression directed toward the formation and maturation of an endospore. Such regulator proteins are highly conserved among various spore formers. Despite this conservation, both regulatory and phenotypic differences are observed between different species of spore forming bacteria. In this study, we demonstrate that deletion of the regulatory sporulation protein SpoVT results in a severe sporulation defect in *Bacillus cereus*, whereas this is not observed in *Bacillus subtilis*. Although spores are initially formed, the process is stalled at a later stage in development, followed by lysis of the forespore and the mother cell. A transcriptomic investigation of *B. cereus* Δ spoVT shows upregulation of genes involved in germination, potentially leading to premature lysis of prespores formed. Additionally, extreme variation in the expression of species-specific genes of unknown function was observed. Introduction of the *B. subtilis* SpoVT protein could partly restore the sporulation defect in the *B. cereus* spoVT mutant strain. The difference in phenotype is thus more than likely explained by differences in promoter targets rather than differences in mode of action of the conserved SpoVT regulator protein. This study stresses that evolutionary variances in regulon members of sporulation regulators can have profound effects on the spore developmental process and that mere protein homology is not a foolproof predictor of similar phenotypes.

Keywords: sporulation, germination, gene regulation, *Bacillus cereus*, SpoVT

INTRODUCTION

Strains of *Bacillus* species are able to form endospores as a survival strategy in response to poor growth conditions. Their metabolic inactive state and sophisticated layered structures lead to strong resistance properties that enable the spore to survive conditions of increased heat, UV radiation, acid concentrations, pressure or low levels of water, or nutrients for extremely long periods of time (Setlow, 2006, 2007; Sella et al., 2014), while maintaining the ability to monitor their surroundings

and respond to improvements through the process of germination and outgrowth (Setlow, 2003, 2013; Moir, 2006; Dworkin and Shah, 2010). Sporulation, spore resistance development, spore germination, and spore outgrowth are processes that are characterized by inter-strain and intra-strain heterogeneity and variety. This hampers the eradication of spores from food products or raw ingredients as it complicates predictability of spore properties and behavior (Cronin and Wilkinson, 2008; Augustin, 2011; Eijlander et al., 2011). Returning to a vegetative state, germinated spores are a major cause of food spoilage and of food poisoning (in the case of toxin production) (Brown, 2000; Abebe et al., 2011; Logan, 2012).

Dormant spores are the final result of sporulation, which involves complex gene regulatory processes taking place in two different compartments of the cell (Eijlander et al., 2014). Sporulation-specific sigma factors govern the expression of dedicated gene sets in various stages, a process that is regulated in a sequential fashion (Hilbert and Piggot, 2004). The early regulator proteins Spo0A and σ^H are responsible for the consecutive expression and activation of σ^F in the forespore and σ^E in the mother cell (Yudkin and Clarkson, 2005). Expression and activation of late-stage sporulation sigma factors σ^G in the forespore and σ^K in the mother cell depend on completion of these earlier sporulation stages (Li and Piggot, 2001; Chary et al., 2005) (Figure 1). Binding of each sigma factor to RNA polymerase leads to interaction with dedicated DNA targets resulting in the spatial and temporal expression of specific sporulation gene sets required for the development and assembly of the forespore (Rudner and Losick, 2001; Hilbert and Piggot, 2004). Most proteins playing key roles in germination are produced during the later stages in sporulation.

The expression levels of sporulation and germination genes are fine-tuned by secondary regulator proteins that are under the control of sigma factors and enable feed forward loops in the regulatory system. One of these proteins is SpoVT (Figure 1). Expressed in the forespore compartment during late-stage sporulation under the control of σ^G , SpoVT enhances the expression of some σ^G -dependent genes and represses others (Bagyan et al., 1996). For DNA binding it forms a tetramer and possibly binds a yet unidentified substrate through means of the GAF domain in the C-terminal part of the protein (Dong et al., 2004; Asen et al., 2009). Deletion of *spoVT* from *B. subtilis* cells results in the formation of spores that have a defective spore coat, a faster nutrient-induced germination response, an increased sensitivity to UV radiation and limited ability for spore outgrowth (Bagyan et al., 1996; Ramirez-Peralta et al., 2012). A recent study in *B. subtilis* has shown that levels of active SpoVT play a crucial role in determining the numbers of important germination proteins, such as nutrient germination receptors (GRs) and small acid-soluble proteins (SASPs), which affects the germination, resistance, and outgrowth properties of the spore (Ramirez-Peralta et al., 2012).

The SpoVT protein is highly conserved amongst spore-forming bacteria, especially *Bacilli* (Asen et al., 2009; Ramirez-Peralta et al., 2012). The extreme sequence similarity (~95%) of the N-terminal domain of SpoVT homologs suggests a similar mode of action concerning DNA binding activity. It must be

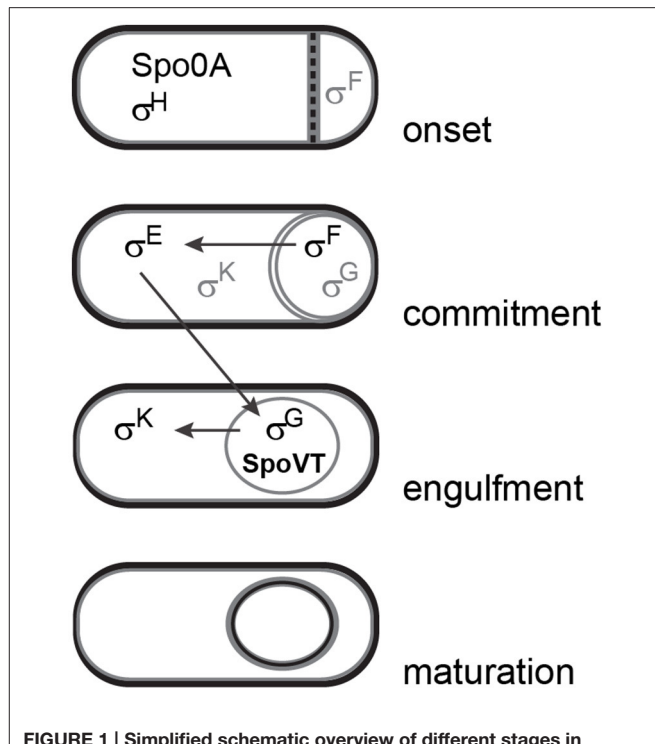


FIGURE 1 | Simplified schematic overview of different stages in sporulation and sequential activation of sporulation-specific sigma factors. Gray lettering indicates inactive forms of sigma factors. This figure was adapted from Piggot and Hilbert (2004).

noted, however, that so far no consensus binding site for SpoVT has been identified (Dong et al., 2004). The C-terminal domain is less conserved (sequence identity of 20–30%) and shows features of a GAF domain that resembles the one of CodY (Asen et al., 2009). Such domains harbor binding pockets for the binding of substrates that are required for structure, sensing, and/or activity. If SpoVT requires substrate-binding for activity, it is possible that this substrate differs amongst various SpoVT homologs (Asen et al., 2009). However, several attempts to identify such a substrate have so far failed.

The SpoVT protein of *Bacillus cereus* (from here on referred to as SpoVT_{BCE}) has been less well studied than its *B. subtilis* counterpart and its precise role in gene expression during sporulation is so far unknown. *B. cereus* is notorious for compromising food quality and safety due to its high diversity, the production of highly heat-resistant spores and cytotoxin-producing properties (Stenfors Arnesen et al., 2008; Lücking et al., 2013). It is part of a wider class of related species that also includes *Bacillus anthracis*, the cause of anthrax, and *Bacillus thuringiensis*, an insect pathogen. The main characteristics of these closely related species are determined by large plasmids that encode specific toxin or other virulence factors (Økstad and Kolstø, 2011). The non-pathogenic *B. subtilis* lacks such plasmids and is part of a different group of Bacilli that also includes *Bacillus licheniformis* and *Bacillus amyloliquefaciens*. Due to a wealth of available experimental data, *B. subtilis* and *B. cereus* are commonly used as model organisms for studies concerning these two groups of species, with in particular *B.*

subtilis 168 and *B. cereus* ATCC 14579. Despite a common ability to form endospores and a conservation of important sporulation and germination genes (de Vries et al., 2004; de Hoon et al., 2010; Galperin et al., 2012), interesting evolutionary diversity can be observed between these two species. This is reflected by differences in gene regulation during sporulation (Pflughoefl et al., 2011) or in various spore properties, such as the spore coat (Wang et al., 2007; Qin and Driks, 2013), spore size (Carrera et al., 2007), germinant receptor protein types (Hornstra et al., 2005; van der Voort et al., 2010), and spore resistance properties (Wang et al., 2003; Black et al., 2008).

In this study, we investigated the role of *SpoVT_{BCE}* in (heterogeneous) gene expression during sporulation of *B. cereus*. We show that, in contrast to what was previously reported for *B. subtilis*, deletion of *spoVT_{BCE}* results in a complete sporulation defect. Transcriptomic investigation during sporulation shows upregulation of genes involved in germination, which indicates premature lysis of prespores. In addition, the data shows differential expression of *B. cereus*-specific genes of unknown function, which potentially play an important role in the extreme phenotype. This is furthermore supported by successful complementation studies using both *SpoVT_{BCE}* and *SpoVT_{BSU}*. Through this study we show that despite strong sequence conservation of *SpoVT* among Bacilli, significant differences exist in the role of this regulator during developmental processes, which are likely due to the specific genes under its control.

MATERIALS AND METHODS

Strains and Plasmids

All strains and plasmids used in this study are listed in **Table 1**. Primers used for the amplification of DNA fragments are listed

in **Table S1**. As reference strains, *B. subtilis* 168 and *B. cereus* ATCC 14579 were used. Foreign DNA was introduced into *B. cereus* via electroporation (Masson et al., 1989), either by using the multicopy plasmid pNW33n or by single crossover DNA integration via non-replicative pMAD and PSG1151 derivatives.

For the construction of the pNWVT vector, the *spoVT* gene (BC0059) including its own promoter was amplified from *B. cereus* ATCC 14579 chromosomal DNA using primers AKUpVT-F and TIFN16. The resulting product was cut with EcoRI and KpnI (Fermentas, FastDigest) and ligated into the corresponding sites of pNW33n (Genbank Accession number, AY237122), which resulted in pNWVT. The pVTSu2 vector was created by replacing *spoVT_{BCE}* with *spoVT_{BSU}* in pNWVT, which was amplified using primers BsuVTF2 and BsuVTR. The primers were specifically designed to ensure that *spoVT_{BSU}* expression would be driven by the *B. cereus* *spoVT* promoter already present in pNWVT. The *spoVT_{BCE}* gene was cut out of pNWVT using BclI and HindIII and replaced with *spoVT_{BSU}* containing compatible sticky ends. Correct construction was verified using restriction analysis and sequencing.

For the construction of the *B. cereus* *spoVT* disruption mutant, we constructed the pDCVT vector by amplifying an upstream *spoVT* flanking region from *B. cereus* ATCC 14579 gDNA using primers dCVT-F1 and dCVT-R1. A downstream flanking region was amplified using primers dCVT-F2 and dCVT-R2. Both flanking regions were fused to HindIII compatible ends of a spectinomycin resistance cassette originating from pDG1726. The fused fragments were ligated into the NcoI and EcoRI sites of pMAD to create pDCVT. The pDCVT was introduced into *B. cereus* ATCC 14579 to disrupt the *spoVT* gene according to the method described by Arnaud et al. (2004). Disruption of *spoVT*

TABLE 1 | Strains and plasmids used in this study.

Strain	Properties	References
<i>B. subtilis</i> 168	<i>trpC2</i>	Kunst et al., 1997
<i>B. subtilis</i> 168 Δ <i>spoVT</i>	<i>spoVT</i> :: <i>spec</i> ^r	Bagyan et al., 1996, kindly provided by Prof. S. Cutting
<i>B. cereus</i> ATCC 14579	Enterotoxic strain of <i>B. cereus</i> wild type isolate	Bacillus Genetic Stock Center, ATCC, BGSC ID6A5
<i>B. cereus</i> ATCC 14579 P _{<i>spoVA</i>} - <i>gfp</i>	P _{<i>spoVA</i>} - <i>gfp</i> , Cm ^r	This study
<i>B. cereus</i> ATCC 14579 Δ <i>spoVT</i>	<i>spoVT</i> :: <i>spec</i> ^r	This study
<i>B. cereus</i> ATCC 14579 Δ <i>spoVT</i> P _{<i>spoVA</i>} - <i>gfp</i>	<i>spoVT</i> :: <i>spec</i> ^r , P _{<i>spoVA</i>} - <i>gfp</i> , Cm ^r	This study
<i>B. cereus</i> ATCC 14579 Δ BC1117	marker-less deletion of the BC1117 ORF	This study
Plasmid	Properties	References
pNW33n	<i>E. coli</i> -Gram + shuttle vector	Bacillus Genetic Stock Center
pNWVT	Cm ^r , <i>spoVT_{BCE}</i>	This study
pVTSu2	Cm ^r , <i>spoVT_{BSU}</i>	This study
pSG1151	Vector for integrative P-gfpmut1 fusions in <i>B. subtilis</i> , Ap ^r , Cm ^r	Lewis and Marston, 1999
pSGCVA	pSG1151 with <i>gfp</i> driven by the <i>Bce</i> <i>spoVAA</i> promoter, Ap ^r , Cm ^r	This study
pMAD	Vector for efficient gene replacement in non-naturally transformable gram-positive bacteria, Ap ^r , Em ^r	Arnaud et al., 2004
pDCVT	pMAD-derivative used for <i>spoVT</i> gene disruption, Ap ^r , Em ^r	This study
pDG1726	<i>E. coli</i> plasmid bearing a spectinomycin resistance cassette	Guérout-Fleury et al., 1995

was verified using PCR analysis and sequencing of the integration site to ensure there were no second-site mutations.

For the construction of a chromosomally integrated P_{spoVA} -*gfp* fusion in *B. cereus*, a 1.5 kb fragment of the upstream region of the *B. cereus* ATCC 14579 *spoVAA* gene (BC4070) was amplified using primers TIFN41 and TIFN42A. The TIFN42A primer was designed as such that the original RBS plus the first two codons of the *spoVAA* gene were included in the amplified fragment. This was then cleaved with EcoRI and KpnI and introduced into the corresponding sites of pSG1151. The resulting pSGCVA vector was introduced into *B. cereus* ATCC 14579 and *B. cereus* ATCC 14579 Δ *spoVT* via electroporation and checked for single crossover integration on the original locus using PCR analysis and sequencing.

A strain bearing an in-frame deletion of the ORF encoded at locus BC1117 was created using a marker-less gene replacement method (Janes and Stibitz, 2006; Lindbäck et al., 2012). Essentially, a modified pMAD-derived vector containing \sim 500 bp of the respective up- and downstream regions of DNA flanking the BC1117 ORF was introduced by electroporation to *B. cereus* ATCC 14579 cells. Plasmid pBKJ233, which encodes I-SceI enzyme, was introduced subsequently to cells identified by blue-white (X-gal) screening and PCR as having inserted the pMAD-derived plasmid at locus BC1117. Clones that had undergone a second recombination event, deleting the BC1117 ORF and leaving behind only the start and stop codons, were identified by screening for erythromycin sensitivity. Finally, the Δ BC1117 strain was validated for the correct construction by PCR.

Culture Preparation and Media

All *B. cereus* strains were cultured at 30°C with aeration at 220 rpm. Media was supplemented with chloramphenicol (4 μ g/ml), erythromycin (2 μ g/ml), or spectinomycin (300 μ g/ml) when appropriate. For the preparation of cells for time-lapse microscopy, cells were prepared as previously described (Eijlander and Kuipers, 2013). For all other sporulation experiments and for the preparation of sporulating cells for RNA isolation, cells were cultured in maltose sporulation medium (MSM) (van der Voort et al., 2010). Spore crops were prepared on MSM agar plates for 7 days at 30°C. Spores were collected from the plates and washed (6000 rpm, 15 min at 4°C) twice a day for 14 days in 10 mM phosphate buffer (pH 6.2) with decreasing concentrations of Tween20 to prevent clumping of the spores (0.1, 0.075, 0.05, 0.04, 0.03, 0.02, and 0.01%). Phase contrast microscopy analysis of the spore crops showed >98% free-lying spores. Spores were stored at 4°C in 10 mM phosphate buffer with 0.01% added Tween20 and were washed twice a week to prevent spontaneous germination.

Complementation of Δ *spoVT* with pNWWT (*spoVT*_{BCE}) and pVTBsu2 (*spoVT*_{BSU})

The vectors pNWWT (containing *spoVT*_{BCE} expressed by its own promoter) and pVTBsu2 (containing *spoVT*_{BSU} expressed by the *P_{spoVTBCE}* promoter) were introduced in the *B. cereus* ATCC 14579 Δ *spoVT* strain by electroporation as described above. Overnight cultures were diluted 1:100 in MSM medium and

incubated at 30°C while shaking for 6 h. Exponentially growing cells were again diluted 1:100 in fresh MSM medium and allowed to grow in the same conditions for 65 h. Samples for phase contrast microscopy analysis were taken after 17, 22, 44, and 65 h. Efficiency in complementation of sporulation was determined using the Cell Counter plugin in ImageJ¹.

Germination Assays

B. cereus spores were washed twice before the experiment and resuspended in ice-cold sterile demineralized water. Spores were heat-activated at 70°C for 15 min and immediately placed on ice for 2 min to cool down. The washing step was repeated after which spores were resuspended in ice-cold sterile germination buffer (10 mM Tris-HCl 7.4 + 10 mM NaCl) to a final OD₆₀₀ of 10. Spores were diluted 10 times in germination buffer containing nutrients (10 mM alanine or 1 mM inosine) or BHI medium supplemented with chloramphenicol (5 μ g/ml) to prevent outgrowth. Changes in optical density were monitored every 2 min for 4 h at 30°C in a TECAN plate reader and the obtained data plotted in Excel.

Imaging, Time-Lapse Microscopy, and Image Analysis

All microscopy imaging was performed using the IX71 Microscope (Olympus) with CoolSNAP HQ2 camera (Princeton Instruments) and DeltaVision softWoRx 3.6.0 (Applied Precision) software. For *B. subtilis* the 100x phase contrast objective was used, for *B. cereus* the 60x phase contrast objective. For the visualization of green fluorescence from GFP or FM46 dye the GFP filterset was used (Chroma, excitation at 470/40 nm, emission at 525/50 nm). Images were taken using 32% APLLC White LED light and 0.05 s exposure for bright field pictures and 10% Xenon light with 0.5 s exposure for fluorescence detection. Pictures were analyzed using ImageJ software.

To monitor gene expression in single cells during sporulation, the time-lapse microscopy technique was applied for the promoter-*gfp* fusion strains of *B. cereus* as previously described (Eijlander and Kuipers, 2013). For quantification of the GFP fluorescence signal distribution, the fluorescence intensity was measured for every cell in the microcolony for every time frame using the ImageJ ROI tool. Fluorescence intensities per cell per frame were exported to Excel and normalized by subtracting background fluorescence levels of the microscopy slide (agarose) and autofluorescence of the cells or spores (highest fluorescent value measured for wt strains). Mean fluorescence values were calculated from ten frames per cell and binned according to set fluorescence value categories. This data was represented in fluorescence distribution plots in Excel.

Total RNA Extraction from Sporulating *B. cereus* Cells

Cells were cultured in sporulation media to induce the sporulation event. Individual stages in sporulation were determined via fluorescence microscopy on agarose patches with

¹<http://imagej.nih.gov/ij/>.

added FM® 1–43 membrane stain (Invitrogen, Ex 479 nm, Em 598 nm) at an end concentration of 1 µg/µl.

Cell samples (5 ml, including biological and technical replicates) were taken every hour for 6 h from transition point onwards (T0, reached after 7 h of growth in MSM). Cells were collected by centrifugation in a pre-cooled centrifuge (4°C, 4000 rpm, 3 min) and immediately frozen in liquid nitrogen. For RNA extraction, cells were thawed on ice in 500 µl TRI-reagent (Life Technologies, Carlsbad, CA USA) and glass beads (<100 µm, Sigma-Aldrich), resuspended and immediately disrupted by 4 rounds of bead beating [45 s at maximal settings (3450 rpm)] in a Mini-Beadbeater-16 (BioSpec products, Bartlesville, OK USA). Direct-zol RNA MiniPrep (Zymo Research, Irvine, CA USA) was used according to manufacturer's instruction for on column RNA purification. Residual chromosomal DNA was removed using the Ambion DNA-free™ kit (Life Technologies®, Thermo Fisher Scientific, USA). The RNA concentration was measured on a NanoDrop ND-1000 spectrophotometer. RNA quality was determined using an Agilent BioAnalyzer RNA 6000 nanokit. The concentration of RNA isolated from wt sporulation cells was a little lower than for $\Delta spoVT$ sporulating cells (3000 ng/µl compared to 3800 ng/µl) but still comparable. Quality of all isolations was within the specified levels for all samples (an OD_{260/280} ratio between 1.8 and 2.0 and an OD_{260/230} ratio of >1.7).

RNA Sequencing

RNA samples (> 1 µg) were sent to PrimBio Research Institute (Exton, PA, USA) where rRNA depletion (using the Ambion MICROBExpress™ Kit) and a library prep (using the Ion Total RNA-Seq Kit v2) were performed. Samples were multiplexed in sets of nine and loaded on an Ion Proton™ chip. In total 80 M reads with an average length of 120 bases were derived per chip. The reads were mapped against the reference genomes for *B. cereus* ATCC 14579 using Bowtie 2 (Langmead and Salzberg, 2012) with optimized parameters setting for Ion Proton data: “ -D 20 -R 3 -N 1 -L 20 -i S, 1, 0.50 -local”. Gene expression profiling was done using SAMtools (Li et al., 2009) and Cufflinks (Trapnell et al., 2012). Subsequent statistical analysis was performed using a modified EdgeR routine on the MolGen webserver².

Spearman Rank correlation analysis was performed to show clustering of biological replicates within one strain and between strains. Correctly clustered data sets were further filtered based on intra-variation < inter-variation. Excel conditional formatting was applied to visualize the degree of intra- and inter-variation for each differentially expressed gene. The biological ratio in gene expression was calculated using log-transformed data in the following formula:

$$\text{Biological ratio} = \log_2(wt1 + wt2) - \log_2(dVT1 + dVT2)$$

where *wt1* and *wt2* are replicate rpkm values for the *wt* strain and *dVT1* and *dVT2* are replicate rpkm values for the $\Delta spoVT$ strain. The fold change in gene expression between the two strains was furthermore determined by raising the number 2 to the power of the absolute value for the ratio ($2^{\text{ABS(ratio)}}$).

²<http://genome2d.molgenrug.nl>, T-Rex DOI: 10.1186/s12864-015-1834-4.

Orthologs of *B. subtilis* sporulation genes (SporeWeb³, Eijlander et al., 2014) in *B. cereus* ATCC 14579 were determined using OrthoMCL (Chen et al., 2006) and (predicted) gene function using the KEGG database⁴ or NCBI Blast⁵.

RESULTS

spoVT* Is Essential for Completion of Sporulation in *Bacillus cereus

All present knowledge on the SpoVT regulator protein so far originates from studies in *B. subtilis*. Cells of *B. subtilis* that lack SpoVT are still able to produce spores, albeit with a defective spore coat structure, an increased initial germination rate in response to nutrients and a severe defect in further germination and outgrowth (Bagyan et al., 1996; Ramirez-Peralta et al., 2012). Despite a strong conservation of SpoVT in endospore-forming bacteria, the effect of removing SpoVT from *B. cereus* cells (SpoVT_{BCE}) proves more severe. In this organism, a similar *spoVT* disruption mutant is unable to complete the sporulation process and produces very few, if any, free-lying spores with a severely defective morphology (Figure 2 $\Delta spoVT$). Re-introduction of *spoVT*_{BCE} only partly restored this defect (14% of the total number of cells restored sporulation, Figure 2 $\Delta spoVT+$). The partial complementation result could be due to differences in plasmid copy number between individual spores. Interestingly, similar complementation experiments with the *spoVT* wt allele of *B. subtilis* (*spoVT*_{BSU} driven by the *PspoVT*_{BCE} promoter) produced comparable results (complementation restored sporulation in 12% of the total number of cells, Figure 2, $\Delta spoVT$ +Bsu). This indicates that the working mechanism of SpoVT_{BSU} and SpoVT_{BCE} is comparable, which is expected given the high sequence conservation between both proteins. The observed difference in phenotypic effect after removal of SpoVT in both organisms must thus have a basis in the promoters of these regulatory proteins interact with to modulate gene expression.

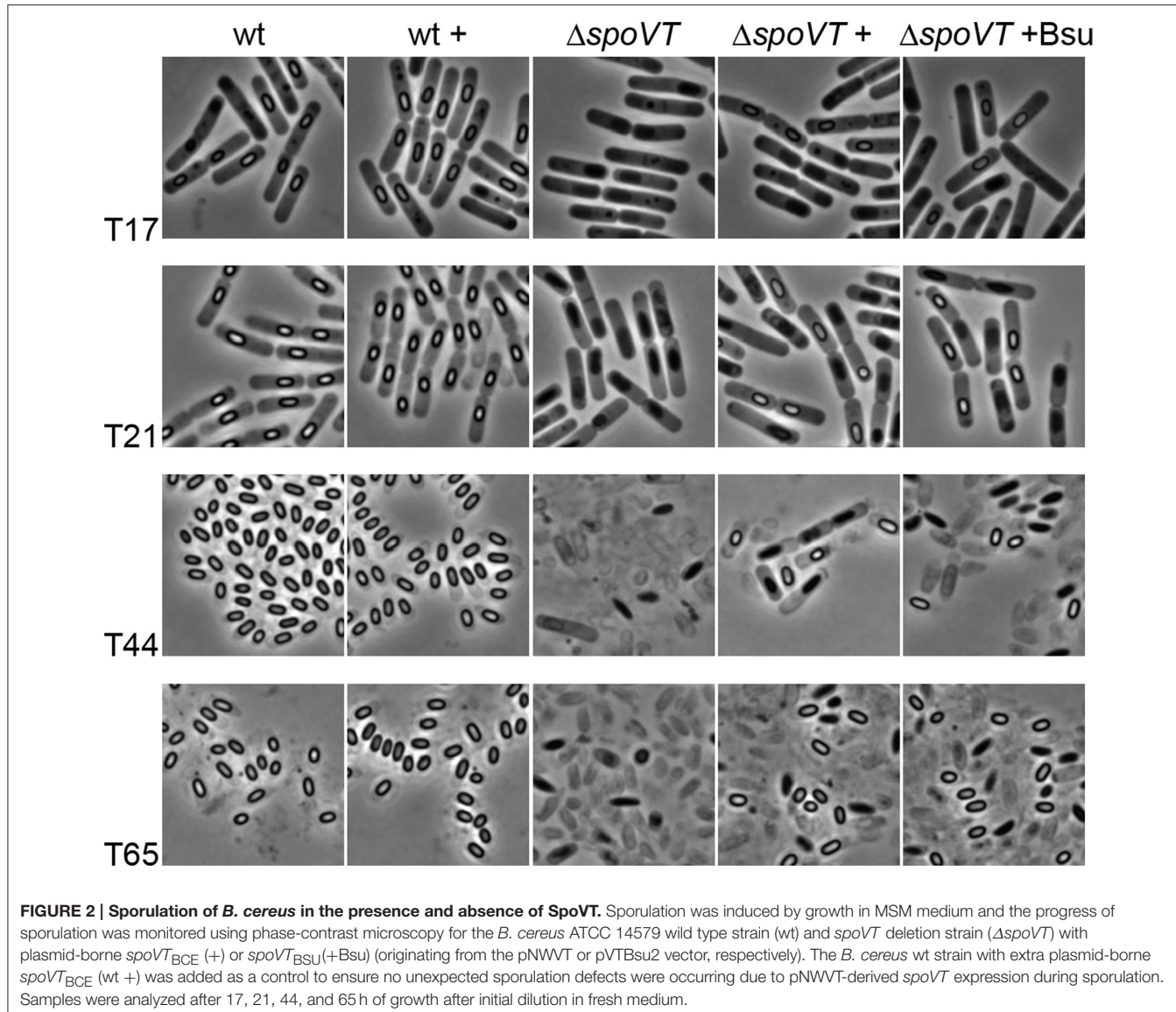
Sporulation of a *spoVT* Deletion Strain of *B. cereus* Is Stalled at a Later Stage Leading to Premature Lysis

Time-lapse fluorescence microscopy is a powerful technique to visualize dynamics in gene expression in time in individual cells and was recently optimized for application with *B. cereus* cells (Eijlander and Kuipers, 2013). In this study, we applied time-lapse fluorescence microscopy to follow the events of forespore-specific gene expression in time in a *spoVT* deletion background of *B. cereus*. Unfortunately, multiple attempts to construct a variety of sporulation-specific promoter-gfp fusions (e.g., *PgerI*, *PcwlJ*, *PgerR*, *PcotD*, *PsspA*) stably integrated into the *B. cereus* genome failed, except for one (i.e., *PspoVA*-gfp). This limited our ability to determine true effects of SpoVT removal on the expression levels of late sporulation genes, but did enable us to

³<http://sporeweb.molgenrug.nl>.

⁴<http://www.genome.jp/kegg/>.

⁵<http://blast.ncbi.nlm.nih.gov/>.



provide insights in the sporulation line of events in the absence of SpoVT.

Time-lapse image analysis of strain *B. cereus* $\Delta spoVT$ $P_{spoVA-BCE-gfp}$ (**Movie S2**) clearly shows that during the earlier stages of sporulation prespores are formed like in the wild type background (**Movie S1**), but that progression of sporulation is stalled at a later stage. First, the formed pre-spores lyse, thereby spreading the produced GFP throughout the mother cell (**Figure 3B** and **Movie S2**). Finally, the mother cell also lyses (**Figure 3A**).

A quantitative analysis of the obtained images was performed to substantiate the difference in *spoVA* gene expression levels in a *spoVT* background. Before pre-spore lysis, the intensity of fluorescence originating from the $P_{spoVA}-gfp$ fusion was significantly higher in the absence of SpoVT_{BCE} than in wild type cells (**Figure 3C** and **Movies S1, S2**). In addition, the distribution of the signal strength was more wide-spread amongst individual

cells. It must be noted, however, that it is possible that this observed effect is not the result of increased (heterogeneity in) promoter activity in the absence of SpoVT, but rather an artifact in the detection of the GFP signal—the *spoVT* spores are severely weakened shortly after the completion of engulfment and, furthermore, it is known that SpoVT enhances rather than represses *spoVA* expression in *B. subtilis* (Wang et al., 2006; Ramirez-Peralta et al., 2012).

Transcriptomic Analysis of *B. cereus* $\Delta spoVT$ during Sporulation

To further investigate the role of SpoVT in gene expression during sporulation of *B. cereus*, we isolated RNA from sporulating cells at three sequential time points (3, 4, and 5 h after the transition point to stationary growth was reached; **Figure S1**). Differentially expressed genes in the *spoVT* deletion strain were compared to the wild type situation using a

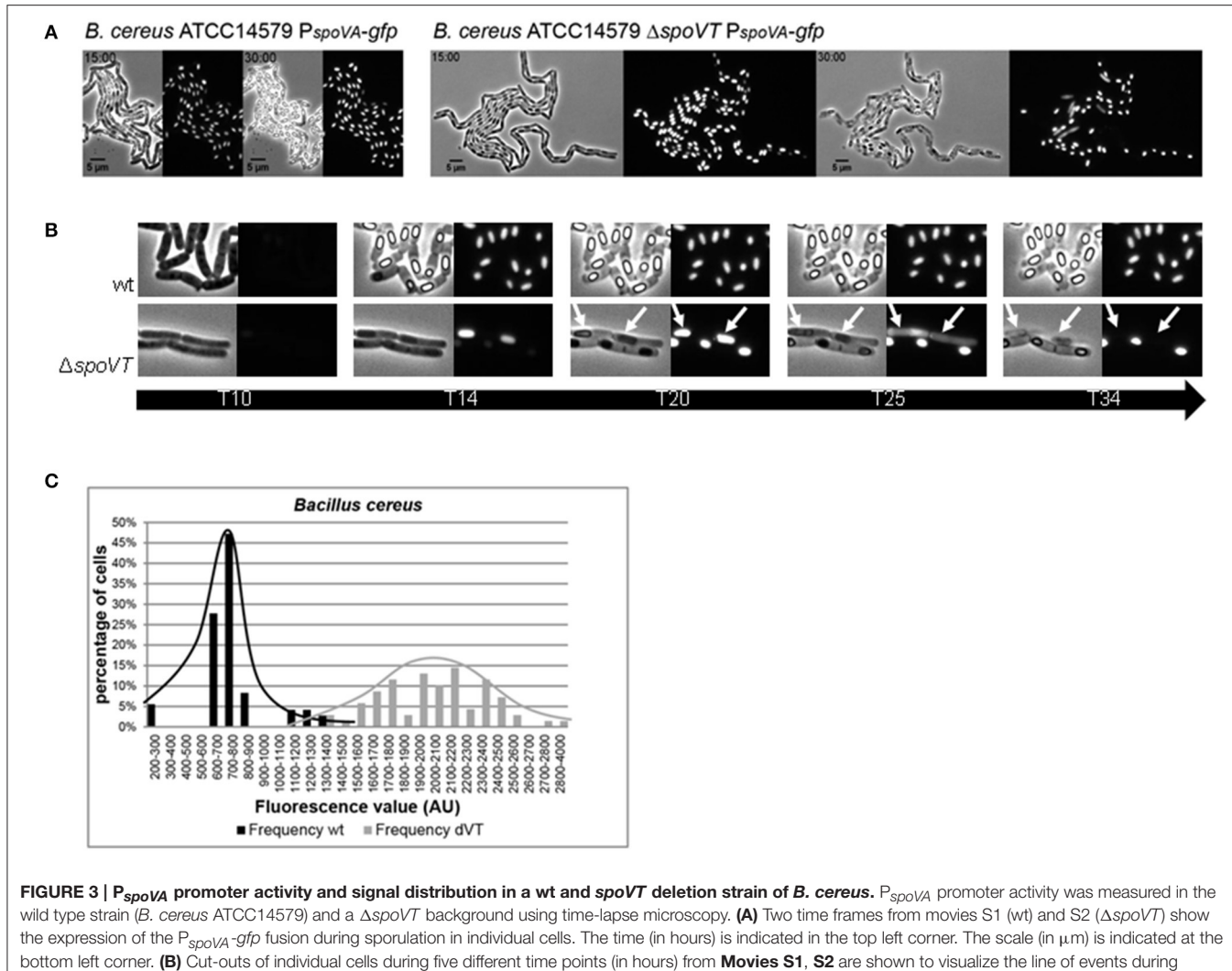


FIGURE 3 | *PspoVA* promoter activity and signal distribution in a wt and *spoVT* deletion strain of *B. cereus*. *PspoVA* promoter activity was measured in the wild type strain (*B. cereus* ATCC14579) and a Δ *spoVT* background using time-lapse microscopy. **(A)** Two time frames from movies S1 (wt) and S2 (Δ *spoVT*) show the expression of the *PspoVA-gfp* fusion during sporulation in individual cells. The time (in hours) is indicated in the top left corner. The scale (in μ m) is indicated at the bottom left corner. **(B)** Cut-outs of individual cells during five different time points (in hours) from Movies S1, S2 are shown to visualize the line of events during sporulation in a wt and a Δ *spoVT* background. Lysing prespores and mothercells in Δ *spoVT* are indicated by white arrows. **(C)** The average fluorescence value distribution in arbitrary units in *B. cereus* wt (black bars) and *spoVT* cells (gray bars) calculated from Movies S1, S2.

transcriptomics approach. Details on RNA isolation, preparation, sequencing, downstream normalization, and statistical analysis of the resulting data are described in the Materials and Methods Section. Resulting normalized expression values [reads per kilobase per million (rpkm)] are provided in Table S2.

Sporulation is a very heterogeneous process, which complicates the synchronization of gene expression in individual cells. This generates a large variety in the absolute gene expression values generated by RNA sequencing. Spearman Rank correlation of the available data showed that two biological replicates of the same strain (wt or Δ *spoVT*) clustered together only for the samples taken at T5. Therefore, further data analysis was performed for that time point only.

The log2-transformed data was used to calculate the fold change in gene expression in the *spoVT* mutant strain compared to the wt strain. A total list of significantly up- and down-regulated genes is provided in Table S3.

Of the differentially expressed genes (with a cut-off of ≥ 2 -fold difference), a total number of 52 genes were down-regulated and 87 genes were up-regulated (Table 2). Both groups contain genes involved in sporulation, germination, regulation, metabolism, and transport and both groups contain a large number of genes encoding hypothetical or unknown proteins. What stands out, is that genes involved in protein synthesis (ribosomal protein subunits) were specifically upregulated in a *spoVT* mutant. In addition, a large number of genes involved in metabolism was also upregulated.

Concerning sporulation and/or germination-specific genes, almost no *B. cereus* orthologs of known SpoVT-regulated genes (as determined by studies in *B. subtilis*; Bagyan et al., 1996; Wang et al., 2006) are present in this list. Only *spoIIIG* (BC3903) and *tepA* (BC3795) were, similarly to their counterparts in *B. subtilis*, repressed by SpoVT in *B. cereus* (Table S3). Amongst significantly down-regulated sporulation genes (>2 -fold difference in gene expression) were some genes

TABLE 2 | Number of genes per functional category up-or down-regulated in a *B. cereus spoVT* deletion background.

Functional category	Number of genes upregulated	Number of genes downregulated
Sporulation	15	9
Germination	4	1
Metabolism and transport	25	10
Protein synthesis	13	0
Regulation	6	4
Hypothetical and unknown	16	20
Other	8	8

encoding spore coat proteins, one germination receptor subunit (GerIA) and a few sporulation proteins of unknown function. Upregulated sporulation genes, on the other hand, were those encoding CwlJ1, SpoIIQ, SpmA, CotD, YaaH, SpoIVA, SpoIIIAB, CdaS, SpoIIIAC, genes encoding sporulation-specific regulators RsfA, SigK, GerE, SigG, and AbrB and a few sporulation proteins of unknown function.

Interestingly, quite a few hypothetical or genes of unknown function were extremely, or at least considerably, downregulated in the *spoVT* deletion strain (Table 3). Although no putative function could be deducted from homology searches using their protein sequences, most of them seem to be specific for *B. cereus* group organisms. One such example is the gene encoded at locus BC1117, expression of which was down-regulated approximately 3000-fold in the *spoVT* mutant strain. BC1117 is predicted to encode a small (50 residue, ~6 kDa) lysine-rich polypeptide. A preliminary examination of the role of BC1117 in *B. cereus* ATCC 14579 was conducted by constructing a strain with a markerless deletion in this locus. However, in contrast to the Δ *spoVT* strain, the Δ BC1117 strain was observed to grow and sporulate normally, releasing mature spores after approximately 24 h of culture (Figure S2).

DISCUSSION

SpoVT is a strongly conserved regulatory protein specifically active during the later sporulation stages in the forespore compartment of cells and is known to play an important role in fine-tuning the regulation of sporulation-specific gene expression (Ramirez-Peralta et al., 2012). The lack of a consensus SpoVT binding sequence complicates the prediction of alternating SpoVT level effects on spore properties and spore germination efficiency. The strongly conserved N-terminal DNA-binding domain of SpoVT suggests a similar conservation in DNA targets for this regulatory protein. However, in this work we show that removing SpoVT from sporulating cells has a dramatic effect on completion of sporulation in *B. cereus*—an effect that is not observed in *B. subtilis*. Unfortunately, we were unable to study single copy integrated SpoVT complementation due to the low efficiency of DNA recombination in *B. cereus* (Arnaud et al., 2004). By making use of a vector-based complementation, restoration of the sporulation phenotype was only partly

accomplished. This could be due to differences in plasmid copy number between individual spores (Turgeon et al., 2008), which would suggest that the tolerated levels of SpoVT_{BCE} protein in sporulating cells fit inside a tight window.

Furthermore, similar complementation results with heterologous SpoVT_{BSU} indicate that the observed difference in the impact of SpoVT removal from sporulating cells of the two species is not due to a difference in the working mechanism, but rather to a difference in regulated target genes. This is supported by transcriptomic analysis of differential gene expression during late-stage sporulation, in which a significant number of *B. cereus*-group specific genes of unknown function were severely down-regulated in the *spoVT* mutant strain. The potential role of one of these genes (BC1117) in sporulation was further investigated using a clean BC1117 deletion mutant strain. This strain sporulated normally, indicating that the sporulation phenotype observed in the Δ *spoVT* strain cannot be solely attributed to the extreme down-regulation of the BC1117 gene. The function of BC1117 and whether it plays a direct or indirect role in sporulation remains to be elucidated. Work is continuing to further characterize the BC1117 polypeptide in terms of its location and role in *B. cereus* spores.

Unfortunately, the synchronization of sporulation for RNA isolation proved challenging, limiting the usability and reliability of the obtained RNA sequencing data sets to time point T5 only. This could be the reason why only a limited number of known SpoVT regulon members were represented in our data set, which does not allow us to define the SpoVT regulon in *B. cereus*. Potentially, the optimization of sporulation protocols for *B. cereus* cells can help overcome this issue.

What can be derived from the transcriptomic data, however, is that the observed sporulation defect caused by lysis of formed prespores in *B. cereus* *spoVT* might be the result of premature germination of the prespores. Genes involved in both metabolism and protein synthesis were upregulated especially in the *spoVT* deletion strain, which is known to occur during the early stages of germination (Horsburgh et al., 2001). In addition, the spore cortex lytic enzyme (SCLE) CwlJ1 and the cortical fragment lytic enzyme (CFLE) SleL were upregulated over 5-fold and almost 4-fold, respectively, in a *spoVT* mutant of *B. cereus*. CwlJ is responsible for the degradation of the cortex layer upon germination and responds specifically to exogenous Ca²⁺-chelated dipicolinic acid (Ca-DPA) (Moir, 2006), whereas SleL cooperates with CwlJ by hydrolysing fragmented peptidoglycan substrates (Lambert et al., 2012), which supports the theory of premature germination in *B. cereus* Δ *spoVT*. Both genes encoding these proteins are known to be expressed in the mother cell under the control of σ^E and SpoIID during early stages of sporulation. This suggests that the observed upregulation in a *spoVT* deletion mutant is more than likely an indirect effect. Such indirect effects may be more abundant, as several other regulatory proteins were also upregulated in the *spoVT* deletion strain (RsfA, SigK, GerE, and SigG). Together with the lack of a consensus SpoVT binding sequence, this complicates the determination of the SpoVT regulon in *B. cereus*.

TABLE 3 | Significantly downregulated hypothetical genes in a *B. cereus* spoVT deletion mutant.

Gene locus tag	Fold-change (down-regulated)	Protein homology
BC1117	2984	Hypothetical protein, homology to <i>B. cereus</i> group-specific hypothetical protein
BC0987	37	Hypothetical protein, homology to hypothetical protein
BC1457	20	Hypothetical protein, homology to hypothetical protein
BC2492	18	Hypothetical protein, homology to <i>B. cereus</i> group-specific hypothetical protein
BC2270	15	Hypothetical protein, homology to <i>B. cereus</i> group-specific hypothetical protein
BC3002	10	Hypothetical protein, homology to <i>B. cereus</i> group-specific hypothetical protein
BC0973	9	Hypothetical protein, <i>B. cereus</i> group membrane protein
BC2426	8	Hypothetical protein, homology to <i>B. cereus</i> group-specific hypothetical protein

The heterogeneous character of SpoVT in sporulating bacteria is intriguing. Through this study we demonstrate an essential role of the SpoVT protein in sporulation of *B. cereus*, whereas in *B. subtilis* SpoVT is not essential, but nevertheless very important for proper formation and maturation of a spore. Further investigation on the essential and/or fine-tuning role of SpoVT in the regulation of sporulation-specific gene expression requires the quantification of active SpoVT levels, preferably in individual cells. This is currently complicated by the gaps in our knowledge on possible SpoVT activity requirements, e.g., the binding of a (yet unidentified) substrate. Obtaining such knowledge will also provide us with more insights on the role of SpoVT in sporulation and germination heterogeneity. Such phenotypic heterogeneity is an outcome of bifurcation in gene regulatory circuits, in which key regulatory proteins are often subjected to multimerization and require additional modification for activation before instigating feed forward loops in gene expression. In *B. subtilis* developmental processes, Spo0A and ComK are well-studied examples of such regulatory proteins (Grossman, 1995; Lopez et al., 2009). Given the requirement of tetramerization and possible substrate binding prior to activation, it is very plausible that SpoVT is equally involved in such complex regulatory circuits and is thus one of the major players responsible for germination heterogeneity. Levels of such a substrate may differ per individual cell, especially if the regulation of its production is part of a signal transduction system. Unfortunately, numerous attempts to identify such a substrate have thus far failed (Dong et al., 2004; Asen et al., 2009). New leads can be defined based on novel findings on the production of signaling molecules during sporulation, such as the recent demonstration of spore-specific production of cyclic di-AMP (c-di-AMP) via the CdaS cyclase during late-stage sporulation (Mehne et al., 2013, 2014). Since the absence of CdaS in sporulating *B. subtilis* cells results in an affected germination profile of resulting spores (Mehne et al., 2014) and since *cdaS* deletion has a negative (direct or indirect) effect on sporulation gene expression levels (qPCR data not shown), it is tempting to assume that CdaS-derived c-di-AMP functions as a trigger molecule for SpoVT activity. Unfortunately, we have so far been unsuccessful in demonstrating an *in vitro* interaction between c-di-AMP and purified SpoVT_{BSU}, whereas a clear interaction of c-di-AMP with the positive control DarA was observed (Jörg Stölke, personal communication, data

not shown). Possibly, forespore-specific interactions between molecules are extra challenging to simulate *in vitro* (Asen et al., 2009), or c-di-AMP plays an important role during spore germination and/or outgrowth not related to SpoVT activity.

Differences in regulons of conserved regulatory proteins are not uncommon. In *B. thuringiensis* for instance, an organism closely related to *B. cereus*, it was found that the SinR regulatory protein was not involved in the regulation of an *eps* operon like in *B. subtilis*, but rather in the biosynthesis of the lipopeptide kurstakain and the Hbl enterotoxin gene that is not part of the *B. subtilis* genome (Fagerlund et al., 2014). In addition, for clostridial species it is well known that the regulatory programs orchestrating sporulation differ significantly from those in *B. subtilis* despite strong regulator protein conservation (Al-Hinai et al., 2015).

In summary, this report further demonstrates that despite conservation in sporulation regulatory proteins amongst Bacilli (de Hoon et al., 2010), future studies on their function and impact should take into account evolutionary differences in regulon members between species underlying important variances in downstream developmental processes.

AUTHOR CONTRIBUTIONS

RE designed the experimental plan, executed the majority of the experiments, analyzed the results, and wrote the manuscript. SH supported in the technical part and read the final manuscript. AD analyzed the transcriptomic results, contributed in writing, and read the final manuscript. AG executed the experiments with the BC1117 mutant, contributed in writing, and read the final manuscript. GC supported in the analysis of the BC1117 mutant results, contributed in writing, and read the final manuscript. OK participated in the experimental plan and read the final manuscript.

FUNDING

This research is funded by TI Food and Nutrition, a public-private partnership on pre-competitive research in food and nutrition. The funders had no role in study design, data

collection and analysis, decision to publish, or preparation of the manuscript.

ACKNOWLEDGMENTS

We would like to thank Dr. Ruud Detert Oude Weme, Prof. Jörg Stülke and Christina Herzberg for technical assistance regarding SpoVT_{BSU} *in vitro* binding studies. We would also like to thank Prof. Simon Cutting for supplying us with the *spoVT* deletion strain of *B. subtilis*.

SUPPLEMENTARY MATERIAL

The Supplementary Material for this article can be found online at: <http://journal.frontiersin.org/article/10.3389/fmicb.2016.01607>

Figure S1 | Fluorescence microscopy analysis of cell sampling for transcriptomic analysis. The sequential stages in sporulation were monitored in time using a fluorescing membrane dye. Time points (in hours) after initiation of sporulation are indicated.

Figure S2 | Light microscopy analysis of *B. cereus* ATCC 14579 cultures approximately 24 h after entry to sporulation. Mature spores are evident in

the **(A)** wild type and **(C)** ΔBC1117 cultures, whereas the ΔSpoVT cells **(B)** have arrested during sporulation. Scale bar indicates 5 μm.

Table S1 | Primers used in this study.

Table S2 | Gene expression during sporulation in *B. cereus* and *B. cereus* ΔspoVT.

Duplicate gene expression values during three time points in sporulation (T3, T4 and T5) for the wild type (WT) and the spoVT deletion strain (delta-VT) are indicated as reads per kilobase per million (rpkm).

Table S3 | Significant up-and downregulated genes in a spoVT deletion background of *B. cereus* during T5.

Down-regulation in gene expression in the spoVT-mutant strain is visualized in red, whereas up-regulation is visualized in green. The data for two biological replicates of the same strain are shown separately. The ratio in gene expression was calculated by taking the difference of the 2log-transformed values at T5 between the wt and the spoVT mutant strain. The fold change in gene expression was calculated by raising the number 2 to the power of the absolute ratio value. Orthologs of known sporulation genes in *B. subtilis* are indicated in bold face. Regulation during sporulation in *B. subtilis* was derived from information on SporeWeb <http://sporeweb.molgenrug.nl>.

Movie S1 | Time-lapse microscopy movie for sporulating wild type *B. cereus* cells. The fluorescence shown in the right panel is derived from GFP expression driven by the P_{SpoVA} promoter.

Movie S2 | Time-lapse microscopy movie for sporulating cells of *B. cereus* delta-spoVT. The fluorescence shown in the right panel is derived from GFP expression driven by the P_{SpoVA} promoter.

REFERENCES

- Abee, T., Groot, M. N., Tempelaars, M., Zwietering, M., Moezelaar, R., and van der Voort, M. (2011). Germination and outgrowth of spores of *Bacillus cereus* group members: diversity and role of germinant receptors. *Food Microbiol.* 28, 199–208. doi: 10.1016/j.fm.2010.03.015
- Al-Hinai, M. A., Jones, S. W., and Papoutsakis, E. T. (2015). The Clostridium sporulation programs: diversity and preservation of endospore differentiation. *Microbiol. Mol. Biol. Rev.* 79, 19–37. doi: 10.1128/MMBR.00025-14
- Arnaud, M., Chastanet, A., and Débarbouillé, M. (2004). New vector for efficient allelic replacement in naturally nontransformable, low-GC-content, gram-positive bacteria. *Appl. Environ. Microbiol.* 70, 6887–6891. doi: 10.1128/aem.70.11.6887-6891.2004
- Asen, I., Djuranovic, S., Lupas, A. N., and Zeth, K. (2009). Crystal structure of SpoVT, the final modulator of gene expression during spore development in *Bacillus subtilis*. *J. Mol. Biol.* 386, 962–975. doi: 10.1016/j.jmb.2008.10.061
- Augustin, J. C. (2011). Challenges in risk assessment and predictive microbiology of foodborne spore-forming bacteria. *Food Microbiol.* 28, 209–213. doi: 10.1016/j.fm.2010.05.003
- Bagyan, I., Hobot, J., and Cutting, S. (1996). A compartmentalized regulator of developmental gene expression in *Bacillus subtilis*. *J. Bacteriol.* 178, 4500–4507.
- Black, E. P., Linton, M., McCall, R. D., Curran, W., Fitzgerald, G. F., Kelly, A. L., et al. (2008). The combined effects of high pressure and nisin on germination and inactivation of *Bacillus* spores in milk. *J. Appl. Microbiol.* 105, 78–87. doi: 10.1111/j.1365-2672.2007.03722.x
- Brown, K. L. (2000). Control of bacterial spores. *Br. Med. Bull.* 56, 158–171. doi: 10.1258/0007142001902860
- Carrera, M., Zandomeni, R. O., Fitzgibbon, J., and Sagripanti, J. L. (2007). Difference between the spore sizes of *Bacillus anthracis* and other *Bacillus* species. *J. Appl. Microbiol.* 102, 303–312. doi: 10.1111/j.1365-2672.2006.03111.x
- Chary, V. K., Meloni, M., Hilbert, D. W., and Piggot, P. J. (2005). Control of the expression and compartmentalization of σ^G activity during sporulation of *Bacillus subtilis* by regulators of σ^F and σ^E. *J. Bacteriol.* 187, 6832–6840. doi: 10.1128/jb.187.19.6832-6840.2005
- Chen, F., Mackey, A. J., Stoeckert, C. J. Jr. and Roos, D. S. (2006). OrthoMCL-DB: querying a comprehensive multi-species collection of ortholog groups. *Nucleic Acids Res.* 34, D363–D368. doi: 10.1093/nar/gkj123
- Cronin, U. P., and Wilkinson, M. G. (2008). *Bacillus cereus* endospores exhibit a heterogeneous response to heat treatment and low-temperature storage. *Food Microbiol.* 25, 235–243. doi: 10.1016/j.fm.2007.11.004
- de Hoon, M. J. L., Eichenberger, P., and Vitkup, D. (2010). Hierarchical evolution of the bacterial sporulation network. *Curr. Biol.* 20, R735–R745. doi: 10.1016/j.cub.2010.06.031
- de Vries, Y. P., Hornstra, L. M., de Vos, W. M., and Abee, T. (2004). Growth and sporulation of *Bacillus cereus* ATCC 14579 under defined conditions: temporal expression of genes for key sigma factors. *Appl. Environ. Microbiol.* 70, 2514–2519. doi: 10.1128/AEM.70.4.2514-2519.2004
- Dong, T. C., Cutting, S. M., and Lewis, R. J. (2004). DNA-binding studies on the *Bacillus subtilis* transcriptional regulator and AbrB homologue, SpoVT. *FEMS Microbiol. Lett.* 233, 247–256. doi: 10.1016/j.femsle.2004.02.013
- Dworkin, J., and Shah, I. M. (2010). Exit from dormancy in microbial organisms. *Nat. Rev. Microbiol.* 8, 890–896. doi: 10.1038/nrmicro2453
- Eijlander, R. T., Abee, T., and Kuipers, O. P. (2011). Bacterial spores in food: how phenotypic variability complicates prediction of spore properties and bacterial behavior. *Curr. Opin. Biotechnol.* 22, 180–186. doi: 10.1016/j.copbio.2010.11.009
- Eijlander, R. T., de Jong, A., Krawczyk, A. O., Holsappel, S., and Kuipers, O. P. (2014). SporeWeb: an interactive journey through the complete sporulation cycle of *Bacillus subtilis*. *Nucleic Acids Res.* 42, D685–D691. doi: 10.1093/nar/gkt1007
- Eijlander, R. T., and Kuipers, O. P. (2013). Live-cell imaging tool optimization to study gene expression levels and dynamics in single cells of *Bacillus cereus*. *Appl. Environ. Microbiol.* 79, 5643–5651. doi: 10.1128/aem.01347-13
- Fagerlund, A., Dubois, T., Økstad, O. A., Verplaetse, E., Gilois, N., Bennaceur, I., et al. (2014). SinR controls enterotoxin expression in *Bacillus thuringiensis* biofilms. *PLoS ONE* 9:e87532. doi: 10.1371/journal.pone.0087532
- Galperin, M. Y., Mekhedov, S. L., Puigbo, P., Smirnov, S., Wolf, Y. I., and Rigden, D. J. (2012). Genomic determinants of sporulation in Bacilli and Clostridia: towards the minimal set of sporulation-specific genes. *Environ. Microbiol.* 14, 2870–2890. doi: 10.1111/j.1462-2920.2012.02841.x
- Grossman, A. D. (1995). Genetic networks controlling the initiation of sporulation and the development of genetic competence in *Bacillus subtilis*. *Annu. Rev. Genet.* 29, 477–508. doi: 10.1146/annurev.ge.29.120195.002401
- Guérout-Fleury, A. M., Shazand, K., Frandsen, N., and Stragier, P. (1995). Antibiotic-resistance cassettes for *Bacillus subtilis*. *Gene* 167, 335–336.

- Hilbert, D. W., and Piggot, P. J. (2004). Compartmentalization of gene expression during *Bacillus subtilis* spore formation. *Microbiol. Mol. Biol. Rev.* 68, 234–262. doi: 10.1128/MMBR.68.2.234-262.2004
- Hornstra, L. M., de Vries, Y. P., de Vos, W. M., Abee, T., and Wells-Bennik, M. H. J. (2005). gerR, a novel ger operon involved in l-alanine- and inosine-initiated germination of *Bacillus cereus* ATCC 14579. *Appl. Environ. Microbiol.* 71, 774–781. doi: 10.1128/AEM.71.2.774-781.2005
- Horsburgh, M. J., Thackray, P. D., and Moir, A. (2001). Transcriptional responses during outgrowth of *Bacillus subtilis* endospores. *Microbiology* 147, 2933–2941. doi: 10.1099/00221287-147-11-2933
- Janes, B. K., and Stibitz, S. (2006). Routine markerless gene replacement in *Bacillus anthracis*. *Infect. Immun.* 74, 1949–1953. doi: 10.1128/IAI.74.3.1949-1953.2006
- Kunst, F., Ogasawara, N., Moszer, I., Albertini, A. M., Alloni, G., Azevedo, V., et al. (1997). The complete genome sequence of the Gram-positive bacterium *Bacillus subtilis*. *Nature* 390, 249–256.
- Lambert, E. A., Sherry, N., and Popham, D. L. (2012). *In vitro* and *In vivo* analyses of the *Bacillus anthracis* spore cortex lytic protein SleL. *Microbiology* 158, 1359–1368. doi: 10.1099/mic.0.056630-0
- Langmead, B., and Salzberg, S. L. (2012). Fast gapped-read alignment with Bowtie 2. *Nat. Methods* 9, 357–359. doi: 10.1038/nmeth.1923
- Lewis, P. J., and Marston, A. L. (1999). GFP vectors for controlled expression and dual labelling of protein fusions in *Bacillus subtilis*. *Gene* 227, 101–110.
- Li, H., Handsaker, B., Wysoker, A., Fennell, T., Ruan, J., Homer, N., et al. (2009). The sequence alignment/map format and samtools. *Bioinformatics* 25, 2078–2079. doi: 10.1093/bioinformatics/btp352
- Li, Z., and Piggot, P. J. (2001). Development of a two-part transcription probe to determine the completeness of temporal and spatial compartmentalization of gene expression during bacterial development. *Proc. Natl Acad. Sci. U.S.A.* 98, 12538–12543. doi: 10.1073/pnas.221454798
- Lindbäck, T., Mols, M., Bassett, C., Granum, P. E., Kuipers, O. P., and Kovács, A. T. (2012). CodY, a pleiotropic regulator, influences multicellular behaviour and efficient production of virulence factors in *Bacillus cereus*. *Environ. Microbiol.* 14, 2233–2246. doi: 10.1111/j.1462-2920.2012.02766.x
- Logan, N. A. (2012). *Bacillus* and relatives in foodborne illness. *J. Appl. Microbiol.* 112, 417–429. doi: 10.1111/j.1365-2672.2011.05204.x
- Lopez, D., Vilamakis, H., and Kolter, R. (2009). Generation of multiple cell types in *Bacillus subtilis*. *FEMS Microbiol. Rev.* 33, 152–163. doi: 10.1111/j.1574-6976.2008.00148.x
- Lücking, G., Stoeckel, M., Atamer, Z., Hinrichs, J., and Ehling-Schulz, M. (2013). Characterization of aerobic spore-forming bacteria associated with industrial dairy processing environments and product spoilage. *Int. J. Food Microbiol.* 166, 270–279. doi: 10.1016/j.ijfoodmicro.2013.07.004
- Masson, L., Préfontaine, G., and Brousseau, R. (1989). Transformation of *Bacillus thuringiensis* vegetative cells by electroporation. *FEMS Microbiol. Lett.* 51, 273–277.
- Mehne, F. M., Gunka, K., Eilers, H., Herzberg, C., Kaever, V., and Stülke, J. (2013). Cyclic di-AMP homeostasis in *Bacillus subtilis*: both lack and high level accumulation of the nucleotide are detrimental for cell growth. *J. Biol. Chem.* 288, 2004–2017. doi: 10.1074/jbc.M112.395491
- Mehne, F. M., Schröder-Tittmann, K., Eijlander, R. T., Herzberg, C., Hewitt, L., Kaever, V., et al. (2014). Control of the diadenylate cyclase CdAS in *Bacillus subtilis*: an autoinhibitory domain limits cyclic di-AMP production. *J. Biol. Chem.* 289, 21098–21107. doi: 10.1074/jbc.M114.562066
- Moir, A. (2006). How do spores germinate? *J. Appl. Microbiol.* 101, 526–530. doi: 10.1111/j.1365-2672.2006.02885.x
- Økstad, O. A., and Kolsto, A. B. (2011). “Food microbiology and food safety,” in *Genomics of Foodborne Bacterial Pathogens*, Vol. 29, eds M. Wiedmann and W. Zhang (Oslo: Springer Science + Business Media, LLC), 29–53. doi: 10.1007/978-1-4419-7686-4_2
- Pflughoef, K. J., Sumby, P., and Koehler, T. M. (2011). *Bacillus anthracis* sin locus and regulation of secreted proteases. *J. Bacteriol.* 193, 631–639. doi: 10.1128/JB.01083-10
- Piggot, P. J., and Hilbert, D. W. (2004). Sporulation of *Bacillus subtilis*. *Curr. Opin. Microbiol.* 7, 579–586. doi: 10.1016/j.mib.2004.10.001
- Qin, H., and Driks, A. (2013). Contrasting evolutionary patterns of spore coat proteins in two *Bacillus* species groups are linked to a difference in cellular structure. *BMC Evol. Biol.* 13:261. doi: 10.1186/1471-2148-13-261
- Ramirez-Peralta, A., Stewart, K. A., Thomas, S. K., Setlow, B., Chen, Z., Li, Y. Q., et al. (2012). Effects of the SpoVT regulatory protein on the germination and germination protein levels of spores of *Bacillus subtilis*. *J. Bacteriol.* 194, 3417–3425. doi: 10.1128/jb.00504-12
- Rudner, D. Z., and Losick, R. (2001). Morphological coupling in development: lessons from prokaryotes. *Dev. Cell* 1, 733–742. doi: 10.1016/S1534-5807(01)00094-6
- Sella, S. R., Vandenberghe, L. P., and Soccol, C. R. (2014). Life cycle and spore resistance of spore-forming *Bacillus atrophaeus*. *Microbiol. Res.* 169, 931–939. doi: 10.1016/j.micres.2014.05.001
- Setlow, P. (2003). Spore germination. *Curr. Opin. Microbiol.* 6, 550–556.
- Setlow, P. (2006). Spores of *Bacillus subtilis*: their resistance to and killing by radiation, heat and chemicals. *J. Appl. Microbiol.* 101, 514–525. doi: 10.1111/j.1365-2672.2005.02736.x
- Setlow, P. (2007). I will survive: DNA protection in bacterial spores. *Trends Microbiol.* 15, 172–180. doi: 10.1016/j.tim.2007.02.004
- Setlow, P. (2013). Summer meeting 2013 - when the sleepers wake: the germination of spores of *Bacillus* species. *J. Appl. Microbiol.* 115, 1251–1268. doi: 10.1111/jam.12343
- Stenfors Arnesen, L. P., Fagerlund, A., and Granum, P. E. (2008). From soil to gut: *Bacillus cereus* and its food poisoning toxins. *FEMS Microbiol. Rev.* 32, 579–606. doi: 10.1111/j.1574-6976.2008.00112.x
- Trapnell, C., Roberts, A., Goff, L., Pertea, G., Kim, D., Kelley, D. R., et al. (2012). Differential gene and transcript expression analysis of RNA-seq experiments with TopHat and Cufflinks. *Nat. Protoc.* 7, 562–578. doi: 10.1038/nprot.2012.016
- Turgeon, N., Laflamme, C., Ho, J., and Duchaine, C. (2008). Evaluation of the plasmid copy number in *B. cereus* spores, during germination, bacterial growth and sporulation using real-time PCR. *Plasmid* 60, 118–124. doi: 10.1016/j.plasmid.2008.05.001
- van der Voort, M., García, D., Moezelaar, R., and Abee, T. (2010). Germinant receptor diversity and germination responses of four strains of the *Bacillus cereus* group. *Int. J. Food Microbiol.* 139, 108–115. doi: 10.1016/j.ijfoodmicro.2010.01.028
- Wang, J. C., Hu, S. H., and Lin, C. Y. (2003). Lethal effect of microwaves on spores of *Bacillus* spp. *J. Food Prot.* 66, 604–609.
- Wang, R., Krishnamurthy, S. N., Jeong, J. S., Driks, A., Mehta, M., and Gingras, B. A. (2007). Fingerprinting species and strains of Bacilli spores by distinctive coat surface morphology. *Langmuir* 23, 10230–10234. doi: 10.1021/la701788d
- Wang, S. T., Setlow, B., Conlon, E. M., Lyon, J. L., Imamura, D., Sato, T., et al. (2006). The forespore line of gene expression in *Bacillus subtilis*. *J. Mol. Biol.* 358, 16–37. doi: 10.1016/j.jmb.2006.01.059
- Yudkin, M. D., and Clarkson, J. (2005). Differential gene expression in genetically identical sister cells: the initiation of sporulation in *Bacillus subtilis*. *Mol. Microbiol.* 56, 578–589. doi: 10.1111/j.1365-2958.2005.04594.x

Conflict of Interest Statement: The authors declare that the research was conducted in the absence of any commercial or financial relationships that could be construed as a potential conflict of interest.

Copyright © 2016 Eijlander, Holsappel, de Jong, Ghosh, Christie and Kuipers. This is an open-access article distributed under the terms of the Creative Commons Attribution License (CC BY). The use, distribution or reproduction in other forums is permitted, provided the original author(s) or licensor are credited and that the original publication in this journal is cited, in accordance with accepted academic practice. No use, distribution or reproduction is permitted which does not comply with these terms.



Variability in DPA and Calcium Content in the Spores of *Clostridium* Species

Jan Jamroskovic^{1,2†}, Zuzana Chromikova^{2†}, Cornelia List^{1†}, Barbora Bartova¹, Imrich Barak^{2*} and Rizlan Bernier-Latmani^{1,*}

¹ Swiss Federal Institute of Technology in Lausanne (EPFL), Lausanne, Switzerland, ² Institute of Molecular Biology, Slovak Academy of Sciences, Bratislava, Slovakia

OPEN ACCESS

Edited by:

Marc Bramkamp,
Ludwig Maximilian University
of Munich, Germany

Reviewed by:

Adam Driks,
Loyola University Chicago, USA
Ralf Moeller,
German Aerospace Center, Germany

*Correspondence:

Imrich Barak
imrich.barak@savba.sk
Rizlan Bernier-Latmani
rizlan.bernier-latmani@epfl.ch

[†]These authors have contributed
equally to this work.

Specialty section:

This article was submitted to
Microbial Physiology and Metabolism,
a section of the journal
Frontiers in Microbiology

Received: 05 August 2016

Accepted: 25 October 2016

Published: 11 November 2016

Citation:

Jamroskovic J, Chromikova Z, List C, Bartova B, Barak I and Bernier-Latmani R (2016) Variability in DPA and Calcium Content in the Spores of *Clostridium* Species. *Front. Microbiol.* 7:1791.
doi: 10.3389/fmicb.2016.01791

Spores of a number of clostridial species, and their resistance to thermal treatment is a major concern for the food industry. Spore resistance to wet heat is related to the level of spore hydration, which is inversely correlated with the content of calcium and dipicolinic acid (DPA) in the spore core. It is widely believed that the accumulation of DPA and calcium in the spore core is a fundamental component of the sporulation process for all endospore forming species. We have noticed heterogeneity in the heat resistance capacity and overall DPA/calcium content among the spores of several species belonging to *Clostridium sensu stricto* group: two *C. acetobutylicum* strains (DSM 792 and 1731), two *C. beijerinckii* strains (DSM 791 and NCIMB 8052), and a *C. collagenovorans* strain (DSM 3089). A *C. beijerinckii* strain (DSM 791) and a *C. acetobutylicum* strain (DSM 792) display low Ca and DPA levels. In addition, these two species, with the lowest average Ca/DPA content amongst the strains considered, also exhibit minimal heat resistance. There appears to be no correlation between the Ca/DPA content and the phylogenetic distribution of the *C. acetobutylicum* and *C. beijerinckii* species based either on the 16S rRNA or the spoVA gene. This finding suggests that a subset of *Clostridium sensu stricto* species produce spores with low resistance to wet heat. Additionally, analysis of individual spores using STEM-EDS and STXM revealed that DPA and calcium levels can also vary amongst individual spores in a single spore population.

Keywords: dipicolinic acid, sporulation, wet heat resistance, STXM, STEM-EDS, *Clostridium sensu stricto*, phylogeny, SpoVA

INTRODUCTION

The process of sporulation is a survival strategy for species belonging to the phylum *Firmicutes*. Bacterial endospores from this phylum, and more specifically the *Bacillales* and *Clostridiales* orders, exhibit remarkable resistance to numerous environmental insults such as heat, dessication, radiation, extremes in pH and pressure, as well as chemical oxidants. Many of clostridial spore-forming species, such as *Clostridium difficile*, *C. perfringens*, *C. botulinum*, *C. tetani*, *C. acetobutylicum*, and *C. beijerinckii*, are medically and industrially important. This group of organisms primarily uses fermentation as a metabolic strategy, but is ubiquitous in the environment and thus can be found in a wide variety of habitats, including mammalian hosts. The mechanism of sporulation is largely conserved amongst these species (Dalla Vecchia et al., 2014).

However, there are large variations in the initiation of sporulation as well as in the process of spore coat formation and germination, due to differences in the environmental niches in which these bacteria thrive (Dalla Vecchia et al., 2014; Paredes-Sabja et al., 2014).

The resistance of spores to environmental attacks is attributable to the unique morphology of the spore, which is formed by several layers: the core, the cortex, the coat, the crust, and in some cases, the exosporium. These structures protect sensitive macromolecules such as DNA and crucial proteins, included in the spore core. Dipicolinic acid (DPA), with its ability to bind and chelate Ca^{2+} ions, plays a key role in the dehydration, and mineralization of the spore core. Dehydration of the spore core is the main factor underlying the resistance of spores to wet heat (Paidhungat et al., 2000).

The process of sporulation has been extensively studied for several decades for the model organism *Bacillus subtilis*. The basic morphological structure of spores is conserved in all the endospore-forming bacteria studied. This unique structure is the basis for the resistance of spores. While some of the resistance determinants of spores have been revealed and it is known that several factors contribute to the development of each type of resistance, the precise mechanism of their action remains to be uncovered (Orsburn et al., 2008). The best-studied mechanism of spore resistance is that to UV, achieved with small-acid soluble proteins (SASPs), which bind to the spore's DNA and promote its conformational change (Setlow, 1995; Raju et al., 2006; Lee et al., 2008). Recently, it was determined that DNA was packed into crystalline nucleoids through binding by α/β type SASPs, hence protecting DNA from modification (Dittmann et al., 2015). Such protein-DNA structures allow spores to endure multiple types of environmental insults such as non-ionizing radiation, wet and dry heat, and desiccation, probably because the movement of internal molecules is restricted (Dittmann et al., 2015). In *B. subtilis*, superdormant spores were identified and were defined as spores able to withstand multiple rounds of germination conditions in the dormant state (Ghosh and Setlow, 2009; Ghosh et al., 2009).

The second most studied type of spore resistance is that to wet heat. This particular form of resistance is of major concern in the food industry because of food spoilage post sterilization. The major factor contributing to spore resistance to wet heat is water content in the spore core. In the dehydrated core, aqueous chemical reactions are inhibited, minimizing damage to biomolecules in case of exposure to thermal extremes (Setlow, 2006). It is well established that dehydration of the spore core directly correlates with its mineralization (Beaman et al., 1982). Thus, water content in the spore core is inversely proportional to the amount of DPA and Ca^{2+} (Douki et al., 2005; Setlow, 2006). DPA in the spore likely provides wet heat resistance through (a) lowering the core water content, (b) protecting proteins from denaturation from wet heat exposure, and (c) helping to stabilize DNA and to afford protection from damage (Raju et al., 2006; Setlow, 2006).

In *B. subtilis*, DPA is synthesized in the mother cell during late sporulation stages and is then taken up together with Ca^{2+} by the engulfed forespore (Tovar-Rojo et al., 2002; Li et al.,

2012). The major component responsible for DPA synthesis is the SpoVF protein complex, which consists of two subunits, SpoVFA and SpoVFB (Daniel and Errington, 1993). A *B. subtilis* *spoVF* mutant strain forms DPA-less spores that contain a high amount of water and are less heat resistant than *spoVF* spores formed in the presence of exogenous DPA (Paidhungat et al., 2000). Exposure of such spores to wet heat results in damage to spore proteins, which is directly proportional to the time of exposure to this condition. After accumulation of defects in proteins, spores may still be able to germinate but growth into viable cells is compromised (Coleman et al., 2007). Genome analysis has revealed that although some Clostridia possess a SpoVF homolog within their genome, it is not the case for species of *Clostridium sensu stricto* (cluster I) (Onyenwoke et al., 2004). In those species, DPA synthesis could be catalyzed by the EtfA protein (electron transfer flavoprotein A), as was shown for *Clostridium perfringens* (Orsburn et al., 2010).

There is strong evidence of heterogeneity in spore populations with respect to resistance of spores to thermal treatment. A single cell analysis approach, where physiology of individual spores was monitored during the incubation at 80–90°C, revealed a variable response of spores to wet heat. The release of DPA from spores itself only takes a few minutes. However, individual spores differ in the so-called lag phase, which is the period from exposure to germination conditions until the commitment of germination, the rapid release of DPA/Ca. The lag period ranges from minutes to hours for individual spores. It is presumed that the spores with the longest lag phase are the most resistant to wet heat. However, molecular, physiological, or environmental factors underpinning this variability in spore populations are poorly understood (Coleman et al., 2007; Zhang et al., 2010, 2011).

Previous studies of resistance of spores have shown that there are large differences regarding the level of resistance to various environmental insults amongst various species (Brul et al., 2011; Maillard, 2011; Paredes-Sabja et al., 2011; Xiao et al., 2011; Setlow, 2013, 2014). In the present work, we focus on several *Clostridium* species belonging to Cluster I of genus *Clostridium* (*sensu stricto*). This cluster is morphologically and physiologically the best described group of the genus *Clostridium*, which contains over 160 species divided into multiple sub-groups according to results of 16S rRNA analysis (Gupta and Gao, 2009). Here, we examine the group of industrially important species belonging to this cluster, specifically *C. acetobutylicum* DSM1731 and DSM792, *C. beijerinckii* strains DSM791 and NCIMB 8052 and *C. collagenovorans* 3089, for their level of resistance to wet heat as well as for their DPA/Ca content. The goal of the study is to evaluate the link between heat resistance and DPA/Ca content, as well as to compare DPA/Ca levels among *Clostridium* species.

MATERIALS AND METHODS

Bacterial Strains

All the strains used in this study are listed in **Table 1**. The *Clostridium* species are closely related phylogenetically (**Figure 1**).

TABLE 1 | Bacterial strains used in the study.

Strain	Source	Sporulation medium	Medium for vegetative growth
<i>B. subtilis</i> PY79	Youngman et al., 1984	DSM	LB
<i>C. acetobutylicum</i> DSM 792	Bernier-Latmani et al., 2010	FLP, CBM	CRM, 2xYTG
<i>C. acetobutylicum</i> DSM 1731	DSMZ	FLP, CBM	CRM, 2xYTG
<i>C. collagenovorans</i> DSM 3089	DSMZ	PBB	CRM, PBB
<i>C. beijerinckii</i> DSM 791	DSMZ	TGY plates, P2	CRM, TGY
<i>C. beijerinckii</i> NCIMB 8052	NCIMB	TGY plates, P2	CRM, TGY
<i>D. reducens</i> MI-1	Bernier-Latmani et al., 2010	WLP	WLP

Medium abbreviations are explained in the text.

DSMZ, German Collection of Microorganisms and Cell Cultures, Braunschweig, Germany

NCIMB, National Collection of Industrial, Food and Marine Bacteria LTD, Aberdeen, UK.

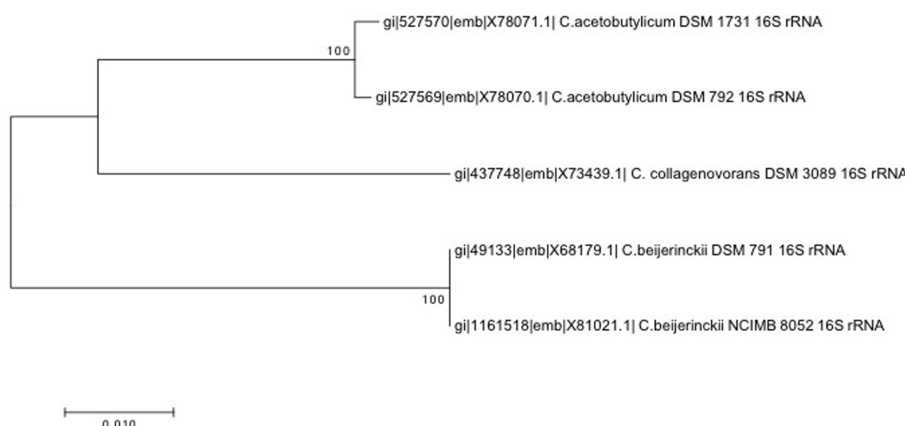


FIGURE 1 | 16S rRNA-based neighbor-joining phylogenetic tree constructed using MEGA7 with the *p*-distance method and the Bootstrap method (1000 replications).

Bacterial Growth and Spore Preparation

Clostridium acetobutylicum DSM 792 and *C. acetobutylicum* DSM 1731 were grown in anoxic conditions in clostridial reinforced media (CRM, Difco) or 2xYTG (per 1 l: Bacto-tryptone, 16 g; yeast, 10 g; sodium chloride, 5 g; glucose, 5 g). For sporulation, bacterial cultures were incubated in Francis low phosphate (FLP) basal medium (per 1 liter: CaCl₂, 0.5 g; K₂HPO₄, 0.03 g; NH₄Cl, 0.5 g; MgSO₄, 0.2 g; FeSO₄, 2.8 mg; glucose, 5 g; glycerol, 0.25 mL; peptone, 0.1 g; yeast extract, 0.1 g. pH was set at a value of 6.8) and cultures were incubated at 30°C (Bernier-Latmani et al., 2010) or on clostridium basal medium (CBM) agar plates (per 1 liter: MgSO₄ × 7H₂O, 0.25 g; MnSO₄ × H₂O, 9.5 mg; FeSO × 7H₂O, 12.5 mg; para-aminobenzoic acid, 1.25 mg; biotin, 0.0025 mg; thiamin hydrochloride, 1.25 mg; casein hydrolysate, 5 g; glucose, 50 g; K₂HPO₄, 0.63 g; KH₂PO₄, 0.63 g) (O'Brien and Morris, 1971) and incubated at 37°C. Several days of incubation on agar plates resulted in sporulation. In fact, samples on CBM agar plates contained more spores than liquid cultures. The presence of spores was confirmed by light microscopy.

Clostridium beijerinckii DSM 791 and *C. beijerinckii* NCIMB 8052 were grown in anoxic conditions in tryptone-glucose-yeast extract (TGY) medium (per 1 liter: Bacto-tryptone, 30 g; glucose, 20 g; yeast extract, 10 g; cysteine, 1 g) or CRM (Difco) at 37°C. For

spore preparation, cells were grown in TGY medium overnight and the next day 1–5% of the inoculum was transferred into P2 sporulation medium (per liter: glucose, 60 g; yeast extract, 1 g; pH was set to 6.6, resazurin, 0.5 mg; thiamine, 1 mg; biotin, 0.01 mg; K₂HPO₄, 0.5 g; KH₂PO₄, 0.5 g; CH₃COONH₄, 2.2 g; MgSO₄ × 7H₂O, 0.2 g; FeSO₄ × 7H₂O, 0.01 g; MnSO₄ × 7H₂O, 0.01 g; para-aminobenzoic acid, 1 mg) (Wang et al., 2013). The presence of spores was verified by light microscopy after several days of growth. Alternatively, a culture growing in TGY medium was spread on TGY plates and grown at 37°C in an anoxic chamber for several days, which resulted in a higher spore yield than sporulation in P2 liquid medium.

Clostridium collagenovorans DSM 3089 was grown in slightly modified PBB medium (for 1 liter: K₂HPO₄, 2.9 g; KH₂PO₄, 1.5 g; MgCl₂ × 6H₂O, 0.1 g; CaCl₂ × 2H₂O, 0.1 g; NaCl, 0.9 g; NH₄Cl, 1 g; trace mineral solution, 10 ml; vitamin solution, 10 ml; resazurin [7-hydroxy-3H-phenoxazin-3-one 10-oxide], 0.2%, pH = 7.8; gelatin, 0.5%, reduced by 0.025% of Na₂S prior to inoculation) for several days at 37°C. This medium also served as a sporulation medium. After several days of growth, the culture contained more than 80% spores without requiring specific conditions for sporulation induction.

Desulfotomaculum reducens M1-1 was grown anaerobically in liquid basal Widdel low-phosphate medium (WLP) for several

days at 37°C (Bernier-Latmani et al., 2010). No induction of sporulation condition was required. The presence of spores was verified by optical microscopy.

Bacillus subtilis PY79 and *B. subtilis* $\Delta spoVF\Delta sleB$ were grown in DSM sporulation medium (Difco) at 37°C. After 48 h of growth, the cultures consisted of 99% spores, as was verified by optical microscopy and sporulation efficiency in case of wild-type *B. subtilis*.

In all cases, spores were collected by centrifugation, washed in cold deionized water to remove the medium and stored at 4°C. The lysis of vegetative cells was carried out using osmotic stress, low temperatures, and in case of *Clostridium* and *Desulfotomaculum* species by long-term exposure to oxygen. We assumed that after several days of storage in aerobic conditions in distilled water at 4°C, all vegetative cells were dead and only spores remained. This spore preparation was used for all subsequent experiments.

Clostridium reinforcement media as a rich complex medium was used in case of all analyzed strains for enumeration of spores by MPN approach, since the quick outgrowth of spores is crucial for this method.

Scanning Transmission X-ray Microscopy (STXM) and Scanning Transmission Electron Microscopy (STEM) Analyses

Spectro-microscopic measurements and data analysis were performed as described elsewhere (Jamroskovic et al., 2014). Briefly, spore samples (2 μ L) diluted to an appropriate number of spores were loaded on carbon grids (Lacey Carbon support grids, EMS) or on silicon nitride (SiNi) non-porous TEM window grids (TEM windows, West Henrietta, NY, USA) and were left to dry completely. Silicon nitride non-porous TEM window were mounted on STXM holders with conventional double-sided sticky tape. STXM analysis was conducted at the SM-beamline end station at the Canadian Light Source (Saskatoon, Canada). Carbon speciation stacks by STXM were collected through serial image collection along C K-edge energies (280–300 eV) extended to capture the calcium LII and LIII edge peaks; thus, the entire energy range considered was 280–355 eV.

Data processing was done using the axis2000 software package (Hitchcock, 1997). Stacks were iteratively aligned to convergence by cross-correlation using the Jacobsen stack analyze algorithm (Jacobsen et al., 2000) with the highest energy image as a reference. Spectra were initially evaluated and normalized to the same thickness using axis2000 before importing into Excel for direct data manipulation. Compared spectra were scaled linearly using 283 and 287 eV as endpoints for the DPA spectra and 346 and 356 eV for calcium spectra.

Scanning Transmission Electron Microscopy with energy dispersive spectroscopy (EDS) was used to obtain elemental composition maps and to perform comparative characterization of elemental content. In this study, an X-ray EDS system (Esprit/Quantax Bruker) in STEM mode in a FEI Tecnai Osiris microscope [200 kV X-FEG field emission gun, X-ray detector (Super-X) with 4 mm \times 30 mm windowless SDD

diodes and 0.9 sr collection angle was applied]. Quantitative EDS analysis was carried out using the Cliff–Lorimer standardless method with thickness correction using K-series. The physical Bremsstrahlung background was calculated based on the sample composition. Some elements such as Cu contributing from the Cu grid were removed from quantification after the deconvolution procedure in the quantification process. Elemental concentrations in atomic % and net counts (signal above background) were derived from deconvoluted line intensities within a 95% confidence level. The process time and acquisition rates were adapted to get the most accurate data for specific element such as Ca, P, and Mn. The experimental spectra were collected with no pile-up artifacts. A correction for specimen drift was applied during acquisition to improve elemental mapping accuracy.

Spore Heat Resistance Determination

To obtain the total number of spores in each spore suspension, 0.5 ml of untreated spore suspension was resuspended in 4.5 ml of appropriate anoxic medium and number of spores was determined by MPN (most probable number) method as follows. For each spore suspension, several 10-fold serial dilutions were prepared. With each increasing dilution, the likelihood of the medium being inoculated by a spore decreases. The growth of bacteria in serial dilutions was evaluated after 2–4 days of incubation at 37°C. The number of tubes with visible turbid cultures was counted and number of spores was estimated using MPN statistic tables. The number of spores in untreated samples obtained for each spore suspension was taken as 100%. Equivalent amounts of spore suspensions (0.5 ml) were treated at 85°C for 10 and 60 min. Serial dilutions of each treated sample were performed and MPN method was used to estimate the number of surviving spores, which is expressed as a percentage of the surviving spores from the untreated sample. All experiments were done in triplicate for each sample (Sutton, 2010).

Quantification of DPA in Spores

Dipicolinic acid concentration was measured using a terbium complexation method (Rosen et al., 1997; Ammann et al., 2011). The calibration curve was prepared using three different concentrations of DPA (0.005, 0.05, and 0.5 μ M) in sterile milli-Q water and TbCl₃ at a final concentration of 30 μ M. A sample containing 30 μ M TbCl₃ was used as a blank. Samples containing various concentrations of DPA without TbCl₃ were also probed for their background photoluminescence, which was subtracted from the measurements. The photoluminescence at defined DPA concentrations was measured at least three times at an excitation/emission wavelength of 276/546 nm on a plate reader (SYNERGYMX, BioTek) and was used for calculation of the calibration curve.

A spore suspension with a known number of spores was autoclaved at 120°C for 30 min to induce the quantitative release of DPA. After autoclaving, the spore suspension was centrifuged and the supernatant was diluted several times by serial dilutions in sterile milli-Q water. TbCl₃ was added to each dilution to a final concentration of 30 μ M and the photoluminescence of terbium-DPA complexes was detected. Every sample was

measured in triplicates. The concentration of DPA per spore was calculated through normalization with the number of spores obtained by the MPN method.

RESULTS

Heat Resistance of Spores Belonging to Clostridial Species

Heat resistance testing of spores of *C. acetobutylicum* DSM 792 and *C. beijerinckii* DSM 791 revealed that they are rather sensitive to wet heat, with 4.6 and 3.9% survival, respectively, after the short wet heat treatment, and only 0.46 and 0.07% survival, respectively, after the prolonged wet heat treatment (**Table 2**).

Clostridium acetobutylicum DSM 1731 spores showed intermediate heat resistance (37% after 10 min) and it is interesting to note that the survival is identical at 60 min of wet heat exposure. This is the only *Clostridium* species probed that exhibits this type of tailing in the survival after extended periods of exposure to wet heat. To a much lesser extent, a similar tailing was observed for *C. collagenovorans* DSM 3089. This strain is the most resistant of all the *Clostridium* strains analyzed, with 100 and 2.5% survival after the short and long wet heat treatment, respectively.

A second strain of *C. beijerinckii*, NCIMB 8052, is not defined as a type strain but has been studied extensively due to its massive solvent production. Wet heat resistance properties of this strain were shown to be distinct from those of *C. beijerinckii* DSM 791 strain, since after the short heat treatment, more than 80% of the NCIMB 8052 spores recovered. However, longer wet heat treatment resulted in significantly diminished survival, only 0.36% (**Table 2**).

The two control strains, *D. reducens* and *B. subtilis*, both show complete wet heat resistance at 10 min and either complete (100%) or significant (20%) resistance after 60 min of exposure to wet heat (**Table 2**).

Overall DPA Levels in Spore Populations of Clostridia Cluster I

The content of DPA in *C. beijerinckii* DSM 791 was the lowest measured within the strains considered here. The average DPA content in spores of this strain was only 0.088 pg of DPA per spore (**Table 2**). In contrast, the spore population of the other *C. beijerinckii* strain (NCIMB 8052) was shown to contain a much higher amount of DPA than DSM 791 (4.4 pg of DPA per spore; **Table 2**). The two *C. acetobutylicum* strains exhibited DPA content ranging from 1.98 pg/spore (strain DSM 792) to 2.6 pg/spore (DSM 1731).

The biochemical analysis of DPA levels in spore population of *C. collagenovorans* shows very high levels of DPA per spore (9.25 pg of DPA/spore), which makes it the highest of all analyzed strains, including the control strains. Because the DPA measurement is carried out for the entire population rather than individual spores, the DPA content per spore does not represent a concentration but rather a total amount. As a result, the size

of the spore is an important determinant of the concentration of DPA, which in turn, is a determinant of heat resistance. Assuming that spores on **Figure 2** represent a typical size for each strain and a cylindrical shape, we computed the volume of spores and the corresponding DPA concentration for each strain (**Table 2**).

Spectromicroscopy Analysis of Individual Clostridial Spores

Raman spectroscopy has been previously used to measure Ca/DPA in single spores (Huang et al., 2007). Here, instead, we employed another single cell analysis approach, using a combination of two advanced spectro-microscopy techniques, STEM-EDS and STXM, which were recently optimized for bacterial spore research (Jamroskovic et al., 2014). Using these methods, we detected DPA and calcium absorption spectra directly in individual spores of each analyzed species. In STXM, the presence of DPA in the spore core appears as a characteristic double peak at 284.7 and 285.3 eV (Jamroskovic et al., 2014), while calcium levels in the spore core are characterized by the presence of a double peak at 349 and 352 eV according to the L_{II} and L_{III} edges of calcium (Jamroskovic et al., 2014).

Scanning Transmission Electron Microscopy-Energy Dispersive Spectroscopy system EDS analysis of the spores of *C. acetobutylicum* DSM 1731 and *C. collagenovorans* DSM 3089 revealed uniformly high levels of calcium in the spore core (8.02 and 8.58%, respectively; **Figure 2**). In contrast, *C. beijerinckii* DSM 791 was found to have very low calcium content both by STXM (**Figure 3**) and STEM-EDS (**Table 2**; **Figure 2**). Average values collected by STXM for all individual spores analyzed indicate relatively low level of DPA in spores (**Figure 3**).

Scanning Transmission X-ray Microscopy analysis of 13 *C. beijerinckii* NCIMB 8052 individual spores revealed a massive DPA peak at 285.3 eV comparable to the DPA peak from *B. subtilis* and *D. reducens* spores, and significantly higher than the DPA-specific peak of *C. beijerinckii* DSM 791 (**Figure 3**). The STXM signal for calcium was also substantially higher when compared to the calcium signal of *C. beijerinckii* DSM 791 (**Figure 3**).

During analysis of *C. beijerinckii* DSM 791 by STXM, we noticed significant heterogeneity in DPA and calcium content between individual spores in the spore population of this strain (**Figure 4**). The example of this heterogeneity is highlighted in comparison of absorption spectra for DPA and calcium in three individual spores of this strain (**Figure 4**) and the STEM-EDS for the same individual spores. In one of analyzed spores (spore 3), the second peak at 285.3 eV characteristic for DPA is missing and thus this spore resembles spores which lack DPA, like *B. subtilis* mutant strain *spoFV sleB* (Jamroskovic et al., 2014). On the other hand, spores 1 and 2 show higher peaks at 284.7 and at 285.3 eV, suggesting the presence of higher amounts of DPA. The signal for calcium (double peak at 249 and 352 eV) mimics that of DPA in all three spores. The same spores were also examined by STEM/EDS microscopy after STXM analysis (**Figure 4B**). High Angle Angular Dark Field STEM microscopy

TABLE 2 | Table of spore survival after 10 and 60 min of wet heat treatment (80°C) expressed as the percentage of spore survival (determined by the MPN method) as compared to an untreated sample.

Strain	Percent survival after heat treatment		DPA (pg) per spore	Qualitative amount of Ca by STEM-EDS and number of spores in that category and Ca atomic % ±SD		Ca in vegetative cells atomic %	Calc. spore DPA conc. (pg/μm³)
	10'	60'					
C. acetobutylicum DSM 792	4.6	0.46	1.98 ± 0.148	High	12 spores at 5.7% ±1.16	0.13	2.1
				Mid	3 spores at 2.94% ±0.50		
				Low	6 spores at 0.44% ±0.14		
C. acetobutylicum DSM 1731	37	37	2.6 ± 0.299	High	10 spores at 8.02% ±0.75	0.46	8.8
<i>C. collagenovorans</i> DSM 3089	100	2.5	9.25 ± 0.910	High	10 spores at 8.58% ±2.45	0.39	18.4
C. beijerinckii DSM 791	3.9	0.07	0.088 ± 0.0033	Low	4 spores at 1.29% ±0.26	0.05	0.3
C. beijerinckii NCIMB 8052	81.5	0.36	4.99 ± 0.377	High	10 spores at 9.04% ±0.83	0.28	4.2
				Low	2 spores at 1.14% ±0.04		
<i>D. reducens</i> MI-1	100	20	2.8 ± 0.338	High	10 spores at 7.96% ±1.47	0.20	4.2
<i>B. subtilis</i> PY79	100	100	1.35 ± 0.35	High	10 spores at 7.29% ±1.23	1.66	4.6

Dipicolinic acid (DPA) per spore was measured by bulk terbium chloride measurement. Calcium per spore was measured by Scanning Transmission Electron Microscopy to energy dispersive spectroscopy (STEM-EDS). Solventogenic strains are indicated in bold.

(HAADF-STEM) images show the morphology of these three representative spores. The spore core, which is denser, and the cortex are clearly distinguishable in all three spores. The atomic percentage of calcium in these three spores, where spore 1 was shown to contain 2.69% Ca, spore 2 contains 1.01%, and spore 3 contains 0.31% of calcium, indicates a correlation between the level of DPA and calcium in the core and thus confirms the STXM data (**Figure 4A**).

We also examined spores of two other Firmicutes, *B. subtilis* and *D. reducens* MI-1, to ascertain whether the variability in levels of DPA and calcium in the spore population is a common feature among other endospore formers. The two species examined formed phase-bright, slightly elliptical spores (**Figure 2**) and STXM and STEM-EDS data showed the presence of high levels of Ca. STXM also indicated high levels of DPA, in contrast to bulk DPA measurements that resulted in significant but not very high values (2.8 and 1.35 μg per spore) relative to the *Clostridium* species considered (**Table 2**). This discrepancy can be attributed to the difference in spore size between the genera considered. In fact, when DPA content is normalized to volume, the content in *B. subtilis* and *D. reducens* is comparable to *C. beijerinckii* NCIMB 8052, which also forms highly wet heat resistant spores.

A major result from the STEM-EDS analysis of spores from the seven strains considered is that some strains (*C. acetobutylicum* DSM 792 and *C. beijerinckii* NCIMB 8052) exhibit great variability in calcium content while other strains (*C. acetobutylicum* DSM 1731, *C. collagenovorans*, *C. beijerinckii* DSM 791, *D. reducens*, and *B. subtilis*) show a uniform distribution of calcium amongst the spore population (**Table 2**).

As noted above, it is exceedingly difficult to obtain a clean spore-only preparation for some *Clostridium* species. However, we measured calcium content in vegetative cells of the *Clostridium* species and found it to be below that in the spores (**Table 2**). Hence, calcium content values greater than the vegetative cell values along with clear spore morphology are pre-requisites for identification of spores in STEM-EDS images.

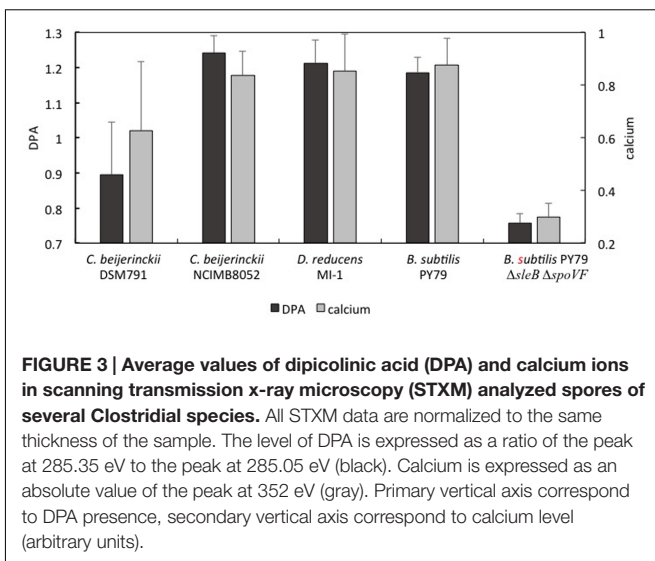
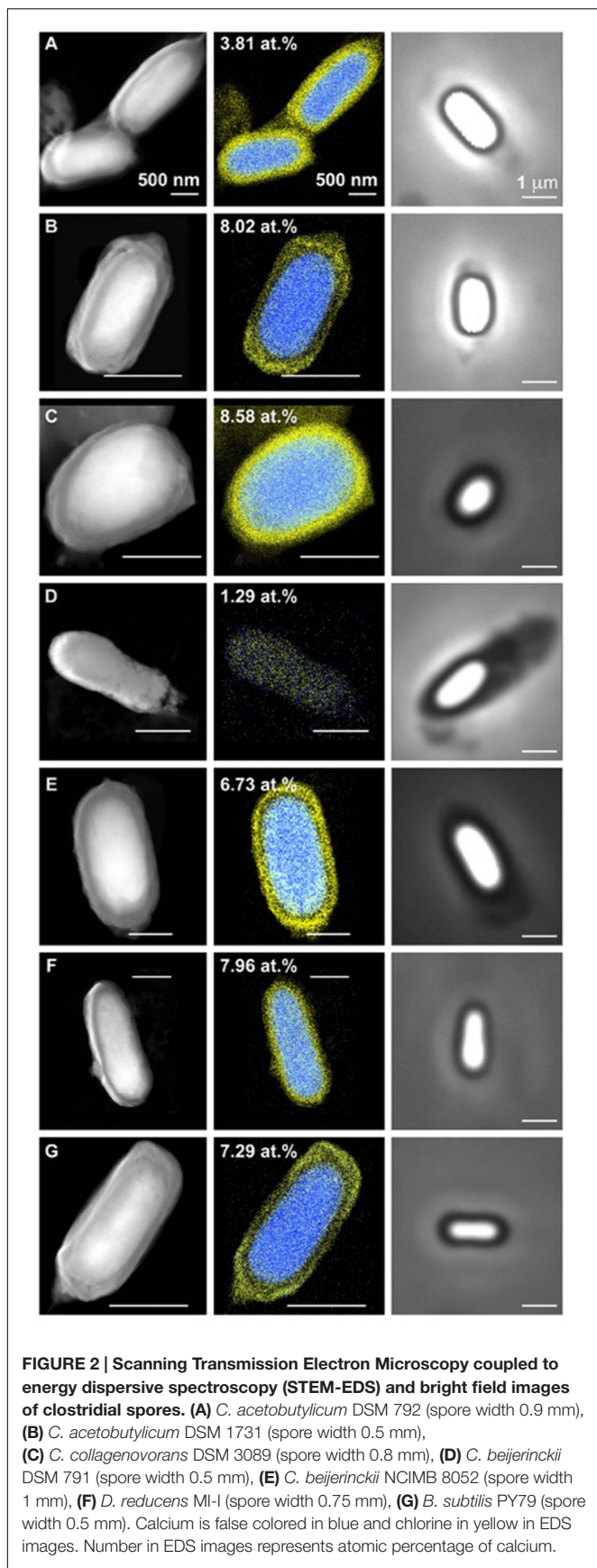
DISCUSSION

Most of the studies of spore resistance strategies have been performed on *B. subtilis* spores due to the easy acquisition and large availability of existing mutants. Here, we focused on the heat resistance properties of spores of species belonging to the genus *Clostridium sensu stricto* (Cluster I).

Species analyzed in this study are very closely related phylogenetically (**Figure 1**), but they also share the same ecological niches as they are ubiquitous in soil, water, and feces; maybe with the exception of *C. collagenovorans* which was isolated from sewage sludge (Jain and Zeikus, 1989). In fact, many *C. beijerinckii* strains were considered to be *C. acetobutylicum*, until DNA fingerprint analyses and sequencing of 16S rRNA proved otherwise (Keis et al., 1995). All of these strains are anaerobic and use a fermentative type of metabolism. *C. acetobutylicum* and *C. beijerinckii* strains also share the same physiology and are able to produce solvents in the process of solventogenesis. Solventogenesis together with sporulation belong to strategies to survive extreme acidic environment, which is induced by acid-generating metabolism of *Clostridia* (Dürre, 2009). During solventogenesis, cells utilize some of the by-product acids to produce neutral solvents, and thus the pH of the environment is restored to favorable levels. In solventogenic *Clostridia*, solventogenesis and sporulation are coincident, and are both regulated by the stationary phase regulator, Spo0A (Ravagnani et al., 2000).

C. collagenovorans DSM 3089 is also closely related to *C. acetobutylicum* (Ludwig et al., 2009) (**Figure 1**). In addition to being acetogenic, it is also able to produce an active collagenase that can hydrolyze collagen and release peptides from animal proteins (Jain and Zeikus, 1989). In contrast to all other *Clostridium* strains considered, it is not solventogenic (Jain and Zeikus, 1988).

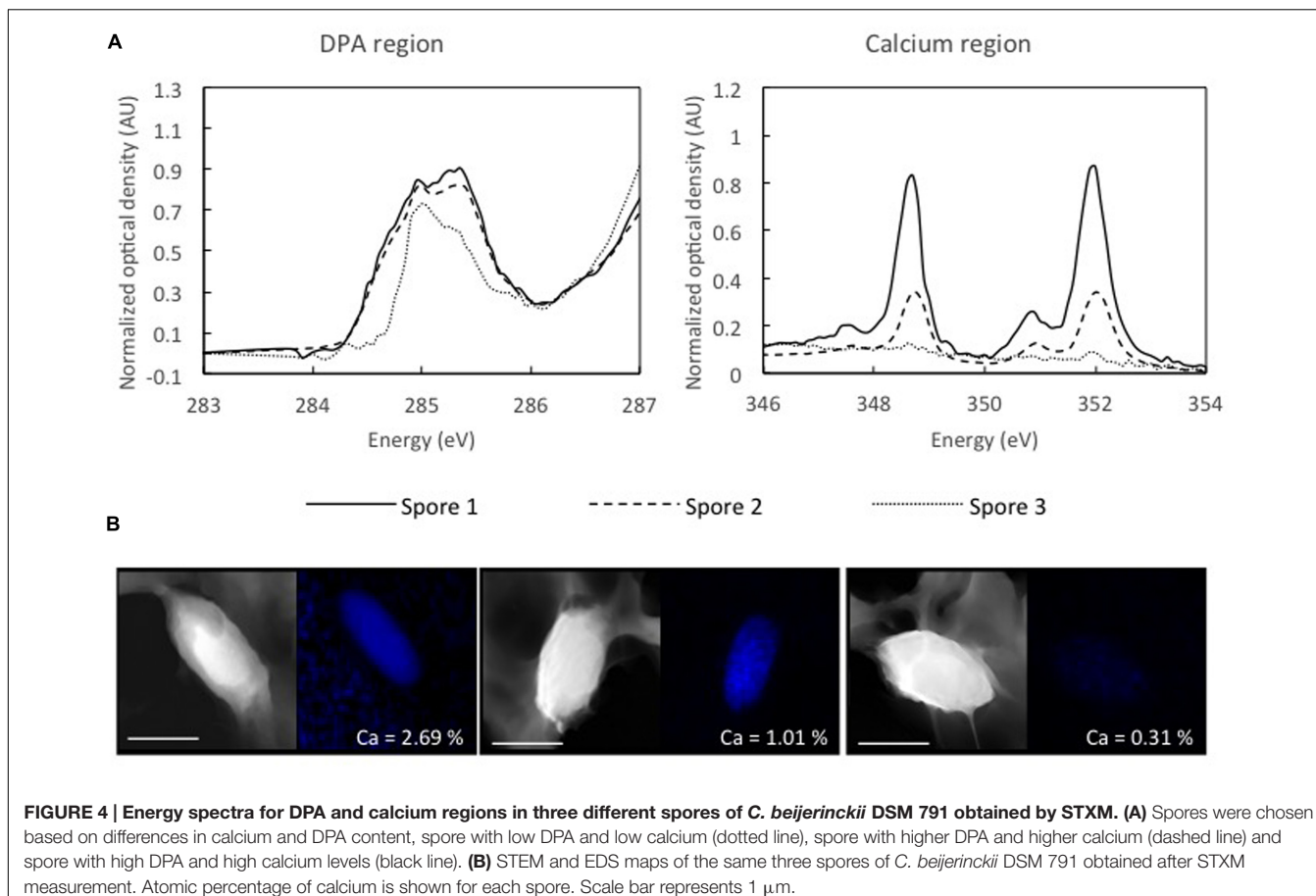
Our results show that despite the close relatedness of analyzed species, they exhibit large variability in calcium and DPA



content as well as heat resistance, regardless of phylogeny. The *Clostridium* species considered here can be divided into several groups.

First, *C. collagenovorans* DSM 3089 behaves similarly to spore-forming organisms outside of the Clostridia. It exhibits high heat resistance, and uniformly high calcium and DPA concentrations in the core. Thus, this organism represents one end of the spectrum of spore-forming organisms. The *Clostridium* species with the next lowest wet heat resistance is *C. beijerinckii* NCIMB 8052 that shows an 81.5% resistance at 10 min of exposure and 0.36% at 60 min. The DPA concentration is comparable to that of *D. reducens* and *B. subtilis* and a large percentage of the spores characterized display a high calcium concentration (Table 2). However, in contrast to *C. collagenovorans*, a few spores contain low calcium concentrations (~1 atomic %). Thus, there is sufficient intra-population variability to be identified from a relatively small sample size (12 spores).

There is a large decrease in heat resistance between the two aforementioned strains and *C. acetobutylicum* DSM 1731. Only 37% of the spores survive 10 min of heat treatment and interestingly, the same fraction survives 60 min of the same treatment. Surprisingly, the calcium and DPA concentrations are high (greater than those in *B. subtilis* and *D. reducens*). It is unclear why the wet heat resistance is much lower in the case of strain DSM 1731 than the control strains. A possible explanation for this discrepancy is that the DPA synthesis pathway is distinct for Cluster I of the *Clostridium* genus as compared to organisms outside that cluster. More specifically, the EtFA flavoprotein encoded by *etfA*, was identified as the DPA synthase in *C. perfringens*, a *Clostridium* that doesn't possess the homolog of SpoVF DPA-synthase from *B. subtilis* (Orsburn et al., 2010). In fact, homologs of SpoVF are missing throughout the whole Cluster I of the *Clostridium* genus and it is very likely that in these species EtFA functions as the only DPA synthase. It is unclear whether this difference in pathway may also impact the



timing of the production of the DPA and how it is distributed within the spore.

Finally, *C. beijerinckii* DSM 791 and *C. acetobutylicum* DSM 792 have very low wet heat resistance (3.9 and 4.6% survival after 10 min, respectively). For *C. beijerinckii* DSM 791, the low wet heat resistance is combined with low DPA and calcium concentrations (**Table 2**). Additionally, in the same strain, there is negligible heat resistance at 60 min of heat exposure, confirming the findings at 10 min. Thus, in this case, low calcium and DPA appear to correspond to low wet heat resistance. While the STEM-EDS results indicated relatively uniform Ca concentrations within the spore population, the STXM data (accompanied by the STEM-EDS data for the same spores) evidenced individual variability with a range of DPA concentrations and Ca concentrations ranging from 0.31 to 2.69 atomic %. Thus, the DPA and Ca are low but display some variability.

For *C. acetobutylicum* DSM 792, we found a wide distribution of calcium concentrations in spores (**Table 2**). A large fraction (57%) of the spores characterized exhibited an average calcium content of 5.7 atomic % while the rest contained an average of 2.94 atomic % for three spores and 0.4 atomic % for six spores. The average spore DPA concentration was 2.1 pg/μm³, approximately half that of the control strains *D. reducens* and *B. subtilis*.

Thus, results obtained from wet heat testing of spores of various clostridial species suggest that DPA/Ca content in spores is correlated to their wet heat resistance level, particularly with respect to short exposure to the treatment. After longer exposure to wet heat (~ 60 min), spores survival decrease dramatically in all strains, with the exception of *C. acetobutylicum* DSM 1731. In this strain, the survival of spores is identical after short wet heat treatment, thus, the survivors retain a relatively high ability to germinate and recover even after prolonged exposure to wet heat.

The relatively low DPA/Ca concentrations in *C. acetobutylicum* DSM 792 and *C. beijerinckii* DSM 791 spores could potentially be a consequence of environmental adaptation. However, the four strains *C. acetobutylicum* and *C. beijerinckii* strains considered in this study have essentially the same type of metabolism (fermentative and solventogenic), and all live in similar environments. Thus, there is little evidence that environmental conditions may lead to this difference.

Another hypothesis was that the strains that produce butanol rather than ethanol may produce more resistant spores. Indeed, *C. acetobutylicum* DSM 1731 and *C. beijerinckii* NCIMB 8052 are known to be some of the most efficient at producing butanol amongst the solventogenic Clostridia (Chua et al., 2013). Thus, we propose that difference in solvent yields amongst the strains

considered may explain the heat resistance and Ca/DPA content discrepancies.

As discussed above, in all Clostridia belonging to Cluster I, EtfA, an electron transfer flavoprotein, is likely the physiological DPA synthase. Some species of this cluster actually contain more homologs of *etfA* in the genome, roles of which are not assigned up to date (Orsburn et al., 2010). The function of EtfA may also include the production of butanol (Boynton et al., 1996). Thus, solventogenic strains that produce abundant butanol (DSM 1731 and NCIMB 8052) may also produce abundant DPA through the activity of EtfA. This link between metabolism and sporulation could also explain the heterogeneity in average DPA content of spores amongst strains, which are otherwise closely related phylogenetically. We can speculate that the heterogeneity in DPA/Ca content of spores within a given spore population may be attributable to differences in expression level of *etfA* prior to sporulation.

Bacillus subtilis, the model organism for the study of physiological and morphological processes in spore formers, also possesses the *etf* locus (*etfA* and *etfB*) in the genome. The function of EtfA flavoprotein in *B. subtilis* resembles the one in solventogenic Clostridia in several aspects. Not only is this protein in *B. subtilis* also involved in fatty acid synthesis, but it also plays a role in de-acidification or the internal environment of the cell by oxidizing NADH and consuming excess protons, thus maintaining the proton motive force of cellular respiration and membrane potential of the cell (Barabesi et al., 2007; Marvasti et al., 2010). While in solventogenic Clostridia the *etf* locus is located in the same operon as solventogenic genes, in *B. subtilis* the *etf* locus is part of *lfA* operon, which is involved in process of calcite formation during biofilm development (Barabesi et al., 2007). Although it may seem that the function of *etfA* differs greatly in the two systems, a connection can be found: the transfer of electrons between NADH/NAD⁺ and consequent regulation of complicated redox reactions. Products of the *etf* operon are thus involved in processes associated with pH homeostasis in the cell, such as solventogenesis in Clostridia, where repeated oxidizing of NADH to NAD⁺ favors formation of reaction intermediates which lead to the production of neutral solvents rather than volatile acids. Because of the buffering properties of calcium carbonate, the precipitation of calcite as a result

of *B. subtilis* metabolism is also a way to maintain the intracellular and extracellular pH within the boundaries suitable for neutrophiles.

It is interesting to note that the only non-solventogenic *Clostridium* strain considered here, *C. collagenovorans*, exhibits the highest Ca and DPA concentrations and the highest spore survival rate to heat treatment among Clostridia.

Overall, this study shows that there is great variability in the calcium, DPA concentrations in *Clostridium* Cluster I spores and that those concentrations correlate well with spore heat resistance. In addition, heat resistance also appears to correlate with the type of metabolism supported by specific organisms. Solventogenic strains generally harbor less DPA/Ca than non-solventogenic strains and within solventogenic strains, the ones producing more butanol appear to harbor more Ca/DPA and hence present greater heat resistance. We propose that the link between DPA synthesis and butanol production is through the *etfA* gene that serves in both pathways. Additional works is required to pinpoint the mechanistic underpinnings of this finding.

AUTHOR CONTRIBUTIONS

JJ carried out the STXM work and initiated the project. ZC and CL carried out most of the experimental work. BB did the electron microscopy. IB and RB-L designed the project and RB-L, ZC, and IB wrote the manuscript.

ACKNOWLEDGMENTS

This work was supported by grant from FNSNF (SCOPES IZ 73Z0_152527/1) to RB-L and IB, by grant VEGA 2/0009/13 from the Slovak Academy of Sciences to IB, by grant APVV-14-0181 to IB and grant ESKAS 2013.0198 to JJ. STXM measurements were performed at the Canadian Light Source, which is supported by the Natural Sciences and Engineering Research Council of Canada, the National Research Council Canada, the Canadian Institutes of Health Research, the Province of Saskatchewan, Western Economic Diversification Canada, and the University of Saskatchewan.

REFERENCES

- Ammann, A. B., Kölle, L., and Brandl, H. (2011). Detection of bacterial endospores in soil by terbium fluorescence. *Int. J. Microbiol.* 2011:435281. doi: 10.1155/2011/435281
- Barabesi, C., Galizzi, A., Mastromei, G., Rossi, M., Tamburini, E., and Perito, B. (2007). *Bacillus subtilis* gene cluster involved in calcium carbonate biomineralization. *J. Bacteriol.* 189, 228–235. doi: 10.1128/JB.01450-06
- Beaman, T. C., Greenamyre, J. T., Corner, T. R., Pankratz, H. S., and Gerhardt, P. (1982). Bacterial spore heat resistance correlated with water content, wet density, and protoplast/sporoplast volume ratio. *J. Bacteriol.* 150, 870–877.
- Bernier-Latmani, R., Veeramani, H., Vecchia, E. D., Junier, P., Lezama-Pacheco, J. S., Suvorova, E. I., et al. (2010). Non-uraninite products of microbial U(VI) reduction. *Environ. Sci. Technol.* 44, 9456–9462. doi: 10.1021/es101675a
- Boynton, Z. L., Bennet, G. N., and Rudolph, F. B. (1996). Cloning, sequencing, and expression of clustered genes encoding beta-hydroxybutyryl-coenzyme A (CoA) dehydrogenase, crotonase, and butyryl-CoA dehydrogenase from *Clostridium acetobutylicum* ATCC 824. *J. Bacteriol.* 178, 3015–3024.
- Brul, S., van Beilen, J., Caspers, M., O'Brien, A., de Koster, C., Oomes, S., et al. (2011). Challenges and advances in systems biology analysis of *Bacillus* spore physiology: molecular differences between an extreme heat resistant spore forming *Bacillus subtilis* food isolate and a laboratory strain. *Food Microbiol.* 28, 221–227. doi: 10.1016/j.fm.2010.06.011
- Chua, T. K., Liang, D.-W., Qi, C., Yang, K.-L., and He, J. (2013). Characterization of a butanol-acetone-producing *Clostridium* strain and identification of its solventogenic genes. *Bioresour. Technol.* 135, 372–378. doi: 10.1016/j.biortech.2012.08.085

- Coleman, W. H., Chen, D., Li, Y. Q., Cowan, A. E., and Setlow, P. (2007). How moist heat kills spores of *Bacillus subtilis*. *J. Bacteriol.* 189, 8458–8466. doi: 10.1128/JB.01242-07
- Dalla Vecchia, E., Visser, M., Stams, A. J., and Bernier-Latmani, R. (2014). Investigation of sporulation in the *Desulfotomaculum* genus: a genomic comparison with the genera *Bacillus* and *Clostridium*. *Environ. Microbiol. Rep.* 6, 756–766. doi: 10.1111/1758-2229.12200
- Daniel, R. A., and Errington, J. (1993). Cloning, DNA sequence, functional analysis and transcriptional regulation of the genes encoding dipicolinic acid synthetase required for sporulation in *Bacillus subtilis*. *J. Mol. Biol.* 232, 468–483. doi: 10.1006/jmbi.1993.1403
- Dittmann, C., Han, H.-M., Grabenbauer, M., and Laue, M. (2015). Dormant *Bacillus* spores protect their DNA in crystalline nucleoids against environmental stress. *J. Struct. Biol.* 191, 156–164. doi: 10.1016/j.jsb.2015.06.019
- Douki, T., Setlow, B., and Setlow, P. (2005). Photosensitization of DNA by dipicolinic acid, a major component of spores of *Bacillus* species. *Photochem. Photobiol. Sci.* 4, 591–597. doi: 10.1039/b503771a
- Dürre, P. (2009). “Metabolic networks in *Clostridium acetobutylicum*: interaction of sporulation, solventogenesis and toxin formation,” in *Clostridia. Molecular Biology in the Post-genomic Era*, eds H. Brüggemann and G. Gottschalk (Norfolk: Caister Academic Press), 215–227.
- Ghosh, S., and Setlow, P. (2009). Isolation and characterization of superdormant spores of *Bacillus* species. *J. Bacteriol.* 191, 1787–1797. doi: 10.1128/JB.01668-08
- Ghosh, S., Zhang, P., Li, Y., and Setlow, P. (2009). Superdormant spores of *Bacillus* species have elevated wet-heat resistance and temperature requirements for heat activation. *J. Bacteriol.* 191, 5584–5591. doi: 10.1128/JB.00736-09
- Gupta, R. S., and Gao, B. (2009). Phylogenomic analyses of clostridia and identification of novel protein signatures that are specific to the genus *Clostridium sensu stricto* (cluster I). *Int. J. Syst. Evol. Microbiol.* 59, 285–294. doi: 10.1099/ijss.0.001792-0
- Hitchcock, A. P. (1997). *AXIS2000 Software, Last Version 2016*. Available at: <http://unicorn.mcmaster.ca/xAxis2000.html>
- Huang, S. S., Chen, D., Pelczar, P. L., Vepachedu, V. R., Setlow, P., and Yong-qing, L. (2007). Levels of Ca2+-dipicolinic acid in individual *Bacillus* spores determined using microfluidic Raman tweezers. *J. Bacteriol.* 189, 4681–4687. doi: 10.1128/jb.00282-07
- Jacobsen, C., Wirick, S., Flynn, G., and Zimba, C. (2000). Soft X-ray spectroscopy from image sequences with sub-100 nm spatial resolution. *J. Microsc.* 197, 173–184. doi: 10.1046/j.1365-2818.2000.00640.x
- Jain, M. K., and Zeikus, J. G. (1988). Taxonomic distinction of two new protein specific, hydrolytic anaerobes: isolation and characterization of *Clostridium proteolyticum* sp. nov. and *Clostridium collagenovorans* sp. nov. *Syst. Appl. Microbiol.* 10, 134–141. doi: 10.1016/S0723-2020(88)80027-4
- Jain, M. K., and Zeikus, J. G. (1989). Bioconversion of gelatin to methane by coculture of *Clostridium collagenovorans* and *Methanosarcina barkeri*. *Appl. Environ. Microbiol.* 55, 366–371.
- Jamroskovic, J., Shao, P., Suvorova, E., Barak, I., and Bernier-Latmani, R. (2014). Combined scanning transmission X-ray and electron microscopy for the characterization of bacterial endospores. *FEMS Microbiol. Lett.* 358, 188–193. doi: 10.1111/1574-6968.12539
- Keis, S., Bennett, C. F., Ward, V. K., and Jones, D. T. (1995). Taxonomy and phylogeny of industrial solvent-producing clostridia. *Int. J. Syst. Bacteriol.* 45, 693–705. doi: 10.1099/00207713-45-4-693
- Lee, K. S., Bumbaca, D., Kosman, J., Setlow, P., and Jedrzejas, M. J. (2008). Structure of a protein-DNA complex essential for DNA protection in spores of *Bacillus* species. *Proc. Natl. Acad. Sci. U.S.A.* 105, 2806–2811. doi: 10.1073/pnas.0708244105
- Li, Y., Davis, A., Korza, G., Zhang, P., Li, Y. Q., Setlow, B., et al. (2012). Role of a SpoVA protein in dipicolinic acid uptake into developing spores of *Bacillus subtilis*. *J. Bacteriol.* 194, 1875–1884. doi: 10.1128/JB.00062-12
- Ludwig, W., Schleifer, K., and Whitman, B. W. (2009). “Taxonomic outline of the phylum Firmicutes,” in *Bergey’s Manual of Systematic Bacteriology*, 2nd Edn, Vol. 3, eds P. de Vos, G. M. Garrity, D. Jones, N. R. Krieg, W. Ludwig, F. Rainey, et al. (New York, NY: Springer).
- Maillard, J.-Y. (2011). Innate resistance to sporicides and potential failure to decontaminate. *J. Hosp. Infect.* 77, 204–209. doi: 10.1016/j.jhin.2010.06.028
- Marvasti, M., Visscher, P. T., Perito, B., Mastromei, G., and Casillas-Martínez, L. (2010). Physiological requirements for carbonate precipitation during biofilm development of *Bacillus subtilis* etfA mutant. *FEMS Microbiol. Ecol.* 71, 341–350. doi: 10.1111/j.1574-6941.2009.00805.x
- O’Brien, R. W., and Morris, J. G. (1971). Oxygen and the growth and metabolism of *Clostridium acetobutylicum*. *J. Gen. Microbiol.* 68, 307–318. doi: 10.1099/00221287-68-3-307
- Onyenwoke, R. U., Brill, J. A., Farahi, K., and Wiegel, J. (2004). Sporulation genes in members of the low G+C Gram-typepositive phylogenetic branch (Firmicutes). *Arch. Microbiol.* 182, 182–192. doi: 10.1007/s00203-004-0696-y
- Orsburn, B. C., Melville, S. B., and Popham, D. L. (2008). Factors contributing to heat resistance of *Clostridium perfringens* endospores. *Appl. Environ. Microbiol.* 74, 3328–3335.
- Orsburn, B. C., Melville, S. B., and Popham, D. L. (2010). Etfa catalyses the formation of dipicolinic acid in *Clostridium perfringens*. *Mol. Microbiol.* 75, 178–186. doi: 10.1111/j.1365-2958.2009.06975.x
- Paidhungat, M., Setlow, B., Dricks, A., and Setlow, P. (2000). Characterization of spores of *Bacillus subtilis* which lack dipicolinic acid. *J. Bacteriol.* 182, 5505–5512. doi: 10.1128/JB.182.19.5505-5512.2000
- Paredes-Sabja, D., Setlow, P., and Sarker, M. R. (2011). Germination of spores of *Bacillales* and *Clostridiales* species: mechanisms and proteins involved. *Trends Microbiol.* 19, 85–94. doi: 10.1016/j.tim.2010.10.004
- Paredes-Sabja, D., Shen, A., and Sorg, J. A. (2014). *Clostridium difficile* spore biology: sporulation, germination, and spore structural proteins. *Trends Microbiol.* 22, 406–416. doi: 10.1016/j.tim.2014.04.003
- Raju, D., Walters, M., Setlow, P., and Sarker, M. R. (2006). Investigating the role of small, acid-soluble spore proteins (SASPs) in the resistance of *Clostridium perfringens* spores to heat. *BMC Microbiol.* 6:50. doi: 10.1186/1471-2180-6-50
- Ravagnani, A., Jennert, K. C. B., Steiner, E., Grunberg, R., Jefferies, J. R., Wilkinson, S. R., et al. (2000). SpoA directly controls the switch from acid to solvent production in solvent-forming Clostridia. *Mol. Microbiol.* 37, 1172–1185. doi: 10.1046/j.1365-2958.2000.02071.x
- Rosen, D. L., Sharpless, C., and McGown, L. B. (1997). Bacterial endospore detection and determination by use of terbium dipicolinate photoluminescence. *Anal. Chem.* 69, 1082–1085. doi: 10.1021/ac960939w
- Setlow, P. (1995). Mechanisms for the prevention of damage to DNA in spores of *Bacillus* species. *Annu. Rev. Microbiol.* 49, 29–54. doi: 10.1146/annurev.mi.49.100195.000333
- Setlow, P. (2006). Spores of *Bacillus subtilis*: their resistance to and killing by radiation, heat and chemicals. *J. Appl. Microbiol.* 101, 514–525. doi: 10.1111/j.1365-2672.2005.02736.x
- Setlow, P. (2013). Summer meeting 2013 – when the sleepers wake: the germination of spores of *Bacillus* species. *J. Appl. Microbiol.* 115, 1251–1268. doi: 10.1111/jam.12343
- Setlow, P. (2014). Spore resistance properties. *Microbiol. Spectr.* 2:TBS-0003-2012. doi: 10.1128/microbiolspec.TBS-0003-2012
- Sutton, S. (2010). The most probable number method and its uses in enumeration, qualification, and validation. *J. Valid Technol.* 16, 35–38.
- Tovar-Rojo, F., Chander, M., Setlow, B., and Setlow, P. (2002). The products of the spoVA operon are involved in dipicolinic acid uptake into developing spores of *Bacillus subtilis*. *J. Bacteriol.* 184, 584–587. doi: 10.1128/JB.184.2.584-587.2002
- Wang, Y., Li, X., and Blaschek, H. P. (2013). Effects of supplementary butyrate on butanol production and the metabolic switch in *Clostridium beijerinckii* NCIMB 8052: genome-wide transcriptional analysis with RNA-Seq. *Biotechnol. Biofuels* 6:138. doi: 10.1186/1754-6834-6-138
- Xiao, Y., Francke, C., Abee, T., and Wells-Bennik, M. H. (2011). Clostridial spore germination versus bacilli: genome mining and current insights. *Food Microbiol.* 28, 266–274. doi: 10.1016/j.fm.2010.03.016
- Youngman, P., Perkins, J. B., and Losick, R. (1984). Construction of a cloning site near one end of Tn917 into which foreign DNA may be inserted without affecting transposition in *Bacillus subtilis* or expression of the transposon-borne erm gene. *Plasmid* 12, 1–9. doi: 10.1016/0147-619X(84)90061-1
- Zhang, P., Kong, L., Setlow, P., and Li, Y. Q. (2010). Characterization of wet heat inactivation of single spores of *Bacillus* species by dual-trap Raman spectroscopy and elastic light scattering. *Appl. Environ. Microbiol.* 76, 1796–1805. doi: 10.1128/AEM.02851-09
- Zhang, P., Kong, L., Wang, G., Setlow, P., and Li, Y.-Q. (2011). Monitoring the wet-heat inactivation dynamics of single spores of *Bacillus* species using Raman

tweezers, differential interference contrast and nucleic acid dye fluorescence microscopy. *Appl. Environ. Microbiol.* 77, 4754–4769. doi: 10.1128/AEM.00194-11

Conflict of Interest Statement: The authors declare that the research was conducted in the absence of any commercial or financial relationships that could be construed as a potential conflict of interest.

Copyright © 2016 Jamroskovic, Chromikova, List, Bartova, Barak and Bernier-Latmani. This is an open-access article distributed under the terms of the Creative Commons Attribution License (CC BY). The use, distribution or reproduction in other forums is permitted, provided the original author(s) or licensor are credited and that the original publication in this journal is cited, in accordance with accepted academic practice. No use, distribution or reproduction is permitted which does not comply with these terms.



Chemical and Stress Resistances of *Clostridium difficile* Spores and Vegetative Cells

Adrienne N. Edwards, Samiha T. Karim, Ricardo A. Pascual, Lina M. Jowhar,
Sarah E. Anderson and Shonna M. McBride*

Emory Antibiotic Resistance Center, Department of Microbiology and Immunology, Emory University School of Medicine, Atlanta, GA, USA

OPEN ACCESS

Edited by:

Neil Fairweather,
Imperial College London, UK

Reviewed by:

Wieg Klaas Smits,
Leiden University, Netherlands
Marcin Dembek,
Newcastle University, UK

***Correspondence:**

Shonna M. McBride
shonna.mcbride@emory.edu

Specialty section:

This article was submitted to
Microbial Physiology and Metabolism,
a section of the journal
Frontiers in Microbiology

Received: 30 June 2016

Accepted: 12 October 2016

Published: 26 October 2016

Citation:

Edwards AN, Karim ST, Pascual RA, Jowhar LM, Anderson SE and McBride SM (2016) Chemical and Stress Resistances of *Clostridium difficile* Spores and Vegetative Cells. *Front. Microbiol.* 7:1698.
doi: 10.3389/fmicb.2016.01698

Clostridium difficile is a Gram-positive, sporogenic and anaerobic bacterium that causes a potentially fatal colitis. *C. difficile* enters the body as dormant spores that germinate in the colon to form vegetative cells that secrete toxins and cause the symptoms of infection. During transit through the intestine, some vegetative cells transform into spores, which are more resistant to killing by environmental insults than the vegetative cells. Understanding the inherent resistance properties of the vegetative and spore forms of *C. difficile* is imperative for the development of methods to target and destroy the bacterium. The objective of this study was to define the chemical and environmental resistance properties of *C. difficile* vegetative cells and spores. We examined vegetative cell and spore tolerances of three *C. difficile* strains, including 630Δerm, a 012 ribotype and a derivative of a past epidemic strain; R20291, a 027 ribotype and current epidemic strain; and 5325, a clinical isolate that is a 078 ribotype. All isolates were tested for tolerance to ethanol, oxygen, hydrogen peroxide, butanol, chloroform, heat and sodium hypochlorite (household bleach). Our results indicate that 630Δerm vegetative cells (630 spo0A) are more resistant to oxidative stress than those of R20291 (R20291 spo0A) and 5325 (5325 spo0A). In addition, 5325 spo0A vegetative cells exhibited greater resistance to organic solvents. In contrast, 630Δerm spores were more sensitive than R20291 or 5325 spores to butanol. Spores from all three strains exhibited high levels of resistance to ethanol, hydrogen peroxide, chloroform and heat, although R20291 spores were more resistant to temperatures in the range of 60–75°C. Finally, household bleach served as the only chemical reagent tested that consistently reduced *C. difficile* vegetative cells and spores of all tested strains. These findings establish conditions that result in vegetative cell and spore elimination and illustrate the resistance of *C. difficile* to common decontamination methods. These results further demonstrate that the vegetative cells and spores of various *C. difficile* strains have different resistance properties that may impact decontamination of surfaces and hands.

Keywords: *Clostridium difficile*, *Clostridium difficile* infection (CDI), anaerobe, spores, resistance, germination, sporulation

INTRODUCTION

Clostridium difficile infection (CDI) is a serious, sometimes fatal, gastrointestinal (GI) disease that has emerged as a major healthcare concern in many hospitals, acute care and long-term care facilities (Rupnik et al., 2009; Dubberke and Olsen, 2012; CDC, 2013; Smits et al., 2016). Susceptibility to CDI can be induced by antibiotic treatment, which disrupts the native intestinal microbiota, creating a niche in which *C. difficile* thrives (Theriot and Young, 2015; Theriot et al., 2016). *C. difficile* spores enter the host by ingestion and germinate into vegetative cells when exposed to bile salts in the GI tract (Sorg and Sonenshein, 2008). *C. difficile* vegetative cells then produce multiple toxins that result in the characteristic diarrhea of CDI (Voth and Ballard, 2005; Shen, 2012; Janoir, 2016). As *C. difficile* vegetative cells transit through the host GI tract, a subset of the cells undergo sporulation, resulting in the formation of dormant spores that are shed in feces, along with vegetative cells (Koenigsknecht et al., 2015). Although CDI is a toxin-mediated disease, the ability for *C. difficile* to form spores is an important virulence factor because the spore serves as the infectious agent and facilitates efficient transmission from host-to-host (Deakin et al., 2012). The physical composition of the spore allows long-term persistence in the environment and confers resistance against desiccation, standard disinfectants and cleaning routines (Driks, 2002, 2003; Ali et al., 2011; Vohra and Poxton, 2011; Dubberke, 2012; Setlow, 2014).

The basic structure of *C. difficile* spores is similar to the spores of *Bacillus subtilis* and other related organisms, with the exception of the exosporium, the outermost layer of the *C. difficile* spore, which is absent in most spore formers (Pizarro-Guajardo et al., 2014, 2016a,b). The spore core, which contains the DNA and other cellular components, is layered by the inner and outer membranes, the cortex and the spore coat (reviewed in Paredes-Sabja et al., 2014). Many orthologs to key proteins that constitute the *B. subtilis* cortex and spore coat are not encoded in *C. difficile* (Henriques and Moran, 2007; Fimlaid et al., 2013), and the receptors and regulatory pathways that govern spore germination are not well conserved (Paredes et al., 2005; de Hoon et al., 2010; Francis et al., 2013; Bhattacharjee et al., 2016), further highlighting the differences between *C. difficile* spores and other bacterial spores. As the individual spore components provide resistance to different stresses (Russell, 1990), from survival in the environment to reactivation within the mammalian gut, elucidating the physical restraints of the *C. difficile* spore is paramount for understanding *C. difficile* biology and developing approaches for the eradication of *C. difficile* in clinical environments.

The purpose of this study was to characterize the resistance properties of the vegetative cells and spores of three *C. difficile* strains, including a derivative of a historical epidemic strain ($630\Delta erm$; 012 ribotype), a current epidemic strain (R20291; 027 ribotype) and a strain that is frequently found in animals and humans (5325; 078 ribotype). We observed that each strain has unique resistance properties that likely contribute to their ability to persist as circulating clinical isolates. Our results emphasize the importance of strain variation in *C. difficile* clinical isolates and

provide additional evidence for stringent approaches to eradicate *C. difficile* spores and vegetative cells from surfaces.

MATERIALS AND METHODS

Bacterial Strains and Growth Conditions

The bacterial strains used in this study are described in Table 1. All *C. difficile* strains were routinely cultured in brain heart infusion-supplemented (BHIS) medium at 37°C in a Coy anaerobic chamber (Bouillaut et al., 2011; Edwards et al., 2013) unless otherwise indicated below.

Construction of 5325 *spoOA* Mutant

The pJS107-*spoOA*178TT plasmid containing the group II intron retargeted to the *spoOA* locus was conjugated into strain 5325 (ATCC BAA-1875, ribotype 078; Ho and Ellermeier, 2011; Fimlaid et al., 2013). Thiamphenicol-resistant colonies containing the pJS107-*spoOA*178TT plasmid were transferred to BHIS plates supplemented with 5 µg ml⁻¹ erythromycin. Erythromycin-resistant colonies were isolated and screened for the 2 kb insertion in the *spoOA* locus using primers oMC444 and oMC1122.

Vegetative Viability Assays

To determine the susceptibility of vegetative cells to a variety of chemical and environmental conditions, the respective *spoOA* mutants of strains $630\Delta erm$, R20291 and 5325 were cultured overnight in BHIS medium. Cultures were grown to mid-exponential phase (OD₆₀₀ ~0.5) and diluted 1:10 into fresh BHIS.

TABLE 1 | Bacterial strains and plasmids.

Plasmid or Strain	Relevant genotype or features	Source, construction or reference
Strains		
<i>Escherichia coli</i>		
HB101	F ⁻ <i>mcrB mrr hsdS20(r_B⁻ m_B⁻) recA13 leuB6 ara-14 proA2 lacY1 galK2 xyl-5 mtl-1 rpsL20</i>	B. Dupuy
MC306	HB101 pRK24 pJS107- <i>spoOA</i> 178TT	Fimlaid et al., 2013
<i>Clostridium difficile</i>		
5325	BAA-1875; ribotype 078	ATCC
$630\Delta erm$	Erm ^S derivative of strain 630; ribotype 012	N. Minton; Hussain et al., 2005
R20291	Clinical isolate; ribotype 027	Stabler et al., 2009
R20291 <i>spoOA</i>	R20291 <i>spoOA::erm</i>	Dawson et al., 2012
MC310 (630 <i>spoOA</i>)	630 Δerm <i>spoOA::erm</i>	Edwards et al., 2014
MC724 (5325 <i>spoOA</i>)	5325 <i>spoOA::erm</i>	This study
Plasmids		
pRK24	Tra ⁺ , Mob ⁺ ; <i>bla, tet</i>	Thomas and Smith, 1987
pS107- <i>spoOA</i> 178TT	Group II intron targeted to <i>spoOA</i>	Fimlaid et al., 2013

When the cultures reached an OD₆₀₀ ~1.0, cells were exposed to various concentrations of chemicals for 15 min as follows: (a) 1 ml culture aliquots were mixed with 5–100 µl butanol (Fisher Scientific), chloroform (Acros Organics), hydrogen peroxide (3% H₂O₂ as a commercially available aqueous solution) or sodium hypochlorite (8.25% NaOCl as commercially available concentrated household bleach) to achieve the indicated final concentrations, (b) 6 ml culture aliquots were placed in 15 ml screw-cap polypropylene conical tubes, cells were pelleted in a benchtop centrifuge at 4,000 rpm for 5 min, suspended in equal volume pre-reduced 1X PBS, divided into 1 ml aliquots and mixed with 5–100 µl concentration of NaOCl as indicated above, (c) 500 µl of culture was combined with 100–300 µl 95% ethanol and brought to a final volume of 1 ml with dH₂O, or (d) 1 ml of culture was placed in 8 ml glass screw-cap tubes and incubated at the indicated temperature in a heated water bath for 20 min. pH was measured using a benchtop Accumet AB150 pH/MV meter. For exposure to oxygen, 2 ml culture was placed in a sterile petri dish, removed from the anaerobic chamber, sealed with parafilm to reduce evaporation and aliquots were removed after 30 min, 1, 3, 6, 9, 12, and 24 h incubation. After exposure, cells were serially diluted in either pre-reduced BHIS medium or 1X PBS and plated onto BHIS supplemented with 0.1% taurocholate. There was no difference in colony forming units (CFU) recovered from either diluent (data not shown). Untreated controls for each culture were diluted and plated to BHIS containing taurocholate prior to treatment to enumerate the initial CFU. Plates were enumerated after at least 24 h incubation at 37°C.

Preparation of Spores

Isolated spores were prepared as previously described Edwards et al. (2013) with the following alterations. Briefly, overnight cultures of *C. difficile* strains grown in BHIS were diluted into fresh BHIS and grown to mid-exponential phase (OD₆₀₀ ~0.5). Two hundred microliter culture was spread onto 70:30 sporulation agar (Fimlaid et al., 2013) and incubated anaerobically at 37°C for ~48 h. The plates were removed from the anaerobic chamber and exposed to oxygen at room temperature for 24 h. Cells were scraped from plates, suspended in 1X PBS and washed once. Spore suspensions were placed in flasks and exposed to oxygen at room temperature for 7–10 days to kill all vegetative cells. The surviving spores were subsequently rinsed twice with 1X PBS. The final spore stocks were enumerated on BHIS supplemented with 0.1% taurocholate and stored at a final concentration of either 1 × 10⁷ CFU ml⁻¹ in 1X PBS supplemented with 1% BSA to prevent clumping of spores or 1 × 10⁸ CFU ml⁻¹ in 1X PBS. BSA was omitted from the higher concentration spore stocks due to precipitation upon addition of some chemicals; however, the presence or absence of BSA did not affect the survival rates of spores in any tested condition. These spore stocks are stable at room temperature for at least a month (data not shown).

Spore Resistance Assays

Hundred microliter aliquots of 1 × 10⁸ CFU ml⁻¹ spores were incubated in the indicated concentration of chemicals for

15 min to ensure a final concentration of 1 × 10⁷ CFU ml⁻¹ spores, which is a concentration commonly used to test spore properties (Lawley et al., 2009). To test spore survival in a range of temperatures, 1 ml 1 × 10⁷ CFU ml⁻¹ spores were placed in 8 ml glass screw-cap tubes and incubated at the indicated temperature in a heated water bath for 20 min. To test the efficacy of NaOCl in BHIS, 0.6 ml spore aliquots in 1X PBS were pelleted at 15000 rpm for 15 min, and 0.55 ml of supernatant was removed to minimize disruption of the spore pellet. Spores were subsequently suspended in equal volume BHIS and treated as described above. At the indicated times, serial dilutions were performed in 1X PBS and plated onto BHIS plates supplemented with 0.1% taurocholate. Colonies were enumerated from plates after a minimum of 36 h incubation.

Phase Contrast Microscopy

Phase contrast microscopy was performed as previously described (Edwards et al., 2014). Briefly, cultures were pelleted or cells were scraped off plates, suspended in 500 µl BHIS and pelleted. The supernatant was decanted, and 2 µl of cell suspension was placed on a prepared slide containing a thin 0.7% agarose pad. Phase contrast microscopy was performed using a X100 Ph3 oil immersion objective on a Nikon Eclipse Ci-L microscope while images were captured using a DS-Fi2 camera.

Statistical Analyses

To evaluate the statistical significance, a two-way analysis of variance (ANOVA), followed by a Dunnett's multiple comparisons test, was used to compare the control to the concentration, length of time or temperature of the indicated conditions. To determine the significance of the germination frequency of purified spores, a one-way ANOVA was performed, followed by a Tukey's multiple comparisons test. $P \leq 0.05$ was considered statistically significant, and all statistical analyses were performed using Microsoft Excel or GraphPad Prism 6.

Accession Numbers

The accession numbers for strains used in this study are as follows: 630 (GenBank accession no. AM180355); R20291 (GenBank accession no. FN545816); M120 (078 reference strain; GenBank accession no. FN665653).

RESULTS

Construction of a spoOA Mutant in 5325 (078 Ribotype)

Because *C. difficile* is shed from the host as both vegetative cells and spores (Wilson et al., 1982; Koenigsknecht et al., 2015; Edwards et al., 2016), we first examined the sensitivities of vegetative cells to environmental stresses. *C. difficile* heterogeneously and asynchronously sporulates (Fimlaid et al., 2013). Thus, to ensure no spores were present in vegetative cell assays, we studied *C. difficile* mutants that are unable to form spores. The transcriptional regulator, Spo0A, serves as the

master regulator of sporulation in all studied endospore-forming bacteria. *Spo0A* is required for the formation of spores and transmission of *C. difficile* (Deakin et al., 2012). To ensure all cells within a studied population were vegetative, we utilized a 630Δ*erm* *spo0A::erm* mutant (hereafter referred to as 630 *spo0A*; MC310; 012 ribotype) and a R20291 *spo0A::erm* mutant (R20291 *spo0A*; 027 ribotype) (Dawson et al., 2012; Edwards et al., 2014). In addition, we created the same insertional mutation in the *spo0A* locus in 5325 (5325 *spo0A*; MC724; 078 ribotype). The insertion of a retargeted group II intron in the 5325 *spo0A* gene was confirmed by PCR amplification (Table 2; Supplementary Figure S1A). Further, phase contrast microscopy of the 5325 *spo0A* mutant revealed the absence of phase bright spores, indicating that the *spo0A* gene product was inactivated (Supplementary Figure S1B), matching the phenotype obtained in a previously published *spo0A* mutant in a 078 ribotype strain (Mackin et al., 2013).

C. difficile Vegetative Cell and Spore Resistance to Ethanol

Alcohol-based hand sanitizers containing 60–80% ethanol or isopropanol have emerged as a primary line of defense in preventing the transmission of infectious agents in healthcare settings. However, *C. difficile* spores are recalcitrant to alcohol exposure and are not removed from hands after use of alcohol rubs (Oughton et al., 2009; Edmonds et al., 2012; Nerandzic et al., 2015). To compare the resilience of *C. difficile* spores and vegetative cells to ethanol exposure, we first performed vegetative viability assays with the *spo0A* mutants in various concentrations of ethanol for 15 min. Both the 630 *spo0A* and R20291 *spo0A* numbers were reduced by ~95% in 14.25% ethanol, whereas survival of the 5325 *spo0A* mutant was marginally affected at this concentration (~35% reduction; Figure 1A). However, the vegetative cells of the three ribotypes tested were consistently reduced to undetectable levels in 28.5% ethanol, indicating that prolonged exposure to relatively high concentrations of alcohol can kill all *C. difficile* vegetative cells.

Depending on the methods used to isolate and purify spores, we have observed that brief ethanol or heat exposure (15–30 min) can enhance spore germination (data not shown). Based on these observations, we chose to isolate *C. difficile* spores following long-term exposure to oxygen, as described in “Materials and Methods,” rather than by ethanol and/or heat exposure. This

method reproducibly produced stocks with phase bright, viable spores containing no viable vegetative cells and some cell debris (Supplementary Figure S2). As previously demonstrated, *C. difficile* spores germinate efficiently in the presence of the bile salt, taurocholate, and the amino acid, glycine (Sorg and Sonenshein, 2008). Remarkably, we observed that regardless of the method used to eliminate vegetative cells, the 5325 (078 ribotype) spores consistently germinated and outgrew in medium lacking taurocholate at a much higher frequency (~75-fold increase) than either the 630Δ*erm* (012) or R20291 (027) spores (Table 3). This observation suggests that 5325 spores germinate using a taurocholate-independent mechanism, or more likely, that this strain has an increased ability to scavenge taurocholate from medium with components from animal by-products [i.e., brain-heart infusion (BHI) medium; see Discussion].

To measure *C. difficile* spore resistance to ethanol, concentrated spore stocks suspended in 1X PBS were mixed to the indicated final concentration of ethanol and incubated for 15 min. The final concentration of spores in these assays was 1×10^7 , which mimics the concentration used in a previous spore resistance study (Lawley et al., 2009) and closely reflects the number of CFUs enumerated from hamster feces during infection (Edwards et al., 2014, 2016). As previously reported (Lawley et al., 2009), *C. difficile* spores were extremely resistant to high levels of ethanol, with all strains exhibiting high survival rates ($\geq 50\%$) even in concentrations of ethanol as high as 85.5% (Figure 1B). Notably, the 5325 spores had higher survival rates in higher concentrations of ethanol than did the 630Δ*erm* or R20291 spores, although this effect was not statistically significant (78% spore survival vs. 56% and 50%, respectively, in 85.5% ethanol; Supplementary Figure S3). Altogether, these results indicate that *C. difficile* spore exposure to ethanol does not inactivate spores.

C. difficile Resistance to Additional Organic Solvents

Clostridium species and related organisms carry out solventogenesis, a process during which growth slows and solvents such as acetone, butanol, and ethanol are produced. For this reason, *Clostridium* and related organisms are used for the production of biofuels, including butanol, which generally inhibit microbial growth. As such, a frequent limiter for solvent production is the high level of solvent toxicity exhibited in relatively low concentrations (Ezeji et al., 2010). As solvent toxicity is understudied in *C. difficile*, we tested the susceptibility of *C. difficile* vegetative cells and spores to butanol as described in “Materials and Methods.” Surprisingly, a significant number of the 5325 *spo0A* cells survived in 2.5% butanol compared to the 630 *spo0A* and R20291 *spo0A* strains (Figure 2A; 50% survival versus 0.003 and 0.01% survival, respectively). While long-term viability and the ability to grow uninhibited in relatively high concentrations of butanol were not tested, these data suggest that the 5325 strain has the ability to withstand greater concentrations of butanol compared to other common *C. difficile* isolates. Spores of all three *C. difficile* strains demonstrated some sensitivity to increasing concentrations of butanol (Figure 2B). However,

TABLE 2 | Oligonucleotides.

Primer	Sequence (5'→3')	Use/locus tag/reference
oMC444	5'-GGAATACACAGGAGGTATCGTACA-3'	Confirmation of 5325 <i>spo0A</i> mutant
oMC819	5'-GTGCGGCTGGATCACCTCCT-3'	PCR ribotyping (Bidet et al., 2000)
oMC820	5'-CCCTGCACCCTTAATAACTTGACC-3'	PCR ribotyping (Bidet et al., 2000)
oMC1122	5'-AACCTACTGGTTACCGTTTCG-3'	Confirmation of 5325 <i>spo0A</i> mutant

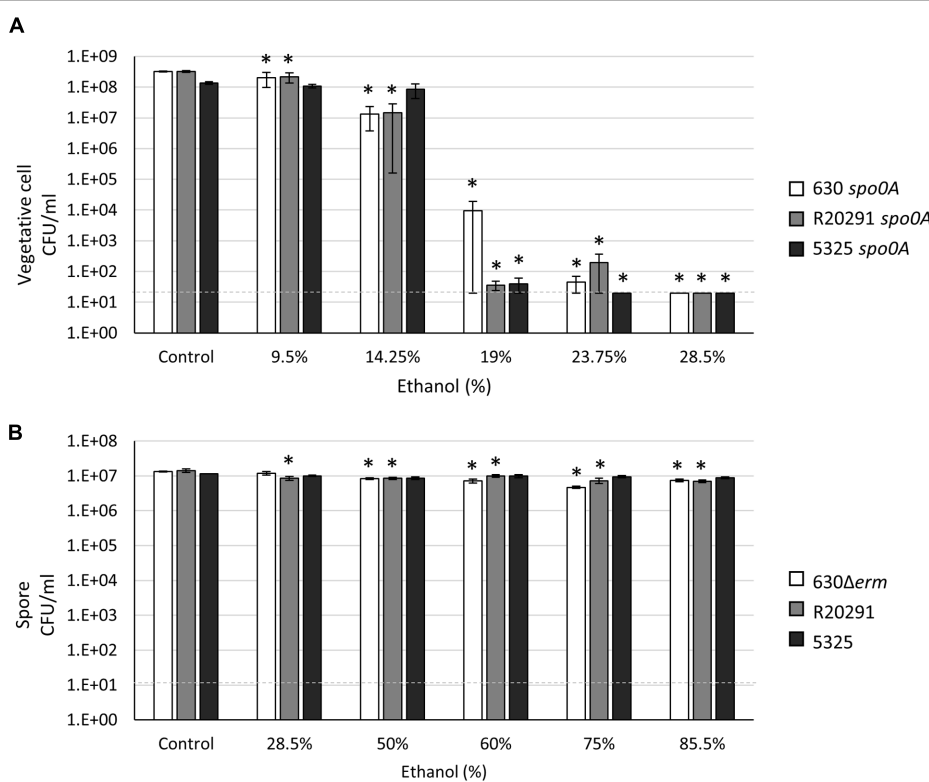


FIGURE 1 | *Clostridium difficile* vegetative cells are sensitive to ethanol, while spores are highly resistant to ethanol. **(A)** Survival of 630 *spoOA*, R20291 *spoOA* and 5325 *spoOA* vegetative cells grown to an OD₆₀₀ ~1.0 in BHIS medium and **(B)** 630Δerm, R20291 and 5325 spores in 1X PBS after exposure to the indicated concentrations (v/v) of ethanol for 15 min. The means and standard error of the means for at least three biological replicates are shown; the limit of detection equals 20 CFU ml⁻¹ for vegetative cells and 10 CFU ml⁻¹ for spores and is denoted by a dashed line. Asterisks indicate a *P* value of <0.05 as determined by two-way ANOVA followed by a Dunnett's multiple comparisons test to compare the condition to the corresponding control of individual strains.

when spores were incubated with 50% butanol, the 630Δerm *C. difficile* spore CFU were reduced to <1%, compared to ~13% and 19% survival rates for the R20291 and 5325 spore populations, respectively, suggesting that the 630Δerm spores are more susceptible to butanol.

We also measured the sensitivity of *C. difficile* vegetative cells and spores to chloroform, an organic solvent sometimes used in sporulation assays for *Bacillus subtilis* and other clostridial organisms (Milhaud and Balassa, 1973; Schiott and Hederstedt, 2000; McBride and Haldenwang, 2004;

Tracy et al., 2011). The 5325 *spoOA* mutant demonstrated greater resistance to chloroform compared to the 630 *spoOA* and R20291 *spoOA* mutants, with 10% of the 5325 *spoOA* population surviving 1% chloroform exposure (Figure 2C), indicating that the 5325 vegetative cells are able to tolerate greater concentrations of chloroform. *C. difficile* spores were unaffected by chloroform exposure, but incubation in chloroform resulted in a small, but not statistically significant, increase in CFU in all strains (Figure 2D). However, this effect was not as consistent in higher concentrations of chloroform.

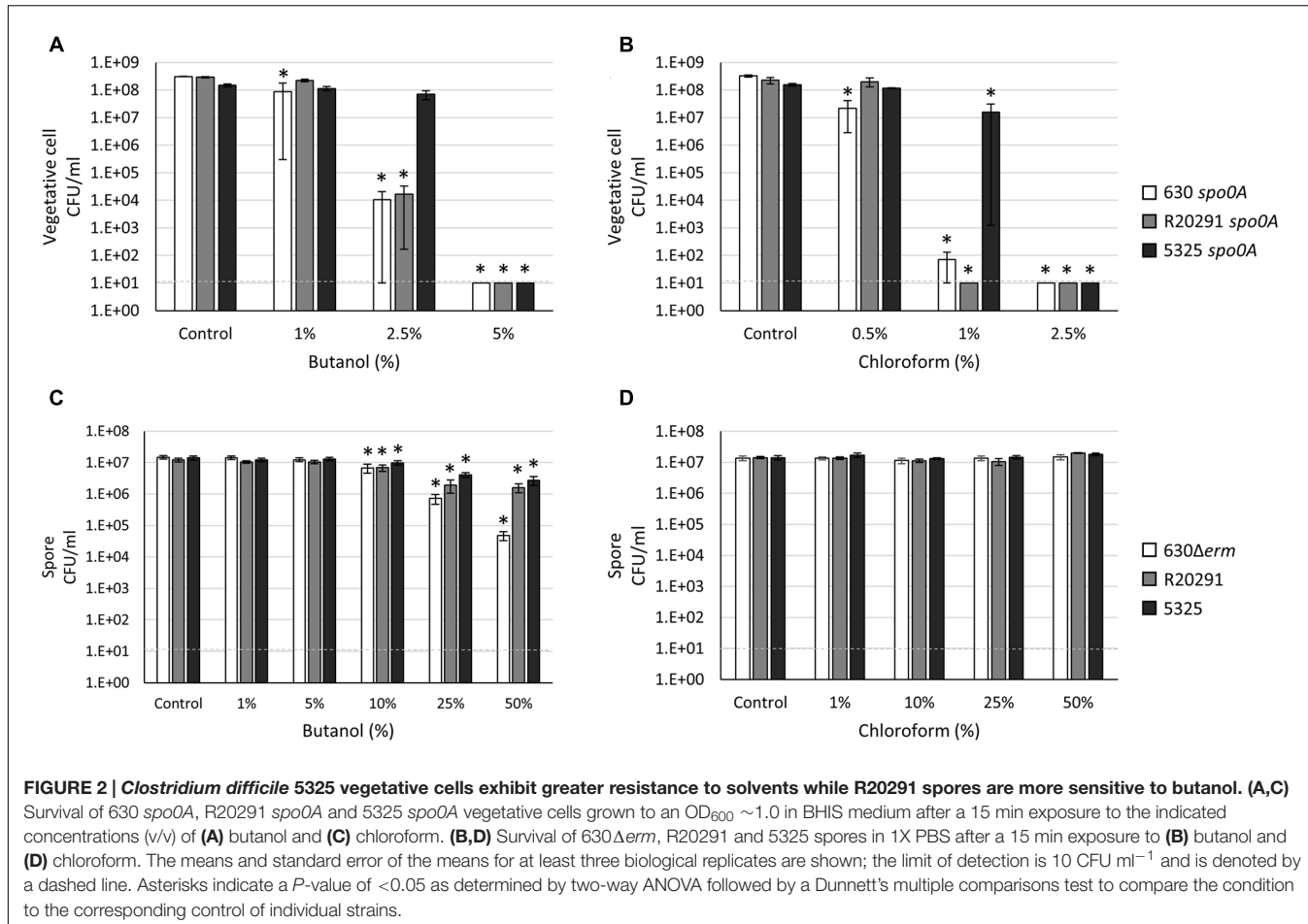
C. difficile Resistance to Oxidative Stress

Clostridium difficile vegetative cells are strict anaerobes and are known to be sensitive to low levels of oxygen (Holy and Chmelar, 2012). However, previous results in our lab demonstrated that some *C. difficile* vegetative cells present in hamster fecal samples survive at least 24 h in fecal pellets suspended in 1X PBS and stored aerobically (Edwards et al., 2016). These data led us to hypothesize that oxygen tolerance may be exhibited by *C. difficile* vegetative cells for short, but significant, periods of time. Although the transmission of non-sporulating *C. difficile* is almost eliminated in the mouse model of *C. difficile* infection (CDI) (Deakin et al., 2012), significant numbers of vegetative cells

TABLE 3 | Germination frequency of *C. difficile* 012, 027, and 078 spores in the absence and presence of taurocholate.

Strain	Ribotype	Taurocholate-independent germination frequency ^a
630Δerm	012	2.04 × 10 ⁻⁴ ± 9.36 × 10 ⁻⁵
R20291	027	2.50 × 10 ⁻⁴ ± 2.24 × 10 ⁻⁴
5325	078	1.72 × 10⁻² ± 9.05 × 10⁻⁵

^aMean germination frequency is calculated from two independently prepared spore stocks as CFU ml⁻¹ enumerated on BHIS divided by CFU ml⁻¹ enumerated on BHIS supplemented with 0.1% taurocholate (total spores). Bold indicates *P* < 0.05 as determined by a one-way ANOVA followed by Tukey's multiple comparisons test.



are shed and recovered in the stool (Koenigsknecht et al., 2015). It is unknown if vegetative cells play a role in transmission in clinical settings. To determine the extent of *C. difficile* vegetative cell oxygen tolerance, the *spoOA* mutant strains were grown to an OD₆₀₀ of 1.0, plated for viability anaerobically and aliquots of the cultures were exposed to atmospheric oxygen for the indicated amount of time, serially diluted and plated anaerobically to enumerate surviving cells. As shown in Figure 3A, the 630 *spoOA* mutant strain was significantly more tolerant to atmospheric oxygen exposure than either the R20291 *spoOA* or 5325 *spoOA* mutant strains. R20291 *spoOA* and 5325 *spoOA* survival dropped precipitously after 1 h exposure to oxygen, and no surviving cells were recovered after 3 h oxygen exposure. These results demonstrate that the 630Δerm strain is able to survive brief oxygen exposure, perhaps providing additional opportunity for spread of the pathogen.

We next determined the effects of an important source of oxidative stress, the common antiseptic and oxidative burst component, hydrogen peroxide (Fawley et al., 2007; Slauch, 2011). Previous studies genetically linked the abilities for *Clostridium acetobutylicum*, a related anaerobe, to tolerate both oxygen and hydrogen peroxide exposures (Hillmann et al., 2008, 2009; Riebe et al., 2009). We asked whether *C. difficile* survival in oxygen correlates with hydrogen peroxide tolerance, as is

observed with *C. acetobutylicum*. Spores from all three strains were resistant to up to 1.5% hydrogen peroxide (Supplementary Figure S4), confirming previous results performed with similar or unknown concentrations of hydrogen peroxide (Fawley et al., 2007; Lawley et al., 2010). In contrast, the vegetative cells of the 630 *spoOA* mutant exhibited increased resistance to hydrogen peroxide exposure compared to the R20291 *spoOA* and 5325 *spoOA* mutants (Figure 3B), similar to the atmospheric oxygen survival trials. These data suggest that the increased vegetative cell oxygen and hydrogen peroxide tolerance exhibited by the 630Δerm strain may be correlative, as in *C. acetobutylicum*.

C. difficile Spores Tolerate High “Wet Heat” Temperatures for a Short Period of Time

One advantage to bacterial spore formation is protection from extreme temperature variations. Wet heat resistance is the ability for spores to survive high temperatures when suspended in an aqueous solution (Setlow, 2006). This property is a universal characteristic of bacterial spores, but differences in heat tolerance between *Bacillus* and other spore-forming species have been noted (Murrell and Scott, 1966; Setlow, 2014). While *B. subtilis* spores can easily survive exposure to 80°C (Milhaud and

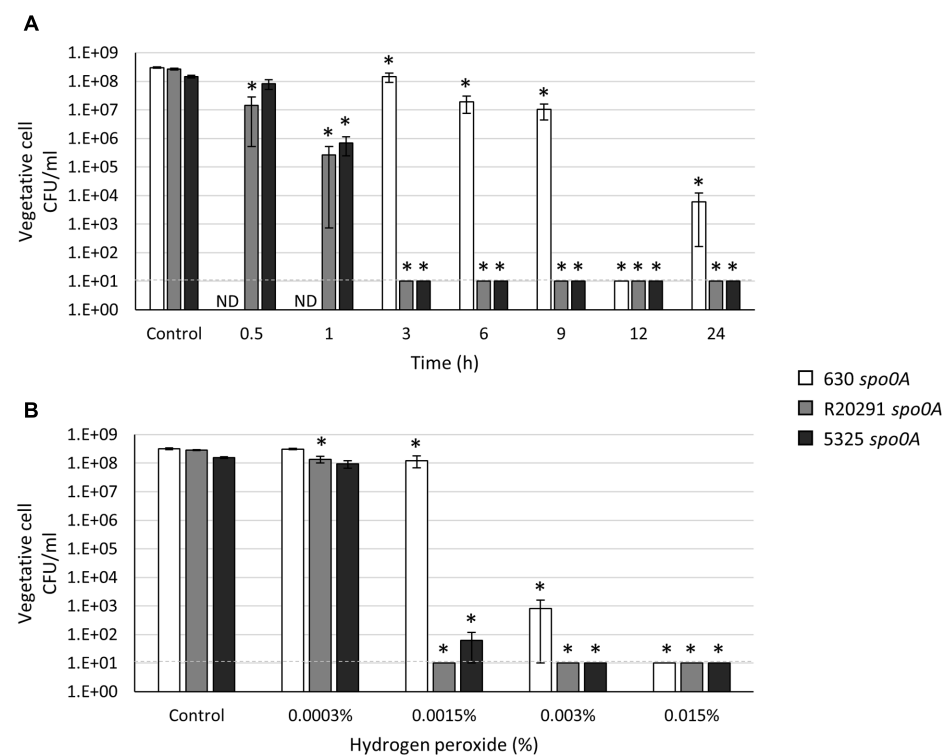


FIGURE 3 | *Clostridium difficile* 630 spoOA vegetative cells demonstrate greater resistance to oxidative stress. Survival of 630 spoOA, R20291 spoOA and 5325 spoOA vegetative cells grown to an OD₆₀₀ ~1.0 in BHIS medium after exposure to (A) atmospheric oxygen after the indicated length of time (h) or (B) hydrogen peroxide (H₂O₂) for 15 min. The means and standard error of the means for at least three biological replicates are shown; the limit of detection is 10 CFU ml⁻¹ and is denoted by a dashed line. Asterisks indicate a P-value of <0.05 as determined by two-way ANOVA followed by a Dunnett's multiple comparisons test to compare the condition to the corresponding control of individual strains. ND, not determined.

Balassa, 1973; Setlow, 2006; Leggett et al., 2012), previous studies in *C. difficile* have demonstrated that *C. difficile* spores are comparatively wet heat-labile (Lawley et al., 2009). *C. difficile* spores have been reported to withstand long-term exposure (>24 h) to 60°C and up to 3 h at 70°C (Lawley et al., 2009), and wet heat-resistance assays are often used to select for *C. difficile* spores in a heterogenous population (Burns et al., 2011; Paredes-Sabja and Sarker, 2011; Fimlaid et al., 2015). We characterized the ability of *C. difficile* vegetative cells and spores to survive exposure to a range of wet heat temperatures for 20 min. The number of *C. difficile* vegetative cells recovered after exposure to 60°C or greater temperature resulted in a ~3-log loss for all three strains; however, we variably recovered some viable vegetative cells following incubation in 80°C (Figure 4A). Exposure to 60°C resulted in a slight, but statistically insignificant, loss of spore viability for all strains (Figure 4B; Supplementary Figure S5). The loss of 630Δerm and 5325 spore viability was more pronounced from 65 to 75°C compared to R20291 spores, while all strains exhibited a significant decrease in spore recovery at 80°C (Figure 4B; Supplementary Figure S5). The R20291 spores exhibited a modest, but consistent, advantage in heat tolerance compared to the 630Δerm and 5325 spores (Figure 4B; Supplementary Figure S5). Viable spores were detectable from all three strains after exposure to 85°C, although the spore load was reduced by at least ~4-logs, comparable to previous

observations (Rodriguez-Palacios and Lejeune, 2011). These data indicate that a substantial proportion of *C. difficile* spores are susceptible to wet heat-killing at temperatures below 85°C, but heat susceptibility is strain-dependent. These results should be taken into consideration when performing heat-resistance assays to quantitate sporulation within a population. Unsurprisingly, temperatures greater than 85°C are required to completely eliminate all *C. difficile* spores when in an aqueous environment.

Household Bleach Is Effective in Eliminating Both *C. difficile* Vegetative Cells and Spores at an Alkaline pH but Loses Efficacy at a Neutral pH

Sodium hypochlorite (NaOCl), the active chemical present in household bleach, is one of the most effective and commonly recommended agents for general disinfection (McDonald et al., 2012). Household bleach is commercially available as an aqueous solution of 5.25–8.25% NaOCl, which correlates to a standard concentration of approximately 5000–8000 mg l⁻¹ free chlorine [FC or parts per million (ppm)]. Previous studies have demonstrated that acidified and household bleach significantly reduce or completely eliminate the number of *C. difficile* spores on hard surfaces (Perez et al., 2005; Alfa et al., 2010; Omidbakhsh, 2010). However, we asked whether household bleach was effective

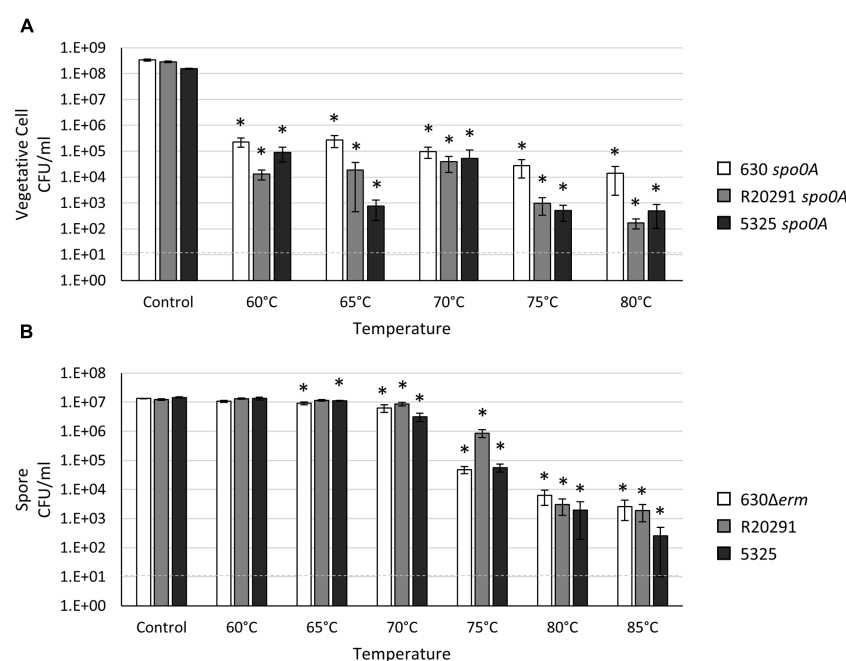


FIGURE 4 | *Clostridium difficile* spores are resistant to high temperatures. Survival of (A) 630 spoOA, R20291 spoOA and 5325 spoOA vegetative cells grown to an OD₆₀₀ ~1.0 in BHIS medium or (B) 630Δerm, R20291 and 5325 spores in 1X PBS after a 20 min exposure to the indicated temperature. The means and standard error of the means for at least three biological replicates are shown; the limit of detection is 10 CFU ml⁻¹ and is denoted by a dashed line. Asterisks indicate a P-value of <0.05 as determined by two-way ANOVA followed by a Dunnett's multiple comparisons test to compare the condition to the corresponding control of individual strains.

in eliminating a high concentration of vegetative cells and spores in an aqueous suspension, as may be the case in some patient care situations. To first assess the microbicidal capacity of household bleach against *C. difficile* vegetative cells in suspension, we added household bleach at 400 mg l⁻¹, 1000 mg l⁻¹, 5000 mg l⁻¹, and 8000 mg l⁻¹ FC (equivalent to 0.5, 1.25, 6.25, and 10% bleach solutions) to the asporogenous population of the three *C. difficile* strains. As before, these strains were grown in the standard medium for cultivation, BHIS, pH 6.8. At an OD₆₀₀ of 1.0, the pH of the culture was 5.98 ± 0.04. When bleach was added to the culture, the pH was increased in a dose-dependent manner, favoring hypochlorite (ClO⁻) formation [final culture pH = 6.04 ± 0.04 in 400 mg l⁻¹ (0.5%) household bleach; final culture pH = 6.60 ± 0.02 in 5000 mg l⁻¹ (6.25%) household bleach.] After a 15 min incubation in 400 mg l⁻¹ (0.5%) household bleach, the vegetative cell population of all three strains was decreased by ~85–90% (Figure 5A). Few vegetative cells were recoverable after incubation in 1000 mg l⁻¹ (1.25%) and 5000 mg l⁻¹ (6.25%) household bleach, and viable *C. difficile* cells were reduced to below the limit of detection (<10 CFU ml⁻¹) in 8000 mg l⁻¹ (10%) household bleach (Figure 5A). As pH alters the ratio of hypochlorite (HOCl) to the hypochlorite ion (OCl⁻), and thus, the effectiveness of bleach (Baumann and Ludwig, 1962), these data suggested that the pH of the aqueous solution may alter the effectiveness of sodium hypochlorite. To test this hypothesis, vegetative cells grown to an OD₆₀₀ of 1.0 in BHIS medium were pelleted and suspended in pre-reduced 1X PBS (pH 7.4). The addition of household bleach to 1X PBS

resulted in an alkaline suspension (pH 8.4–10, depending on the final concentration of bleach). A 15 min incubation in household bleach at all concentrations reduced the number of recoverable viable vegetative cells to below the limit of detection (<10 CFU ml⁻¹; data not shown).

We next determined the efficacy of household bleach against *C. difficile* spores suspended in either 1X PBS or BHIS medium. As with *C. difficile* vegetative cells suspended in 1X PBS, a 15 min exposure to all concentrations of bleach was effective in reducing viable spores to below the limit of detection (<10 CFU ml⁻¹; data not shown). Surprisingly, *C. difficile* 630Δerm, R20291 and 5325 spores suspended in BHIS were able to withstand a 15 min exposure to household bleach, even at the highest concentration of 8000 mg l⁻¹ (10%) household bleach (Figure 5B). These data suggest that the pH of liquid biohazard spills (e.g., feces) may alter the effectiveness of sodium hypochlorite. As a result, higher concentrations of bleach and/or the use of additional components to ensure an alkaline pH may be necessary to completely eliminate *C. difficile* vegetative cells and spores in biohazard spills.

DISCUSSION

Clostridium difficile infections have quickly emerged as a significant healthcare burden, and result in billions of dollars per year in additional healthcare-related expenses (Kwon et al., 2015; Levy et al., 2015). The environmental reduction of

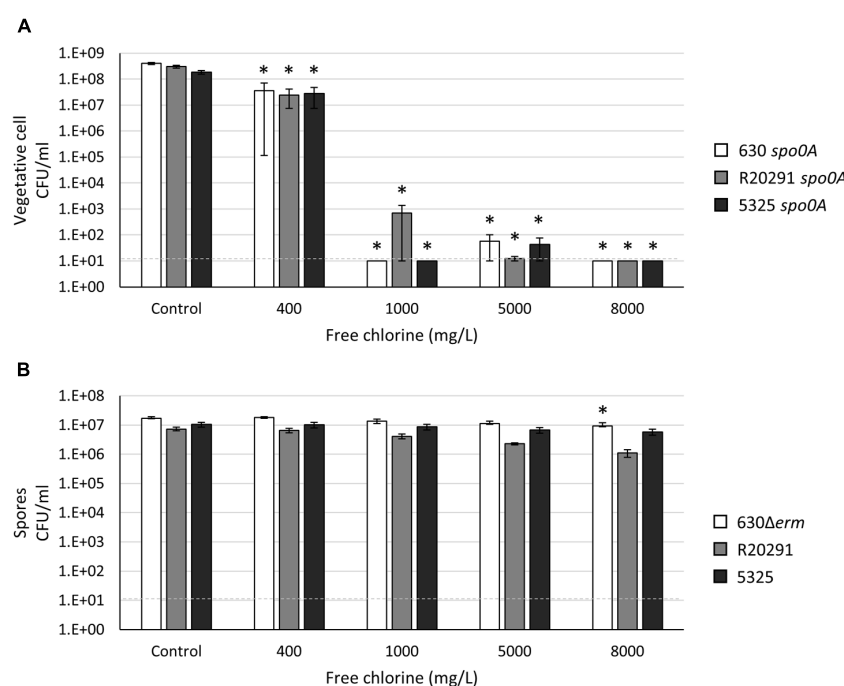


FIGURE 5 | *Clostridium difficile* vegetative cells and spores are resistant to sodium hypochlorite (household bleach) at a physiological pH. Survival of (A) 630 *spoOA*, R20291 *spoOA* and 5325 *spoOA* vegetative cells grown to an OD₆₀₀ ~1.0 in BHIS medium or (B) 630Δerm, R20291 and 5325 spores suspended in BHIS medium after exposure to 400 mg l⁻¹, 1000 mg l⁻¹, 5000 mg l⁻¹, 8000 mg l⁻¹ free chlorine (FC) for 15 min. The means and standard error of the means for at least three biological replicates are shown; the limit of detection is 10 CFU ml⁻¹ and is denoted by a dashed line. Asterisks indicate a P-value of <0.05 as determined by two-way ANOVA followed by a Dunnett's multiple comparisons test to compare the condition to the corresponding control of individual strains.

C. difficile spores is a major concern in the prevention of efficient transmission in hospitals and acute and long-term care facilities. While sodium hypochlorite (household bleach) has traditionally been recommended for sanitization in these settings, studies have shown that without frequent and thorough cleaning, detection and transmission of *C. difficile* can occur (Macleod-Glover and Sadowski, 2010; Lessa et al., 2012). To better understand how the resistance properties of *C. difficile* could impact survival and transmission, this study investigated the persistence of vegetative cells and spores after exposure of different *C. difficile* strains to a variety of chemicals and temperatures.

As expected, we observed greater effects for all of the chemicals and conditions tested on the viability of vegetative cells, compared to that of spores. The highest concentrations of ethanol (28.5%), butanol (5%), chloroform (2.5%), hydrogen peroxide (0.015%) or bleach (8000 mg l⁻¹) tested were sufficient to decrease the vegetative cell counts for all strains to below detectable limits (~10 CFU/ml). But, some treatments were more effective against vegetative cells of some strains than others. In particular, the 630 *spoOA* strain demonstrated higher resistance to oxygen exposure and hydrogen peroxide than the R20291 *spoOA* and 5325 *spoOA* strains examined. Conversely, the 5325 *spoOA* strain displayed greater resistance to killing by the organic compounds butanol and chloroform than the 630 *spoOA* and R20291 *spoOA* strains. These results reveal strain-dependent differences in survival that are specific to actively growing cells and independent of spore structure. Because *C. difficile* *spoOA*

mutants exhibit pleiotropic phenotypes, we tested the 630 *spoOA* isogenic parent, 630Δerm, in a subset of conditions, and found no difference in survival rates (Supplementary Figure S6), indicating that the *spoOA* mutant strain behaves similarly to the parent strain.

To our knowledge, aerotolerance of *C. difficile* vegetative cells has not been mechanistically studied. The observation that oxygen sensitivity and hydrogen peroxide resistance are strain-dependent properties may provide insight into the mechanisms by which *C. difficile* tolerates low levels of oxidative stress. A mutation in the oxidative stress repressor (*perR*) in the related organism, *Clostridium acetobutylicum*, confers prolonged aerotolerance and higher resistance to hydrogen peroxide (H₂O₂; Hillmann et al., 2008). A single genetic pathway in *C. acetobutylicum*, which includes PerR, is responsible for detoxifying both atmospheric oxygen and reactive oxygen species (ROS), including those produced by hydrogen peroxide (Riebe et al., 2009). Although *C. acetobutylicum* is more aerotolerant than *C. difficile*, the fact that resistance to oxygen exposure and ROS correlates with individual strains suggests that *C. difficile* may also utilize a single genetic pathway to combat multiple sources of oxidative stress. The infectious dose of *C. difficile* is unknown, but is presumed to be extremely low (<10), as is observed for the hamster model of acute CDI (Larson et al., 1978). Consequently, it is possible that vegetative cells play a minor role in the spread of *C. difficile* if vegetative cells from feces can survive short periods of exposure to atmospheric oxygen.

As anticipated, spores of all three strains were inherently resistant to many of the chemicals tested, with ethanol, chloroform and hydrogen peroxide proving ineffective at any practical concentration that could be assessed. Strain-dependent differences were observed for spore resistance to butanol, which was more effective against strain 630Δ*erm*, and wet heat, which more readily killed 630Δ*erm* and 5325. The highest wet-heat temperature examined, 85°C, was not sufficient to completely destroy all spores for any of the strains examined.

As environmental control is one of the critical measures in preventing the spread of CDI, the use of the most effective cleaning products, along with adequate cleaning procedures (Eckstein et al., 2007), is necessary to reduce the environmental sources of *C. difficile* spores (Macleod-Glover and Sadowski, 2010). Our results confirm that spores are recalcitrant to high concentrations of ethanol, the primary active ingredient in alcohol-based hand sanitizers, and relatively high concentrations of hydrogen peroxide (<3%), which is an active ingredient in several hospital cleaning agents. A previous study demonstrated that 1% hydrogen peroxide can reduce spore viability by ~75% when incubated with 10⁶ spores/ml. We observed ~25–40% reduction that was not statistically significant (Supplementary Figure S4), and we used a higher concentration of spores in our tests (10⁶ vs. 10⁷ spore CFU/ml) (Lawley et al., 2010). Further, Lawley et al. (2010) found that exposure to a 10% hydrogen peroxide solution reduced viable spores to below their limit of detection (<2 CFU ml⁻¹). Some studies have shown that the use of hydrogen peroxide-based hospital cleaning agents [e.g., G-force, accelerated hydrogen peroxide (AHP) and stabilized hydrogen peroxide (SHP)] in clinical settings can reduce, but not completely eliminate, detection of *C. difficile* or patient cases of CDI (Alfa et al., 2010; Horn and Otter, 2015; Steindl et al., 2015). Because spores are highly resistant to these compounds in the laboratory and strong, stable solutions of hydrogen peroxide are necessary for spore inactivation, our results strongly suggest that these products not be used for decontamination, and confirm that a strong dilution of household bleach at an alkaline pH is the best choice for environmental control of *C. difficile* (Wilcox et al., 2003; Eckstein et al., 2007).

We observed that spores of the 5325 strain appeared to germinate in a taurocholate-independent manner on BHIS plates at a significantly higher frequency than 630Δ*erm* or R20291 spores. Other *C. difficile* clinical isolates have exhibited germination in the absence of bile salts, and no correlation between ribotypes was noted (Heeg et al., 2012). However, these spores were heat treated at 60°C for 25 min before plating, which may increase the germination frequency (Rodriguez-Palacios and Lejeune, 2011). A recent study revealed that all tested *C. difficile* strains, including those in the previous study that germinated and resumed growth in medium lacking taurocholate, required taurocholate and glycine to germinate *in vitro*, with the exception of CD 2351, a 078 clinical isolate, which did not require glycine (Bhattacharjee et al., 2016). Further, some spores exhibited a significantly increased affinity to taurocholate (Bhattacharjee et al., 2016), suggesting that spores from these strains require lower concentrations of taurocholate to activate germination. Thus, the difference in frequencies of taurocholate-independent

germination by 5325 compared to 630Δ*erm* and R20291 may result from an increased ability for 5325 to bind low levels of taurocholate. The variation in affinity to bile salts of various *C. difficile* clinical isolates may reflect the availability of nutrients and ratio of bile salts present in the primary host GI tract.

This study further highlights the broad variations observed in *C. difficile* clinical and animal isolates in regards to many physiological processes, including sporulation, germination and toxin production (Burns et al., 2010; Heeg et al., 2012; Carlson et al., 2015; Nawrocki et al., 2015; Bhattacharjee et al., 2016). Although an attractive hypothesis is that the distinct properties of each strain are genotypic and reflect the GI environment of the primary host in which each strain evolved, there are likely many variable environmental factors that contribute to the physical composition of the spore, such as the prominence of different spore proteins and the number of germinant receptors.

Further studies are required to determine which features of the *C. difficile* spore coat and cortex confer resistance to various chemicals and environmental insults. Resistances often arise sequentially, not simultaneously, as additional components are built onto the prespore, as seen in *B. subtilis* (Balassa, 1971; Russell, 1990). Determining the order of resistances as *C. difficile* sporulation progresses will provide insight into the biochemical mechanisms of spore formation and may serve as a useful tool for studying late sporulation events.

AUTHOR CONTRIBUTIONS

AE, SK, RP, LJ, SA, and SM contributed to the acquisition and analysis of the data. AE drafted the manuscript and AE, SK, RP, LJ, SA, and SM edited and approved the content.

FUNDING

This research was supported by the U.S. National Institutes of Health (NIH) through grants AI116933, AI109526, DK087763 and DK101870 to SM, AI106699 to SA, and GM099644 to RP. The content of this manuscript is solely the responsibility of the authors and does not necessarily reflect the official views of the National Institutes of Health.

ACKNOWLEDGMENTS

We thank the members of the McBride lab for helpful suggestions and discussions throughout the course of this study. We are grateful to Brendan Wren for the gift of the R20291 *spo0A* mutant and to Aimee Shen for the *spo0A* plasmid.

SUPPLEMENTARY MATERIAL

The Supplementary Material for this article can be found online at: <http://journal.frontiersin.org/article/10.3389/fmicb.2016.01698/full#supplementary-material>

REFERENCES

- Alfa, M. J., Lo, E., Wald, A., Dueck, C., DeGagne, P., and Harding, G. K. (2010). Improved eradication of *Clostridium difficile* spores from toilets of hospitalized patients using an accelerated hydrogen peroxide as the cleaning agent. *BMC Infect. Dis.* 10:268. doi: 10.1186/1471-2334-10-268
- Ali, S., Moore, G., and Wilson, A. P. (2011). Spread and persistence of *Clostridium difficile* spores during and after cleaning with sporicidal disinfectants. *J. Hosp. Infect.* 79, 97–98. doi: 10.1016/j.jhin.2011.06.010
- Balassa, G. (1971). The genetic control of spore formation in bacilli. *Curr. Top. Microbiol. Immunol.* 56, 99–192.
- Baumann, E. R., and Ludwig, D. D. (1962). Free available chlorine residuals for small nonpublic water supplies. *J. Am. Water Works Assoc.* 54, 1379–1388.
- Bhattacharjee, D., Francis, M. B., Ding, X., McAllister, K. N., Shrestha, R., and Sorg, J. A. (2016). Reexamining the germination phenotypes of several *Clostridium difficile* strains suggests another role for the CspC germinant receptor. *J. Bacteriol.* 198, 777–786. doi: 10.1128/JB.00908-915
- Bidet, P., Lalande, V., Salauze, B., Burghoffer, B., Avesani, V., Delmee, M., et al. (2000). Comparison of PCR-ribotyping, arbitrarily primed PCR, and pulsed-field gel electrophoresis for typing *Clostridium difficile*. *J. Clin. Microbiol.* 38, 2484–2487.
- Bouillaut, L., McBride, S. M., and Sorg, J. A. (2011). Genetic manipulation of *Clostridium difficile*. *Curr. Protoc. Microbiol.* Chap. 9, Unit9A.2. doi: 10.1002/9780471729259.mc09a02s20
- Burns, D. A., Heap, J. T., and Minton, N. P. (2010). The diverse sporulation characteristics of *Clostridium difficile* clinical isolates are not associated with type. *Anaerobe* 16, 618–622. doi: 10.1016/j.anaerobe.2010.10.001
- Burns, D. A., Heeg, D., Cartman, S. T., and Minton, N. P. (2011). Reconsidering the sporulation characteristics of hypervirulent *Clostridium difficile* BI/NAP1/027. *PLoS ONE* 6:e24894. doi: 10.1371/journal.pone.0024894
- Carlson, P. E. Jr., Kaiser, A. M., McColm, S. A., Bauer, J. M., Young, V. B., Aronoff, D. M., et al. (2015). Variation in germination of *Clostridium difficile* clinical isolates correlates to disease severity. *Anaerobe* 33, 64–70. doi: 10.1016/j.anaerobe.2015.02.003
- CDC (2013). *Antibiotic Resistance Threats in the United States, 2013*. Available at: <http://www.cdc.gov/features/AntibioticResistanceThreats/>
- Dawson, L. F., Valiente, E., Faulds-Pain, A., Donahue, E. H., and Wren, B. W. (2012). Characterisation of *Clostridium difficile* biofilm formation, a role for Spo0A. *PLoS ONE* 7:e50527. doi: 10.1371/journal.pone.0050527
- de Hoon, M. J., Eichenberger, P., and Vitkup, D. (2010). Hierarchical evolution of the bacterial sporulation network. *Curr. Biol.* 20, R735–R745. doi: 10.1016/j.cub.2010.06.031
- Deakin, L. J., Clare, S., Fagan, R. P., Dawson, L. F., Pickard, D. J., West, M. R., et al. (2012). The *Clostridium difficile* spo0A gene is a persistence and transmission factor. *Infect. Immun.* 80, 2704–2711. doi: 10.1128/IAI.00147-12
- Driks, A. (2002). Overview: development in bacteria: spore formation in *Bacillus subtilis*. *Cell. Mol. Life Sci.* 59, 389–391. doi: 10.1007/s00018-002-8430-x
- Driks, A. (2003). The dynamic spore. *Proc. Natl. Acad. Sci. U.S.A.* 100, 3007–3009. doi: 10.1073/pnas.0730807100
- Dubberke, E. (2012). Strategies for prevention of *Clostridium difficile* infection. *J. Hosp. Med.* 7(Suppl. 3), S14–S17. doi: 10.1002/jhm.1908
- Dubberke, E. R., and Olsen, M. A. (2012). Burden of *Clostridium difficile* on the healthcare system. *Clin. Infect. Dis.* 55(Suppl. 2), S88–S92. doi: 10.1093/cid/cis335
- Eckstein, B. C., Adams, D. A., Eckstein, E. C., Rao, A., Sethi, A. K., Yadavalli, G. K., et al. (2007). Reduction of *Clostridium difficile* and vancomycin-resistant *Enterococcus* contamination of environmental surfaces after an intervention to improve cleaning methods. *BMC Infect. Dis.* 7:61. doi: 10.1186/1471-2334-7-61
- Edmonds, S. L., Macinga, D. R., Mays-Suko, P., Duley, C., Rutter, J., Jarvis, W. R., et al. (2012). Comparative efficacy of commercially available alcohol-based hand rubs and World Health Organization-recommended hand rubs: formulation matters. *Am. J. Infect. Control* 40, 521–525. doi: 10.1016/j.ajic.2011.08.016
- Edwards, A. N., Nawrocki, K. L., and McBride, S. M. (2014). Conserved oligopeptide permeases modulate sporulation initiation in *Clostridium difficile*. *Infect. Immun.* 82, 4276–4291. doi: 10.1128/IAI.02323-14
- Edwards, A. N., Suarez, J. M., and McBride, S. M. (2013). Culturing and maintaining *Clostridium difficile* in an anaerobic environment. *J. Vis. Exp.* 79, e50787. doi: 10.3791/50787
- Edwards, A. N., Tamayo, R., and McBride, S. M. (2016). A novel regulator controls *Clostridium difficile* sporulation, motility and toxin production. *Mol. Microbiol.* 100, 954–971. doi: 10.1111/mmi.13361
- Ezeji, T., Milne, C., Price, N. D., and Blaschek, H. P. (2010). Achievements and perspectives to overcome the poor solvent resistance in acetone and butanol-producing microorganisms. *Appl. Microbiol. Biotechnol.* 85, 1697–1712. doi: 10.1007/s00253-009-2390-0
- Fawley, W. N., Underwood, S., Freeman, J., Baines, S. D., Saxton, K., Stephenson, K., et al. (2007). Efficacy of hospital cleaning agents and germicides against epidemic *Clostridium difficile* strains. *Infect. Control Hosp. Epidemiol.* 28, 920–925. doi: 10.1086/519201
- Finlay, K. A., Bond, J. P., Schutz, K. C., Putnam, E. E., Leung, J. M., Lawley, T. D., et al. (2013). Global analysis of the sporulation pathway of *Clostridium difficile*. *PLoS Genet.* 9:e1003660. doi: 10.1371/journal.pgen.1003660
- Finlay, K. A., Jensen, O., Donnelly, M. L., Francis, M. B., Sorg, J. A., and Shen, A. (2015). Identification of a novel lipoprotein regulator of *Clostridium difficile* spore germination. *PLoS Pathog.* 11:e1005239. doi: 10.1371/journal.ppat.1005239
- Francis, M. B., Allen, C. A., Shrestha, R., and Sorg, J. A. (2013). Bile acid recognition by the *Clostridium difficile* germinant receptor, CspC, is important for establishing infection. *PLoS Pathog.* 9:e1003356. doi: 10.1371/journal.ppat.1003356
- Heeg, D., Burns, D. A., Cartman, S. T., and Minton, N. P. (2012). Spores of *Clostridium difficile* clinical isolates display a diverse germination response to bile salts. *PLoS ONE* 7:e32381. doi: 10.1371/journal.pone.0032381
- Henrikens, A. O., and Moran, C. P. Jr. (2007). Structure, assembly, and function of the spore surface layers. *Annu. Rev. Microbiol.* 61, 555–588. doi: 10.1146/annurev.micro.61.080706.093224
- Hillmann, F., Doring, C., Riebe, O., Ehrenreich, A., Fischer, R. J., and Bahl, H. (2009). The role of PerR in O₂-affected gene expression of *Clostridium acetobutylicum*. *J. Bacteriol.* 191, 6082–6093. doi: 10.1128/JB.00351-09
- Hillmann, F., Fischer, R. J., Saint-Prix, F., Girbal, L., and Bahl, H. (2008). PerR acts as a switch for oxygen tolerance in the strict anaerobe *Clostridium acetobutylicum*. *Mol. Microbiol.* 68, 848–860. doi: 10.1111/j.1365-2958.2008.06192.x
- Ho, T. D., and Ellermeier, C. D. (2011). PrsW is required for colonization, resistance to antimicrobial peptides, and expression of extracytoplasmic function sigma factors in *Clostridium difficile*. *Infect. Immun.* 79, 3229–3238. doi: 10.1128/IAI.00019-11
- Holy, O., and Chmelar, D. (2012). Oxygen tolerance in anaerobic pathogenic bacteria. *Folia Microbiol. (Praha)* 57, 443–446. doi: 10.1007/s12223-012-0149-y
- Horn, K., and Otter, J. A. (2015). Hydrogen peroxide vapor room disinfection and hand hygiene improvements reduce *Clostridium difficile* infection, methicillin-resistant *Staphylococcus aureus*, vancomycin-resistant enterococci, and extended-spectrum beta-lactamase. *Am. J. Infect. Control* 43, 1354–1356. doi: 10.1016/j.ajic.2015.06.029
- Hussain, H. A., Roberts, A. P., and Mullany, P. (2005). Generation of an erythromycin-sensitive derivative of *Clostridium difficile* strain 630 (630Δerm) and demonstration that the conjugative transposon Tn916ΔE enters the genome of this strain at multiple sites. *J. Med. Microbiol.* 54, 137–141. doi: 10.1099/jmm.045790-0
- Janoir, C. (2016). Virulence factors of *Clostridium difficile* and their role during infection. *Anaerobe* 37, 13–24. doi: 10.1016/j.anaerobe.2015.10.009
- Koenigsknecht, M. J., Theriot, C. M., Bergin, I. L., Schumacher, C. A., Schloss, P. D., and Young, V. B. (2015). Dynamics and establishment of *Clostridium difficile* infection in the murine gastrointestinal tract. *Infect. Immun.* 83, 934–941. doi: 10.1128/IAI.02768-14
- Kwon, J. H., Olsen, M. A., and Dubberke, E. R. (2015). The morbidity, mortality, and costs associated with *Clostridium difficile* infection. *Infect. Dis. Clin. North Am.* 29, 123–134. doi: 10.1016/j.idc.2014.11.003
- Larson, H. E., Price, A. B., Honour, P., and Borriello, S. P. (1978). *Clostridium difficile* and the aetiology of pseudomembranous colitis. *Lancet* 1, 1063–1066. doi: 10.1016/S0140-6736(78)90912-1
- Lawley, T. D., Clare, S., Deakin, L. J., Goulding, D., Yen, J. L., Raisen, C., et al. (2010). Use of purified *Clostridium difficile* spores to facilitate evaluation of health care disinfection regimens. *Appl. Environ. Microbiol.* 76, 6895–6900. doi: 10.1128/AEM.00718-10

- Lawley, T. D., Croucher, N. J., Yu, L., Clare, S., Sebaihia, M., Goulding, D., et al. (2009). Proteomic and genomic characterization of highly infectious *Clostridium difficile* 630 spores. *J. Bacteriol.* 191, 5377–5386. doi: 10.1128/JB.00597-09
- Leggett, M. J., McDonnell, G., Denyer, S. P., Setlow, P., and Maillard, J. Y. (2012). Bacterial spore structures and their protective role in biocide resistance. *J. Appl. Microbiol.* 113, 485–498. doi: 10.1111/j.1365-2672.2012.05336.x
- Lessa, F. C., Gould, C. V., and McDonald, L. C. (2012). Current status of *Clostridium difficile* infection epidemiology. *Clin. Infect. Dis.* 55(Suppl. 2), S65–S70. doi: 10.1093/cid/cis319
- Levy, A. R., Szabo, S. M., Lozano-Ortega, G., Lloyd-Smith, E., Leung, V., Lawrence, R., et al. (2015). Incidence and costs of *Clostridium difficile* infections in Canada. *Open Forum Infect. Dis.* 2, ofv076. doi: 10.1093/ofid/ofv076
- Mackin, K. E., Carter, G. P., Howarth, P., Rood, J. I., and Lytras, D. (2013). SpoA differentially regulates toxin production in evolutionarily diverse strains of *Clostridium difficile*. *PLoS ONE* 8:e79666. doi: 10.1371/journal.pone.0079666
- Macleod-Glover, N., and Sadowski, C. (2010). Efficacy of cleaning products for *C. difficile*: environmental strategies to reduce the spread of *Clostridium difficile*-associated diarrhea in geriatric rehabilitation. *Can. Fam. Physician* 56, 417–423.
- McBride, S., and Haldenwang, W. G. (2004). Sporulation phenotype of a *Bacillus subtilis* mutant expressing an unprocessable but active sigmaE transcription factor. *J. Bacteriol.* 186, 1999–2005. doi: 10.1128/JB.186.7.1999-2005.2004
- McDonald, L. C., Lessa, F., Sievert, D., Wise, M., Herrera, R., Gould, C., et al. (2012). Vital signs: preventing *Clostridium difficile* infections. *Morb. Mortal. Wkly. Rep.* 61, 157–162.
- Milhaud, P., and Balassa, G. (1973). Biochemical genetics of bacterial sporulation. IV. Sequential development of resistances to chemical and physical agents during sporulation of *Bacillus subtilis*. *Mol. Gen. Genet.* 125, 241–250. doi: 10.1007/BF00270746
- Murrell, W. G., and Scott, W. J. (1966). The heat resistance of bacterial spores at various water activities. *J. Gen. Microbiol.* 43, 411–425. doi: 10.1099/00221287-43-3-411
- Nawrocki, K. L., Edwards, A. N., Daou, N., Bouillaut, L., and McBride, S. M. (2015). CodY-dependent regulation of sporulation in *Clostridium difficile*. *J. Bacteriol.* 198, 2113–2120. doi: 10.1128/JB.00220-16
- Nerandzic, M. M., Sunkesula, V. C. C. T. S., Setlow, P., and Donskey, C. J. (2015). Unlocking the sporicidal potential of ethanol: induced sporicidal activity of ethanol against *Clostridium difficile* and *Bacillus* spores under altered physical and chemical conditions. *PLoS ONE* 10:e0132805. doi: 10.1371/journal.pone.0132805
- Omidbakhsh, N. (2010). Evaluation of sporicidal activities of selected environmental surface disinfectants: carrier tests with the spores of *Clostridium difficile* and its surrogates. *Am. J. Infect. Control* 38, 718–722. doi: 10.1016/j.ajic.2010.02.009
- Oughton, M. T., Loo, V. G., Dendukuri, N., Fenn, S., and Libman, M. D. (2009). Hand hygiene with soap and water is superior to alcohol rub and antiseptic wipes for removal of *Clostridium difficile*. *Infect. Control Hosp. Epidemiol.* 30, 939–944. doi: 10.1086/605322
- Paredes, C. J., Alsaker, K. V., and Papoutsakis, E. T. (2005). A comparative genomic view of clostridial sporulation and physiology. *Nat. Rev. Microbiol.* 3, 969–978. doi: 10.1038/nrmicro1288
- Paredes-Sabja, D., and Sarker, M. R. (2011). Germination response of spores of the pathogenic bacterium *Clostridium perfringens* and *Clostridium difficile* to cultured human epithelial cells. *Anaerobe* 17, 78–84. doi: 10.1016/j.anaerobe.2011.02.001
- Paredes-Sabja, D., Shen, A., and Sorg, J. A. (2014). *Clostridium difficile* spore biology: sporulation, germination, and spore structural proteins. *Trends Microbiol.* 22, 406–416. doi: 10.1016/j.tim.2014.04.003
- Perez, J., Springthorpe, V. S., and Sattar, S. A. (2005). Activity of selected oxidizing microbicides against the spores of *Clostridium difficile*: relevance to environmental control. *Am. J. Infect. Control* 33, 320–325. doi: 10.1016/j.ajic.2005.04.240
- Pizarro-Guajardo, M., Calderon-Romero, P., Castro-Cordova, P., Mora-Uribe, P., and Paredes-Sabja, D. (2016a). Ultrastructural variability of the exosporium layer of *Clostridium difficile* spores. *Appl. Environ. Microbiol.* 82, 2202–2209. doi: 10.1128/AEM.03410-15
- Pizarro-Guajardo, M., Calderon-Romero, P., and Paredes-Sabja, D. (2016b). Revising the ultrastructure variability of the exosporium layer of *Clostridium difficile* spores from sporulating cultures and biofilms. *Appl. Environ. Microbiol.* 82, 5892–5898. doi: 10.1128/AEM.01463-16
- Pizarro-Guajardo, M., Olgun-Araneda, V., Barra-Carrasco, J., Brito-Silva, C., Sarker, M. R., and Paredes-Sabja, D. (2014). Characterization of the collagen-like exosporium protein, BclA1, of *Clostridium difficile* spores. *Anaerobe* 25, 18–30. doi: 10.1016/j.anaerobe.2013.11.003
- Riebe, O., Fischer, R. J., Wampler, D. A., Kurtz, D. M. Jr., and Bahl, H. (2009). Pathway for H₂O₂ and O₂ detoxification in *Clostridium acetobutylicum*. *Microbiology* 155(Pt 1), 16–24. doi: 10.1099/mic.0.022756-0
- Rodriguez-Palacios, A., and Lejeune, J. T. (2011). Moist-heat resistance, spore aging, and superdormancy in *Clostridium difficile*. *Appl. Environ. Microbiol.* 77, 3085–3091. doi: 10.1128/AEM.01589-1510
- Rupnik, M., Wilcox, M. H., and Gerding, D. N. (2009). *Clostridium difficile* infection: new developments in epidemiology and pathogenesis. *Nat. Rev. Microbiol.* 7, 526–536. doi: 10.1038/nrmicro2164
- Russell, A. D. (1990). Bacterial spores and chemical sporicidal agents. *Clin. Microbiol. Rev.* 3, 99–119. doi: 10.1128/CMR.3.2.99
- Schiott, T., and Hederstedt, L. (2000). Efficient spore synthesis in *Bacillus subtilis* depends on the CcdA protein. *J. Bacteriol.* 182, 2845–2854. doi: 10.1128/JB.182.10.2845-2854.2000
- Setlow, P. (2006). Spores of *Bacillus subtilis*: their resistance to and killing by radiation, heat and chemicals. *J. Appl. Microbiol.* 101, 514–525. doi: 10.1111/j.1365-2672.2005.02736.x
- Setlow, P. (2014). Spore resistance properties. *Microbiol. Spectr.* 2. doi: 10.1128/microbiolspec.TBS-0003-2012
- Shen, A. (2012). *Clostridium difficile* toxins: mediators of inflammation. *J. Innate Immun.* 4, 149–158. doi: 10.1159/000332946
- Slauch, J. M. (2011). How does the oxidative burst of macrophages kill bacteria? Still an open question. *Mol. Microbiol.* 80, 580–583. doi: 10.1111/j.1365-2958.2011.07612.x
- Smits, W. K., Lytras, D., Lacy, D. B., Wilcox, M. H., and Kuijper, E. J. (2016). *Clostridium difficile* infection. *Nat. Rev. Dis. Primers* 2, 16020. doi: 10.1038/nrdp.2016.20
- Sorg, J. A., and Sonenshein, A. L. (2008). Bile salts and glycine as cogerminants for *Clostridium difficile* spores. *J. Bacteriol.* 190, 2505–2512. doi: 10.1128/JB.01765-07
- Stabler, R. A., He, M., Dawson, L., Martin, M., Valiente, E., Corton, C., et al. (2009). Comparative genome and phenotypic analysis of *Clostridium difficile* 027 strains provides insight into the evolution of a hypervirulent bacterium. *Genome Biol.* 10, R102. doi: 10.1186/gb-2009-10-9-r102
- Steindl, G., Fiedler, A., Huhulescu, S., Wewalka, G., and Allerberger, F. (2015). Effect of airborne hydrogen peroxide on spores of *Clostridium difficile*. *Wien Klin. Wochenschr.* 127, 421–426. doi: 10.1007/s00508-014-0682-6
- Theriot, C. M., Bowman, A. A., and Young, V. B. (2016). Antibiotic-induced alterations of the gut microbiota alter secondary bile acid production and allow for *Clostridium difficile* spore germination and outgrowth in the large intestine. *mSphere* 1, e45–e15. doi: 10.1128/mSphere.00045-15
- Theriot, C. M., and Young, V. B. (2015). Interactions between the gastrointestinal microbiome and *Clostridium difficile*. *Annu. Rev. Microbiol.* 69, 445–461. doi: 10.1146/annurev-micro-091014-104115
- Thomas, C. M., and Smith, C. A. (1987). Incompatibility group P plasmids: genetics, evolution, and use in genetic manipulation. *Annu. Rev. Microbiol.* 41, 77–101. doi: 10.1146/annurev.mi.41.100187.000453
- Tracy, B. P., Jones, S. W., and Papoutsakis, E. T. (2011). Inactivation of sigmaE and sigmaG in *Clostridium acetobutylicum* illuminates their roles in clostridial-cell-form biogenesis, granulose synthesis, solventogenesis, and spore morphogenesis. *J. Bacteriol.* 193, 1414–1426. doi: 10.1128/JB.01380-10
- Vohra, P., and Poxton, I. R. (2011). Efficacy of decontaminants and disinfectants against *Clostridium difficile*. *J. Med. Microbiol.* 60(Pt 8), 1218–1224. doi: 10.1099/jmm.0.030288-30280
- Voith, D. E., and Ballard, J. D. (2005). *Clostridium difficile* toxins: mechanism of action and role in disease. *Clin. Microbiol. Rev.* 18, 247–263. doi: 10.1128/CMR.18.2.247-263.2005
- Wilcox, M. H., Fawley, W. N., Wigglesworth, N., Parnell, P., Verity, P., and Freeman, J. (2003). Comparison of the effect of detergent versus hypochlorite cleaning on environmental contamination and incidence of *Clostridium difficile* infection. *J. Hosp. Infect.* 54, 109–114. doi: 10.1016/S0195-6701(02)00400-0

Wilson, K. H., Kennedy, M. J., and Fekety, F. R. (1982). Use of sodium taurocholate to enhance spore recovery on a medium selective for *Clostridium difficile*. *J. Clin. Microbiol.* 15, 443–446.

Conflict of Interest Statement: The authors declare that the research was conducted in the absence of any commercial or financial relationships that could be construed as a potential conflict of interest.

Copyright © 2016 Edwards, Karim, Pascual, Jowhar, Anderson and McBride. This is an open-access article distributed under the terms of the Creative Commons Attribution License (CC BY). The use, distribution or reproduction in other forums is permitted, provided the original author(s) or licensor are credited and that the original publication in this journal is cited, in accordance with accepted academic practice. No use, distribution or reproduction is permitted which does not comply with these terms.



The Influence of Sporulation Conditions on the Spore Coat Protein Composition of *Bacillus subtilis* Spores

Wishwas R. Abhyankar^{1,2*}, Kiki Kamphorst¹, Bhagyashree N. Swarge^{1,2}, Henk van Veen³, Nicole N. van der Wel³, Stanley Brul², Chris G. de Koster¹ and Leo J. de Koning¹

¹ Department of Mass Spectrometry of Bio-macromolecules, Swammerdam Institute for Life Sciences, University of Amsterdam, Amsterdam, Netherlands, ² Department of Molecular Biology and Microbial Food Safety, Swammerdam Institute for Life Sciences, University of Amsterdam, Amsterdam, Netherlands, ³ Department of Cell Biology and Histology, Electron Microscopy Centre Amsterdam, Academic Medical Center, Amsterdam, Netherlands

OPEN ACCESS

Edited by:

Simon Michael Cutting,
Royal Holloway, University of London,
UK

Reviewed by:

Daniel Paredes-Sabja,
Universidad Andres Bello, Chile
Susan Schlimpert,
Biotechnology and Biological
Sciences Research Council, UK

*Correspondence:

Wishwas R. Abhyankar
w.r.abhyankar@uva.nl

Specialty section:

This article was submitted to
Microbial Physiology and Metabolism,
a section of the journal
Frontiers in Microbiology

Received: 30 June 2016

Accepted: 30 September 2016

Published: 13 October 2016

Citation:

Abhyankar WR, Kamphorst K, Swarge BN, van Veen H, van der Wel NN, Brul S, de Koster CG and de Koning LJ (2016) The Influence of Sporulation Conditions on the Spore Coat Protein Composition of *Bacillus subtilis* Spores. *Front. Microbiol.* 7:1636.
doi: 10.3389/fmicb.2016.01636

Spores are of high interest to the food and health sectors because of their extreme resistance to harsh conditions, especially against heat. Earlier research has shown that spores prepared on solid agar plates have a higher heat resistance than those prepared under a liquid medium condition. It has also been shown that the more mature a spore is, the higher is its heat resistance most likely mediated, at least in part, by the progressive cross-linking of coat proteins. The current study for the first time assesses, at the proteomic level, the effect of two commonly used sporulation conditions on spore protein presence. ¹⁴N spores prepared on solid Schaeffer's-glucose (SG) agar plates and ¹⁵N metabolically labeled spores prepared in shake flasks containing 3-(N-morpholino) propane sulfonic acid (MOPS) buffered defined liquid medium differ in their coat protein composition as revealed by LC-FT-MS/MS analyses. The former condition mimics the industrial settings while the latter conditions mimic the routine laboratory environment wherein spores are developed. As seen previously in many studies, the spores prepared on the solid agar plates show a higher thermal resistance than the spores prepared under liquid culture conditions. The ¹⁴N:¹⁵N isotopic ratio of the 1:1 mixture of the spore suspensions exposes that most of the identified inner coat and crust proteins are significantly more abundant while most of the outer coat proteins are significantly less abundant for the spores prepared on solid SG agar plates relative to the spores prepared in the liquid MOPS buffered defined medium. Sporulation condition-specific differences and variation in isotopic ratios between the tryptic peptides of expected cross-linked proteins suggest that the coat protein cross-linking may also be condition specific. Since the core dipicolinic acid content is found to be similar in both the spore populations, it appears that the difference in wet heat resistance is connected to the differences in the coat protein composition and assembly. Corroborating the proteomic analyses, electron microscopy analyses show a significantly thinner outer coat layer of the spores cultured on the solid agar medium.

Keywords: *Bacillus*, sporulation conditions, spores, proteomics, quantitative proteomics

INTRODUCTION

Bacterial spores are of high interest because of their extreme resistance properties, especially toward nutritional and environmental stresses (Rose et al., 2007), and the heterogeneity amongst them. Due to their resistant nature, the methods to prevent bacterial contamination do not eliminate spores easily. This is not only a concern to the food processing and production industries but also to the cleaning rooms of industries as well as the medical sectors (Checinska et al., 2015). To develop spore prevention methods, the mechanisms of development and resistance of spores have to be understood completely. For a long time, the heat resistance of spores is of high interest in microbiology and therefore this property has been highly examined (Mundra et al., 2014). Stress resistant spores can germinate to form vegetative cells when the conditions become favorable resulting in food spoilage or sometimes food intoxication (Checinska et al., 2015). The spore germination behavior is heterogeneous and therefore an additional challenge to the food industries. The multiple layers of spores all contribute in some way to their resistance properties (Driks, 2002). It is believed that next to the dehydrated core, the cortex and coat contribute to the spores' heat resistance. The core consists of the cell's DNA, ribosomes, dipicolinic acid (DPA), and small acid-soluble proteins or SASPs (Setlow, 1988). The SASPs protect the DNA, while DPA forms a chelate complex with cations like calcium (Checinska et al., 2015). These chelate complexes are suggested to play a role in dehydration of the core, which in turn protects the spore from heat stress and UV light (Setlow et al., 2006). The major function of the external coat layers is to protect the spore from any enzyme or chemical assault and preserve the genome (McKenney et al., 2013). A peculiarity of these proteinaceous layers is that ~30% of it is said to be composed of insoluble cross-linked proteins.

The resistance of spores is affected by more than one factor during their development. The group of Sanchez-Salas et al. (2011) compared the wet heat resistance of young spores with the total produced (matured) spores from the same culture and found young spores to have a significantly lower wet heat resistance. Sanchez-Salas et al. (2011) concluded that changes in the spore coat during maturation are responsible for the higher wet heat resistance. Furthermore, a recent study from our group suggested that the inter-protein cross-linking might contribute to the heat resistance of the spores (Abhyankar et al., 2015). However, the influence of initial sporulation conditions on spore resistance properties was here not explicitly assessed. In a previous study, it had been shown that spores made at higher temperatures had a higher wet heat resistant than spores generated at lower sporulation temperatures (Melly et al., 2002). In addition, effects of the sporulation medium on spore's stress resistance properties have been assessed in a number of studies. Dadd et al. (1983) showed that the level of nutrients and the amount of available divalent cations affect spore thermal stress resistance properties (Dadd et al., 1983). Rose et al. (2007) performed a study comparing the wet heat resistance of *Bacillus subtilis* spores

prepared in 2x Schaeffer's-glucose (2x SG) liquid and solid medium. The spores made on plates were more resistant to a temperature of 90°C in water than the spores made in liquid medium (Rose et al., 2007). The same group also concluded that there was no difference in the core water, DPA levels between two spore populations but these populations differed in their germination behavior. Yet, the effect of sporulation conditions on the spore's (coat) proteome remains elusive.

The current research has focused on three main questions – (1) What is the influence of different sporulation conditions used in industries and research laboratories on the spore coat protein composition? (2) What is the influence of different sporulation conditions on spore coat inter-protein cross-linking and coat ultrastructure? (3) Does the (sporulation) condition-induced specific changes in spore thermal resistance, correlate with the changes in the spore coat proteome and changes in the extent of cross-linking of proteins such as CotG, CotU, GerQ, etc.? To answer these questions a quantitative proteomic analysis of *B. subtilis* spores made in liquid and on agar plates has been set-up under two commonly used sporulation conditions using two of the most common sporulation media. To that end ¹⁴N and metabolically labeled ¹⁵N vegetative cells are sporulated on ¹⁴N 2x SG agar solid plates or in a ¹⁵N-labeled 3-(N-morpholino) propane sulfonic acid (MOPS) buffered defined liquid medium, respectively. The former condition is generally used in industry as a condition known to yield most stress resistant spores and one that bears similarity to the conditions in the food chain. The latter condition is commonly used in fundamental microbiology laboratories as it allows for the dissection of the effects of individual medium components as well as provides homogenous conditions to maximize spore homogeneity useful for numerous biochemical studies. The spore suspensions are mixed 1:1 based on the optical density values and the protein ratios for the two different sporulation conditions are determined as the ¹⁴N: ¹⁵N protein abundance ratios with LC-FTMS analyses. DPA contents of two spore populations are determined to check the effect of each sporulation condition on the DPA content. Finally, to support our proteomics data, electron microscopy (EM) has been used and the thickness of different spore layers is measured. It appears that the spore coat protein composition of the two spore populations differs significantly. Especially, the outer coat proteome is affected by the sporulation conditions. The EM analyses show that the spores developed on the solid medium possess thinner outer coats compared to the spores formed in the liquid sporulation medium. Though the DPA levels of both spore populations are similar, the spores formed on plates are significantly more heat resistant. Interestingly, the crust proteins and certain coat proteins known to be involved in cross-linking in the spores are identified in higher abundance in the spores developed on solid medium relative to those developed in liquid medium. For these proteins, variations in peptide ratios are seen. This suggests that the enhanced heat resistance is possibly linked to the specific cross-linked coat proteins and the degree of cross-linking therein.

MATERIALS AND METHODS

Bacterial Strain and Sporulation Conditions

The *B. subtilis* wild-type strain PY79 used in this work was obtained from Dr. Eichenberger's lab (New York University, USA). The aim was to study the effect of two of the most common yet drastically different sporulation conditions used in practice in industries and fundamental studies, respectively. Therefore we chose 2x SG agar as a solid medium and liquid defined medium buffered with MOPS in our study. Initially, the cells were cultured on a Tryptic Soy agar plate and incubated overnight at 37°C. A single colony was then inoculated in the liquid Tryptic Soy broth medium and cultivated until early exponential phase. The exponentially growing cells were then subjected to growth in serial dilutions (as shown in Figure 1) of 2x SG liquid medium (^{14}N medium; further referred to as ^{14}N cells) and a defined medium, buffered with MOPS supplemented with $^{15}\text{NH}_4\text{Cl}$ (further referred to as ^{15}N cells). Further, the culture enrichment was done in 20 ml 2x SG and MOPS liquid media, respectively. For sporulation, the conditions differed significantly. The enriched ^{14}N cells (0.1 ml) were spread on 10 plates of 2x SG agar (incubated at 37°C) whereas the enriched ^{15}N cells were inoculated (1% final volume) to 500 ml of MOPS medium (incubated at 37°C at 200 rpm). The cells were allowed to sporulate for 5 days when the sporulation was induced by glucose exhaustion as described elsewhere (Abhyankar et al., 2011). Four independent biological replicates were prepared and analyzed.

Spore Harvesting

After 5 days of incubation, the ^{14}N spores were collected by scraping them off from the 2x SG agar plates and centrifugation whereas the ^{15}N spores were harvested by centrifugation and removal of the supernatant. Both sets of spores were further purified as described in the literature (Abhyankar et al., 2011). In short, the spores were washed once with 0.01% Tween to kill the vegetative cells and further washed seven times with Milli-Q water. Any remaining vegetative cells were removed using a Histodenz gradient centrifugation, if needed as described elsewhere (Abhyankar et al., 2015). The yield of ^{14}N spores was lower (10^9 spores/mL) compared to the ^{15}N spores (10^{11} spores/mL). The purified spore crops contained >99% phase bright spores.

Mixing of ^{14}N and ^{15}N - Labeled Spores and Spore Coat Isolation

The harvested ^{14}N and ^{15}N spores were mixed in 1:1 ratio based on OD₆₀₀ and re-suspended in cold 10 mM Tris-HCl (pH 7.5). Subsequently the spores were disintegrated with 0.1-mm Zirconia Silica beads in a Bio-Savant Fast Prep 120 machine (Qbiogene, Carlsbad, CA, USA). A program of nine Fast-prepping rounds was set. One round lasted for 40 s at a maximum speed of 6. After every three rounds, the samples were placed on ice for 5 min to prevent protein degradation by over-heating. To remove non-covalently

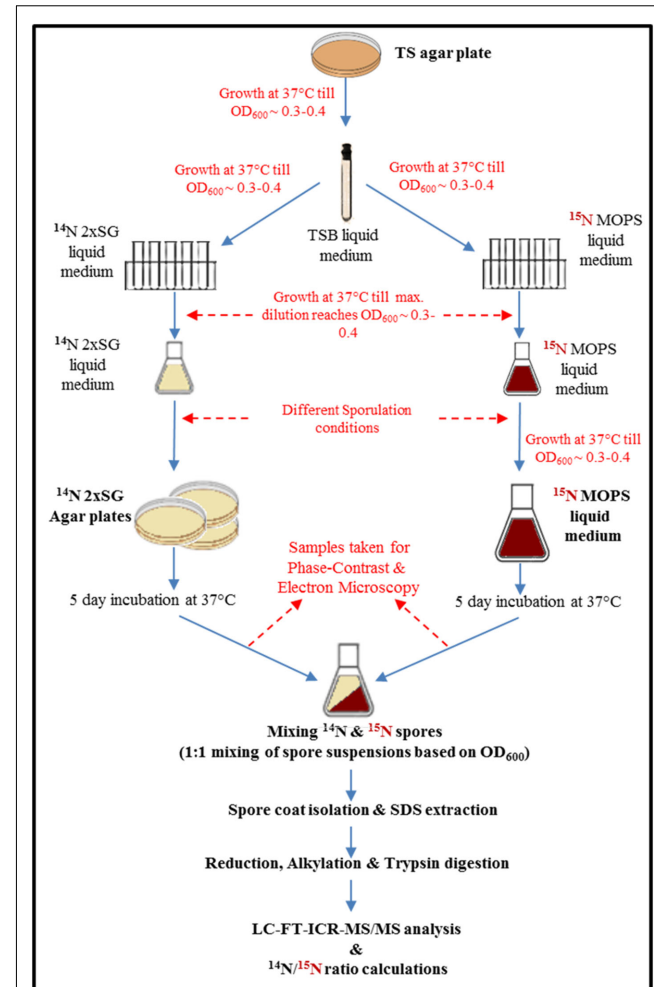


FIGURE 1 | Workflow of quantitative proteomics of spores prepared under the most common sporulation conditions used in industries (solid agar plates) and in routine microbiology laboratories (liquid medium). The magenta color indicates presence of ^{15}N in the medium, cells, and therefore also in spores.

linked proteins and intracellular contaminants, isolated layers of insoluble spore material were washed extensively with 1 M NaCl and thermally treated for 10 min at 80°C in a water bath, with 50 mM Tris-HCl, pH 7.8 containing 2% SDS, 100 mM Na-EDTA, 150 mM NaCl, and 100 mM β -mercaptoethanol (Abhyankar et al., 2011). SDS-treated coats were washed four times with Milli-Q water and freeze dried overnight for immediate use for mass spectrometric (MS) analysis.

Sample Preparation for MS Analysis

The freeze-dried coat material was subjected to reduction with 10 mM dithiothreitol in 100 mM NH₄HCO₃ (1 h at 55°C). To avoid the re-formation of the di-sulfide bridges, alkylation of the reduced coat material was performed with 55 mM iodoacetamide in 100 mM NH₄HCO₃ for 45 min at room temperature in the dark. Subsequently the proteins

were digested for 18 h at 37°C with trypsin (Trypsin Gold Promega, Madison, WI, USA) using a 1:60 (w/w) protease: protein ratio. After 18 h, the tryptic digests were desalting using Omix μC18 pipette tips (80 µg capacity, Varian, Palo Alto, CA, USA) according to the manufacturer's instructions. The peptides were collected in 25 µL 50% acetonitrile (ACN), 0.1% trifluoroacetic acid (TFA), and stored at -80°C (Abhyankar et al., 2011). Before analysis a fraction of eluted peptide material was freeze-dried and concentrated in 10 µL of 0.1% TFA and peptide concentration was measured at 205 nm (Scopes, 1974) with a Nanodrop ND1000 spectrophotometer (Isogen Life Sciences, De Meern, The Netherlands).

Liquid Chromatography-Fourier Transform Ion Cyclotron Tandem Mass Spectrometry (LC-FT-ICR MS/MS) Analysis

LC-MS/MS data were acquired with an Bruker ApexUltra Fourier Transform Ion Cyclotron Resonance Mass Spectrometer (Bruker Daltonics, Bremen, Germany) equipped with a 7T magnet and a nano-electrospray Apollo II DualSourceTM coupled to an Ultimate 3000 (Dionex, Sunnyvale, CA, USA) High-Performance Liquid Chromatography system. For each digest, samples containing up to 200 ng of tryptic peptides were injected as a 20 µL 0.1% TFA, 3% ACN aqueous solution, and loaded onto a PepMap100 C18 (5 µm particle size, 100 Å pore size, 300 µm inner diameter × 5 mm length) precolumn. Following injection, the peptides were eluted via an Acclaim PepMap 100 C18 (3 µm particle size, 100 Å pore size, 75 µm inner diameter × 500 mm length.) analytical column (Thermo Scientific, Etten-Leur, The Netherlands) to the nano-electrospray source. LC gradient profiles of up to 120 min were used with 0.1% formic acid/99.9% H₂O (A) and 0.1% formic acid/80% ACN/19.9% H₂O (B) at a flow rate of 300 nL/min at a column temperature of 60°C. The gradient profiles were as follows 0 min 97%A/3%B, 2 min 94%A/6%B, 110 min 70%A/30%B, 120 min 60%A/40%B, 125 min 100%B. Data dependent Q-selected peptide ions were fragmented in the hexapole collision cell at an Argon pressure of 6×10^{-6} mbar (measured at the ion gage) and the fragment ions were detected in the ICR cell at a resolution of up to 60,000. In the MS/MS duty cycle, three different precursor peptide ions were selected from each survey MS. The MS/MS duty cycle time for one survey MS and three MS/MS acquisitions was about 2 s. Instrument mass calibration was better than 2 ppm over an m/z range of 250–1500. Raw FT-MS/MS data were processed with the MASCOT DISTILLER program, version 2.4.3.1 (64 bits), MDRO 2.4.3.0 (MATRIX science, London, UK), including the Search toolbox and the Quantification toolbox. Peak-picking for both MS and MS/MS spectra were optimized for the mass resolution of up to 60,000. Peaks were fitted to a simulated isotope distribution with a correlation threshold of 0.7, with minimum signal to noise of 2. The processed data, from the four independent biological replicates, were searched with the MASCOT server program 2.3.02 (MATRIX science, London, UK) against a complete *B. subtilis* 168 ORF translation database

(Uniprot 2011 update, downloaded from <http://www.uniprot.org/uniprot>) combined with a protein contamination data base (compiled by and downloaded from Max Planck Institute of Biochemistry, Martinsried). Quantification using ¹⁵N-Metabolic [MD] labeling was included. Trypsin was used as enzyme and one missed cleavage was allowed. Carbamidomethylation of cysteine was used as a fixed modification and oxidation of methionine as a variable modification. The peptide mass tolerance was set to 25 ppm and the peptide fragment mass tolerance was set to 0.03 Dalton. MASCOT MudPIT peptide identification score was set to a cut-off of 18. The MASCOT protein identification reports were exported as XML and then imported in custom made Visual Basic (VBA) software program Protein Browser running in Microsoft Excel. The program facilitates organization and data mining of large sets of proteomics data. The identified proteins for each of the four replica of ¹⁴N/¹⁵N spore mixture coat isolate samples are listed in Supplementary Table S1A, together with their protein MASCOT score and number of peptide spectrum matches. These proteins were identified in at least two out of four replicates with at least two unique peptides. Using the quantification toolbox, the isotopic ratios for a subset of identified proteins were determined as an average of the isotopic ratios of the corresponding light over heavy tryptic peptides. This subset represents a selection of known and putative spore coat proteins, based on literature, sigma regulations, and localization studies. Critical settings were: require bold red: on, significance threshold: 0.05; Protocol type: precursor; Correction: Element ¹⁵N; Value 99.6; Report ratio L/H; Integration method: Simpson's integration method; Integration source: survey; Allow elution time shift: on; Elution time delta: 20 s; Std. Err. Threshold: 0.15, Correlation Threshold (Isotopic distribution fit): 0.98; XIC threshold: 0.1; All charge states: on; Max XIC width: 200 s; Threshold type: at least homology; Peptide threshold value: 0.05; unique pepseq: on. All reported isotopic peptide ratios were manually validated by inspection of the spectral MS data. The MASCOT DISTILLER protein quantification reports were exported in excel format and then imported in the Protein Browser program. To correct for possible errors in ¹⁴N/¹⁵N 1:1 culture mixing, the ¹⁴N/¹⁵N ratios were normalized on the median for each replicate dataset. For quantification a sub-selection of putative and known coat proteins was made based on previous literature (Abhyankar et al., 2015), localization studies and their regulating sigma factors. The quantified putative coat proteins for each of the four replica ¹⁴N/¹⁵N spore mixture coat isolate samples are included in Supplementary Table S1B, together with their protein MASCOT score and light over heavy (L/H) isotopic ratio. The proteins that were quantified at least in two of the four replicates have been included in the results. The proteomics data has been deposited to the ProteomeXchange Consortium (Vizcaíno et al., 2014) via the PRIDE partner repository with the dataset identifier PXD004473.

Measurement of Thermal Resistance of ¹⁴N and ¹⁵N Spores

One milliliter of spores (¹⁴N as well as ¹⁵N spores) with an OD₆₀₀ of 2 were heat activated (70°C, 30 min) in a water bath. The

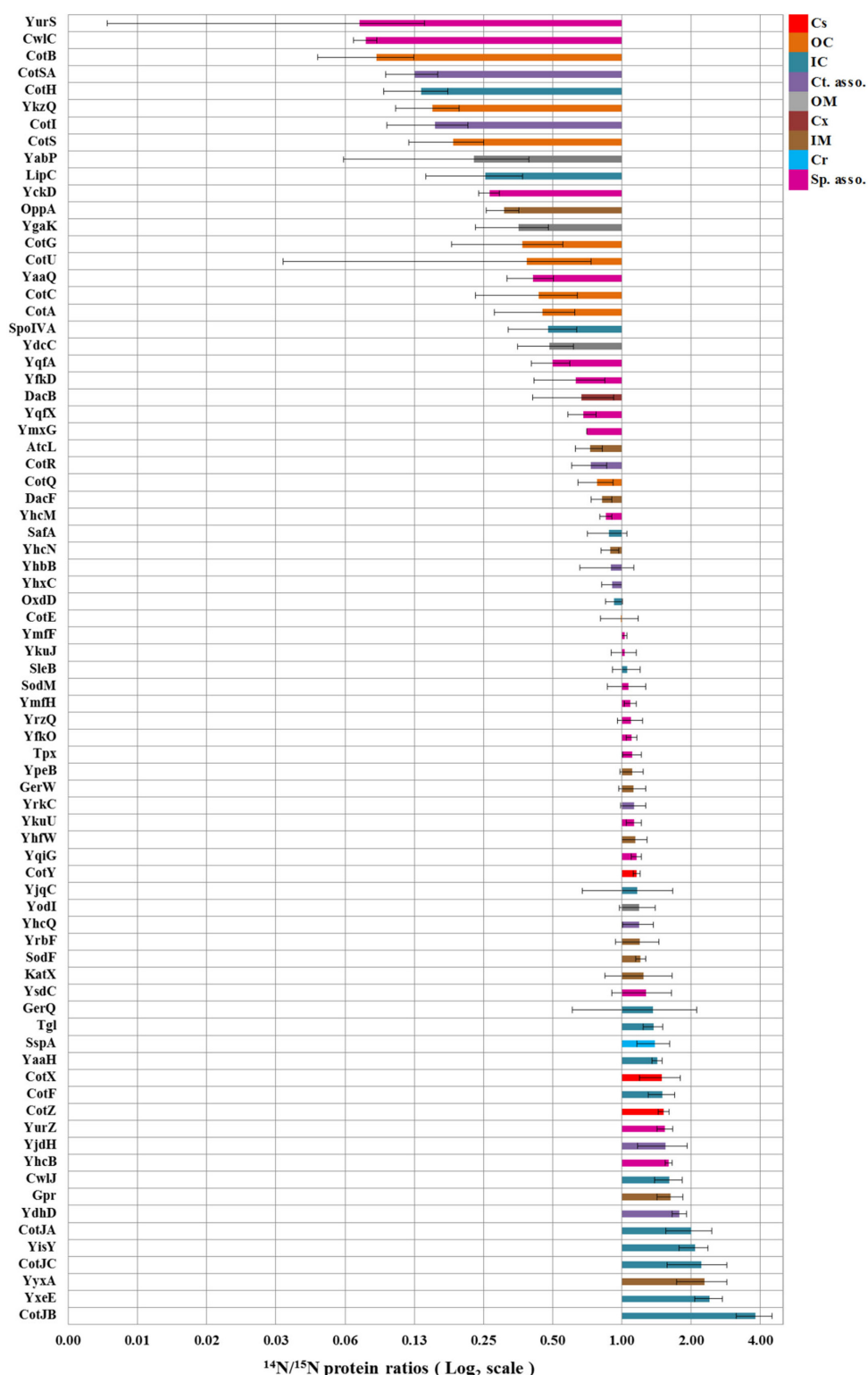


FIGURE 2 | Fold changes in spore coat protein expression in spores cultured on solid agar plates and in shake flask with liquid medium. The bars indicate the mean ratios of proteins across four replicates while error bars indicate the standard deviations in these ratios. By definition, the values are within 95.40% confidence interval in the range of the error bars. The protein localization is based upon their sigma factor regulations and the available literature (van Ooij et al., 2004; Immura et al., 2010; McKenney et al., 2010; Driks and Eichenberger, 2016). Cs, Crust; OC, Outer coat; IC, Inner coat; Ct. asso., Spore coat associated proteins; OM, Outer membrane; Cx, Cortex; IM, Inner membrane; Cr, Core; Sp. asso., Spore associated proteins.

vegetative cells, if any, were inactivated by the heat activation. After heat activation the 1 ml of spores were injected with a syringe into metal screw-cap tubes with 9 ml of sterile Milli-Q water which were pre-heated for 20 min in a glycerol bath (85°C). The spore suspensions from three biological replicates were heated for 10 min (85°C) in the glycerol bath inducing thermal stress. After 10 min, the tubes were cooled on ice. One milliliter of the spore suspension was serially diluted in sterile Milli-Q water and 100 µl of sample from last three dilutions was spread on Tryptic Soy agar plates. The heat resistance was determined by counting the number of colonies after 48 h incubation at 37°C (Kooiman et al., 1973). Two technical replicates were performed for each biological replicate.

Measurement of DPA Concentration in ^{14}N and ^{15}N Spores

Dipicolinic acid analysis was performed according to an established protocol (Janssen et al., 1958). Spore suspension with a fixed OD₆₀₀ was freeze dried and weighed. Consequently, the spores were suspended in 5 ml of sterile Milli-Q water and autoclaved for 15 min at 121°C. The spores were then cooled on ice, acidified with 100 µl of 1 N acetic acid and incubated for 1 h at room temperature. After 1 h, the spores were centrifuged (10 min at 1500 × g) and 4 ml of the supernatant was transferred to new test tube. One milliliter of the color reagent [1 % Fe(NH₄)₂(SO₄)₂.6H₂O along with 1 % ascorbic acid in 0.5 M acetate buffer of pH 5.5] was added to the supernatant. By measuring the A₄₄₀, a standard curve was prepared for the concentration range of 20–140 µg/ml DPA. The A₄₄₀ of the mixture was measured and the amounts were calculated from the standard curve.

Electron Microscopy

For each sporulation condition, the spores were fixed in 1% glutaraldehyde and 4% paraformaldehyde in 0.1 M Phosphate buffer (pH 7.4) for 60 min. After fixation the spores were washed in distilled water, block stained overnight in 1.5% uranyl acetate to enhance contrast in the electron microscope, washed in distilled water, and osmicated for 60 min in 1% OsO₄ in water (Electron Microscopy Sciences, Hatfield, PA, USA). Subsequently, the spores were dehydrated in an alcohol series (of ethanol) and embedded into propylene oxide/Epon 1:1 before embedding into LX-112 resin (Ladd Research, Williston, VT, USA). Between each step, the spores were centrifuged down. After polymerization at 60°C the Epon blocks with the spores were prepared for ultrathin sectioning. Ultrathin sections of 90 nm were cut on a Reichert EM UC6 with a diamond knife, collected on Formvar coated grids and stained with uranyl acetate and lead citrate. Sections were examined with a FEI Technai-12 G2 Spirit Biotwin transmission electron microscope (TEM). Images were taken with a Veleta camera (Olympus, SIS). For measurement of the thickness of the coat layers, using the iTEM software (Emsis) the images of cross-sectioned spores were taken at a magnification of 120,000×. For these measurements, 80 spores per replicate were used.

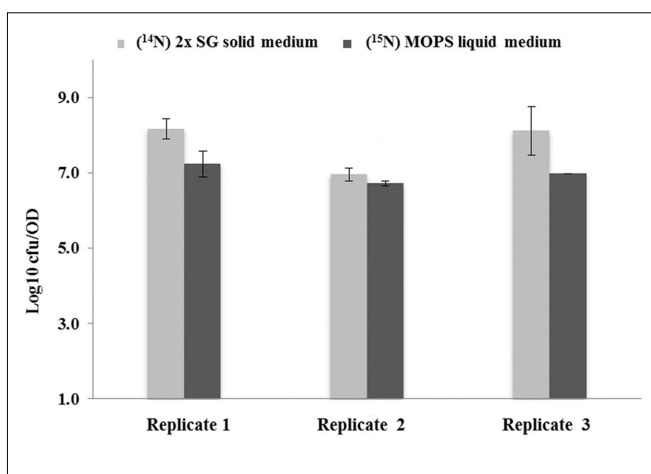


FIGURE 3 | Thermal resistance of spores developed under different sporulation conditions. Log₁₀ values of colony forming units (CFU) obtained after 48 h incubation per OD₆₀₀ of spores. The values represent the mean averages for three biological replicates where the error bars represent the standard deviation observed for two technical replicates. By definition, the values are within 95.40% confidence interval in the range of the error bars.

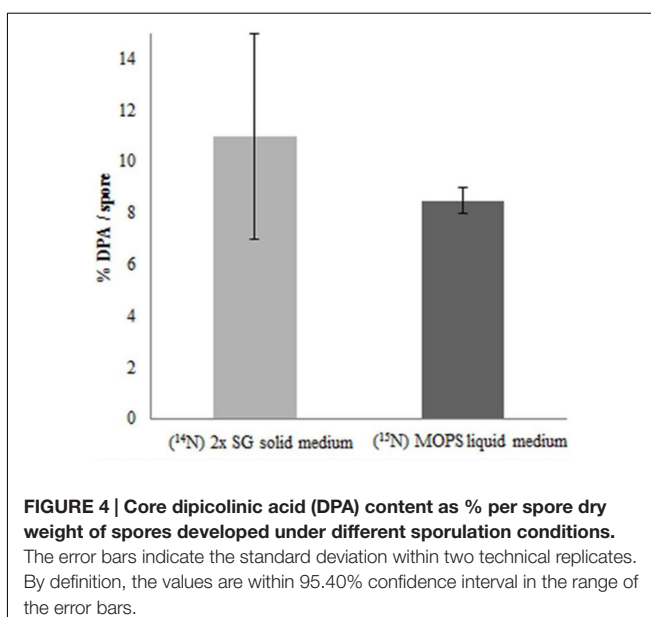


FIGURE 4 | Core dipicolinic acid (DPA) content as % per spore dry weight of spores developed under different sporulation conditions.

The error bars indicate the standard deviation within two technical replicates. By definition, the values are within 95.40% confidence interval in the range of the error bars.

RESULTS

Differences in Coat Protein Levels of Spores Developed under Solid and Liquid Medium Conditions

A total of 351 proteins have been identified across four replicates (Supplementary Table S1A). Because part of the identified proteins are co-isolated cytosolic proteins, only a selected group of spore proteins have been quantified by calculating their $^{14}\text{N}/^{15}\text{N}$ isotopic ratio (Supplementary Table S1B). This sub-selection includes outer coat, inner coat, and crust proteins as identified based on their sigma factor regulation and/or

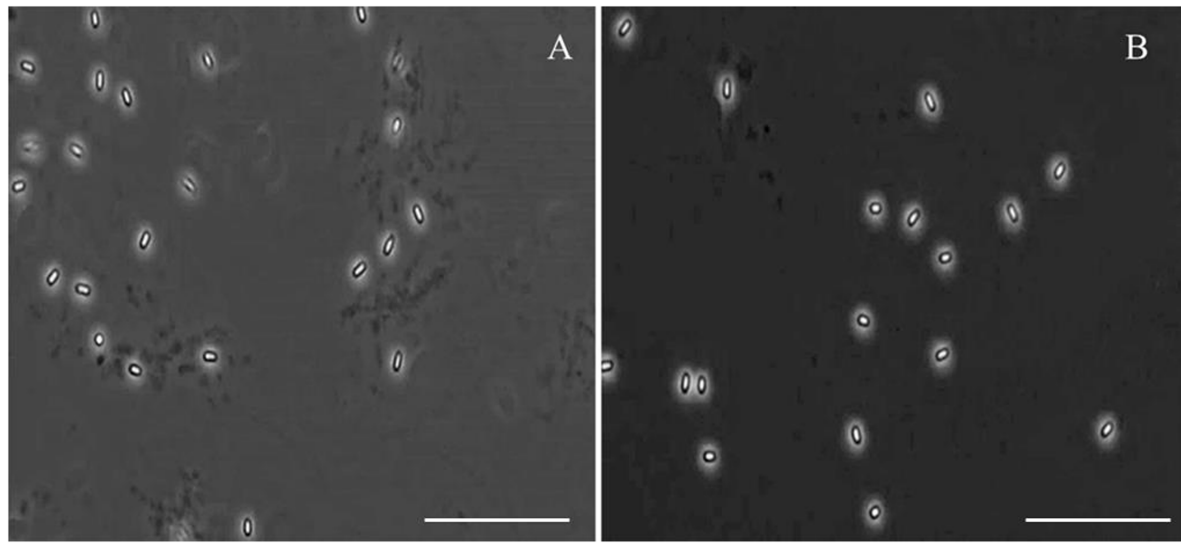


FIGURE 5 | Phase contrast microscopic images of spores cultured on solid agar plates (A) and in shake flasks containing liquid medium (B). The spores are observed under 100 \times magnification with oil under simple phase contrast microscope. Scale bars indicate 10 μ m.

localization (Abhyankar et al., 2011). The mean average of light/heavy ratios of the proteins over the four replicates are plotted on a Log₂ scale (**Figure 2**) as coat protein fold changes between the spores cultured under solid and in liquid medium conditions. The error bars indicate the standard deviation per protein. The results in **Figure 2** show that most of the outer coat proteins such as CotA, CotG, CotC, CotU, etc., are lower in abundance in spores developed on solid sporulation medium (represented in the upper part of the figure with isotopic ratios lower than 1). Also all known crust proteins CotX, CotY, and CotZ as well as many of the inner coat proteins such as CotJA, CotJB, etc., are seen to be highly abundant in the spores obtained from solid sporulation media (represented in the lower part of the figure with isotopic ratios greater than 1).

Thermal Resistance of ^{14}N and ^{15}N Spores Obtained from SG Plates and MOPS in Shake Flask Conditions

The results for the thermal resistance test for spores at 85°C for 10 min are shown in **Figure 3**. The data shows the Log₁₀ number of colonies, grown on the TSA plates 48 h after the thermally induced stress had been given. Shown are mean values, averaged over two technical replicates performed for three biological replicates. It appears that the spores prepared on the 2x SG solid medium plates yield significantly more colonies thereby indicating a higher thermal resistance than observed for the spores generated under liquid medium condition.

The Core DPA Content of ^{14}N and ^{15}N Spores Obtained from SG Plates and MOPS in Shake Flask Conditions

In order to check the role of DPA on thermal resistance of spore cultured under different sporulation conditions, the DPA



FIGURE 6 | Appearance of liquid suspensions of spores cultured on 2x SG agar plates (A) and in 3-(N-morpholino) propane sulfonic acid (MOPS) buffered defined liquid medium in shake flask (B). Two spore crops differ in their color as liquid suspensions in sterile Milli-Q water with equal OD₆₀₀.

concentrations were measured. For both spore populations, the DPA content analyses show no significant differences. As shown in **Figure 4** the DPA amount, mean averaged over two technical replicate analyses in both spore populations, is between the previously reported range of 5–15% (by weight) per spore (Gerhardt and Marquis, 1989).

Morphology of ^{14}N and ^{15}N Spores Obtained from SG Plates and MOPS in Shake Flask Conditions

The spores prepared on solid and in liquid media under the phase contrast microscope show no significant morphological difference in terms of size and shape of both spore populations

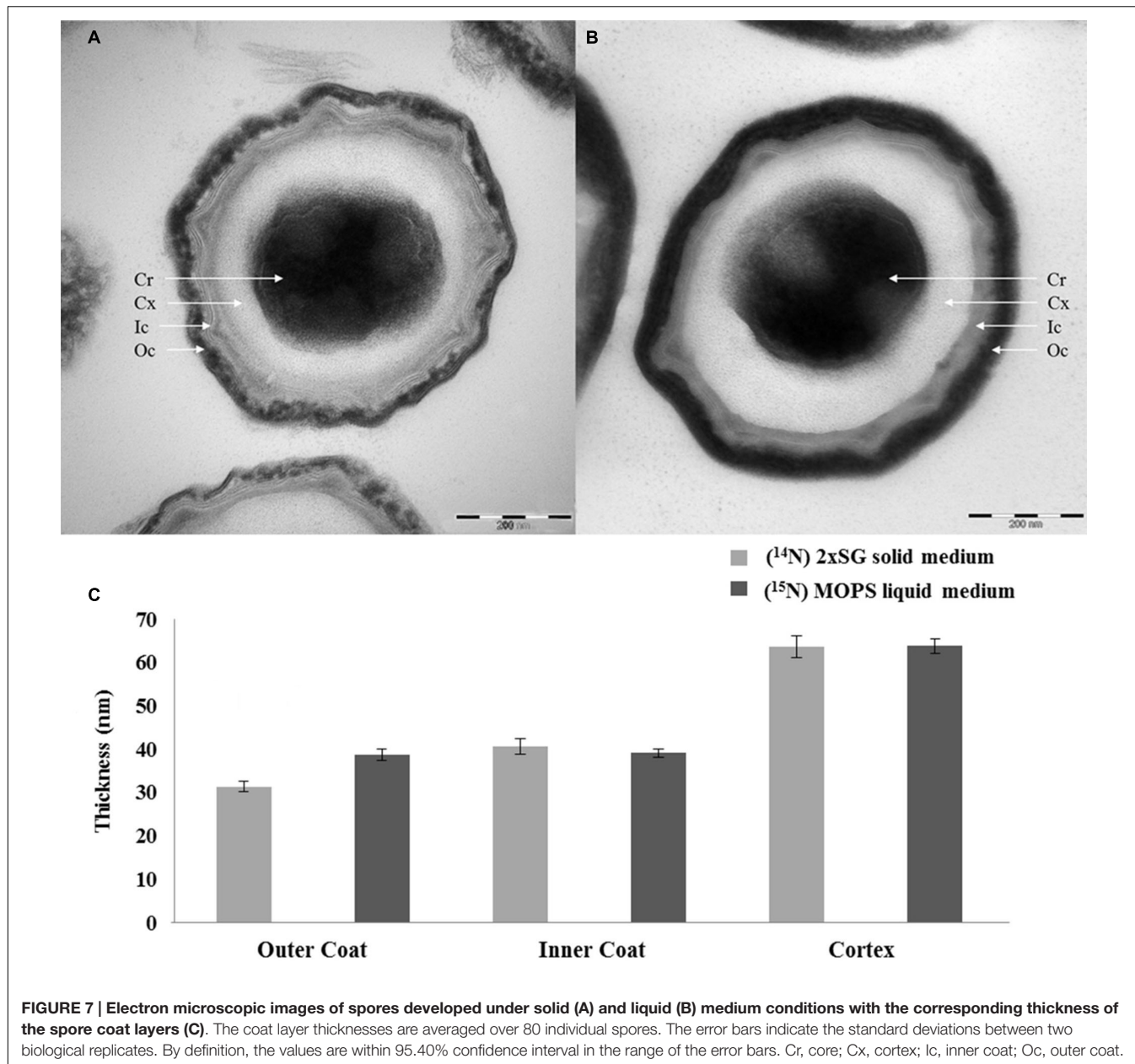


FIGURE 7 | Electron microscopic images of spores developed under solid (A) and liquid (B) medium conditions with the corresponding thickness of the spore coat layers (C). The coat layer thicknesses are averaged over 80 individual spores. The error bars indicate the standard deviations between two biological replicates. By definition, the values are within 95.40% confidence interval in the range of the error bars. Cr, core; Cx, cortex; Ic, inner coat; Oc, outer coat.

(Figure 5). However, the spores prepared on the 2x SG agar plates and those prepared in MOPS liquid medium in shake flasks show a clear color difference when seen as liquid suspensions of similar OD (Figure 6). The spores prepared on the 2x SG agar plates have a light brown/beige color, while spores prepared in the liquid MOPS medium are colored dark brown. The electron microscopic images of the spores (Figure 7) clearly show characteristic differences between the spores cultured under solid and liquid medium conditions. While the outer coat layer of the spores cultured under solid medium condition is significantly thinner, the thicknesses of the inner coat and the cortex layers are comparable to the corresponding layers in the spores prepared under liquid medium condition (Figure 7).

DISCUSSION

The protein fold changes depicted in Figure 2 show that most of the inner coat and all the known crust morphogenetic proteins (CotX, CotY, and CotZ; Imamura et al., 2011; Driks and Eichenberger, 2016) are more abundant (¹⁴N:¹⁵N ratio > 1) and most of the outer coat proteins such as CotA, CotB, CotC, CotG, CotQ, and CotU (Driks and Eichenberger, 2016) are less abundant (¹⁴N:¹⁵N ratio < 1) in spores obtained from cultures grown on solid agar plates relative to the cells that were sporulated in liquid medium. Significantly, CotE levels are not affected. CotE is a pivotal protein coordinating the formation of the outer coat (Driks, 2002) and directing the assembly of a large

set of inner and outer coat proteins (Kim et al., 2006). Different regions of CotE are responsible for the assembly and deposition of spore coat proteins. Proteins CotA, YaaH, CotR, CotG, CotB, CotS, and CotSA are dependent on the C-terminal of CotE for their deposition (Little and Driks, 2001). It is remarkable that most of these proteins are found to be less abundant in spores cultured on solid 2x SG agar plates. No tryptic peptide from C-terminal region of CotE has been identified in this study. This can be either due to the lack of lysine and arginine cleavage sites in this region or due to the involvement of the C-terminal in linking and depositing other proteins. Both CotJC and CotJB (~ 17 kDa) are found to be significantly abundant in spores prepared on solid agar plates which is consistent with the report that CotJC and CotJA, which are part of the same operon as CotJB, directly influence each other (Kim et al., 2006).

In the current study, we compare the two well-known sporulation conditions, one used often in industries to generate high heat resistant spores on solid plates, and one in defined liquid medium that provides a basis for laboratory experiments that seek for the molecular mechanisms of spore resistance. Although, the phase contrast microscopic images in **Figure 5** show no significant differences in the morphology and spore size of the two spore crops, the spore suspensions in **Figure 6** show a more intense browning for the spores cultured in the shake flask, which agrees with the observed increased abundance of the outer coat protein CotA in those spores. This protein is known to produce the brown melanin-like pigment in spores (Hullo et al., 2001). These results are in contrast with those obtained by Rose et al. (2007) as they observed no major difference in the CotA levels but a large difference in pigment production, i.e., CotA activity when they compared two different sporulation conditions using the same medium. This indicates that the CotA activity and CotA levels might not always be comparable. This observation also calls for a detailed EM studies of these spore populations. Upon zooming in with an electron microscope, the images clearly show that the crust and outer coat layer, averaged over 80 spore images is about 10 nm thicker for the spores cultured in the liquid defined medium (**Figure 7**). This agrees with the quantitative proteomic results, which show high abundance for most of the crust and outer coat proteins in these spores. The EM images further show no significant differences between the thickness of the inner coat and cortex layers, while no significant difference has been found in the DPA content in the core of both spore crops (**Figure 4**). Also Rose et al. (2007) have found no significant difference in the core water levels of spores prepared in the same medium but with different sporulation conditions. The DPA content, linked to the thermal resistance of spores (Orsburn et al., 2008), is comparable in both ^{14}N and ^{15}N spores in our study and yet the thermal resistance of the spores cultured on the solid agar is significantly higher. For the coat proteins Tgl, GerQ, KatX (catalase), YjqC (catalase), SodM unusual large variations in the isotopic ratios have been found between the four replicates as shown by their large standard deviation (**Figure 2**). These proteins are suggested to be involved in inter-protein cross-linking during spore maturation (Driks, 1999; Ragkousi and

Setlow, 2004; Checinska et al., 2015), and variations in peptide ratios suggest that cross-linking during maturation hampers the efficient digestion of these proteins (Abhyankar et al., 2015) and that the progress of cross-linking is critical to reproduce. Similarly, the cysteine rich crust proteins CotX, CotY, and CotZ are also assumed to be cross-linked via di-sulfide bonds. Yet, no large variations of protein isotopic ratios are observed for these proteins. This is because the di-sulfide links in the crust are cut during processing of the spores before the tryptic digestion. These proteins like the ones mentioned above are present at higher abundance in the spores cultured on the solid agar plates. This suggests that the enhanced heat resistance is likely to be linked to the sum of specific cross-linked coat proteins and the degree of cross-linking.

CONCLUSION

It appears that the spores developed on solid 2x SG agar plates and those in liquid defined medium in a shake flask, have a distinct coat protein composition, which is correlated, and likely functionally connected, to the difference in thermal resistance. Despite the higher abundance of most of the outer coat proteins and consequently a thicker outer coat layer, the spores obtained from cells sporulated under liquid medium conditions have a lower thermal resistance. Coat and crust proteins typically involved in cross-linking are more abundant in the thermally resistant spores (prepared on agar plates) that possess thinner outer coats. With the DPA contents of both spore crops being comparable, the difference in thermal resistance could well be linked to the difference in the degree of cross-linking in the coat.

AUTHOR CONTRIBUTIONS

WA and LdK formulated the research concept, contributed equally to drafting of the manuscript, and performed data analysis. KK and BS performed the laboratory work. HvV and NvW carried out the electron microscopy measurements. SB and CdK contributed by guiding the laboratory work and by critically reading the manuscript.

ACKNOWLEDGMENT

Authors thank the Netherlands Organization for Scientific Research (NWO) for financial support.

SUPPLEMENTARY MATERIAL

The Supplementary Material for this article can be found online at: <http://journal.frontiersin.org/article/10.3389/fmicb.2016.01636>

REFERENCES

- Abhyankar, W., Pandey, R., Ter Beek, A., Brul, S., De Koning, L. J., and De Koster, C. G. (2015). Reinforcement of *Bacillus subtilis* spores by cross-linking of outer coat proteins during maturation. *Food Microbiol.* 45, 54–62. doi: 10.1016/j.fm.2014.03.007
- Abhyankar, W., Ter Beek, A., Dekker, H., Kort, R., Brul, S., and De Koster, C. G. (2011). Gel-free proteomic identification of the *Bacillus subtilis* insoluble spore coat protein fraction. *Proteomics* 11, 4541–4550. doi: 10.1002/pmic.201100003
- Checinska, A., Paszczynski, A., and Burbank, M. (2015). *Bacillus* and other spore-forming genera: variations in responses and mechanisms for survival. *Annu. Rev. Food Sci. Technol.* 6, 351–369. doi: 10.1146/annurev-food-030713-092332
- Dadd, A. H., McCormick, K. E., and Daley, G. M. (1983). Factors influencing the resistance of biological monitors to ethylene oxide. *J. Appl. Bacteriol.* 55, 39–48. doi: 10.1111/j.1365-2672.1983.tb02645.x
- Driks, A. (1999). *Bacillus subtilis* spore coat. *Microbiol. Mol. Biol. Rev.* 63, 1–20.
- Driks, A. (2002). Maximum shields: the assembly and function of the bacterial spore coat. *Trends Microbiol.* 10, 251–254. doi: 10.1016/S0966-842X(02)02373-9
- Driks, A., and Eichenberger, P. (2016). The spore coat. *Microbiol. Spectr.* 4, 1–22. doi: 10.1128/microbiolspec.TBS-0023-2016
- Gerhardt, P., and Marquis, R. E. (1989). “Spore thermoresistance mechanisms,” in *Regulation of Prokaryotic Development*, eds I. Smith, R. A. Slepecky, and P. Setlow (Washington, DC: American Society for Microbiology), 43–63.
- Hullo, M. F., Moszer, I., Danchin, A., and Martin-Verstraete, I. (2001). CotA of *Bacillus subtilis* is a copper-dependent laccase. *J. Bacteriol.* 183, 5426–5430. doi: 10.1128/JB.183.18.5426-5430.2001
- Imamura, D., Kuwana, R., Takamatsu, H., and Watabe, K. (2010). Localization of proteins to different layers and regions of *Bacillus subtilis* spore coats. *J. Bacteriol.* 192, 518–524. doi: 10.1128/JB.01103-09
- Imamura, D., Kuwana, R., Takamatsu, H., and Watabe, K. (2011). Proteins involved in formation of the outermost layer of *Bacillus subtilis* spores. *J. Bacteriol.* 193, 4075–4080. doi: 10.1128/JB.05310-11
- Janssen, F. W., Lund, A. J., and Anderson, L. E. (1958). Colorimetric assay for dipicolinic acid in bacterial spores. *Science* 127, 26–27. doi: 10.1126/science.127.3288.26
- Kim, H., Hahn, M., Grabowski, P., Mcpherson, D. C., Otte, M. M., Wang, R., et al. (2006). The *Bacillus subtilis* spore coat protein interaction network. *Mol. Microbiol.* 59, 487–502. doi: 10.1111/j.1365-2958.2005.04968.x
- Kooiman, W. J., Barker, A. N., Gould, G. W., and Wolf, J. (1973). “The screw cap tube technique: a new and accurate technique for the determination of the wet heat resistance of bacterial spores,” in *Spore Research*, eds A. N. Barker, G. W. Gould, and J. Wolf (London: Academic Press), 87–92.
- Little, S., and Driks, A. (2001). Functional analysis of the *Bacillus subtilis* morphogenetic spore coat protein CotE. *Mol. Microbiol.* 42, 1107–1120. doi: 10.1046/j.1365-2958.2001.02708.x
- McKenney, P. T., Driks, A., and Eichenberger, P. (2013). The *Bacillus subtilis* endospore: assembly and functions of the multilayered coat. *Nat. Rev. Microbiol.* 11, 33–44. doi: 10.1038/nrmicro2921
- McKenney, P. T., Driks, A., Eskandarian, H. A., Grabowski, P., Guberman, J., Wang, K. H., et al. (2010). A distance-weighted interaction map reveals a previously uncharacterized layer of the *Bacillus subtilis* spore coat. *Curr. Biol.* 20, 934–938. doi: 10.1016/j.cub.2010.03.060
- Melly, E., Genest, P. C., Gilmore, M. E., Little, S., Popham, D. L., Driks, A., et al. (2002). Analysis of the properties of spores of *Bacillus subtilis* prepared at different temperatures. *J. Appl. Microbiol.* 92, 1105–1115. doi: 10.1046/j.1365-2672.2002.01644.x
- Mundra, R. V., Mehta, K. K., Wu, X., Paskaleva, E. E., Kane, R. S., and Dordick, J. S. (2014). Enzyme-driven *Bacillus* spore coat degradation leading to spore killing. *Biotechnol. Bioeng.* 111, 654–663. doi: 10.1002/bit.25132
- Orsburn, B., Melville, S. B., and Popham, D. L. (2008). Factors contributing to heat resistance of *Clostridium perfringens* endospores. *Appl. Environ. Microbiol.* 74, 3328–3335. doi: 10.1128/AEM.02629-07
- Ragkousi, K., and Setlow, P. (2004). Transglutaminase-mediated cross-linking of GerQ in the coats of *Bacillus subtilis* spores. *J. Bacteriol.* 186, 5567–5575. doi: 10.1128/JB.186.17.5567-5575.2004
- Rose, R., Setlow, B., Monroe, A., Mallozzi, M., Driks, A., and Setlow, P. (2007). Comparison of the properties of *Bacillus subtilis* spores made in liquid or on agar plates. *J. Appl. Microbiol.* 103, 691–699. doi: 10.1111/j.1365-2672.2007.03297.x
- Sanchez-Salas, J. L., Setlow, B., Zhang, P., Li, Y. Q., and Setlow, P. (2011). Maturation of released spores is necessary for acquisition of full spore heat resistance during *Bacillus subtilis* sporulation. *Appl. Environ. Microbiol.* 77, 6746–6754. doi: 10.1128/AEM.05031-11
- Scopes, R. K. (1974). Measurement of protein by spectrophotometry at 205 nm. *Anal. Biochem.* 59, 277–282. doi: 10.1016/0003-2697(74)90034-7
- Setlow, B., Atluri, S., Kitchel, R., Koziol-Dube, K., and Setlow, P. (2006). Role of dipicolinic acid in resistance and stability of spores of *Bacillus subtilis* with or without DNA-protective alpha/beta-type small acid-soluble proteins. *J. Bacteriol.* 188, 3740–3747. doi: 10.1128/JB.00212-06
- Setlow, P. (1988). Small, acid-soluble spore proteins of *Bacillus* species: structure, synthesis, genetics, function, and degradation. *Annu. Rev. Microbiol.* 42, 319–338. doi: 10.1146/annurev.mi.42.100188.001535
- van Ooij, C., Eichenberger, P., and Losick, R. (2004). Dynamic patterns of subcellular protein localization during spore coat morphogenesis in *Bacillus subtilis*. *J. Bacteriol.* 186, 4441–4448. doi: 10.1128/JB.186.14.4441-4448.2004
- Vizcaíno, J. A., Deutsch, E. W., Wang, R., Csordas, A., Reisinger, F., Rios, D., et al. (2014). ProteomeXchange provides globally coordinated proteomics data submission and dissemination. *Nat. Biotech.* 32, 223–226. doi: 10.1038/nbt.2839

Conflict of Interest Statement: The authors declare that the research was conducted in the absence of any commercial or financial relationships that could be construed as a potential conflict of interest.

Copyright © 2016 Abhyankar, Kamphorst, Swarge, van Veen, van der Wel, Brul, de Koster and de Koning. This is an open-access article distributed under the terms of the Creative Commons Attribution License (CC BY). The use, distribution or reproduction in other forums is permitted, provided the original author(s) or licensor are credited and that the original publication in this journal is cited, in accordance with accepted academic practice. No use, distribution or reproduction is permitted which does not comply with these terms.



The Exosporium of *Bacillus megaterium* QM B1551 Is Permeable to the Red Fluorescence Protein of the Coral *Discosoma* sp.

Mariamichela Lanzilli¹, Giuliana Donadio¹, Roberta Addevico¹, Anella Saggese¹, Giuseppina Cangiano¹, Loredana Baccigalupi¹, Graham Christie², Ezio Ricca¹ and Rachele Iстicato^{1*}

¹ Department of Biology, University of Naples Federico II, Naples, Italy, ² Department of Chemical Engineering and Biotechnology, University of Cambridge, Cambridge, UK

OPEN ACCESS

Edited by:

Martin Koenneke,
University of Bremen, Germany

Reviewed by:

Claes Von Wachenfeldt,
Lund University, Sweden
Daniel Paredes-Sabja,
Universidad Andres Bello, Chile

*Correspondence:

Rachele Iстicato
isticato@unina.it

Specialty section:

This article was submitted to
Microbial Physiology and Metabolism,
a section of the journal
Frontiers in Microbiology

Received: 29 July 2016

Accepted: 19 October 2016

Published: 04 November 2016

Citation:

Lanzilli M, Donadio G, Addevico R, Saggese A, Cangiano G, Baccigalupi L, Christie G, Ricca E and Iстicato R (2016) The Exosporium of *Bacillus megaterium* QM B1551 Is Permeable to the Red Fluorescence Protein of the Coral *Discosoma* sp.. *Front. Microbiol.* 7:1752.
doi: 10.3389/fmicb.2016.01752

Bacterial spores spontaneously interact and tightly bind heterologous proteins. A variety of antigens and enzymes have been efficiently displayed on spores of *Bacillus subtilis*, the model system for spore formers. Adsorption on *B. subtilis* spores has then been proposed as a non-recombinant approach for the development of mucosal vaccine/drug delivery vehicles, biocatalysts, bioremediation, and diagnostic tools. We used spores of *B. megaterium* QM B1551 to evaluate their efficiency as an adsorption platform. Spores of *B. megaterium* are significantly larger than those of *B. subtilis* and of other *Bacillus* species and are surrounded by the exosporium, an outermost surface layer present only in some *Bacillus* species and lacking in *B. subtilis*. Strain QM B1551 of *B. megaterium* and a derivative strain totally lacking the exosporium were used to localize the adsorbed monomeric Red Fluorescent Protein (mRFP) of the coral *Discosoma* sp., used as a model heterologous protein. Our results indicate that spores of *B. megaterium* adsorb mRFP more efficiently than *B. subtilis* spores, that the exosporium is essential for mRFP adsorption, and that most of the adsorbed mRFP molecules are not exposed on the spore surface but rather localized in the space between the outer coat and the exosporium.

Keywords: surface display, protein delivery, spores, *Bacillus megaterium*, exosporium

INTRODUCTION

Gram-positive bacteria of the *Bacillus* and *Clostridium* genera can differentiate to form an endospore (spore), a metabolically quiescent cell produced in response to conditions that do not allow cell growth (McKenney et al., 2012). Once released in the environment, the spore survives in its dormant state for extremely long periods, resisting to a vast range of stresses such as high temperatures, dehydration, absence of nutrients and the presence of toxic chemicals (McKenney et al., 2012). However, the quiescent spore is able to continuously monitor the environment and respond to the presence of water and nutrients by germinating and originating a vegetative cell that is able to grow and sporulate (McKenney et al., 2012). Resistance to non-physiological conditions is, in part, due to the spore surface structures. In *Bacillus subtilis*, the model system for spore formers, the spore surface is organized in a multilayered coat and in a crust, a recently discovered layer

that surrounds the spore coat (McKenney et al., 2012). *B. subtilis* spores are negatively charged (Huang et al., 2010; Pesce et al., 2014) and have a relative hydrophobicity that is in part due to the glycosylation of some spore surface proteins (Cangiano et al., 2014; Rusciano et al., 2014). In several *Bacillus* and *Clostridium* species, including *B. cereus*, *B. anthracis*, *B. megaterium*, and *C. difficile*, the outermost spore structure is the exosporium, a morphologically distinct layer composed of proteins and glycoproteins that surrounds the coat (Díaz-González et al., 2015; Manetsberger et al., 2015b; Stewart, 2015).

The bacterial spore has been proposed as a platform to display heterologous proteins, with potential applications ranging from the development of mucosal vaccines to re-usable biocatalysts, diagnostic tools, and bioremediation devices (Knecht et al., 2011; Istitato and Ricca, 2014; Ricca et al., 2014). The remarkable and well documented resistance of the spore (McKenney et al., 2012), the amenability of several spore-forming species to the genetic manipulation (Harwood and Cutting, 1990) and the safety record of several species (Cutting, 2011; Baccigalupi et al., 2015) support the use of the spore as a display and delivery system. Two strategies have been developed to display heterologous proteins on the spore surface. A recombinant strategy, based on the construction of gene fusions between DNA coding for a selected spore surface protein and DNA coding for the protein to be displayed, has been used over the years to display a variety of heterologous proteins (Istitato and Ricca, 2014). A non-recombinant approach, based on the spontaneous adsorption between purified spores and purified proteins, has been also used to display various enzymes and antigens (Ricca et al., 2014). The molecular details controlling spore adsorption have not been fully elucidated. It is known that the adsorption is more efficient when the pH of the binding buffer is acidic (pH 4) (Huang et al., 2010; Sirec et al., 2012) and that a combination of electrostatic and hydrophobic interactions are likely involved in the interaction (Huang et al., 2010; Sirec et al., 2012). It is also known that mutant spores with severely altered spore surfaces interact more efficiently than isogenic wild type spores with model proteins (Sirec et al., 2012; Donadio et al., 2016).

Here, we used a fluorescent protein, the monomeric form of the Red Fluorescent Protein (mRFP) of the coral *Discosoma* sp. (Campbell et al., 2002), to evaluate whether spores of *B. megaterium* are able to interact with and adsorb a model heterologous protein. *B. megaterium* comprises a number of morphologically distinct strains sharing the unusual large dimensions of both cells (length up to 4 μm and a diameter of 1.5 μm) and spores (length up to 3 μm and diameter of 1 μm) (Di Luccia et al., 2016). Spores of some strains of *B. megaterium* are surrounded by an exosporium, and since so far only spores of species that lack an exosporium have been considered as adsorption platforms, no data are available on the impact of the exosporium in the interaction with heterologous proteins.

The QM B1551 strain is the best-characterized strain of *B. megaterium*. This strain carries about 11% of its genome on seven indigenous plasmids (Rosso and Vary, 2005; Vary et al., 2007; Eppinger et al., 2011), two of which – pBM500

and pBM600 – have been identified as carrying genes that are essential to the formation of this strain's distinctive "walnut-shaped" exosporium (Manetsberger et al., 2015a). The protein composition of the QM B1551 exosporium is as yet poorly characterized, with only a few genes encoding orthologs of recognized exosporium protein in spores of other species being identified by genomic analyses. These include genes encoding BclA nap proteins, which form a localized nap in *B. megaterium* QM B1551 spores, plus an ortholog of the BxpB protein that forms the basal layer of the exosporium in *B. cereus* family spores. The latter appears to fulfill a different role in *B. megaterium* QM B1551 spores, since a null mutant strain retained an apparently normal exosporium (Manetsberger et al., 2015a).

In this paper, we present data that demonstrates that spores of *B. megaterium* QM B1551 can efficiently adsorb mRFP, and provide evidence that protein molecules are able to cross the permeability barrier presented by the exosporium to localize in the inter-coat space.

MATERIALS AND METHODS

Bacterial Strains, Spore, and RFP Production

The *B. megaterium* strains employed in this study are QM B1551 and its plasmid-less derivative PV361 (Rosso and Vary, 2005). The *B. subtilis* strain used in this study was PY79 (Youngman et al., 1984). Sporulation of all *Bacillus* strains was induced by the exhaustion method (Cutting and Vander Horn, 1990). After 30 h of growth in Difco Sporulation (DS) medium at 37°C with vigorous shaking spores were collected and purified as described by Nicholson and Setlow (1990) using overnight incubation in H₂O at 4°C to lyse residual sporangial cells. The number of purified spores obtained was measured by direct counting with a Bürker chamber under an optical microscope (Olympus BH-2 with 40× lens).

For mRFP production, cells of *Escherichia coli* strain RH161 (Donadio et al., 2016), bearing the expression vector pRSET-A carrying an in-frame fusion of the 5' end of the *rfp* coding region to six histidine codons under the transcriptional control of a T7 promoter, were grown for 18 h at 37°C in 100 ml of autoinduction medium to express the heterologous protein (Istitato et al., 2010). The His₆-tagged RFP protein was purified under native conditions using a His-Trap column as recommended by the manufacturer (GE Healthcare Life Science). Purified protein was desalted using a PD10 column (GE Healthcare Life Science) to remove high NaCl and imidazole concentrations.

Adsorption Reaction

Unless otherwise specified 5 μg of purified recombinant mRFP was added to a suspension of spores (5×10^8) in 50 mM Sodium Citrate pH 4.0 at 25°C in a final volume of 200 μl . After 1 h of incubation, the binding mixture was centrifuged (10 min at 13,000 g) to fractionate mRFP bound-spores in the pellet from free mRFP in the supernatant.

Western and Dot-Blot Analysis

Spore pellets from adsorption reactions were resuspended in 40 µl of spore coat extraction buffer (Nicholson and Setlow, 1990; Giglio et al., 2011), incubated at 68°C for 1 h to solubilize spore coat proteins and loaded onto a 12% SDS-PAGE gel. The proteins were then electro-transferred to nitrocellulose filters (Amersham Pharmacia Biotech) and used for Western blot analysis as previously reported (Isticato et al., 2008) using monoclonal mRFP-recognizing anti-His antibody (Sigma). A quantitative determination of the amount of mRFP was obtained by dot blot experiments comparing serial dilutions of purified mRFP and binding assay supernatant. Filters were then visualized by the ECL-prime method (Amersham Pharmacia Biotech) and subjected to densitometric analysis by Quantity One 1-D Analysis Software (Bio-Rad). Dot blot and relative densitometric analyses were performed three times to verify the significance of the results.

Fluorescence and Immunofluorescence Microscopy

Post-adsorption spores were resuspended in 50 µl of 1x PBS pH 4.0 and 5 µl of the suspension placed on microscope slides and covered with a coverslip previously treated for 30 s with poly-L-lysine (Sigma). Immunofluorescence was performed as described by Isticato et al. (2013), with the following modifications: 2.0×10^6 RFP-adsorbed spores of QM B1551 and PV361 *B. megaterium* strains were pretreated with 1% bovine serum albumin (BSA) – 1x PBS pH 4.0 for 30 min prior to 2 h-incubation at 4°C with the anti-polyHistidine antibodies (mouse; Sigma) diluted 1:20 in 1x PBS pH 4.0–1% BSA. As a control of the specificity of this technique, non-adsorbed spores were directly treated with anti-His antibodies. After three washes, the samples were incubated with a 64-fold diluted anti-mouse secondary antibody conjugated with fluorescein isothiocyanate, FITC (Santa Cruz Biotechnology, Inc.) and washed four times with 1x PBS pH 4.0. Washed samples were resuspended in 20 µl of 1x PBS pH 4.0 and 10 µl were analyzed. All samples were observed with an Olympus BX51 fluorescence microscope fitted with a 100× UPlan F1 oil objective; U-MNG or U-MWIBBP cube-filters were used to detect the red fluorescence emission of mRFP or the green emission of FITC-conjugated antibodies, respectively. Exposure times were in the range between 200 and 3000 ms. Images were captured using an Olympus DP70 digital camera and processed with Image Analysis Software (Olympus) for minor adjustments of brightness, contrast and color balance (McCloy et al., 2014). ImageJ (v1.48, NIH) was used to draw an outline around 80 spores for each strain and minimum, maximum and mean fluorescence values per pixel were recorded for each spore. Values of fluorescence intensity were displayed subsequently as box-plots with 5–95% confidence intervals (McCloy et al., 2014).

Statistical Analysis

Results from dot blot and fluorescence microscopy analysis are the averages from three independent experiments. Statistical significance was determined by the Student *t*-test, and the significance level was set at $P < 0.05$.

RESULTS

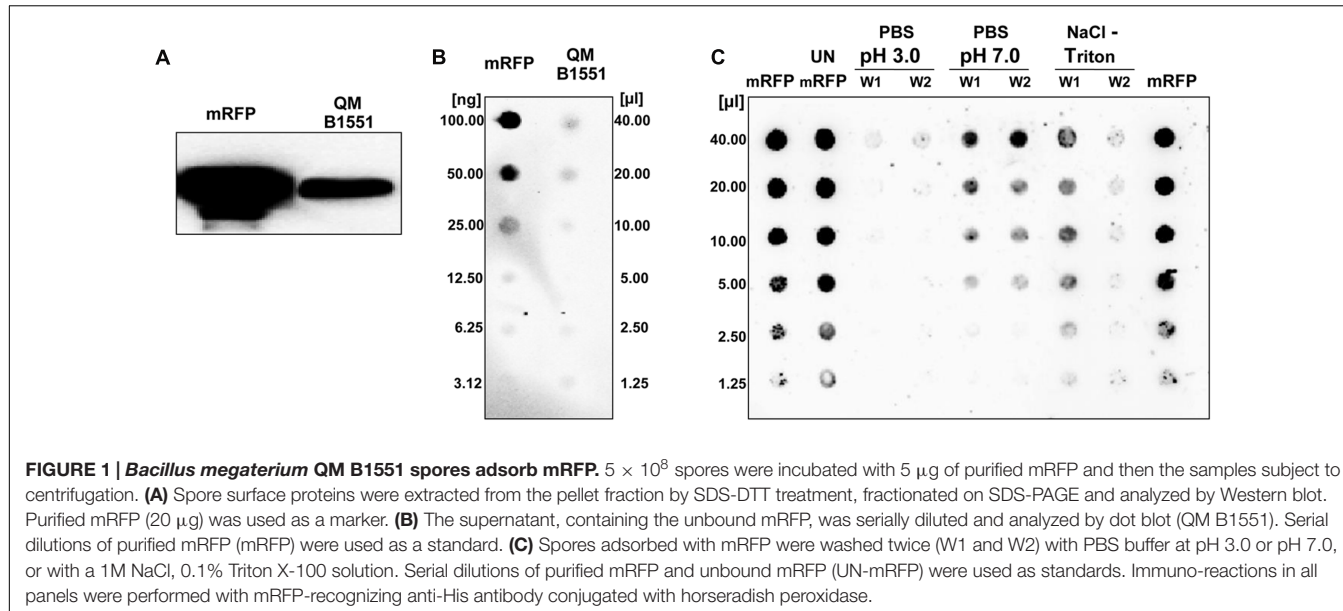
mRFP of *Discosoma* sp. is Adsorbed by *B. megaterium* Spores

To verify whether spores of *B. megaterium* QM B1551 were able to adsorb mRFP, 5 µg of the purified protein (Materials and Methods) were incubated with 5.0×10^8 purified spores. The adsorption reaction was performed in 50 mM sodium citrate at pH 4.0, as previously described (Sirec et al., 2012). After the reaction, spores were extensively washed with 1x PBS pH 4.0, spore surface proteins were extracted as described in Materials and Methods and analyzed by western blotting with anti-polyHistidine-Peroxidase antibody (Sigma), which recognizes the histidine-tagged N terminus of mRFP. As shown in **Figure 1A**, mRFP was extracted from spores, indicating that it was adsorbed during the reaction and then released by the extraction treatment. To evaluate the efficiency of adsorption, we analyzed the amount of mRFP left unbound, i.e., post-adsorbed spores were collected by centrifugation and the supernatant serially diluted and analyzed by dot blotting (**Figure 1B**). A densitometric analysis of the dot blot (**Supplementary Table 1**) showed that when 5 µg of mRFP was used in the adsorption reaction less than 1% was left unbound, indicating that about 99% of the heterologous protein was adsorbed to *B. megaterium* spores.

To analyze whether adsorbed mRFP molecules were tightly bound to the spore surface, post-adsorption reaction spores were washed twice with PBS buffer at pH 3.0 or pH 7.0, or with a 1M NaCl, 0.1% Triton X-100 solution as previously described (Donadio et al., 2016). As shown in **Figure 1C**, and supported by densitometric analysis of the dot blot (**Supplementary Table 2**), the washes at pH 3.0 did not cause any release of the adsorbed mRFP, while the washes at pH 7.0 or with 1M NaCl, 0.1% Triton X-100 caused a minimal, less than 1%, release of mRFP molecules. Therefore, results presented in **Figure 1** suggest that mRFP was efficiently adsorbed and tightly bound to *B. megaterium* spores. To assess whether spore-adsorbed mRFP molecules retained their fluorescence properties, we performed a fluorescence microscopy analysis. As shown in **Figure 2**, post-adsorption reaction spores were associated with a strong fluorescence signal visible around the entire spore surface.

The Exosporium has an Essential Role in mRFP Adsorption

Strain QM B1551 of *B. megaterium* contains seven indigenous plasmids (Rosso and Vary, 2005; Eppinger et al., 2011) and plasmid-encoded genes are essential for exosporium formation (Manetsberger et al., 2015a). PV361 is a QM B1551-cured strain lacking all seven plasmids and, as a consequence, totally lacking the exosporium (Manetsberger et al., 2015a). We used spores of strain PV361 to analyze the role of the exosporium in mRFP adsorption. In parallel, we also used spores of *B. subtilis* PY79 that in a previous study have been shown to adsorb mRFP (Donadio et al., 2016). To compare the adsorption efficiency of spores of the *B. subtilis* PY79 and *B. megaterium* QM B1551 and PV361

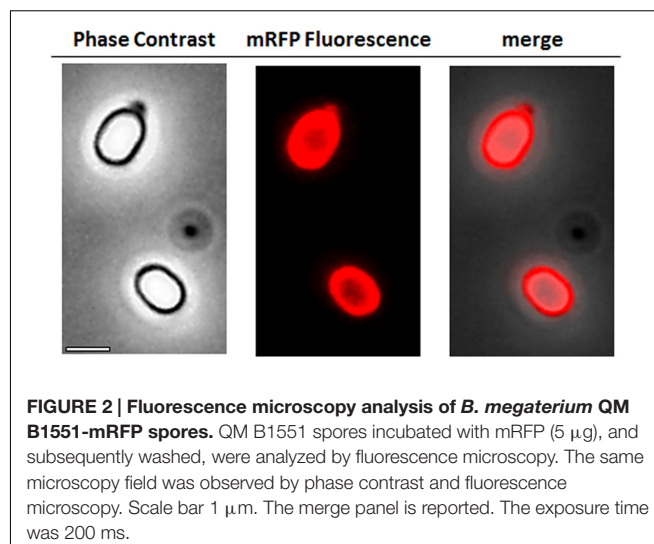


strains, we adsorbed 5 μg of purified mRFP with 5.0×10^8 spores of each of the three strains. After the adsorption reactions spores were collected by centrifugation, proteins extracted by SDS-DTT treatment and analyzed by western blotting with mRFP-recognizing anti-His antibody. As shown in Figure 3A, mRFP was apparently extracted in larger amounts from spores of QM B1551 than from spores of the other two strains. In an attempt to quantify these apparent differences, unbound mRFP from the adsorption reactions was serially diluted and analyzed by dot blotting (Figure 3B). A densitometric analysis of the dot blot of Figure 3B (Supplementary Table 3) indicated that PY79 and PV361 spores adsorbed about 90% of the total mRFP while QM B1551 spores adsorbed almost all (over 99%) purified mRFP.

The adsorption efficiency of spores of the three strains was also analyzed by fluorescence microscopy (Figure 4A and Supplementary Figure S1). Microscopy images were analyzed by ImageJ software (v1.48, NIH) to perform quantitative fluorescence image analysis and spore fluorescence was calculated as described in Materials and Methods. The analysis of 80 spores of each strain indicated an average fluorescence value per pixel of 52.43 (± 5.94), 20.81 (± 2.71), and 32.33 (± 2.97 ; arbitrary units) for QM B1551, PV361, and PY79, respectively (Figure 4B), conferring further evidence that QM B1551 spores adsorbed more mRFP than spores of the other two strains.

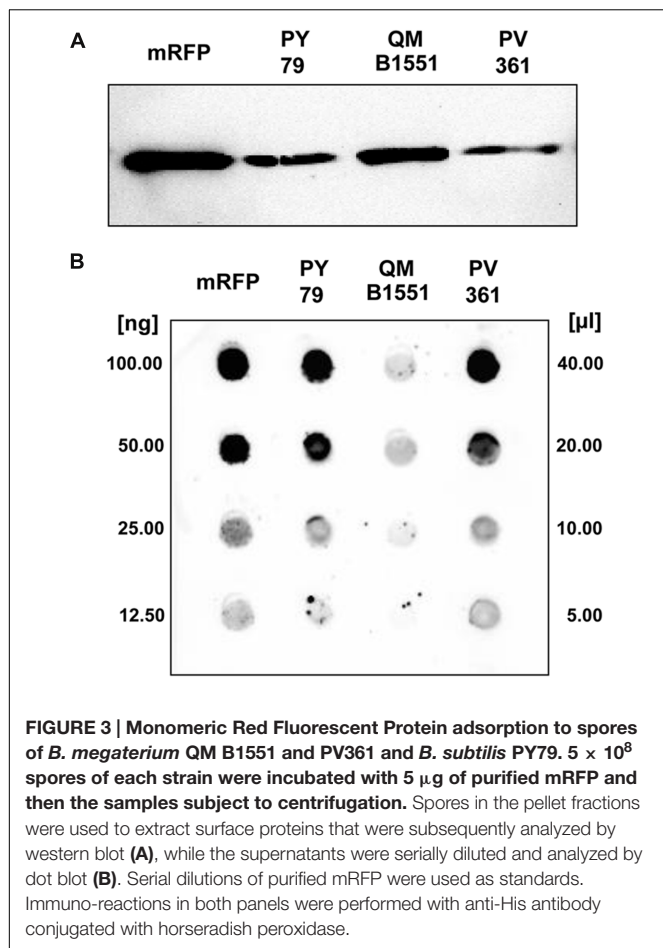
Based on the results of Figures 3 and 4, we conclude that the exosporium, present in QM B1551 and lacking in PV361 has a relevant role in the adsorption of mRFP.

In addition, results of Figure 4 indicated that *B. subtilis* PY79 spores are more efficient than *B. megaterium* PV361 spores in adsorbing mRFP, whereas dot blotting reported in Figure 3B indicated similar adsorption efficiencies for the two strains. We believe that this discrepancy is due to a strong reduction of fluorescence when mRFP is bound to PV361 but not to PY79 or QM B1551 spores (see below).



Quantitative Assessment of mRFP Adsorption to QM B1551 Spores

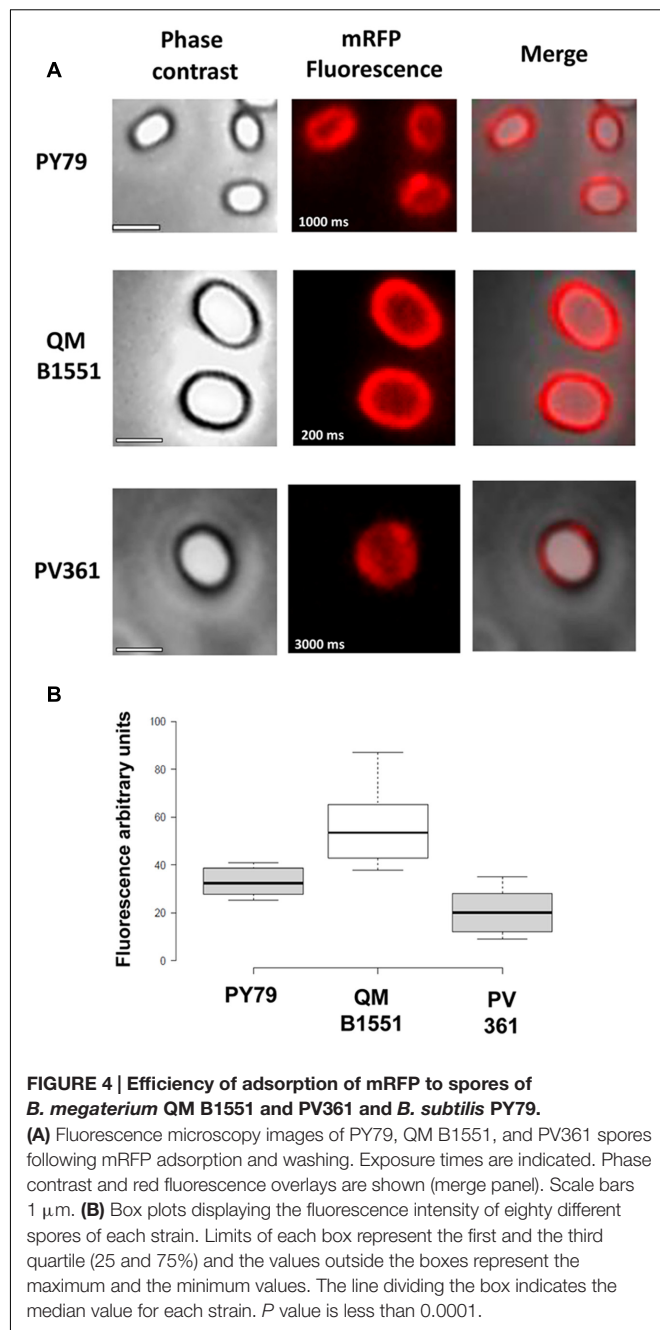
Dot blot experiments (Figure 3B) indicated that when 5 μg of purified mRFP was used in adsorption reactions with 5.0×10^8 spores of the QM B1551 strain almost all heterologous protein was bound to the spore. In order to define the maximal amount of mRFP that can be adsorbed to QM B1551 spores, we repeated the reactions with increasing concentrations of purified mRFP, i.e., 5.0×10^8 QM B1551 spores were reacted with 5, 10, 20, 40, 80, and 160 μg of purified mRFP. After the reactions spores were collected by centrifugation and the supernatants containing unbound mRFP were serially diluted and analyzed by dot blotting (Figure 5A). Figure 5B displays the results of a densitometric analyses of the dot blot (Supplementary Table 4), which indicates that when 5–80 μg of mRFP was



reacted with 5 × 10⁸ spores, the percentage of protein bound to spores was over 90%. A decrease of bound mRFP was observed when 160 µg of purified protein were used in the reaction. However, even when 160 µg of purified mRFP was used over 60% of the protein was absorbed, indicating that 5.0 × 10⁸ spores of QM B1551 can adsorb about 100 µg of mRFP.

mRFP Localizes to the Inter-Coat Space in *B. megaterium* QM B1551 Spores

An immuno-fluorescence microscopy approach was employed to assess whether adsorbed mRFP molecules were exposed on the surface of *B. megaterium* QM B1551 spores. QM B1551 spores adsorbed with various amounts of mRFP were reacted with monoclonal anti-His antibody recognizing the recombinant mRFP, then with fluorescent anti-mouse secondary antibody (Santa Cruz Biotechnology, Inc.) and observed under the fluorescence microscope (Figure 6). With the lowest amount of mRFP used in this experiment (2 µg) the mRFP fluorescence signal (red) was observed all around the spore while the immunofluorescence signal (green) was weak and mainly concentrated at the spore poles, suggesting that only in those points mRFP was exposed on the spore surface. Increasing the amount of mRFP used in the reaction the number of green spots



increased (5 and 10 µg) and with highest amount of mRFP used in the reaction (20 µg) an almost complete green ring was observed around the spores. Based on the results presented in Figure 6, we hypothesized that mRFP molecules infiltrate through the exosporium and localizes in the inter-coat space between the outer coat and the exosporium, i.e., when a low amount of mRFP is used almost all protein molecules are internal to the exosporium and are available to the antibody at only a few locations. Increasing amounts of mRFP in adsorption reactions results in the inter-coat space “filling up,” until ultimately more mRFP molecules are available to the antibody on the

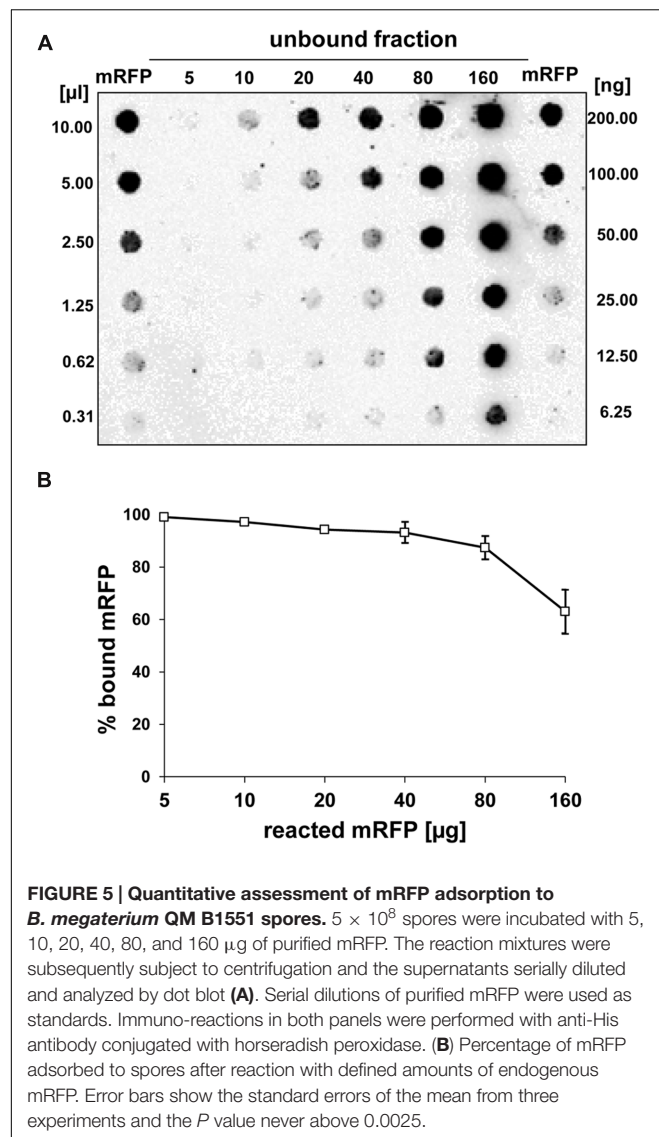


FIGURE 5 | Quantitative assessment of mRFP adsorption to *B. megaterium* QM B1551 spores. 5×10^8 spores were incubated with 5, 10, 20, 40, 80, and 160 μ g of purified mRFP. The reaction mixtures were subsequently subject to centrifugation and the supernatants serially diluted and analyzed by dot blot (**A**). Serial dilutions of purified mRFP were used as standards. Immuno-reactions in both panels were performed with anti-His antibody conjugated with horseradish peroxidase. (**B**) Percentage of mRFP adsorbed to spores after reaction with defined amounts of endogenous mRFP. Error bars show the standard errors of the mean from three experiments and the *P* value never above 0.0025.

spore surface. This hypothesis implies that if the exosporium is lacking then all mRFP should be available to the antibody. To test this, we compared by immunofluorescence microscopy equal numbers of spores of QM B1551 (with exosporium) and of PV361 (without exosporium) incubated with the same amount of mRFP (5 μ g). When the exosporium was present (QM B1551) mRFP was only partially available to the antibody and green spots were observed (Figure 7 and Supplementary Figure S2). When the exosporium was not present (PV361) adsorbed mRFP was available to the antibody all around the spore and a complete green ring was formed, supporting the hypothesis that mRFP is internal to the exosporium in QM B1551 spores.

While QM B1551 spores used in the experiments of Figure 7 showed a complete red fluorescent ring as in Figure 2, PV361 spores showed a very weak red fluorescent signal. With PV361 spores a red signal was only observed using long exposure times at the fluorescence microscope (Figure 4). Since mRFP is present

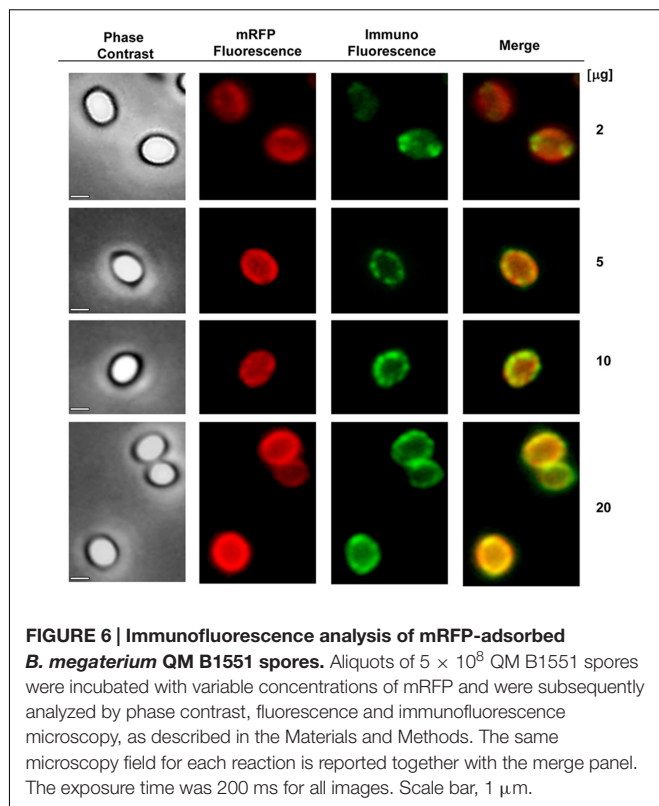


FIGURE 6 | Immunofluorescence analysis of mRFP-adsorbed *B. megaterium* QM B1551 spores. Aliquots of 5×10^8 QM B1551 spores were incubated with variable concentrations of mRFP and were subsequently analyzed by phase contrast, fluorescence and immunofluorescence microscopy, as described in the Materials and Methods. The same microscopy field for each reaction is reported together with the merge panel. The exposure time was 200 ms for all images. Scale bar, 1 μ m.

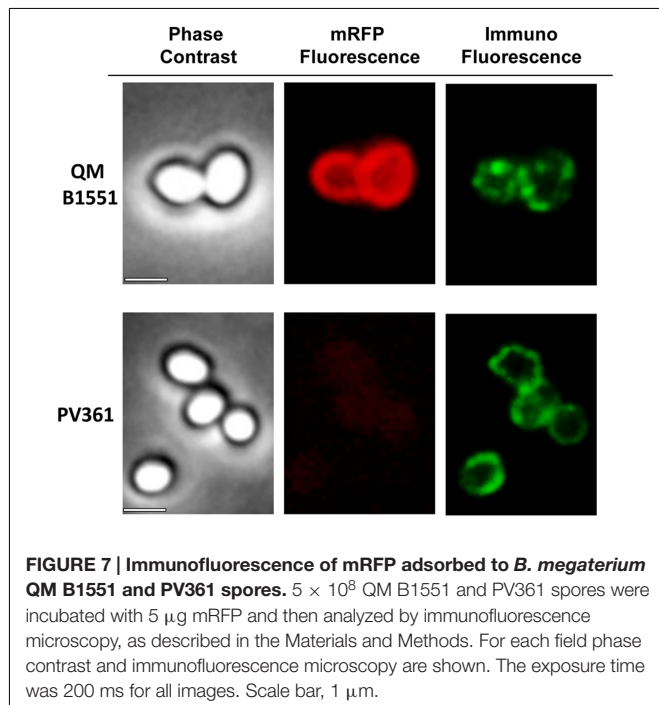


FIGURE 7 | Immunofluorescence of mRFP adsorbed to *B. megaterium* QM B1551 and PV361 spores. 5×10^8 QM B1551 and PV361 spores were incubated with 5 μ g mRFP and then analyzed by immunofluorescence microscopy, as described in the Materials and Methods. For each field phase contrast and immunofluorescence microscopy are shown. The exposure time was 200 ms for all images. Scale bar, 1 μ m.

around PV361 spores (Figures 3 and 7), we conclude that mRFP fluorescence is weakened when the protein is adsorbed to PV361 spores. Further experiments will be needed to fully address this point.

DISCUSSION

The main findings of this report are that spores of *B. megaterium* are extremely efficient in adsorbing the heterologous model protein mRFP, that the exosporium has an important role in this process, and that mRFP molecules infiltrate through the exosporium localizing between the outer coat and the exosporium. These results expand previous work performed on spores of *B. subtilis* and demonstrate that spores of a different species may also be used to deliver heterologous proteins via the adsorption method. The high efficiency of adsorption observed with *B. megaterium* spores is in part due to the large size of its spore compared with that of *B. subtilis*. Indeed, the *B. megaterium* spore surface area is about 2.5-fold larger than the *B. subtilis* spore, with a surface of $5.33 \mu\text{m}^2$ (h: 1.60 ± 0.16 w: 0.84 ± 0.07) vs. $1.98 \mu\text{m}^2$ (h: 1.07 ± 0.09 w: 0.48 ± 0.03). The large dimensions allow the adsorption of up to $100 \mu\text{g}$ of mRFP when $160 \mu\text{g}$ of protein are reacted with spores.

The observation that mRFP crosses the exosporium indicates that it is permeable to mRFP, a 27 kDa protein. Permeability of the exosporium is not totally surprising since germinants present in the environment have to cross the external layers of the spore to reach their receptors, albeit germinants are typically small molecules with molecular masses typically <200 Da. Additionally, the mRFP data are broadly in agreement with the results of previous studies conducted with labeled dextrans and related molecules (Koshikawa et al., 1984; Nishihara et al., 1989). In those studies, the *B. megaterium* QM B1551 exosporium was suggested to represent a permeability barrier to molecules with molecular weights greater than 100 KDa, while influencing the passage of molecules with masses somewhere between 2 and 40 kDa (Koshikawa et al., 1984; Nishihara et al., 1989).

An interesting challenge for future work will be to establish the mechanism or route of infiltration that mRFP, and by inference other heterologous proteins of interest, takes to enter the inter-coat space. Examination by transmission electron microscopy of sectioned *B. megaterium* QM B1551 spores indicates that the exosporium comprises two identical “shells” (Manetsberger et al., 2015a), and it may be that the interface between each of these structures (described as “apical openings” in early papers) permits ingress of relatively large molecules. Discerning the basis for the apparent loss of mRFP fluorescence upon adsorption to PV361 spores, and whether mRFP molecules are able to infiltrate the outer coat layers, as observed for *B. subtilis* spores (Donadio et al., 2016), will also be of interest.

In the current study, we hypothesize that mRFP molecules preferentially cross the exosporium and accumulate in the inter-coat space between the outer coat and the exosporium. In this model, mRFP molecules are only adsorbed and displayed on the spore surface once adsorption sites (or volumetric capacity?) in the inter-coat space are sufficiently occupied. This implies that the adsorption approach to surface display can be used

with *B. megaterium* QM B1551 spores, although the system is dependent on the spore to protein ratio used in adsorption reactions. Since various strains of *B. megaterium* have long been used industrially for the production of enzymes such as amylases and dehydrogenases, vitamins and antimicrobial molecules (Vary et al., 2007), our data suggest a new biotechnological application for the *B. megaterium* spore as a vehicle to bind and deliver heterologous proteins.

AUTHOR CONTRIBUTIONS

ML and GD – performed most of the experiments; RA and AS – contributed to interpretation of data for the work; GiC, LB, and GrC – contributed to drafting the work and revising it critically; ER – contributed to discussions and suggestions during the work and contributed to writing the manuscript; RI – led the work and contributed to writing the manuscript. All authors read and approved the final manuscript.

FUNDING

This work was supported by a grant (STAR Linea1- 2014) from the Federico II University of Naples and Compagnia di San Paolo, Italy to RI.

SUPPLEMENTARY MATERIAL

The Supplementary Material for this article can be found online at: <http://journal.frontiersin.org/article/10.3389/fmicb.2016.01752/full#supplementary-material>

FIGURE S1 | Whole field images of fluorescence microscopy analysis reported in Figure 4. The same microscopy field was observed by phase contrast and fluorescence microscopy. Scale bar $5 \mu\text{m}$. The merge panel is reported. The exposure time is indicated.

FIGURE S2 | Whole field images of Immunofluorescence analysis reported in Figure 7. The same microscopy field was observed by phase contrast and fluorescence microscopy. Scale bar $5 \mu\text{m}$. The exposure time was 200 ms for all images.

TABLE S1 | Densitometric analysis of dot blot experiments with the supernatants of the adsorption reaction with QM B1551 spores (Figure 1B).

TABLE S2 | Densitometric analysis of dot blot experiments with the supernatants of various washes after the adsorption reaction (Figure 1C).

TABLE S3 | Densitometric analysis of dot blot experiments with the supernatants of the adsorption reaction performed with spores of strains PY79, QM B1551, and PV361 (Figure 3B).

TABLE S4 | Densitometric analysis of dot blot experiments with the supernatants of the adsorption reaction performed with different amounts of mRFP.

REFERENCES

- Baccigalupi, L., Ricca, E., and Ghelardi, E. (2015). "Non-LAB probiotics: spore Formers," in *Probiotics and Prebiotics: Current Research and Future Trends*, eds K. Venema and A. P. do Carmo (Norfolk, VA: Caister Academic Press), 93–103. doi: 10.21775/9781910190098.06
- Campbell, R. E., Tour, O., Palmer, A. E., Steinbach, P. A., Baird, G. S., Zacharias, D. A., et al. (2002). A monomeric red fluorescent protein. *Proc. Natl. Acad. Sci. U.S.A.* 99, 7877–7882. doi: 10.1073/pnas.082243699
- Cangiano, G., Sirec, T., Panarella, C., Isticato, R., Baccigalupi, L., De Felice, M., et al. (2014). The sps gene products affect germination, hydrophobicity and protein adsorption of *Bacillus subtilis* spores. *Appl. Environ. Microbiol.* 80, 7293–7302. doi: 10.1128/AEM.02893-14
- Cutting, S. M. (2011). *Bacillus* probiotics. *Food Microbiol.* 28, 214–220. doi: 10.1016/j.fm.2010.03.007
- Cutting, S., and Vander Horn, P. B. (1990). "Genetic analysis," in *Molecular Biological Methods for Bacillus*, eds C. Harwood and S. Cutting (Chichester: John Wiley and Sons), 27–74.
- Díaz-González, F., Milano, M., Olguín-Araneda, V., Pizarro-Cerda, J., Castro-Córdova, P., Tzeng, S. C., et al. (2015). Protein composition of the outermost exosporium-like layer of *Clostridium difficile* 630 spores. *J. Proteom.* 123, 1–13. doi: 10.1016/j.jprot.2015.03.035
- Di Luccia, B., D'Apuzzo, E., Varriale, F., Baccigalupi, L., Ricca, E., and Pollice, A. (2016). *Bacillus megaterium* SF185 induces stress pathways and affects the cell cycle distribution of human intestinal epithelial cells. *Benef. Microb.* 7, 609–620. doi: 10.3920/BM2016.0020
- Donadio, G., Lanzilli, M., Sirec, T., Ricca, E., and Isticato, R. (2016). Protein adsorption and localization on wild type and mutant spores of *Bacillus subtilis*. *Microb. Cell Fact.* 15:153. doi: 10.1186/s12934-016-0551-2
- Eppinger, M., Bunk, B., Johns, M. A., Edirisinghe, J. N., Kutumbaka, K. K., Koenig, S. S., et al. (2011). Genome sequences of the biotechnologically important *Bacillus megaterium* strains QM B1551 and DSM319. *J. Bacteriol.* 193, 4199–4213. doi: 10.1128/JB.00449-11
- Giglio, R., Fani, R., Isticato, R., De Felice, M., Ricca, E., and Baccigalupi, L. (2011). Organization and evolution of the cotG and cotH genes of *Bacillus subtilis*. *J. Bacteriol.* 193, 6664–6673. doi: 10.1128/jb.06121-11
- Harwood, C. R., and Cutting, S. M. (1990). *Molecular Biological Methods for Bacillus*. Chichester: John Wiley and Sons.
- Huang, J. M., Hong, H. A., Van Tong, H., Hoang, T. H., Brisson, A., and Cutting, S. M. (2010). Mucosal delivery of antigens using adsorption to bacterial spores. *Vaccine* 28, 1021–1030. doi: 10.1016/j.vaccine.2009.10.127
- Isticato, R., Pelosi, A., De Felice, M., and Ricca, E. (2010). CotE binds to CotC and CotU and mediates their interaction during spore coat formation in *Bacillus subtilis*. *J. Bacteriol.* 192, 949–954. doi: 10.1128/JB.01408-09
- Isticato, R., Pelosi, A., Zilhão, R., Baccigalupi, L., Henriques, A. O., De Felice, M., et al. (2008). CotC-CotU heterodimerization during assembly of the *Bacillus subtilis* spore coat. *J. Bacteriol.* 190, 1267–1275. doi: 10.1128/JB.01425-07
- Isticato, R., and Ricca, E. (2014). Spore surface display. *Microbiol. Spectr.* 2, 351–366. doi: 10.1128/microbiolspec.TBS-0011-2012
- Isticato, R., Sirec, T., Treppiccione, L., Maurano, F., De Felice, M., Rossi, M., et al. (2013). Nonrecombinant display of the B subunit of the heat labile toxin of *Escherichia coli* on wild type and mutant spores of *Bacillus subtilis*. *Microb. Cell Fact.* 12:98. doi: 10.1186/1475-2859-12-98
- Knecht, L. D., Pasini, P., and Daunert, S. (2011). Bacterial spores as platforms for bioanalytical and biomedical applications. *Anal. Bioanal. Chem.* 400, 977–989. doi: 10.1007/s00216-011-4835-4
- Koshikawa, T., Beaman, T. C., Pankratz, H. S., Nakashio, S., Corner, T. R., and Gerhardt, P. (1984). Resistance, germination, and permeability correlates of *Bacillus megaterium* spores successively divested of integument layers. *J. Bacteriol.* 159, 624–632.
- Manetsberger, J., Hall, E. A. H., and Christie, G. (2015a). Plasmid-encoded genes influence exosporium assembly and morphology in *Bacillus megaterium* QM B1551 spores. *FEMS Microbiol. Lett.* 362:fvn147. doi: 10.1093/femsle/fvn147
- Manetsberger, J., Manton, J. D., Erdelyi, M. J., Lin, H., Rees, D., Christie, G., et al. (2015b). Ellipsoid localization microscopy infers the size and order of protein layers in *Bacillus* spore coats. *Biophys. J.* 109, 2058–2066. doi: 10.1016/j.bpj.2015.09.023
- McCloy, R., Rogers, S., Caldon, E., Lorca, T., Castro, A., and Burgess, A. (2014). Partial inhibition of Cdk1 in G2 phase overrides the SAC and decouples mitotic events. *Cell Cycle* 13, 1400–1412. doi: 10.4161/cc.28401
- McKenney, P. T., Draks, A., and Eichemberger, P. (2012). The *Bacillus subtilis* endospore: assembly and functions of the multilayered coat. *Nat. Rev. Microbiol.* 11, 33–44. doi: 10.1038/nrmicro2921
- Nicholson, W. L., and Setlow, P. (1990). "Sporulation, germination and outgrowth," in *Molecular biological methods for Bacillus*, eds C. Harwood and S. Cutting (Chichester: John Wiley and Sons), 391–450.
- Nishihara, T., Takubo, Y., Kawamata, E., Koshikawa, T., Ogaki, J., and Kondo, M. (1989). Role of outer coat in resistance of *Bacillus megaterium* spore. *J. Biochem.* 106, 270–273.
- Pesce, G., Rusciano, G., Sirec, T., Isticato, R., Sasso, A., and Ricca, E. (2014). Surface charge and hydrodynamic coefficient measurements of *Bacillus subtilis* spore by optical tweezers. *Colloids Surf. B Biointerfaces* 116C, 568–575. doi: 10.1016/j.colsurfb.2014.01.039
- Ricca, E., Baccigalupi, L., Cangiano, G., De Felice, M., and Isticato, R. (2014). Mucosal vaccine delivery by non-recombinant spores of *Bacillus subtilis*. *Microb. Cell Fact.* 13, 115. doi: 10.1186/s12934-014-0115-2
- Rosso, M. L., and Vary, P. S. (2005). Distribution of *Bacillus megaterium* QM B1551 plasmids among other *B. megaterium* strains and *Bacillus* species. *Plasmid* 53, 205–217. doi: 10.1016/j.plasmid.2004.10.005
- Rusciano, G., Zito, G., Isticato, R., Sirec, T., Ricca, E., Bailo, E., and Sasso, A. (2014). Nanoscale chemical imaging of *Bacillus subtilis* spores by combining tip-enhanced Raman scattering and advanced statistical tools. *ACS Nano* 8, 12300–12309. doi: 10.1021/nn504595k
- Sirec, T., Strazzulli, A., Isticato, R., De Felice, M., Moracci, M., and Ricca, E. (2012). Adsorption of beta-galactosidase of *Alicyclobacillus acidocaldarius* on wild type and mutants spores of *Bacillus subtilis*. *Microb. Cell Fact.* 11:100. doi: 10.1186/1475-2859-11-100
- Stewart, G. C. (2015). The Exosporium layer of bacterial spores: a connection to the environment and the infected host. *Microbiol. Mol. Biol. Rev.* 79, 437–457. doi: 10.1128/MMBR.00050-15
- Vary, P. S., Biedendieck, R., Fuerch, T., Meinhardt, F., Rohde, M., Deckwer, W. -D., et al. (2007). *Bacillus megaterium*—from simple soil bacterium to industrial protein production host. *Appl. Microbiol. Biotechnol.* 76, 957–967 doi: 10.1007/s00253-007-1089-3
- Youngman, P., Perkins, J. B., and Losick, R. (1984). A novel method for the rapid cloning in *Escherichia coli* of *Bacillus subtilis* chromosomal DNA adjacent to *Tn917* insertion. *Mol. Gen. Genet.* 195, 424–433. doi: 10.1007/BF00341443
- Conflict of Interest Statement:** The authors declare that the research was conducted in the absence of any commercial or financial relationships that could be construed as a potential conflict of interest.
- Copyright © 2016 Lanzilli, Donadio, Addevico, Saggese, Cangiano, Baccigalupi, Christie, Ricca and Isticato. This is an open-access article distributed under the terms of the Creative Commons Attribution License (CC BY). The use, distribution or reproduction in other forums is permitted, provided the original author(s) or licensor are credited and that the original publication in this journal is cited, in accordance with accepted academic practice. No use, distribution or reproduction is permitted which does not comply with these terms.



Diversity of the Germination Apparatus in *Clostridium botulinum* Groups I, II, III, and IV

Jason Brunt^{1*}, Arnoud H. M. van Vliet^{1,2}, Féodor van den Bos¹, Andrew T. Carter¹ and Michael W. Peck¹

¹ Gut Health and Food Safety, Institute of Food Research, Norwich, UK, ² School of Veterinary Medicine, Faculty of Health and Medical Sciences, University of Surrey, Guildford, UK

OPEN ACCESS

Edited by:

Simon Michael Cutting,
Royal Holloway – University
of London, UK

Reviewed by:

Joseph Sorg,
Texas A&M University, USA
Peter Setlow,
University of Connecticut Health
Center, USA

*Correspondence:

Jason Brunt
jason.brunt@ifr.ac.uk

Specialty section:

This article was submitted to
Microbial Physiology and Metabolism,
a section of the journal
Frontiers in Microbiology

Received: 29 June 2016

Accepted: 12 October 2016

Published: 28 October 2016

Citation:

Brunt J, van Vliet AHM, van den Bos F, Carter AT and Peck MW (2016) Diversity of the Germination Apparatus in *Clostridium botulinum* Groups I, II, III, and IV. *Front. Microbiol.* 7:1702.
doi: 10.3389/fmicb.2016.01702

Clostridium botulinum is a highly dangerous pathogen that forms very resistant endospores that are ubiquitous in the environment, and which, under favorable conditions germinate to produce vegetative cells that multiply and form the exceptionally potent botulinum neurotoxin. To improve the control of botulinum neurotoxin-forming clostridia, it is important to understand the mechanisms involved in spore germination. Here we present models for spore germination in *C. botulinum* based on comparative genomics analyses, with *C. botulinum* Groups I and III sharing similar pathways, which differ from those proposed for *C. botulinum* Groups II and IV. All spores germinate in response to amino acids interacting with a germinant receptor, with four types of germinant receptor identified [encoded by various combinations of *gerA*, *gerB*, and *gerC* genes (*gerX*)]. There are three gene clusters with an ABC-like configuration; ABC [*gerX1*], ABABCB [*gerX2*] and ACx BBB [*gerX4*], and a single CA-B [*gerX3*] gene cluster. Subtypes have been identified for most germinant receptor types, and the individual GerX subunits of each cluster show similar grouping in phylogenetic trees. *C. botulinum* Group I contained the largest variety of *gerX* subtypes, with three *gerX1*, three *gerX2*, and one *gerX3* subtypes, while *C. botulinum* Group III contained two *gerX1* types and one *gerX4*. *C. botulinum* Groups II and IV contained a single germinant receptor, *gerX3* and *gerX1*, respectively. It is likely that all four *C. botulinum* Groups include a SpoVA channel involved in dipicolinic acid release. The cortex-lytic enzymes present in *C. botulinum* Groups I and III appear to be CwlJ and SleB, while in *C. botulinum* Groups II and IV, SleC appears to be important.

Keywords: *C. botulinum*, *C. sporogenes*, spore, germination, germinant receptors, cortex-lytic enzymes

INTRODUCTION

All strains of *Clostridium botulinum* form the highly potent botulinum neurotoxin, the agent responsible for botulism, a severe and often fatal neuroparalytic disease of humans and animals (Hatheway, 1988; Hauschild, 1989; Lindström et al., 2009; Peck, 2009; Peck et al., 2011; Johnson, 2013; Carter and Peck, 2015). There are seven confirmed botulinum neurotoxins (types A to G), and approximately forty different subtypes (Carter and Peck, 2015; Hill et al., 2015; Williamson et al., 2016). The botulinum neurotoxin is the most powerful toxin known, with as little as 30–100 ng sufficient to cause human botulism. Humans

are susceptible to three distinct types of botulism. Foodborne botulism is an intoxication associated with consumption of botulinum neurotoxin preformed in food. Infant/intestinal (adult) botulism is an infection associated with growth and neurotoxin formation in the infant gut, while wound botulism is an infection associated with growth and neurotoxin formation in a wound (often following drug abuse). In humans, symptoms of botulism typically commence with blurred vision, followed by an acute symmetrical descending bilateral paralysis, and eventually paralysis of the respiratory/cardiac muscles (Hatheway, 1988; Hauschild, 1989; Lindström et al., 2009; Peck, 2009; Peck et al., 2011; Johnson, 2013; Carter and Peck, 2015).

All strains of *C. botulinum* also form highly resistant endospores that are ubiquitous in the environment and may contaminate foods (Dodds, 1992; Carlin et al., 2004; Peck, 2010; Peck et al., 2010; Barker et al., 2016) and which, under favorable conditions germinate to produce vegetative cells that multiply and form neurotoxin. Spore germination is commonly initiated by a germinant receptor (GR) responding to nutrient germinants, and is followed by the release of dipicolinic acid (DPA) and partial core hydration. Next, cortex-lytic enzymes (CLEs) degrade the spore cortex, permitting additional core hydration and core expansion. Since spore germination is the key stage in the transition from dormant spore to vegetative cell, a greater understanding of the mechanisms involved in this process may contribute to an improved control of *C. botulinum*. Spore germination is relatively well understood in *Bacillus* (Setlow, 2014), and significant developments have been recently made in various species of *Clostridium*, including *C. botulinum* (Broussolle et al., 2002; Alberto et al., 2003; Paredes-Sabja et al., 2008b, 2009a; Burns et al., 2010; Adam et al., 2011; Banawas et al., 2013; Brunt et al., 2014, 2015; Meaney et al., 2015; Kevorkian et al., 2016).

Clostridium botulinum is not a homogeneous species, but a collection of four discrete bacterial groups (*C. botulinum* Groups I–IV) that share the common feature of forming botulinum neurotoxin. While all are obligately anaerobic bacteria, the four groups are sufficiently distinct to merit allocation to individual species. For each *C. botulinum* group, closely related non-toxigenic bacteria are known. *C. botulinum* Group I (proteolytic *C. botulinum*) is a major cause of botulism in humans (foodborne, infant, and wound), and strains form one or more neurotoxins of types A, B, or F (Hatheway, 1988; Peck et al., 2011; Johnson, 2013). *C. botulinum* Group I is a highly proteolytic and mesophilic bacterium that forms very heat resistant spores. The “Botulinum cook” (121°C/3 min) given to low acid canned foods is designed to inactivate these spores (Peck, 2009). *C. sporogenes* and *C. botulinum* Group I are closely related bacteria (Collins et al., 1994; Sebaihia et al., 2007; Jacobson et al., 2008; Carter et al., 2009; Bradbury et al., 2012). *C. sporogenes* is a significant cause of food spoilage (McClure, 2006), and due to its close physiological similarity to *C. botulinum* Group I is widely used as a surrogate in demonstrating the effectiveness of food preservation processes (Brown et al., 2012; Taylor et al., 2013). Recent analysis indicates

that several strains that form type B neurotoxin, and were previously classified as *C. botulinum* Group I, appear more like strains of *C. sporogenes* that have acquired a neurotoxin gene (Carter et al., 2009; Weigand et al., 2015; Williamson et al., 2016). *C. botulinum* Group II (non-proteolytic *C. botulinum*) is an important cause of foodborne botulism in humans, and is a concern for the safe production of minimally heat-processed refrigerated foods (Peck and Stringer, 2005; Peck, 2006; Peck et al., 2008). Strains form a single neurotoxin of type B, E, or F. *C. botulinum* Group II is a saccharolytic and psychrotrophic bacterium that forms spores of moderate heat resistance (Peck, 2009; Stringer et al., 2013). Strains of *C. botulinum* Group III form a single neurotoxin of type C or type D or more commonly a hybrid neurotoxin that comprises elements of each (type C/D or D/C), and are responsible for botulism in a wide range of animal species (Lindstrom et al., 2004; Sharpe et al., 2008; Woudstra et al., 2015). *C. botulinum* Group III is a saccharolytic and mesophilic bacterium that closely resembles *C. novyi* and *C. haemolyticum* (Skarin and Segerman, 2014) and forms spores of high heat resistance (Sasaki et al., 2001; Woudstra et al., 2015). *C. botulinum* Group IV (also known as *C. argentinense*) is the least studied *C. botulinum* group. This proteolytic and mesophilic bacterium forms type G neurotoxin and spores of high heat resistance. While experiments have shown its type G toxin to be toxigenic in animals, it has been weakly associated with botulism cases (Peck, 2009). Closely related non-toxigenic bacteria include *C. subterminale*.

The rapid technical development in genome sequencing, as well as the reductions in cost, now allow for comparative genomics of large collections of bacteria. In the present study, genome sequences have been used to establish the spore germination pathways, from germination receptors to spore-cortex-lytic hydrolases, for *C. botulinum* Groups I–IV. These bioinformatic approaches have been coupled to experimental analysis of germination stimuli. *C. botulinum* spores were found to contain GRs that responded to amino acids, and CLEs that resembled those described in other species. Spore germination appeared similar in *C. botulinum* Groups I and III, with subtle differences to that in *C. botulinum* Groups II and IV.

MATERIALS AND METHODS

Genome Sequences Included in This Study

Genome sequences were downloaded in FASTA file format as contigs or complete genome sequences from the NCBI website¹. Supplementary Table S1 contains GenBank/EMBL/DDBJ accession numbers of each genome sequence used, as well as assignment to *C. botulinum* Groups I–IV. The *C. botulinum* Group I data set comprised 92 *C. botulinum* and 8 *C. sporogenes* genome sequences, while those for *C. botulinum* Groups II and III comprised 24 and 31 *C. botulinum* genome sequences,

¹<http://www.ncbi.nlm.nih.gov/genome/browse/>

respectively. A single *C. botulinum* Group IV genome was also included.

Phylogenetic Analyses

A combined phylogenetic tree of all 156 genome sequences was generated using Feature Frequency Profiling with FFPry version 3.19² (Sims et al., 2009) with a word length of $L = 18$ as described in (van Vliet and Kusters, 2015). The program FFPboot was used for bootstrap analysis of the tree generated, using the default settings, and run for 100 replicates. Individual phylogenetic trees of *C. botulinum* Groups I–III were generated from core genome single nucleotide polymorphisms (SNPs), identified using the parSNP version 1.2 program from the Harvest suite (Treangen et al., 2014) with the “-a 13 -c -x” switches, with bootstrap values provided by the ParSNP output.

Comparative Genomics of GerX and Cortex-Lytic Enzymes

Genome sequences were provisionally annotated using Prokka version 1.12 (Seemann, 2014) and used for comparative genomics using Roary version 3.5.7 (Page et al., 2015). The *gerX* clusters and associated upstream and downstream genes were extracted from the comparisons to assess conservation of the genomic organization of the *gerX* clusters, as outlined in **Figure 1D** and Supplementary Table S2. Alignments were made with MEGA version 6.0 (Tamura et al., 2011), and used for generation of phylogenetic trees using the Neighbor Joining option. Figtree³ was used for annotation of phylogenetic trees. Genome sequences were genotyped for the different *gerX* clusters by *in silico* hybridisation using 60 nt oligonucleotides from the different *gerX* gene clusters, using the Microbial In Silico Typing (MIST) software package (Kruczkiewicz et al., 2013) and the NCBI Blast+ version 2.28 executables. Representative gene numbers for the *gerX* clusters and CLE genes from reference genomes are given in Supplementary Table S2. BLAST searches of the Prokka-annotated genomes were used to assess the level of variation between predicted GerX and CLE proteins encoded by the genomes. All generated data and phylogenetic trees are available in Supplementary Data Sheet 1.

Protein Bioinformatics

Relevant predicted amino acid sequences of the germination proteins of interest were imported into the Geneious 8.1.7 software (Biomatters⁴) package from NCBI. Signal cleavage sites were predicted using sigcleave, which is part of the EMBOSS suite (Rice et al., 2000). Protein domain analysis was performed using Pfam (Punta et al., 2012) and InterProScan to annotate proteins with families and domains (Quevillon et al., 2005). Transmembrane helices were characterized using Transmembrane Hidden Markov models (TMHMM; Krogh et al., 2001). Protein structure predictions were also analyzed using the PSIPRED Protein Sequence Analysis Workbench (Buchan et al., 2013).

²<http://sourceforge.net/projects/ffp-phylogeny/>

³<http://tree.bio.ed.ac.uk/software/figtree/>

⁴<http://www.geneious.com>

Bacterial Strains and Growth Conditions

Clostridium sporogenes strain ATCC15579 was grown at 37°C in anaerobic tryptone-yeast-glucose medium (TYG). *Escherichia coli* strain Top10 (Invitrogen) was used for plasmid maintenance and the *E. coli* strain CA434 (Purdy et al., 2002) was used for conjugal transfer. *E. coli* strains were grown aerobically in Luria-Bertani medium (LB) at 37°C. Where appropriate, growth medium was supplemented with antibiotics at the following final concentrations; chloramphenicol 25 µg/ml, cycloserine 250 µg/ml, thiampenicol 15 µg/ml, erythromycin 2.5 µg/ml, and the chromogenic substrate 5-bromo-4-chloro-3-indolyl-β-D-galactopyranoside (X-Gal) 80 µg/ml. All bacterial media supplements were purchased from Sigma.

PCR and Cloning

Constructed mutants and plasmids utilized in this study are presented in Supplementary Table S3. Primers used for verification of successful insertion events are also listed in Supplementary Table S3. PCR experiments were performed using Phusion High-Fidelity PCR Master Mix with GC Buffer kit (Thermo Fisher). Plasmid isolation and PCR purification was performed using the Wizard Plus SV Minipreps DNA Purification System and the Wizard SV Gel and PCR Clean-Up System (Promega) respectively, as defined in the provided Technical Manual. Chromosomal DNA isolation from potential mutants was prepared as previously described (Sebaihia et al., 2007).

Generation and Characterisation of spoVA Mutants and Their Complements

Mutants of *C. sporogenes* strain ATCC15579 were generated using the Clostron system as previously described (Brunt et al., 2014). Briefly, target sites were identified using the Perutka method (Perutka et al., 2004) and mutants were generated (Supplementary Table S3) as described (Heap et al., 2010). Re targeted introns were synthesized and ligated into the pMTL007C-E2 vector by DNA 2.0 (Menlo Park, USA). Retargeted intron plasmids were transformed into *E. coli* CA434. Confirmed (sequenced) plasmids were then transferred by conjugation into their respective clostridial host. For mutant complementation, plasmid pMTL83151 was used (Heap et al., 2009). Primers bearing restriction sites compatible with pMTL83151 (*Bam*HI and *Nhe*I) were used to amplify the *spoVA* gene cluster and its 5' non-coding region, covering the predicted putative promoter. The resulting PCR product was digested with *Bam*HI and *Nhe*I before being ligated into the pMTL83151 plasmid. Following confirmation by sequencing, complementation plasmids were transconjugated into their respective mutants using *E. coli* CA434 as described previously. The capacity of *C. sporogenes* *spoVA* mutants to form spores was assessed following incubation in anaerobic TYG broth at 37°C for 72 h. Spore formation was visualized every 24 h, in at least twenty fields, using phase-contrast microscopy. The number of heat resistant spores formed after 72 h was determined by heating the culture (80°C, 15 min), serial dilution in 0.85% saline, and plating in

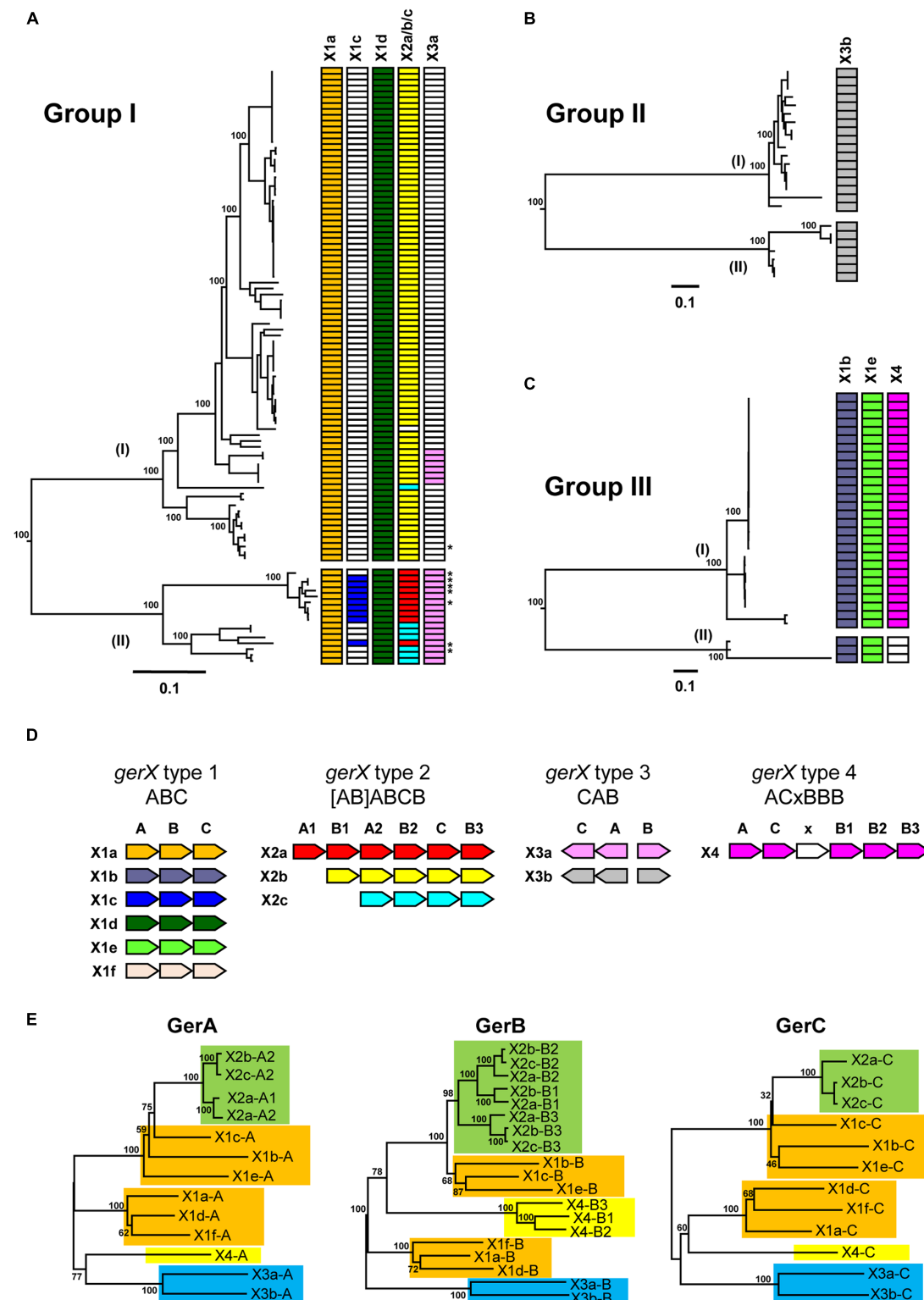


FIGURE 1 | Distribution of GerX receptor gene clusters in *Clostridium botulinum* Groups I to IV and *C. sporogenes* genomes. (A) Distribution of gerX types in *C. botulinum* Group I and *C. sporogenes* genomes. The asterisks represent *C. sporogenes* strains. The colors in trees (A–C) correspond with the colors attributed to each individual gerX subtype shown in (D). White blocks represent absence of the specific germinant receptor subtype. **(B)** Distribution of gerX types in *C. botulinum* Group II genomes. **(C)** Distribution of gerX types in *C. botulinum* Group III genomes. A full list of isolates included and their gerX gene clusters is given (Continued)

FIGURE 1 | Continued

in Supplementary Table S4. The phylogenetic trees in (A–C) are based on single nucleotide polymorphisms (SNPs) as determined using ParSNP (Treangen et al., 2014). Values shown at branches represent bootstrap values provided by ParSNP. (D) Genetic organization of the *gerX* subtypes. Type 1 represents the *gerABC* layout, Type 2 represents the (AB) ABCB layout, Type 3 the CA-B layout as a bicistronic gene cluster, and Type 4 an ACxBBB gene cluster. Subtype *gerX1f* is only found in *C. botulinum* Group IV which is not shown in (A–C). (E) Phylogenetic tree of Ger proteins. Representative reference genomes used are given in Supplementary Table S2. Colors represent the clustering based on GerX type. GerX type 1 is highlighted in gold, GerX type 2 in green, GerX type 3 in blue, GerX type 4 in yellow. The GerA, GerB, and GerC amino acid sequences each cluster into different subtypes. GerA, GerB, and GerC amino acid sequences were aligned with MEGA v 7.0, followed by creation of a phylogenetic tree using the Neighbor joining algorithm. Values shown at branches represent bootstrap values from 100 replicates.

triplicate on to TYG agar before incubation anaerobically (37°C, 72 hrs).

RESULTS AND DISCUSSION

Core Genome SNP Analysis of *C. botulinum* Genomes Confirms Clustering into Four Distinct Groups

To investigate the relationship between germination genes and genome phylogeny, we obtained 156 *C. botulinum* genome sequences. These were first clustered using feature frequency profiling (Sims et al., 2009; van Vliet and Kusters, 2015), to obtain an overview of the phylogenetic relationships within these 156 genome sequences. This initial analysis showed that the 156 genomes separated into four distinct phylogenetic groups (Supplementary Figure S1), thus giving 100 *C. botulinum* Group I (including *C. sporogenes*), 24 *C. botulinum* Group II, 31 *C. botulinum* Group III, and 1 *C. botulinum* Group IV genomes. The phylogenetic relationships within each group were determined using core genome SNP analysis, highlighting that Groups I–III each consisted of two distinct clusters of isolates, thus confirming the heterogeneity of the *C. botulinum* species. All but one of the *C. sporogenes* genomes clustered in *C. botulinum* Group I (lineage II), together with nine *C. botulinum* genomes forming a more distantly related lineage (Figure 1A, lineage II and Supplementary Table S4). It was recently reported that *C. botulinum* strains CDC68016, ATCC 51387, Prevot 1662, Osaka05, and Okayama2011 were defined as *C. sporogenes*-like strains that may have acquired a neurotoxin gene via horizontal transfer of plasmid DNA (Weigand et al., 2015). Conversely, *C. sporogenes* strain CDC24533 belonging to lineage I is a *C. botulinum* Group I strain that probably lost its neurotoxicogenic plasmid (Weigand et al., 2015). *C. botulinum* Group II strains were separated into two distinct lineages (Figure 1B; Supplementary Table S4). Lineage I comprises BoNT/E producing strains only, and while lineage II is dominated by BoNT/B producing strains some BoNT/E and /F producing strains are also present, confirming a previous microarray study (Stringer et al., 2013). Members of *C. botulinum* Group III also split into two distinct lineages (Figure 1C; Supplementary Table S4). Finally, a single strain of *C. botulinum* Group IV was examined. In summary, our phylogenetic analysis agrees with previous work that the lack of phylogenetic relationship between the Groups is sufficient to consider each Group as a separate species.

Germinant Receptor Subunits May Have Co-evolved and Could Allow Adaptation to New Environmental Niches

Under suitable conditions, the dormancy of bacterial spores is broken, and germination occurs. This is often initiated by a GR located in the spore inner membrane responding to nutrient germinants, followed by the release of DPA and partial core hydration. The *C. botulinum* and *C. sporogenes* GR is generally composed of three proteins (GerA, GerB, and GerC) that are encoded by their respective *ger* genes in a multi gene locus (Brunt et al., 2014). The designation, *gerX* implies that the cognate germinant molecule for the receptor encoded by this gene cluster is unknown. All 156 *C. botulinum* and *C. sporogenes* genome sequences were interrogated for *gerX* clusters and their flanking genes to assess conservation of the *gerX* cluster genomic organization. Four different types of *gerX* cluster were identified (Figure 1D). These different cluster types were further separated into subtypes based on similarity of DNA and predicted protein sequences of their *gerA*, *gerB*, and *gerC* genes, together with their genomic organization (Figure 1D). Analysis showed six subtypes displaying a monocistronic *gerABC* gene order (*gerX* type 1a–f), three subtypes that possess a *gerABCB* core, preceded by *gerAB*, *gerB* or nothing (*gerX* type 2a–c), two subtypes with a bicistronic divergent *gerCA* and *gerB* gene cluster (*gerX* type 3a–b), and one with a *gerACxBBB* configuration (*gerX* type 4; Figure 1D). Using BLASTP, the similarity within each GerX1 and GerX3 subtype was more than ca. 90% (except GerX1c ~85%), while the similarity between each subtype was ca. 20–65%.

Comparison of the amino acid sequences of the respective GerA, GerB, and GerC proteins showed that these form clusters according to the GerX subtype (Figure 1E). For example, the GerA, GerB, and GerC proteins of the X2 type each clustered together, as do the GerA, GerB, and GerC components of the X1a, X1b and, X1f subtypes, and the X1c, X1d, and X1e subtypes. Interestingly, the three GerB proteins of the GerX4 type all clustered closely together, and separately from the other GerB proteins (Figure 1E). The fact that all three GerX subunits group together within these four distinct lineages may imply that individual genes within each cluster could have co-evolved, and that the different cluster subtypes may have not arisen through insertional events (except for type 2).

gerX type 1 is an archetypal tricistronic ABC configuration receptor, with six subtypes (Figure 1D). Each subtype is unique to a single *C. botulinum* Group. All *C. botulinum* Group I/*C. sporogenes* strains possess *gerX1a* and *gerX1d*, while several strains in *C. botulinum* Group I/*C. sporogenes* lineage II also

possess *gerX1c* (**Figure 1A**). *gerX1b* and *gerX1e* are both present in all *C. botulinum* Group III strains (**Figure 1C**), and *gerX1f* is found in *C. botulinum* Group IV. *gerX1a* and *gerX1d* (but not *gerX1c*) are present in *C. botulinum* Group I strain ATCC 3502 and *C. sporogenes* ATCC 15579, and their functionality has been demonstrated (Brunt et al., 2014). The mutation of putative germination *gerXA* receptor genes revealed that both *gerX1s* were essential for amino acid stimulated germination in *C. botulinum* Group I strain ATCC 3502, while in *C. sporogenes* ATCC 15579 only *gerX1d* was essential for amino acid stimulated germination (Brunt et al., 2014). The fact that no obvious structural evidence could be found to explain the functional differences between this receptor in *C. botulinum* and *C. sporogenes* suggests that the answer may lie in subtle differences between their respective primary amino acid sequences. Interestingly, receptor types *gerX1a* (*C. botulinum* Group I/C. *sporogenes*), *gerX1b* (*C. botulinum* Group III), and *gerX1f* (*C. botulinum* Group IV), are flanked by homologs of a hypothetical protein immediately upstream of *gerXA* and a stage II sporulation protein immediately downstream of *gerXC*. This suggests a conserved location in *C. botulinum* Group I/C. *sporogenes*, and in *C. botulinum* Groups III and IV. However, the other slightly more distantly related *gerX1* subtypes (*gerX1c*, *gerX1d*, and *gerX1e*; **Figure 1E**) are not immediately flanked by the same genes.

The GerXA, GerXB, and GerXC proteins present in GerX type 2 each form a distinct clade separate from other GR proteins (and are shaded green in **Figure 1E**). GerX type 2 is exclusively possessed by strains of *C. botulinum* Group I and *C. sporogenes*, and all strains carry a single version of this larger GR gene cluster except for strain 20497 (**Figure 1A**; Supplementary Table S4). Further examination of the genome of strain 20497 reveals a ~77 kb deletion compared to the closely related strain 20427, and this ~77 kb region includes this putative GR gene cluster. The genes encoding the GerX type 2 proteins appear to be in a stable genomic environment, as the GR gene clusters always bear on their 5' flank an alanine racemase CDS and on their 3' flank a small conserved hypothetical protein CDS. Alanine racemase is able to convert the germinant L-alanine into the germination inhibitor D-alanine in *B. cereus* (Dodatko et al., 2009). This locus is conceivably a ‘transferable plasticity region’ as the configuration and number of GerX CDSs appears to be interchangeable, implying that this region may serve as a recombinational hot-spot for the *gerX* subunits. In addition, a small fragment of a *gerXA* gene apparently was often inserted into the 5' end of the first ‘extra’ *gerXB* gene of *C. botulinum* Group I; one example of which has been recently described in some detail (Brunt et al., 2014). The functionality of two of these gene clusters (*gerX2b* and *gerX2c* configurations) has recently been tested in *C. botulinum* Group I strain ATCC 3502 and *C. sporogenes* ATCC 15579 (Brunt et al., 2014). Mutagenesis of these multi gene loci revealed that neither was able to promote germination alone, although *gerX2c* formed part of a complex involved in controlling the germination rate in *C. sporogenes* (Brunt et al., 2014). Moreover, it is conceivable that they could individually respond to some other as yet unknown germinant or environmental niche. It is perhaps pertinent to consider why these putative GR gene clusters vary in their configuration and in

particular have additional *gerXB* genes (except for *gerX2a* which has an additional *gerXA*). Why does this not appear to be the case with *gerXA* or *gerXC* genes? Furthermore, the genomes of all *C. botulinum* Group I strains also contain a gene encoding an orphan *gerB* subunit. Although a monocistronic *gerA* gene subunit has been shown to be functional in *C. perfringens*, albeit only having a minor role (Paredes-Sabja et al., 2008b; Banawas et al., 2013), there is no current evidence of a functioning monocistronic *gerB* gene in the genus *Clostridium*. From our bioinformatics analysis the GerXB protein subunits are up to 457 residues in length and consist of 7–10 transmembrane helices. The GerXB proteins belong to the superfamily of membrane-associated single-component membrane transporters (Setlow, 2014; Moir and Cooper, 2016). However, this homology is largely based on structure as the sequence homology is low. Current evidence also suggests that the GerB protein is responsible for germinant binding (Christie et al., 2008; Christie et al., 2010) and may stabilize and/or influence the quantity of GerC proteins (Cooper and Moir, 2011). Perhaps one attractive proposal is that if the GerXB protein does indeed contain the germinant binding site, then the ability of strains to swap GerXB units or to possess multiple GerXB units may enable them to adapt to exploit new environmental niches.

GerX type 3 is present in some *C. botulinum* Group I lineage (I) strains and all lineage (II) strains (*gerX3a*), and in all *C. botulinum* Group II strains (*gerX3b*; **Figures 1A,B**). It is the only complete GR present in *C. botulinum* Group II, with the caveat that there are currently fewer sequenced *C. botulinum* Group II genomes available for analysis than there are *C. botulinum* Group I genomes. Analysis of this locus revealed an organization that is quite different to the ‘classical’ receptor organization with a GerXA CDS in the middle of the receptor (CA-B; **Figure 1D**), and a bicistronic transcriptional organization with *gerAC* and *gerB* genes in the opposite orientation. The organization of this receptor gene cluster is similar to the single one also observed in *C. perfringens* where the *gerK* locus includes a monocistronic *gerKB* in an orientation opposite to that of a bicistronic *gerKA-gerKC* (Paredes-Sabja et al., 2008b; Banawas et al., 2013). Furthermore, it has been demonstrated that the GerKC protein is the main GR protein involved in nutrient and non-nutrient germination (Banawas et al., 2013). Although no function has yet been formally assigned to this *ger* gene cluster, the fact that amino acid induced spore germination of three *C. botulinum* Group II strains has been previously reported makes it the prime candidate for encoding a functional germination receptor (Plowman and Peck, 2002). The GerXA, GerXB, and GerXC proteins present in GerX type 3 each form a separate clade from other *C. botulinum* GR proteins (shaded blue in **Figure 1E**).

There is a single example of GerX type 4, the receptor ACxBBB from some strains of *C. botulinum* Group III (**Figures 1C,D**). All three GerXB subunits clustered together [and are shaded yellow (**Figure 1E**)], and while similar to each other were more distantly related to other GerXB proteins (**Figure 1E**). GerXA and GerXC from GerX type 4 were also distinct from other related GR proteins (**Figure 1E**). The GerX(x) putative subunit, located in the middle of *C. botulinum* Group III germination

cluster is a hypothetical protein of 74 residues and comprises a non-cytoplasmic domain (ca. 22 residues) at the N-terminus and a single transmembrane region (ca. 23 residues) in the centre. The protein is also predicted to have its own ribosome binding site and a predicted signal peptide; evidence that it is probably expressed. It also contains the ribosome binding site for the next gene (*gerXB*) in this locus. The amino acid sequences of GerX(x) revealed no homology to any other proteins outside of *C. botulinum* Group III. However, unrelated small (ca. 75 residues) proteins in or adjacent to other GR clusters have been described previously (Paredes-Sabja et al., 2011; Ramirez-Peralta et al., 2013). The functionality of GerX(x) remains to be tested but it is tempting to speculate that as this protein is only present in *C. botulinum* Group III, a pathogen strongly associated with animal botulism, this putative receptor subunit may be associated with a particular environmental niche.

Spores Respond to a Diverse Range of Germinants

Germination of *Clostridium* spores is usually initiated by germinants that include amino acids and sugars (Table 1), and often proceeds more slowly than that observed with *Bacillus* (Brunt et al., 2014). Spore germination in *C. botulinum* Group I and *C. sporogenes* is triggered by a variety of amino acids, often in combination with L-lactate; although previous studies have described a variable effect of L-lactate (Broussolle et al., 2002; Alberto et al., 2003; Peck, 2009). A literature review of germination characteristics of *C. botulinum* Group I reveals that although most strains germinate with the addition of L-alanine, germination responses are strain, pH, temperature, and buffer dependent (Broussolle et al., 2002; Alberto et al., 2003; Peck, 2009; Brunt et al., 2014). Recently, analysis of *C. botulinum* strain ATCC 3502 revealed that GerX1a and GerX1d responded to a variety of amino acids and that they act in synergy and cannot function individually. *C. sporogenes* strain ATCC15579 also responded to a variety of amino acids. Although, only GerX1d was essential, GerX3a and GerX2c GRs form part of a complex involved in controlling the rate of amino acid stimulated germination (Brunt et al., 2014).

Spores of *C. botulinum* Group II also respond to a variety of amino acids (Table 1) (Ando and Iida, 1970; Ando, 1971; Plowman and Peck, 2002). In contrast to *C. botulinum* Group I, L-lactate is considered essential for amino acid induced germination in *C. botulinum* Group II (Plowman and Peck, 2002). The germination responses of *C. botulinum* Group II is dependent on strain, pH, temperature, and buffer (Ando and Iida, 1970; Ando, 1971; Plowman and Peck, 2002; Peck, 2009).

While various aspects of the physiology and genomics of *C. botulinum* Group III have been studied in some detail (Eklund and Dowell, 1987; Woudstra et al., 2015), relatively little is known about the properties of their spores or their spore germination characteristics. Based on analysis of the encoded GRs, it is anticipated that these spores will also respond to amino acid germinants. Current knowledge of spore germination in *C. botulinum* Group IV is also limited. However, one study has shown that spores optimally germinate with a mixture of

L-cysteine, L-lactate, and bicarbonate and sub-optimally with L-alanine, L-lactate, and bicarbonate (Takeshi et al., 1988).

Observed inconsistencies in the results from different publications, together with our own experience, indicate that strain differences and the method used to produce spores, how they are maintained, and which buffer is used to evaluate germination, invariably has a direct effect on germination rates and extents.

SpoVA Is Implicated in Sporulation and DPA Release

Clostridium and *Bacillus* spores contain a large store of a 1:1 chelate of Ca²⁺ and pyridine-2, 6-dicarboxylic acid (DPA) within its core which contributes to spore dormancy and heat resistance (Paidhungat et al., 2000). It has been proposed that the SpoVA proteins are associated with the inner membrane and may form a mechanosensitive channel through which DPA may be transported, and thereby packaged during sporulation (Li et al., 2012; Korza and Setlow, 2013; Velasquez et al., 2014). One line of evidence supporting this hypothesis comes from work showing that SpoVAC can act as a non-selective solute channel when expressed in *E. coli* (Velasquez et al., 2014). There are three SpoVA proteins, and it is yet to be determined whether all three act together and/or interact with other proteins. For most spore-formers (including *C. perfringens*), DPA release precedes cortex hydrolysis during germination and is reported to also activate the CwlJ protein (Paidhungat et al., 2001). However, it has recently been found that in *Clostridium difficile* spore cortex hydrolysis precedes DPA release (Francis et al., 2015). It is presently unknown whether DPA release in *C. botulinum* and *C. sporogenes* follows that observed in *C. perfringens* or *C. difficile*. A role for SpoVA proteins in clostridial spore germination has been demonstrated in *C. perfringens* and *C. difficile* (Paredes-Sabja et al., 2008a; Donnelly et al., 2016).

In the present study, bioinformatics analysis revealed that strains of *C. botulinum* Groups I–III and *C. sporogenes* each contain one gene cluster encoding spoVAC, spoVAD, and spoVAE. In contrast the single strain of *C. botulinum* Group IV studied to date possesses two gene clusters encoding the SpoVA proteins. *C. botulinum* SpoVAC, a paralog of SpoVAE, is typically 153 residues long and contains three or four membrane-spanning regions. SpoVAE is approximately 118 residues long and also contains three or four membrane-spanning regions and a predicted signal peptide (*C. botulinum* Group III). SpoVAD is typically 333 residues long. SpoVAD has been shown to bind specifically to DPA and Ca-DPA (Li et al., 2012). To characterize the functionality of SpoVA proteins in *C. sporogenes* ATCC 15579, a series of single insertion mutants (*spoVAE-1864⁻*, *spoVAC-1862⁻*, *spoVAD-1863⁻*) were constructed and subsequently complemented (*spoVAE-1864⁺*, *spoVAC-1862⁺*, *spoVAD-1863⁺*). Phenotypic analysis of the *spoVA* mutations revealed that the products of all three genes were required for successful sporulation, and complementation restored similar wild type levels of sporulation, except for *spoVAE-1864⁻* (Figure 2). Furthermore, attempts to complement the *spoVAE-1864⁻* using a plasmid that contained the entire *spoVA* locus (i.e.,

TABLE 1 | Germinants of *Clostridium botulinum* Groups I–IV and *C. sporogenes* spores.

	Germinant	Reference
Group I	L-alanine, L-cysteine, L-methionine, L-serine, L-phenylalanine, glycine	Broussolle et al., 2002; Alberto et al., 2003; Brunt et al., 2014
<i>C. sporogenes</i>	L-alanine, L-cysteine, L-methionine, L-serine, L-phenylalanine,	Broussolle et al., 2002; Brunt et al., 2014
Group II	L-alanine, L-serine, L-cysteine, L-threonine, glycine	Ando and Iida, 1970; Ando, 1971; Plowman and Peck, 2002
Group III	No information	–
Group IV	L-cysteine, L-alanine*	Takeshi et al., 1988

L-lactate is often required as a co-germinant with the amino acids listed. *sub-optimal germination observed with L-alanine in *C. botulinum* Group IV.

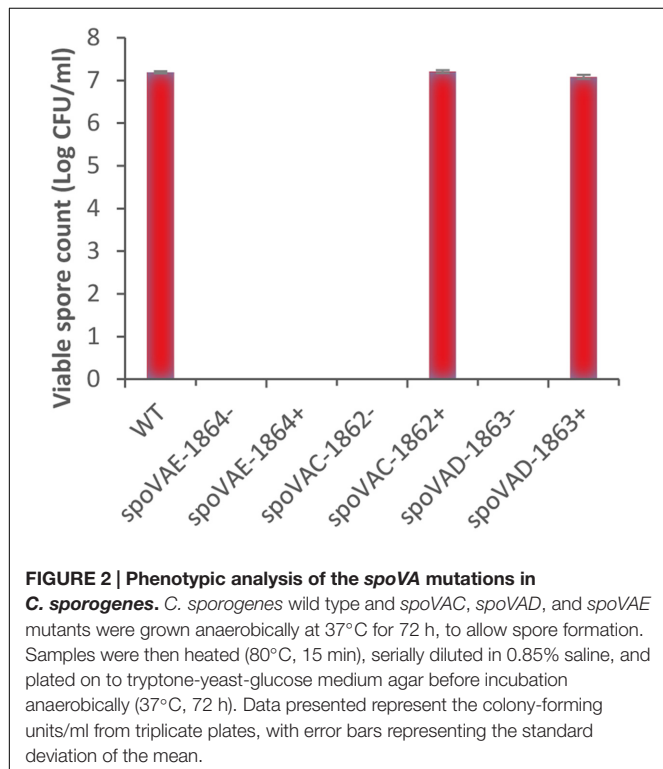


FIGURE 2 | Phenotypic analysis of the spoVA mutations in *C. sporogenes*. *C. sporogenes* wild type and spoVAC, spoVAD, and spoVAE mutants were grown anaerobically at 37°C for 72 h, to allow spore formation. Samples were then heated (80°C, 15 min), serially diluted in 0.85% saline, and plated on to tryptone-yeast-glucose medium agar before incubation anaerobically (37°C, 72 h). Data presented represent the colony-forming units/ml from triplicate plates, with error bars representing the standard deviation of the mean.

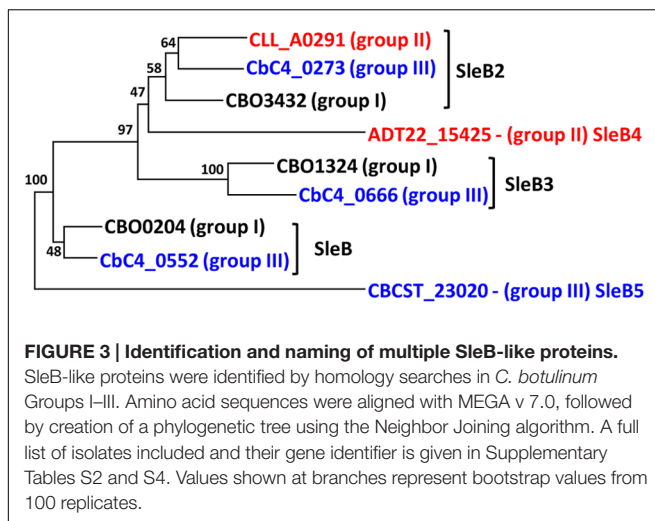
spoVAE, *spoVAC*, *spoVAD*) also failed to complement *spoVAE*-1864[−] mutant. The failure of some plasmid complemented mutants to regain wild type sporulation levels in clostridia has been reported previously (Li et al., 2011; Brunt et al., 2014; Meaney et al., 2015). Mutations in the *spoVA* operon of *B. subtilis* strains result in the lysis of immature spores during sporulation, most likely due to their lack of DPA (Tovar-Rojo et al., 2002). The cause of this lysis is unknown but it may be due in part to the CLE SleB (see below) which is activated in spores lacking DPA (Tovar-Rojo et al., 2002). Similarly, although we did initially observe occasional endospores produced by SpoVA mutants by phase microscopy, these endospores lysed during sporulation and none were observed at the end of the sporulation experiment. Furthermore, no heat resistant endospores were detected following heating (80°C, 15 min) and subsequent plating on microbiological growth medium. In contrast to our findings

for *C. sporogenes* and those of *B. subtilis*, mutations of the *spoVA* operon in *C. perfringens* and *spoVAC* in *C. difficile* did not result in the lysis of immature spores and spores germinated relatively normally, but also had a high water content and decreased heat resistance (Paredes-Sabja et al., 2008a; Donnelly et al., 2016). Taken together, the sequence homology and phenotypic results presented here suggest that the SpoVA proteins may perform a similar role in *C. botulinum* and *C. sporogenes* to those reported in *Bacillus*, specifically the SpoVA proteins may be involved in DPA uptake during sporulation and DPA release during germination. Further studies are required, however, to confirm this assertion.

Spore Cortex Hydrolysis and the Identification of Multiple Enzymes

In all *Bacillus* and *Clostridium* species [except *C. difficile* (Francis et al., 2015)], the release of DPA and various ions from the germinating spore is followed by the hydrolysis of the peptidoglycan in the spore cortex (Johnstone, 1994). The spore cortex peptidoglycan plays an important role in conserving spore dormancy and heat resistance (Atri and Foster, 2001; Peck, 2009). Analysis of the spore cortex peptidoglycan reveals that its structure is highly conserved between *Bacillus* and *Clostridium* (Atri and Foster, 2001). Cortex hydrolysis is reliant on activation of preformed CLEs that cleave the spore cortex peptidoglycan. Spores of *Bacillus* and some *Clostridium* species contain two redundant CLEs, CwlJ and SleB (Setlow et al., 2009; Paredes-Sabja et al., 2011; Meaney et al., 2015). CwlJ is activated by Ca²⁺-DPA release from the spore core (Paidhungat et al., 2001). The mechanism of SleB activation remains unknown, although YpeB is required for its localization and may be involved in regulating its activity (Li et al., 2013). *C. perfringens* and *C. difficile* have a solitary CLE, SleC, which is essential for peptidoglycan hydrolysis and germination (Miyata et al., 1995; Paredes-Sabja et al., 2009b; Burns et al., 2010). SleC is present as an inactive zymogen which becomes activated by cleavage of Pro-SleC by a Csp protease (Paredes-Sabja et al., 2009a).

The genomes of 156 strains of *C. botulinum* Groups I–IV and *C. sporogenes* all contained CLE homologs, with the level of conservation in the predicted protein sequences within each Group >90%, with the exception of SleB3 and YpeB in Group III (89 and 88%, respectively), similar to the variation in GerX subunit sequences (Figure 1E). All *C. botulinum* Groups I and III strains carry at least one copy of sleB, with a single exception



(Supplementary Table S4). *C. botulinum* Group I strain Af84 appears to lack a SleB homolog, and this is associated with a deletion of a ~159 kb region in the genome when compared to *C. botulinum* Group I strain U21076. This ~159 kb deletion also

includes the SpoVA channel forming proteins. However, there is a second copy of the gene cluster encoding the SpoVA proteins at a different locus. Furthermore, at the site of the deletion, small fragments of *spoVAD* and *spoVAC* are observed. All *C. botulinum* Group I and *C. botulinum* Group III strains also carry a single copy of a *cwlJ* and *ypeB* gene. Recent studies have shown that, at least for *C. botulinum* Group I ATCC 3502, SleB and YpeB are required for optimal germination and that while a gene encoding CwlJ is present, a functional enzyme is not formed (Meaney et al., 2015). These findings are in contrast to *B. subtilis* in which CwlJ plays a prominent role in degrading the spore cortex (Ishikawa et al., 1998; Yi and Setlow, 2010). Furthermore, studies in our lab (unpublished data) revealed that insertional inactivation of *cwlJ* in *C. sporogenes* ATCC15579 resulted in a decrease in germination rate, indicating that CwlJ is functional in this strain. Our bioinformatic analysis also revealed the presence of genes encoding four additional ‘SleB-like’ proteins (tentatively named SleB2, SleB3, SleB4, and SleB5), with at least one example present in each strain of *C. botulinum* Groups I–III (Figures 3 and 4; Supplementary Table S4).

Interestingly, *C. botulinum* Group II, which possess the SleC cortex hydrolysis system, also contain *sleB2*, and strains CB11/1-1, 20536 and ATCC17786 contain a second *sleB*-like

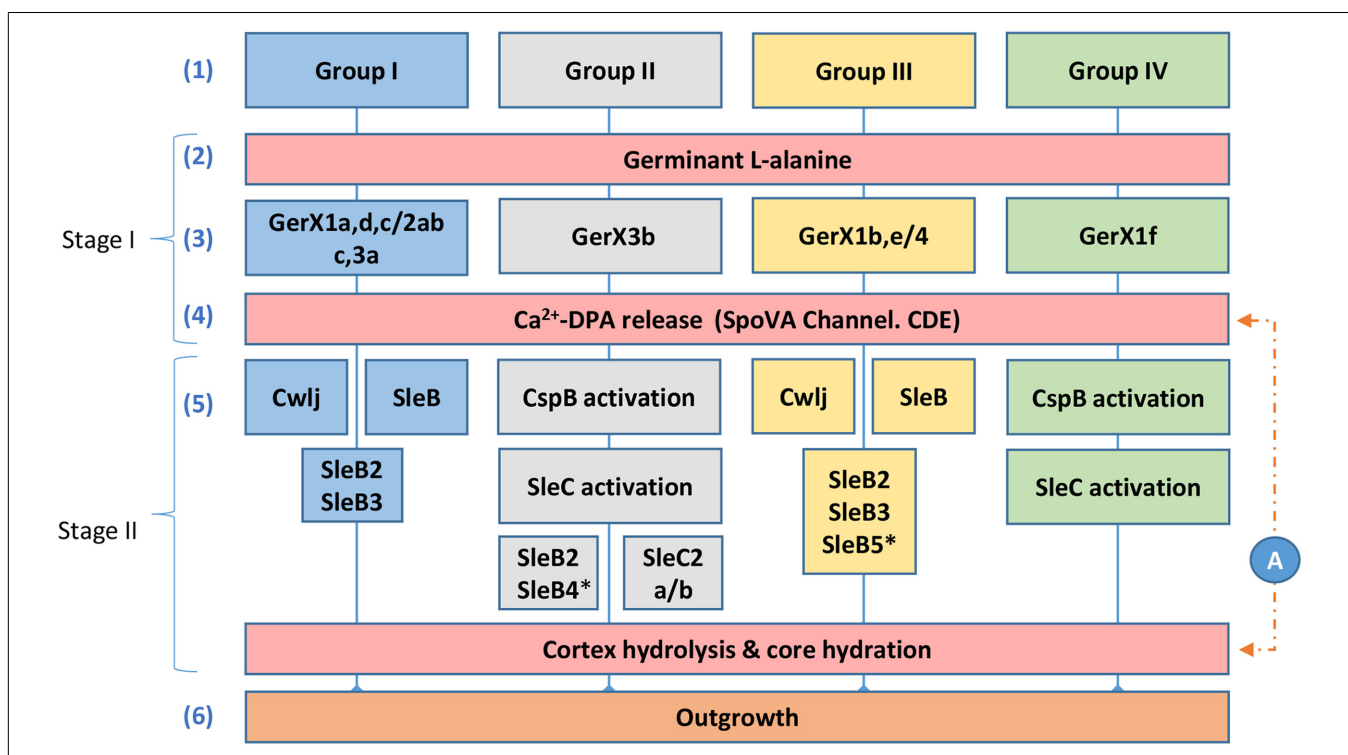


FIGURE 4 | Diagrammatic model for the proposed germination pathways of *C. botulinum* Groups I–IV. One model for spore germination is proposed for *C. botulinum* Groups I and III, and a second related model is proposed for *C. botulinum* Groups II and IV. (1) *C. botulinum* Groups. Germination stage I; (2) and (3) germinant e.g., L-alanine binds to its cognate receptor located in the inner membrane (see Figure 1). (4) Ca^{2+} -DPA is released through the SpoVA channel. Germination stage II; (5) Cortex-lytic enzymes (CLEs) are activated and then cleave the spore cortex peptidoglycan. *C. botulinum* Group I and Group III involves the CLEs CwlJ and SleB. *C. botulinum* Groups II and IV the CLE SleC is activated by CspB, followed by cortex hydrolysis. (6) Membrane and coat degradation, the recommencement of metabolism and eventually cell outgrowth of the newly formed cell. (A) The timing of the release of Ca^{2+} -DPA is unknown in *C. botulinum* and may be released following germinant binding or after cortex hydrolysis. *only observed in a small set of Groups II and III genomes, as identified in Supplementary Table S4.

CDS (encoding SleB4). The latter *sleB*-like gene may, however, be involved in bacterial conjugation as in strains CB11/1-1 and ATCC17786 it is present on a plasmid, situated adjacent to genes predicted to encode the conjugation pilus (Carter et al., 2016). We did not detect genes encoding YpeB or CwlJ homologs in *C. botulinum* Group II genomes. Similarly, *C. botulinum* Group IV encodes a SleC cortex hydrolysis system, and does not encode SleB-like homologs. *C. botulinum* Group II strains also contain a second *sleC*-like CDS (*sleC2a/b*; Supplementary Table S4). Alignment and secondary structural analysis revealed that SleC, which is ~443 residues long, consists of two domains; a SpoIID/LytB domain plus a peptidoglycan-binding domain. SleC2a/b, annotated as a spore CLE, pre-pro-form, is also a multi-domain protein consisting of a SpoIID/LytB domain and 4–5 peptidoglycan-binding domains. SleC2a is ~792 residues and SleC2b is ~698 residues. SleC2b, which has one less peptidoglycan-binding domain in comparison to SleC2a, is largely found in *C. botulinum* Group II type E strains.

SleB2, which is usually annotated in the databases as being ‘SleB-like’ with a similar C-terminus to *B. cereus* SleB, is ~177 residues and is defined as a cell wall hydrolase. SleB3 is ~260 residues, consists of two LysM domains, which are involved in peptidoglycan-binding, and is also associated with the Hydrolase_2 superfamily. Both SleB2 and SleB3 CDSs are immediately preceded by an *ydaO* element (except in *C. botulinum* Group II strains). The *ydaO* element is a riboswitch that is often associated with genes responsible for degradation of polysaccharides in *Bacillus* (Block et al., 2010). SleB4 is ~214 residues, is only found in three *C. botulinum* Group II strains and belongs to the cell wall hydrolase family. SleB5 is only found in one *C. botulinum* Group III strain, has two peptidoglycan-binding domains and is annotated as belonging to the spore cortex-lytic family. It is interesting that strains which use the SleC CLE system also contain these SleB-like proteins and it is tempting to speculate that these proteins may be involved in an alternative cortex hydrolysis pathway. Certainly, the functionality of these *sleB* and *sleC*-like CDSs merits further investigation, including determination of the ligand for the *ydaO* motif.

A Diagrammatic Germination Model for Spore Germination in *C. botulinum* Groups I–IV

Although the germination mechanisms in *Bacillus* are better understood, significant progress is now being made in understanding germination processes in *Clostridium* (Paredes-Sabja et al., 2011; Kevorkian et al., 2016). Despite this progress, germination mechanisms in *C. botulinum* Groups I–IV are still relatively poorly understood. Based on our findings and on studies in *Bacillus* and *C. perfringens* (Paredes-Sabja et al., 2011) we propose two germination systems for *C. botulinum* spores (Figure 4). The first system, which applies to strains of *C. botulinum* Group I (and *C. sporogenes*) and *C. botulinum* Group III, involves the recognition of nutrient germinants by their cognate receptor, followed by Ca^{2+} -DPA release through

the proposed SpoVA channel (Stage I). In stage II, the CLEs CwlJ and SleB are activated, followed by cortex hydrolysis, membrane and coat degradation, the recommencement of metabolism and eventually cell outgrowth (Figure 4). The second germination system, present in strains of *C. botulinum* Group II and *C. botulinum* Group IV, again involves the recognition of nutrient germinants by their cognate receptor, followed by Ca^{2+} -DPA release through the proposed SpoVA channel (Stage I). In stage II, the CLE SleC is activated by CspB (a protein only found in Groups II and IV, see Supplementary Tables S2 and S4), followed by cortex hydrolysis, membrane, and coat degradation, the recommencement of metabolism and eventually cell outgrowth (Figure 4). These are the first models proposed for spore germination in *C. botulinum* Groups I–IV.

CONCLUSION

This work describes the first models to be developed of spore germination in *C. botulinum* Groups I–IV. Of particular interest is the discovery that two different pathways exist which lead to spore germination and subsequently to outgrowth. Spore germination followed the phylogenetic groupings, with germination in *C. botulinum* Groups I and III similar, and subtly different to that in *C. botulinum* Groups II and IV. The bioinformatic comparisons and comparative genomics analyses suggest that it is most likely that the individual GerA/B/C components of the GerX clusters have co-evolved, although we cannot exclude a contribution from recombination and horizontal gene transfer. The next few years may be a fascinating period of discovery, in which the different specific role of each class of GR is uncovered.

AUTHOR CONTRIBUTIONS

JB and MP conceived the study. JB, MP, AvV, AC, and FvdB analysed the data. JB, AvV, and FvdB performed the experiments. JB, MP, AC, and AvV wrote the paper. All authors read and approved the final manuscript.

ACKNOWLEDGMENT

The authors acknowledge support from the Biotechnology and Biological Sciences Research Council as part of the BBSRC Institute Strategic Programme on Gut Health and Food Safety BB/J004529/1.

SUPPLEMENTARY MATERIAL

The Supplementary Material for this article can be found online at: <http://journal.frontiersin.org/article/10.3389/fmicb.2016.01702/full#supplementary-material>

REFERENCES

- Adam, K. H., Brunt, J., Brightwell, G., Flint, S. H., and Peck, M. W. (2011). Spore germination of the psychrotolerant, red meat spoiler, *Clostridium frigidicarnis*. *Lett. Appl. Microbiol.* 53, 92–97. doi: 10.1111/j.1472-765X.2011.03071.x
- Alberto, F., Broussolle, V., Mason, D. R., Carlin, F., and Peck, M. W. (2003). Variability in spore germination response by strains of proteolytic *Clostridium botulinum* types A, B and F. *Lett. Appl. Microbiol.* 36, 41–45. doi: 10.1046/j.1472-765X.2003.01260.x
- Ando, Y. (1971). The germination requirements of spores of *Clostridium botulinum* type E. *Jpn. J. Microbiol.* 15, 515–525. doi: 10.1111/j.1348-0421.1971.tb00613.x
- Ando, Y., and Iida, H. (1970). Factors affecting the germination of spores of *Clostridium botulinum* type E. *Jpn. J. Microbiol.* 14, 361–370. doi: 10.1111/j.1348-0421.1970.tb00536.x
- Atrih, A., and Foster, S. J. (2001). Analysis of the role of bacterial endospore cortex structure in resistance properties and demonstration of its conservation amongst species. *J. Appl. Microbiol.* 91, 364–372. doi: 10.1046/j.1365-2672.2001.01394.x
- Banawas, S., Paredes-Sabja, D., Korza, G., Li, Y., Hao, B., Setlow, P., et al. (2013). The *Clostridium perfringens* germinant receptor protein GerKC is located in the spore inner membrane and is crucial for spore germination. *J. Bacteriol.* 195, 5084–5091. doi: 10.1128/JB.00901-13
- Barker, G. C., Malakar, P. K., Plowman, J., and Peck, M. W. (2016). Quantification of nonproteolytic *Clostridium botulinum* spore loads in food materials. *Appl. Environ. Microbiol.* 82, 1675–1685. doi: 10.1128/AEM.03630-15
- Block, K. F., Hammond, M. C., and Breaker, R. R. (2010). Evidence for widespread gene control function by the ydaO riboswitch candidate. *J. Bacteriol.* 192, 3983–3989. doi: 10.1128/JB.00450-10
- Bradbury, M., Greenfield, P., Midgley, D., Li, D., Tran-Dinh, N., Vriesekoop, F., et al. (2012). Draft genome sequence of *Clostridium sporogenes* PA 3679, the common nontoxigenic surrogate for proteolytic *Clostridium botulinum*. *J. Bacteriol.* 194, 1631–1632. doi: 10.1128/JB.06765-11
- Broussolle, V., Alberto, F., Shearman, C. A., Mason, D. R., Botella, L., Nguyen-The, C., et al. (2002). Molecular and physiological characterisation of spore germination in *Clostridium botulinum* and *Clostridium sporogenes*. *Anaerobe* 8, 89–100. doi: 10.1006/anae.2002.0424
- Brown, J. L., Tran-Dinh, N., and Chapman, B. (2012). *Clostridium sporogenes* PA 3679 and its uses in the derivation of thermal processing schedules for low-acid shelf-stable foods and as a research model for proteolytic *Clostridium botulinum*. *J. Food Prot.* 75, 779–792. doi: 10.4315/0362-028X.JFP-11-391
- Brunt, J., Cross, K. L., and Peck, M. W. (2015). Apertures in the *Clostridium sporogenes* spore coat and exosporium align to facilitate emergence of the vegetative cell. *Food Microbiol.* 51, 45–50. doi: 10.1016/j.fm.2015.04.013
- Brunt, J., Plowman, J., Gaskin, D. J., Itchner, M., Carter, A. T., and Peck, M. W. (2014). Functional characterisation of germinant receptors in *Clostridium botulinum* and *Clostridium sporogenes* presents novel insights into spore germination systems. *PLoS Pathog.* 10:e1004382. doi: 10.1371/journal.ppat.1004382
- Buchan, D. W., Minneci, F., Nugent, T. C., Bryson, K., and Jones, D. T. (2013). Scalable web services for the PSIPRED protein analysis workbench. *Nucleic Acids Res.* 41, W349–W357. doi: 10.1093/nar/gkt381
- Burns, D. A., Heap, J. T., and Minton, N. P. (2010). SleC is essential for germination of *Clostridium difficile* spores in nutrient-rich medium supplemented with the bile salt taurocholate. *J. Bacteriol.* 192, 657–664. doi: 10.1128/JB.01209-09
- Carlin, F., Broussolle, V., Perelle, S., Litman, S., and Fach, P. (2004). Prevalence of *Clostridium botulinum* in food raw materials used in REPFEDs manufactured in France. *Int. J. Food Microbiol.* 91, 141–145. doi: 10.1016/S0160-1605(03)00371-4
- Carter, A. T., Austin, J. W., Weedmark, K. A., and Peck, M. W. (2016). Evolution of chromosomal *Clostridium botulinum* type E neurotoxin gene clusters: evidence provided by their rare plasmid-borne counterparts. *Genome Biol. Evol.* 8, 540–555. doi: 10.1093/gbe/evw017
- Carter, A. T., Paul, C. J., Mason, D. R., Twine, S. M., Alston, M. J., Logan, S. M., et al. (2009). Independent evolution of neurotoxin and flagellar genetic loci in proteolytic *Clostridium botulinum*. *BMC Genomics* 10:115. doi: 10.1186/1471-2164-10-115
- Carter, A. T., and Peck, M. W. (2015). Genomes, neurotoxins and biology of *Clostridium botulinum* Group I and Group II. *Res. Microbiol.* 166, 303–317. doi: 10.1016/j.resmic.2014.10.010
- Christie, G., Gotzke, H., and Lowe, C. R. (2010). Identification of a receptor subunit and putative ligand-binding residues involved in the *Bacillus megaterium* QM B1551 spore germination response to glucose. *J. Bacteriol.* 192, 4317–4326. doi: 10.1128/JB.00335-10
- Christie, G., Lazarevska, M., and Lowe, C. R. (2008). Functional consequences of amino acid substitutions to GerVB, a component of the *Bacillus megaterium* spore germinant receptor. *J. Bacteriol.* 190, 2014–2022. doi: 10.1128/JB.01687-07
- Collins, M. D., Lawson, P. A., Willems, A., Cordoba, J. J., Fernandez-Garayzabal, J., Garcia, P., et al. (1994). The phylogeny of the genus *Clostridium*: proposal of five new genera and eleven new species combinations. *Int. J. Syst. Bacteriol.* 44, 812–826. doi: 10.1093/ijs/0207713-44-4-812
- Cooper, G. R., and Moir, A. (2011). Amino acid residues in the GerAB protein important in the function and assembly of the alanine spore germination receptor of *Bacillus subtilis* 168. *J. Bacteriol.* 193, 2261–2267. doi: 10.1128/JB.01397-10
- Dodatko, T., Akoachere, M., Muehlbauer, S. M., Helfrich, F., Howerton, A., Ross, C., et al. (2009). *Bacillus cereus* spores release alanine that synergizes with inosine to promote germination. *PLoS ONE* 4:e6398. doi: 10.1371/journal.pone.0006398
- Dodds, K. (1992). “*Clostridium botulinum* in the environment,” in *Clostridium Botulinum: Ecology and Control in Foods*, eds A. H. W. Hauschild and K. L. Dodds (New York, NY: Marcel Dekker), 21–52.
- Donnelly, M. L., Fimlaid, K. A., and Shen, A. (2016). Characterization of *Clostridium difficile* spores lacking either SpoVAC or DPA synthetase. *J. Bacteriol.* 198, 1694–1707. doi: 10.1128/JB.00986-15
- Eklund, M. W., and Dowell, V. R. (1987). *Avian Botulism*. Springfield, IL: Thomas.
- Francis, M. B., Allen, C. A., and Sorg, J. A. (2015). Spore cortex hydrolysis precedes dipicolinic acid release during *Clostridium difficile* spore germination. *J. Bacteriol.* 197, 2276–2283. doi: 10.1128/JB.02575-14
- Hatheway, C. L. (1988). “Botulism,” in *Laboratory Diagnosis of Infectious Diseases: Principles and Practice*, eds A. Balows, W. J. Hausler, M. Ohashi, A. Turano, and E. H. Lennette (New York, NY: Springer), 111–133.
- Hauschild, A. H. W. (1989). “*Clostridium botulinum*,” in *Foodborne Bacterial Pathogens*, ed. M. P. Doyle (New York, NY: Marcel Dekker).
- Heap, J. T., Kuehne, S. A., Ehsaan, M., Cartman, S. T., Cooksley, C. M., Scott, J. C., et al. (2010). The ClosTron: mutagenesis in *Clostridium* refined and streamlined. *J. Microbiol. Methods* 80, 49–55. doi: 10.1016/j.mimet.2009.10.018
- Heap, J. T., Pennington, O. J., Cartman, S. T., and Minton, N. P. (2009). A modular system for *Clostridium* shuttle plasmids. *J. Microbiol. Methods* 78, 79–85. doi: 10.1016/j.mimet.2009.05.004
- Hill, K. K., Xie, G., Foley, B. T., and Smith, T. J. (2015). Genetic diversity within the botulinum neurotoxin-producing bacteria and their neurotoxins. *Toxicon* 107, 2–8. doi: 10.1016/j.toxicon.2015.09.011
- Ishikawa, S., Yamane, K., and Sekiguchi, J. (1998). Regulation and characterization of a newly deduced cell wall hydrolase gene (cwl) which affects germination of *Bacillus subtilis* spores. *J. Bacteriol.* 180, 1375–1380.
- Jacobson, M. J., Lin, G., Whittam, T. S., and Johnson, E. A. (2008). Phylogenetic analysis of *Clostridium botulinum* type A by multi-locus sequence typing. *Microbiology* 154, 2408–2415. doi: 10.1099/mic.0.2008/016915-0
- Johnson, E. A. (2013). “*Clostridium botulinum*,” in *Food Microbiology: Fundamentals and Frontiers*, 4th Edn, eds M. P. Doyle and R. L. Buchanan (Washington, DC: ASM Press), 441–463.
- Johnstone, K. (1994). The trigger mechanism of spore germination: current concepts. *Soc. Appl. Bacteriol. Symp. Ser.* 23, 17S–24S. doi: 10.1111/j.1365-2672.1994.tb04354.x
- Kevorkian, Y., Shirley, D. J., and Shen, A. (2016). Regulation of *Clostridium difficile* spore germination by the CspA pseudoprotease domain. *Biochimie* 122, 243–254. doi: 10.1016/j.biochi.2015.07.023
- Korza, G., and Setlow, P. (2013). Topology and accessibility of germination proteins in the *Bacillus subtilis* spore inner membrane. *J. Bacteriol.* 195, 1484–1491. doi: 10.1128/JB.02262-12
- Krogh, A., Larsson, B., von Heijne, G., and Sonnhammer, E. L. (2001). Predicting transmembrane protein topology with a hidden Markov model: application to complete genomes. *J. Mol. Biol.* 305, 567–580. doi: 10.1006/jmbi.2000.4315

- Kruczkiewicz, P., Mutschall, S., Barker, D., Thomas, J., Van Domselaar, G., Gannon, V. P. J., et al. (2013). "MIST: a tool for rapid in silico Generation of Molecular Data from Bacterial Genome Sequences," in *Proceedings of the International Conference on Bioinformatics Models, Methods and Algorithms: Bioinformatics 2013*, Porto, 316–323. doi: 10.5220/0004249003160323
- Li, J., Chen, J., Vidal, J. E., and McClane, B. A. (2011). The Agr-like quorum-sensing system regulates sporulation and production of enterotoxin and beta2 toxin by *Clostridium perfringens* type A non-food-borne human gastrointestinal disease strain F5603. *Infect. Immun.* 79, 2451–2459. doi: 10.1128/IAI.00169-11
- Li, Y., Butzin, X. Y., Davis, A., Setlow, B., Korza, G., Ustok, F. I., et al. (2013). Activity and regulation of various forms of CwlJ, SleB, and YpeB proteins in degrading cortex peptidoglycan of spores of *Bacillus* species in vitro and during spore germination. *J. Bacteriol.* 195, 2530–2540. doi: 10.1128/JB.00259-13
- Li, Y., Davis, A., Korza, G., Zhang, P., Li, Y. Q., Setlow, B., et al. (2012). Role of a SpoVA protein in dipicolinic acid uptake into developing spores of *Bacillus subtilis*. *J. Bacteriol.* 194, 1875–1884. doi: 10.1128/JB.00062-12
- Lindström, M., Fredriksson-Ahomaa, M., and Korkeala, H. (2009). "Molecular epidemiology of group I and group II *Clostridium botulinum*," in *Clostridia, Molecular Biology in the Post-Genomic Era*, eds H. Brüggemann and G. Gottschalk (Norfolk, UK: Caister Academic Press), 103–130.
- Lindstrom, M., Nevas, M., Kurki, J., Sauna-aho, R., Latvala-Kiesila, A., Polonen, I., et al. (2004). Type C botulism due to toxic feed affecting 52,000 farmed foxes and minks in Finland. *J. Clin. Microbiol.* 42, 4718–4725. doi: 10.1128/JCM.42.10.4718-4725.2004
- McClure, P. J. (2006). "Spore-forming bacteria," in *Food Spoilage Microorganisms*, Vol. 21, ed. C. D. W. Blackburn (Sawston: Woodhead Publishing limited), 579–623.
- Meaney, C. A., Cartman, S. T., McClure, P. J., and Minton, N. P. (2015). Optimal spore germination in *Clostridium botulinum* ATCC 3502 requires the presence of functional copies of SleB and YpeB, but not CwlJ. *Aerobe* 34, 86–93. doi: 10.1016/j.aerobe.2015.04.015
- Miyata, S., Moriyama, R., Miyahara, N., and Makino, S. (1995). A gene (sleC) encoding a spore-cortex-lytic enzyme from *Clostridium perfringens* S40 spores; cloning, sequence analysis and molecular characterization. *Microbiology* 141(Pt 10), 2643–2650. doi: 10.1099/13500872-141-10-2643
- Moir, A., and Cooper, G. (2016). Spore Germination. *Microbiol. Spectr.* 3, 217–236. doi: 10.1128/microbiolspec.TBS-0014-2012
- Page, A. J., Cummins, C. A., Hunt, M., Wong, V. K., Reuter, S., Holden, M. T., et al. (2015). Roary: rapid large-scale prokaryote pan genome analysis. *Bioinformatics* 31, 3691–3693. doi: 10.1093/bioinformatics/btv421
- Paidhungat, M., Ragkousi, K., and Setlow, P. (2001). Genetic requirements for induction of germination of spores of *Bacillus subtilis* by Ca(2+)-dipicolinate. *J. Bacteriol.* 183, 4886–4893. doi: 10.1128/JB.183.16.4886-4893.2001
- Paidhungat, M., Setlow, B., Driks, A., and Setlow, P. (2000). Characterization of spores of *Bacillus subtilis* which lack dipicolinic acid. *J. Bacteriol.* 182, 5505–5512. doi: 10.1128/JB.182.19.5505-5512.2000
- Paredes-Sabja, D., Setlow, B., Setlow, P., and Sarker, M. R. (2008a). Characterization of *Clostridium perfringens* spores that lack SpoVA proteins and dipicolinic acid. *J. Bacteriol.* 190, 4648–4659. doi: 10.1128/JB.00325-08
- Paredes-Sabja, D., Setlow, P., and Sarker, M. R. (2009a). The protease CspB is essential for initiation of cortex hydrolysis and dipicolinic acid (DPA) release during germination of spores of *Clostridium perfringens* type A food poisoning isolates. *Microbiology* 155, 3464–3472. doi: 10.1099/mic.0.030965-0
- Paredes-Sabja, D., Setlow, P., and Sarker, M. R. (2009b). SleC is essential for cortex peptidoglycan hydrolysis during germination of spores of the pathogenic bacterium *Clostridium perfringens*. *J. Bacteriol.* 191, 2711–2720. doi: 10.1128/JB.01832-08
- Paredes-Sabja, D., Setlow, P., and Sarker, M. R. (2011). Germination of spores of *Bacillales* and *Clostridiales* species: mechanisms and proteins involved. *Trends Microbiol.* 19, 85–94. doi: 10.1016/j.tim.2010.10.004
- Paredes-Sabja, D., Torres, J. A., Setlow, P., and Sarker, M. R. (2008b). *Clostridium perfringens* spore germination: characterization of germinants and their receptors. *J. Bacteriol.* 190, 1190–1201. doi: 10.1128/JB.01748-07
- Peck, M. W. (2006). *Clostridium botulinum* and the safety of minimally heated, chilled foods: an emerging issue? *J. Appl. Microbiol.* 101, 556–570. doi: 10.1111/j.1365-2672.2006.02987.x
- Peck, M. W. (2009). Biology and genomic analysis of *Clostridium botulinum*. *Adv. Microb. Physiol.* 55, 320. doi: 10.1016/S0065-2911(09)05503-9
- Peck, M. W. (2010). "*Clostridium botulinum*," in *Pathogens and Toxins in Foods: Challenges and Interventions*, eds V. K. Juneja and J. N. Sofos (Washington, DC: ASM Press), 31–52.
- Peck, M. W., Goodburn, K. E., Betts, R. P., and Stringer, S. C. (2008). Assessment of the potential for growth and neurotoxin formation by non-proteolytic *Clostridium botulinum* in short shelf-life commercial foods designed to be stored chilled. *Trends Food Sci. Technol.* 19, 207–216. doi: 10.1016/j.tifs.2007.12.006
- Peck, M. W., Plowman, J., Aldus, C. F., Wyatt, G. M., Izurieta, W. P., Stringer, S. C., et al. (2010). Development and application of a new method for specific and sensitive enumeration of spores of nonproteolytic *Clostridium botulinum* types B, E, and F in foods and food materials. *Appl. Environ. Microbiol.* 76, 6607–6614. doi: 10.1128/AEM.01007-10
- Peck, M. W., and Stringer, S. C. (2005). The safety of pasteurised in-pack chilled meat products with respect to the foodborne botulism hazard. *Meat Sci.* 70, 461–475. doi: 10.1016/j.meatsci.2004.07.019
- Peck, M. W., Stringer, S. C., and Carter, A. T. (2011). *Clostridium botulinum* in the post-genomic era. *Food Microbiol.* 28, 183–191. doi: 10.1016/j.fm.2010.03.005
- Perutka, J., Wang, W. J., Goerlitz, D., and Lambowitz, A. M. (2004). Use of computer-designed group II introns to disrupt *Escherichia coli* DExH/D-box protein and DNA helicase genes. *J. Mol. Biol.* 336, 421–439. doi: 10.1016/j.jmb.2003.12.009
- Plowman, J., and Peck, M. W. (2002). Use of a novel method to characterize the response of spores of non-proteolytic *Clostridium botulinum* types B, E and F to a wide range of germinants and conditions. *J. Appl. Microbiol.* 92, 681–694. doi: 10.1046/j.1365-2672.2002.01569.x
- Punta, M., Coggill, P. C., Eberhardt, R. Y., Mistry, J., Tate, J., Boursnell, C., et al. (2012). The Pfam protein families database. *Nucleic Acids Res.* 40, D290–D301. doi: 10.1093/nar/gkr1065
- Purdy, D., O'Keeffe, T. A. T., Elmore, M., Herbert, M., McLeod, A., Bokor-Brown, M., et al. (2002). Conjugative transfer of clostridial shuttle vectors from *Escherichia coli* to *Clostridium difficile* through circumvention of the restriction barrier. *Mol. Microbiol.* 46, 439–452. doi: 10.1046/j.1365-2958.2002.03134.x
- Quevillon, E., Silventoinen, V., Pillai, S., Harte, N., Mulder, N., Apweiler, R., et al. (2005). InterProScan: protein domains identifier. *Nucleic Acids Res.* 33, W116–W120. doi: 10.1093/nar/gki442
- Ramirez-Peralta, A., Gupta, S., Butzin, X. Y., Setlow, B., Korza, G., Leyva-Vazquez, M.-A., et al. (2013). Identification of new proteins that modulate the germination of spores of *Bacillus* species. *J. Bacteriol.* 195, 3009–3021. doi: 10.1128/jb.00257-13
- Rice, P., Longden, I., and Bleasby, A. (2000). EMBOSS: the European molecular biology open software suite. *Trends Genet.* 16, 276–277. doi: 10.1016/S0168-9525(00)02044-2
- Sasaki, Y., Takikawa, N., Kojima, A., Norimatsu, M., Suzuki, S., and Tamura, Y. (2001). Phylogenetic positions of *Clostridium novyi* and *Clostridium haemolyticum* based on 16S rDNA sequences. *Int. J. Syst. Evol. Microbiol.* 51, 901–904. doi: 10.1099/00207713-51-3-901
- Sebaihia, M., Peck, M. W., Minton, N. P., Thomson, N. R., Holden, M. T., Mitchell, W. J., et al. (2007). Genome sequence of a proteolytic (Group I) *Clostridium botulinum* strain Hall A and comparative analysis of the clostridial genomes. *Genome Res.* 17, 1082–1092. doi: 10.1101/gr.628207
- Seemann, T. (2014). Prokka: rapid prokaryotic genome annotation. *Bioinformatics* 30, 2068–2069. doi: 10.1093/bioinformatics/btu153
- Setlow, B., Peng, L., Loshon, C. A., Li, Y. Q., Christie, G., and Setlow, P. (2009). Characterization of the germination of *Bacillus megaterium* spores lacking enzymes that degrade the spore cortex. *J. Appl. Microbiol.* 107, 318–328. doi: 10.1111/j.1365-2672.2009.04210.x
- Setlow, P. (2014). Germination of spores of *Bacillus* species: what we know and do not know. *J. Bacteriol.* 196, 1297–1305. doi: 10.1128/JB.01455-13
- Sharpe, A. E., Brady, C. P., Byrne, W., Moriarty, J., O'Neill, P., and McLaughlin, J. G. (2008). Major outbreak of suspected botulism in a dairy herd in the Republic of Ireland. *Vet. Rec.* 162, 409–412. doi: 10.1136/vr.162.13.409
- Sims, G. E., Jun, S. R., Wu, G. A., and Kim, S. H. (2009). Alignment-free genome comparison with feature frequency profiles (FFP) and optimal resolutions. *Proc. Natl. Acad. Sci. U.S.A.* 106, 2677–2682. doi: 10.1073/pnas.0813249106

- Skarin, H., and Segerman, B. (2014). Plasmidome interchange between *Clostridium botulinum*, *Clostridium novyi* and *Clostridium haemolyticum* converts strains of independent lineages into distinctly different pathogens. *PLoS ONE* 9:e107777. doi: 10.1371/journal.pone.0107777
- Stringer, S. C., Carter, A. T., Webb, M. D., Wachnicka, E., Crossman, L. C., Sebaihia, M., et al. (2013). Genomic and physiological variability within Group II (non-proteolytic) *Clostridium botulinum*. *BMC Genomics* 14:333. doi: 10.1186/1471-2164-14-333
- Takeshi, K., Ando, Y., and Oguma, K. (1988). Germination of Spores of *Clostridium botulinum* Type-G. *J. Food Prot.* 51, 37–38.
- Tamura, K., Peterson, D., Peterson, N., Stecher, G., Nei, M., and Kumar, S. (2011). MEGA5: molecular evolutionary genetics analysis using maximum likelihood, evolutionary distance, and maximum parsimony methods. *Mol. Biol. Evol.* 28, 2731–2739. doi: 10.1093/molbev/msr121
- Taylor, R. H., Dunn, M. L., Ogden, L. V., Jefferies, L. K., Eggett, D. L., and Steele, F. M. (2013). Conditions associated with *Clostridium sporogenes* growth as a surrogate for *Clostridium botulinum* in nonthermally processed canned butter. *J. Dairy Sci.* 96, 2754–2764. doi: 10.3168/jds.2012-6209
- Tovar-Rojo, F., Chander, M., Setlow, B., and Setlow, P. (2002). The products of the spoVA operon are involved in dipicolinic acid uptake into developing spores of *Bacillus subtilis*. *J. Bacteriol.* 184, 584–587. doi: 10.1128/JB.184.2.584-587.2002
- Treangen, T. J., Ondov, B. D., Koren, S., and Phillippy, A. M. (2014). The Harvest suite for rapid core-genome alignment and visualization of thousands of intraspecific microbial genomes. *Genome Biol.* 15, 524. doi: 10.1186/PREACCEPT-2573980311437212
- van Vliet, A. H., and Kusters, J. G. (2015). Use of alignment-free phylogenetics for rapid genome sequence-based typing of *Helicobacter pylori* virulence markers and antibiotic susceptibility. *J. Clin. Microbiol.* 53, 2877–2888. doi: 10.1128/JCM.01357-15
- Velasquez, J., Schuurman-Wolters, G., Birkner, J. P., Abree, T., and Poolman, B. (2014). *Bacillus subtilis* spore protein SpoVAC functions as a mechanosensitive channel. *Mol. Microbiol.* 92, 813–823. doi: 10.1111/mmi.12591
- Weigand, M. R., Pena-Gonzalez, A., Shirey, T. B., Broeker, R. G., Ishaq, M. K., Konstantinidis, K. T., et al. (2015). Implications of genome-based discrimination between *Clostridium botulinum* Group I and *Clostridium sporogenes* strains for bacterial taxonomy. *Appl. Environ. Microbiol.* 81, 5420–5429. doi: 10.1128/AEM.01159-15
- Williamson, C. H., Sahl, J. W., Smith, T. J., Xie, G., Foley, B. T., Smith, L. A., et al. (2016). Comparative genomic analyses reveal broad diversity in botulinum-toxin-producing Clostridia. *BMC Genomics* 17:180. doi: 10.1186/s12864-016-2502-z
- Woudstra, C., Le Marechal, C., Souillard, R., Bayon-Auboyer, M. H., Mermoud, I., Desoutter, D., et al. (2015). Draft genome sequences of 17 French *Clostridium botulinum* Group III strains. *Genome Announc.* 3:e01105-15. doi: 10.1128/genomeA.01105-15
- Yi, X., and Setlow, P. (2010). Studies of the commitment step in the germination of spores of bacillus species. *J. Bacteriol.* 192, 3424–3433. doi: 10.1128/JB.00326-10

Conflict of Interest Statement: The authors declare that the research was conducted in the absence of any commercial or financial relationships that could be construed as a potential conflict of interest.

Copyright © 2016 Brunt, van Vliet, van den Bos, Carter and Peck. This is an open-access article distributed under the terms of the Creative Commons Attribution License (CC BY). The use, distribution or reproduction in other forums is permitted, provided the original author(s) or licensor are credited and that the original publication in this journal is cited, in accordance with accepted academic practice. No use, distribution or reproduction is permitted which does not comply with these terms.



Identification of Differentially Expressed Genes during *Bacillus subtilis* Spore Outgrowth in High-Salinity Environments Using RNA Sequencing

Katja Nagler¹, Antonina O. Krawczyk², Anne De Jong², Kazimierz Madela³, Tamara Hoffmann⁴, Michael Laue³, Oscar P. Kuipers², Erhard Bremer⁴ and Ralf Moeller^{1*}

¹ Space Microbiology Research Group, Radiation Biology Department, Institute of Aerospace Medicine, German Aerospace Center, Cologne, Germany, ² Department of Molecular Genetics, Groningen Biomolecular Sciences and Biotechnology Institute, University of Groningen, Groningen, Netherlands, ³ Advanced Light and Electron Microscopy, Center for Biological Threats and Special Pathogens, Robert Koch Institute, Berlin, Germany, ⁴ Laboratory of Microbiology, Department of Biology, Philipps-University Marburg, Marburg, Germany

OPEN ACCESS

Edited by:

Imrich Barak,
Slovak Academy of Sciences, Slovakia

Reviewed by:

Claes Von Wachenfeldt,
Lund University, Sweden

Kai Papenfort,
Ludwig-Maximilians Universität,
Germany

*Correspondence:

Ralf Moeller
ralf.moeller@dlr.de

Specialty section:

This article was submitted to
Microbial Physiology and Metabolism,
a section of the journal
Frontiers in Microbiology

Received: 21 July 2016

Accepted: 20 September 2016

Published: 06 October 2016

Citation:

Nagler K, Krawczyk AO, De Jong A, Madela K, Hoffmann T, Laue M, Kuipers OP, Bremer E and Moeller R (2016) Identification of Differentially Expressed Genes during *Bacillus subtilis* Spore Outgrowth in High-Salinity Environments Using RNA Sequencing. *Front. Microbiol.* 7:1564.
doi: 10.3389/fmicb.2016.01564

In its natural habitat, the soil bacterium *Bacillus subtilis* often has to cope with fluctuating osmolality and nutrient availability. Upon nutrient depletion it can form dormant spores, which can revive to form vegetative cells when nutrients become available again. While the effects of salt stress on spore germination have been analyzed previously, detailed knowledge on the salt stress response during the subsequent outgrowth phase is lacking. In this study, we investigated the changes in gene expression during *B. subtilis* outgrowth in the presence of 1.2 M NaCl using RNA sequencing. In total, 402 different genes were upregulated and 632 genes were downregulated during 90 min of outgrowth in the presence of salt. The salt stress response of outgrowing spores largely resembled the osmospecific response of vegetative cells exposed to sustained high salinity and included strong upregulation of genes involved in osmoprotectant uptake and compatible solute synthesis. The σ^B -dependent general stress response typically triggered by salt shocks was not induced, whereas the σ^W regulon appears to play an important role for osmoadaptation of outgrowing spores. Furthermore, high salinity induced many changes in the membrane protein and transporter transcriptome. Overall, salt stress seemed to slow down the complex molecular reorganization processes ("ripening") of outgrowing spores by exerting detrimental effects on vegetative functions such as amino acid metabolism.

Keywords: *B. subtilis* spore germination, outgrowth, ripening, high salinity, osmotic stress, NaCl, RNA-seq

INTRODUCTION

In its natural habitat, the soil bacterium *Bacillus subtilis* is frequently confronted with fluctuating environmental conditions and has therefore evolved a broad range of elaborate stress responses (Marles-Wright and Lewis, 2007, 2010; Lopez et al., 2009; Schultz et al., 2009). Two common environmental stresses in soil are changes in osmolality and limitation of nutrient availability (Wood et al., 2001; Bremer, 2002; Nicholson, 2002).

When soil desiccation creates hyperosmotic conditions, cells have to adjust their internal osmolality to avoid water efflux and plasmolysis (Wood et al., 2001; Hoffmann and Bremer, 2016). In a first response, *B. subtilis* cells quickly take up large amounts of K⁺ via the KtrAB and KtrCD transport systems to restore internal osmotic pressure (Whatmore et al., 1990; Holtmann et al., 2003). However, prolonged high intracellular K⁺ concentrations are not compatible with various cellular functions (Whatmore et al., 1990; Record et al., 1998). Therefore, *B. subtilis* subsequently replaces K⁺ by compatible solutes, highly soluble organic compounds that do not disturb cell physiology, to adjust its intracellular osmotic potential (Whatmore et al., 1990; Kempf and Bremer, 1998). Compatible solutes can either be synthesized (*de novo* or from precursors) or taken up from the environment via five osmotically inducible osmoprotectant uptake transporters (OpuA, OpuB, OpuC, OpuD, OpuE) that differ in their affinities and substrate specificities (Kempf and Bremer, 1998; Hoffmann and Bremer, 2016). The most important compatible solutes for *B. subtilis* are glycine betaine (GB) and proline (Hoffmann and Bremer, 2016).

Depending on how salt stress is imposed, *B. subtilis* cells can react in distinct manners (Spiegelhalter and Bremer, 1998; Steil et al., 2003; Young et al., 2013). When *B. subtilis* is subjected to a sudden osmotic up-shock, the σ^B-governed general stress response is activated (Spiegelhalter and Bremer, 1998; Nannapaneni et al., 2012; Young et al., 2013). In contrast, upon incremental and sustained salt stress, cells activate a specific osmotic stress response under the regulation of the house-keeping sigma factor σ^A (Spiegelhalter and Bremer, 1998; Steil et al., 2003; Young et al., 2013; Hoffmann and Bremer, 2016). Nevertheless, it is still not understood how increases in the environmental osmolality are perceived and how this information is processed to adjust gene expression according to the cells' needs (Hoffmann and Bremer, 2016).

A different strategy of *B. subtilis* to cope with environmental (albeit not osmotic) stress is sporulation: upon nutrient depletion *B. subtilis* can form dormant spores that are highly resistant against a broad range of environmental extremes such as heat, desiccation, and chemicals (Ruzal et al., 1998; Nicholson et al., 2000; Setlow, 2006, 2013). A dormant spore consists of a dehydrated spore core (analogous to a growing cell's protoplast) that is enveloped by a dense inner membrane, a germ cell wall, a cortex, and a proteinaceous spore coat (Setlow, 2006). Although spores can remain dormant for extended periods of time, they can convert back to vegetative cells via a process called germination when nutrients become available (Nicholson, 2002; Setlow, 2013). Throughout germination, spores release ions and Ca²⁺-dipicolinate (Ca²⁺-DPA), hydrolyze their cortex, and rehydrate, which causes the loss of their refractivity and resistance properties (reviewed in Setlow, 2013). After germination is completed, the former spores enter a phase called

outgrowth, which is defined as the time period between the onset of metabolic activity and the first cell division (Setlow, 2003; Keijser et al., 2007). Throughout outgrowth the germinated spores undergo molecular reorganization ("ripening"), escape from their spore coats, and elongate (Keijser et al., 2007; Segev et al., 2013; Setlow, 2013; Sinai et al., 2015). Important events in early outgrowth are the generation of ATP, nucleotides, and amino acids from endogenous resources, as well as the onset of macromolecular synthesis (Paidhungat and Setlow, 2002; Setlow, 2003; Keijser et al., 2007; Sinai et al., 2015). On the genomic level, the importance of σ^A as well as the temporal activation of at least 30% of all *B. subtilis* genes during a well-regulated spore outgrowth program have been reported (Horsburgh et al., 2001; Keijser et al., 2007). Correspondingly, outgrowing spores synthesize more than 650 different proteins before entering vegetative growth (Sinai et al., 2015).

While the effects of high salinity on *B. subtilis* spore germination have been analyzed previously (Nagler et al., 2014, 2015; Nagler and Moeller, 2015), detailed knowledge on the salt stress response during the subsequent outgrowth phase, especially on a transcriptomic level, is lacking. Therefore, we investigated changes in the gene expression profile of outgrowing *B. subtilis* spores in the presence of 1.2 M NaCl by RNA sequencing (RNA-seq). A key result of our study was the observation that the transcriptional profile of salt-stressed outgrowing spores exhibits many similarities to continuously salt-stressed vegetative cells, whereas the σ^B-controlled general stress regulon was not engaged.

MATERIALS AND METHODS

Spore Production and Purification

Spores of *B. subtilis* 168 (*trpC2*; DSM402) were produced in liquid cultures of modified Schaeffer's Sporulation Medium with glucose (2x SG; as described in Nicholson and Setlow, 1990). All chemicals were ordered from Sigma-Aldrich (St. Louis, MO, USA). The sporulation cultures were incubated at 37°C for 48 h in a shaking incubator (200 rpm). Spores were harvested, washed with distilled, sterile water at least seven times, and retrieved by centrifugation. The purity of the spore stocks, as checked by phase-contrast microscopy, was ≥99%. Spores were stored in distilled water in screw-capped glass tubes at 4°C until use.

Spore Germination and Outgrowth Experiments

Spores were heat activated at 70°C for 30 min in order to ensure synchronized germination. Germination and outgrowth experiments were performed in germination media composed of Spizizen Minimal Medium (SMM; as described in Nicholson and Setlow, 1990) with or without 1.2 M NaCl, which additionally contained 50.5 mM D-glucose, 0.5 mM L-tryptophan, and 10 mM of the germination trigger L-alanine.

The transcriptomics outgrowth experiments were performed in 45 ml germination medium (500 ml flasks). The medium was inoculated with 1.2×10^{10} heat-activated spores (in total) and 15 ml samples were withdrawn at 30, 60, and 90 min after inoculation. The samples were immediately mixed with ice-cold

Abbreviations: 2x SG, Modified Schaeffer's Sporulation Medium with glucose; DPA, Dipicolinic acid (pyridine-2,6-dicarboxylic acid); FC, Fold change; GB, Glycine betaine; OD_{600 nm}, Optical density at 600 nm; RNA-seq, RNA sequencing; SASP, Small, acid-soluble spore protein; SEM, Scanning electron microscopy; SMM, Spizizen Minimal Medium.

killing buffer (Nicolas et al., 2012) and washed with ice cold water by centrifugation (1 min at 10,000 $\times g$ at 4°C). The pellet was resuspended in 400 μl ice-cold LETS buffer (0.1 M LiCl, 0.01 M Na₂EDTA, 0.1 M Tris-HCl pH 7.4, 0.2% SDS), transferred to a pre-cooled Lysing Matrix B tube (MP Biomedicals, Santa Ana, CA, USA) containing 500 μl phenol:chloroform (1:1) and 25 μl 10% SDS, and used for RNA isolation. For the dormant spore RNA samples, spore suspensions were also heat-treated for consistency. Subsequently they were centrifuged, the pellets were resuspended in LETS buffer, and transferred to Lysing Matrix B tube for RNA isolation. The transcriptomics outgrowth experiments were performed in duplicate using two independent spore batches.

For spectrophotometric measurements, germination was carried out in triplicate in 96-well plates, each containing 200 μl of germination media. Each well was inoculated with 40 μl heat-activated spores to a starting optical density of ca. 0.5 at 600 nm (OD_{600nm}) corresponding to a total of ca. 4×10^7 spores per well. The plate was incubated at 37°C in a multi-plate reader (ELx808IU, BioTek, Bad Friedrichshall, Germany) that read the OD_{600nm} of the culture, with 5 s of shaking before all readings. The OD_{600nm} data was normalized by division of each reading by the first measured value (t_{0min}), yielding the relative OD_{600nm} given in %. A 60% decrease in relative OD_{600nm} corresponds to germination of the whole spore population (Atluri et al., 2006; Nagler et al., 2014).

Microscopy

For scanning electron microscopy (SEM) of outgrowing spores, dormant spores were germinated as described above. Samples were withdrawn 30, 60, and 90 min after germination initiation, washed with distilled water and fixed in 2.5% glutaraldehyde. Fixed samples were washed with distilled water, adsorbed to an Alcian blue-coated cover slip, and stored in 2.5% glutaraldehyde (in 0.05 M HEPES) overnight. Then, samples were washed with distilled water, treated with 1% osmium, washed again, dehydrated with increasing concentrations of ethanol, and dried by critical-point drying (Emitech K850, UK). Dried samples were sputter-coated with 3 nm Au/Pd (Polaron E5100) and analyzed by SEM (Gemini 1530, Carl Zeiss Microscopy GmbH, Germany) using an acceleration voltage of 5 kV and the in-lens secondary electron detector.

For live cell imaging of individual spores, dormant spores were dried in a plastic dish (μ -dish, ibidi, Germany). The dried spores were covered with germination medium (as described above) that was solidified with 1.5% agarose. Germination and outgrowth were observed by phase-contrast with a Nikon TE2000-E Eclipse microscope and a Plan Fluor 100/1.3 Oil objective. Photos were taken every 5 s and merged into time-lapse videos. Germination parameters (starting time of change from bright to dark and duration of change) were determined using ImageJ (Rasband, 1997) and are given as median-values (with spore counts ranging from 74 to 124 spores per condition) in **Figure 1B**.

To monitor germination by phase-contrast microscopy, spores were germinated in 96-well plates as described above. At appropriate time points, 5 μl samples were withdrawn and fixed by applying to a microscope slide coated with 1% agar.

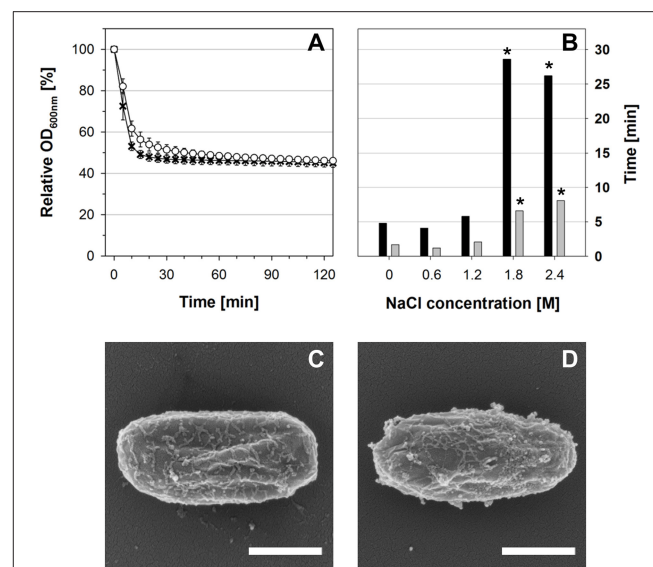


FIGURE 1 | (A) Spore germination and outgrowth profiles in SMM supplemented with glucose, L-tryptophan, and L-alanine as measured by OD_{600nm} . The medium contained either 1.2 M NaCl (white circles) or no NaCl (black crosses). **(B)** Single-spore live cell imaging analyses. The times required for start of refractivity loss (black bars) and duration of refractivity loss (gray bars) at different NaCl concentrations are shown as median-values ($n \geq 74$ spores). Asterisks indicate significant ($p \leq 0.01$) differences to the values at 0 M NaCl. **(C,D)** SEM pictures 90 min after germination initiation **(C)** in the absence of NaCl or **(D)** in the presence of 1.2 M NaCl. Scale bars = 500 nm.

Micrographs were taken using a Zeiss fluorescence microscope (Axio Imager M2, Carl Zeiss MicroImaging GmbH, Germany) equipped with an AxioCam MRm.

RNA Isolation

RNA isolation was performed with a phenol-chloroform extraction method as follows. The samples (in Lysing Matrix B tubes, see above) were immediately disrupted using a FastPrep device (Eubio, Austria), with four subsequent disruptions (45 s at 6.5 m/s) separated by 1–2 min incubation on ice to avoid overheating. After disruption, samples were centrifuged at 4°C and the supernatant was mixed with chloroform. After centrifugation at 4°C, the RNA was precipitated by 0.3 M sodium acetate (pH 5.3) in isopropanol for 3 h on ice. The pellet was washed with 70% ethanol, dried, resuspended in nuclease-free water, and treated with a RNase-free DNase Set (Qiagen, Hilden, Germany) according to the manufacturer's manual (incubation for 1 h at 37°C). The treated samples were diluted with nuclease-free water and mixed with the same amount of phenol:chloroform:isoamylalcohol (25:24:1). After centrifugation at 4°C, the RNA was precipitated by 0.3 M sodium acetate (pH 5.3) in isopropanol overnight at 4°C. The pellet was washed with 70% ethanol, dried, and resuspended in 50 μl nuclease-free water.

RNA Sequencing and Data Analyses

RNA concentration of the samples was quantified using a NanoDrop 2000c instrument (Wilmington, DE, USA). Sample

quality was determined with an Agilent 2100 Bioanalyzer and an Agilent RNA 6000 Nano Kit (Agilent Technologies, Waldbronn, Germany) according to the manufacturer's manual. The samples were stored at -80°C until analysis. RNA-seq was performed by the PrimBio Research Institute (Exton, PA, USA). The obtained raw data containing 4391 genes were then subjected to analyses using the webserver-based RNA-seq analysis pipeline T-Rex as described by De Jong et al. (2015). Unless noted otherwise, the transcriptomics data are expressed as the contrast of the RNA that was present in outgrowing spores in the presence of NaCl ("target") against RNA in the absence of NaCl ("control"). T-Rex includes two different significance thresholds termed "TopHits" [\log_2 fold change ($\log_2\text{FC}$) ≥ 2 and $p \leq 0.05$] and "HighFold" ($\log_2\text{FC} \geq 5$ and a $p \leq 0.01$); unless noted otherwise TopHits values are shown. Additionally, the transcriptomics data was analyzed in JBrowse 1.11.6 (Skinner et al., 2009). Hierarchical clustering of transcription profiles was performed with the TIGR Multiexperiment Viewer (MeV, <http://mev.tm4.org/>). Functional categorization was performed according to the SubtiWiki platform (<http://www.subtiwiki.uni-goettingen.de>; Mäder et al., 2012; Michna et al., 2016). The RNA-seq data was deposited in the Gene Expression Omnibus (GEO) database (<http://www.ncbi.nlm.nih.gov/geo/>) under the accession number GSE81238.

RESULTS AND DISCUSSION

Spore Germination and Outgrowth at High Salinity

B. subtilis spore germination at high salinity has previously been investigated (Nagler et al., 2014, 2015; Nagler and Moeller, 2015), but only little is known about the effects of salt stress on the transcriptional profile of outgrowing spores. In our study, spores of *B. subtilis* 168 were germinated with L-alanine in minimal medium containing either no NaCl or 1.2 M NaCl. This salt concentration was chosen in accordance with former studies on the salt stress response in vegetative *B. subtilis* cells and studies on *B. subtilis* spore germination at high salinity (Boch et al., 1994; Steil et al., 2003; Nagler et al., 2014, 2015, 2016).

In agreement with previous results (Nagler et al., 2014), the OD_{600nm} decrease of the germination culture that corresponds to germination was slightly slower in the presence of 1.2 M NaCl, but ultimately almost the complete spore population germinated successfully within 30 min (Figure 1A). Due to the low nutrient-content in the minimal medium, no growth could be observed by OD_{600nm} and phase-contrast microscopy within 2 h (Figure 1A and data not shown). Single-spore live cell imaging and student's *t*-test analysis showed that neither the starting time of the change from highly refractive to dark nor the duration of this refractivity change were significantly different in the presence or absence of 1.2 M NaCl (Figure 1B). In contrast, both processes were significantly prolonged at NaCl concentrations ≥ 1.8 M. Furthermore, phase-contrast microscopy and SEM revealed that stressed and non-stressed outgrowing spores had essentially the same morphology at all sample time points (30, 60, 90 min) of

the transcriptomics experiment and were still encased in their spore coats after 90 min, thus resembling dormant spores by SEM (Figures 1C,D; Figure S1, and data not shown). This indicates that the spores germinated under both conditions were in their ripening phase of outgrowth, throughout which the outgrowing spores undergo molecular reorganization, but do not exhibit morphological changes (Segev et al., 2013). Altogether these data show that the transcriptomes of outgrowing spores in the presence and absence of 1.2 M NaCl can be compared to each other and reflect the impact of NaCl on gene expression within the ripening phase of outgrowth.

Dormant Spore RNA

Dormant spores contain RNA, including sporulation- and spore-related transcripts that are remnants from the spore formation process (e.g., Keijser et al., 2007; Segev et al., 2012; Bassi et al., 2016). This RNA can be degraded during early outgrowth, thus serving as a ribonucleotide reservoir for *de novo* RNA synthesis (Setlow and Kornberg, 1970; Keijser et al., 2007; Segev et al., 2012). Other transcripts may have a functional relevance, potentially being rapidly translated at the beginning of spore revival (Keijser et al., 2007; Segev et al., 2013; Sinai et al., 2015). Preliminary microarray data have suggested that degradation of spore-related RNA may be slower during outgrowth under salt stress, thereby falsely indicating these genes as "upregulated" under stress conditions (Nagler, 2012). Hence, to allow for discrimination of RNA that is newly transcribed during outgrowth from the dormant spore transcripts and to investigate the composition of the dormant spore transcriptome, we analyzed the RNA content of dormant spores.

Overall, 955 common transcripts were detected in dormant spore samples of two independent spore batches, albeit partially with low abundance (GSE81238). Yet, a high consistency of transcripts with high abundance among the two samples and a notable overlap with previous studies (Keijser et al., 2007; Segev et al., 2013) suggest that the RNA content of dormant spores was not random. In total, we found 21 out of the 25 mostly sporulation- or spore-specific transcripts that were detected by Keijser et al. (2007), as well as 103 out of 369 different dormant spore transcripts reported by Segev et al. (2012). The latter overlap of ca. 35% can still be considered substantial, regarding the different genetic background (PY79 vs. 168) and various differences in the experimental setup.

Out of the 955 detected common dormant spore transcripts, $\sim 25\%$ encode membrane proteins with one-third thereof coding for transporters (Figure 2). Another prevalent group of dormant spore RNAs detected is involved in information processing (34%), especially in proteins synthesis, modification and degradation (216 transcripts). About half of these 216 transcripts were tRNA and tRNA-related genes, which had the overall highest abundances in both replicates. The tRNA reservoir may facilitate a rapid start of translation after germination is completed. Furthermore, 106 mRNAs belong to the "Coping with stress" functional category, one-third of which is a part of the σ^B regulon (Figure 2). If indeed translated, they may play an important role during outgrowth under

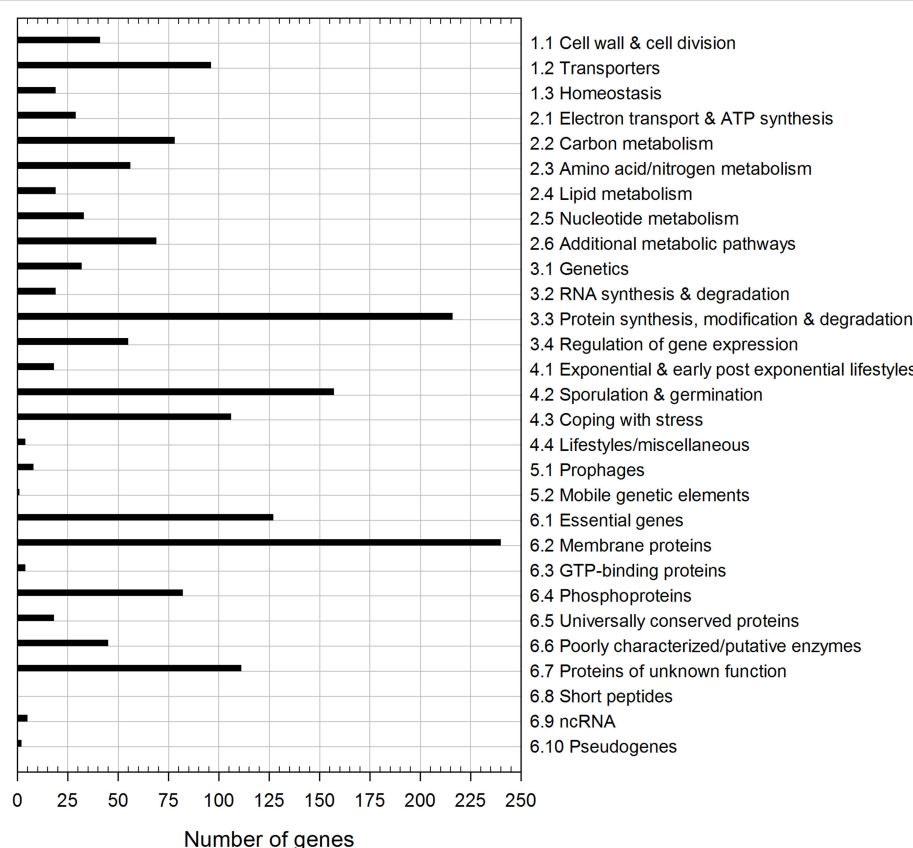


FIGURE 2 | Functional classification of dormant spore transcripts. The 955 transcripts common to both dormant spore replicates were categorized according to SubtiWiki (<http://subtiwiki.uni-goettingen.de>).

suboptimal conditions. Besides, 157 dormant spore transcripts encode proteins for sporulation and germination, including the highly abundant mRNAs for small acid-soluble spore proteins (SASPs). These mRNAs are most likely residues from sporulation and might support outgrowth by providing nucleotides for *de novo* RNA synthesis (Setlow and Kornberg, 1970; Keijser et al., 2007). Finally, in agreement with previous reports (Segev et al., 2012; Bassi et al., 2016), many dormant spore RNAs (partially with very high abundance, e.g., *ytzL*, *yrzQ*, and *ypzG*) code for proteins of unknown function, whose characterization could yield new insights into sporulation and/or spore composition.

Differential Gene Expression during Outgrowth at High Salinity

To investigate the impact of salt stress on the ripening phase of outgrowth, RNA was extracted 30, 60, and 90 min after the initiation of germination in the absence and presence of 1.2 M NaCl. The RNA was subjected to RNA-seq and the results were evaluated using the T-REx analysis pipeline (De Jong et al., 2015). T-REx offers two different significance thresholds, i.e., “TopHits” ($\log_2 FC \geq 2, p \leq 0.05$) and “HighFold” ($\log_2 FC \geq 5, p \leq 0.01$), but unless noted otherwise, TopHits-values are shown (in the following paragraph, the respective HighFold-values are given in parentheses). In all cases, the RNA-seq data obtained from

outgrowth in the presence of NaCl was contrasted against the data from outgrowth in the absence of NaCl.

In total, 402 (85) genes were upregulated and 632 (190) genes were downregulated during outgrowth in the presence of 1.2 M NaCl (Table 1). At all investigated time points, the transcriptomes of dormant spores, salt-stressed outgrowing spores, and non-salt-stressed outgrowing spores were clearly distinct from each other according to principal component analysis (Figure S2). The strongest alteration of gene expression caused by the presence of NaCl was detected at 30 min of outgrowth (Table 1; Figure S2). This may be due to major salt stress response and adaptation processes occurring at this time point. In addition, high salinity might have postponed the molecular reorganization processes of early outgrowth in a similar manner as it causes a reduced growth rate of vegetative cells (Boch et al., 1994; Hahne et al., 2010). In any case, the transcriptomes of stressed vs. non-stressed outgrowing spores became more similar over time, as indicated by the lower number of differentially expressed genes in the 60 and 90 min samples (Table 1). Consistently, the 30 min transcriptome contained much more genes that were exclusively differentially expressed at this time point than the 60 and 90 min transcriptomes (Table 2). Yet, 134 (76) genes were differentially expressed at all three time points of outgrowth under salt stress (Table 2).

TABLE 1 | Differentially expressed genes during outgrowth in the presence of 1.2 M NaCl^a.

Time (min) ^b	TopHits		HighFold	
	$\log_2\text{FC} \geq 2; p \leq 0.05$		$\log_2\text{FC} \geq 5; p \leq 0.01$	
	Upregulated	Downregulated	Upregulated	Downregulated
30	321	523	64	153
60	157	184	41	25
90	118	161	31	38
Total	402	632	85	190

^aGene expression in the presence of 1.2 M NaCl was contrasted against gene expression in the absence of NaCl at each respective time point.

^bTime of sample withdrawal after mixing spores with germinants.

For functional interpretation, differentially expressed genes were categorized according to the SubtiWiki database (Mäder et al., 2012; Michna et al., 2016). Strong alterations of gene expression—at all-time points and in both directions—could be observed in the functional categories “Membrane proteins” (category number 6.2, see **Figure 3**), “Transporters” (1.2), “Coping with stress” (4.3), and “Proteins of unknown function” (6.7) (**Figure 3**; Tables S1, S2; Database S1). To a lesser extent and predominantly after 30 min outgrowth, genes belonging to the functional categories “Protein synthesis, modification and degradation” (3.3), “Regulation of gene expression” (3.4), and “Essential genes” (6.1) were also notably differentially expressed (**Figure 3**; Tables S1, S2; Database S1). While most enriched categories exhibited similar extents of up- and downregulation, genes in the categories “Amino acid/nitrogen metabolism” (2.3), “Additional metabolic pathways” (2.6), and “Phosphoproteins” (6.4) were greatly downregulated (**Figure 3**; Tables S1, S2; Database S1). This might relate to the aforementioned potential high-salinity-dependent retardation of the molecular reorganization processes during the ripening period and/or the reallocation of cellular resources toward salt stress response. The most relevant functional categories and groups are discussed in detail below.

Hyperosmotic Stress Response

The functional category “Coping with hyperosmotic stress” includes genes encoding proteins involved in the specific hyperosmotic stress response, i.e., all Opu transporters (OpuA–OpuE); the K⁺ uptake systems KtrAB and KtrCD; GbsA, GbsB, and GbsR required for GB synthesis from the precursor choline; ProA, ProH, and ProJ responsible for osmoadaptive proline synthesis; and the amino-peptidases PapA and PapB that can degrade proline-containing peptides (Boch et al., 1994, 1996; Kempf and Bremer, 1998; Holtmann et al., 2003; Brill et al., 2011a; Zaprasis et al., 2013). In our study, 20 of the 25 genes in this category were differentially expressed (**Figure 4A**). No significant differential expression was detected for *ktrC*, *ktrD*, *papA*, *papB*, and *opuBC* (Dataset S1). Seventeen of the twenty differentially expressed genes were upregulated, including the operons *proHJ*, *gbsAB*, *opuA*,

TABLE 2 | Cohesion of contrasts: specific and shared differentially expressed genes among the sample time points.

30 min	60 min	90 min	Sample time point(s)		Number of genes ^a	
			TopHits	HighFold	TopHits	HighFold
			564	329		
			90	54		
			68	44		
			93	42		
			24	15		
			53	30		
			134	76		

^aThe numbers of genes are either specific to the time point (only one gray-filled box), or shared exclusively by the time points indicated by gray fills.

opuB (except *opuBC*), *opuC*, and the genes *gbsR*, *opuD*, and *opuE* (**Figure 4A**). All of these genes encode proteins involved in uptake and synthesis of osmoprotectants, which play a central role in the hyperosmotic stress response of vegetative *B. subtilis* cells (Kempf and Bremer, 1998; Bremer, 2002). Our results indicate that the same genes have an important function in the salt stress response of outgrowing spores as well.

In agreement with previous reports, salt-stressed induced upregulation of *opu* genes was already very strong after 30 min of outgrowth (**Figure 4A**) and was independent of the transporters’ substrate availability (as no substrates were in the medium), reflecting their osmotic control (Hahne et al., 2010). It should be noted that *opuBC* from the *opuB* operon was likewise upregulated (around 2.5 log₂FC; Dataset S1), but the difference may not have been significant as *opu* genes are reportedly also expressed to some extent in non-stressed outgrowing spores (Keijser et al., 2007). Interestingly, the different *opu* operons had variable temporal expression patterns (**Figure 4A**): *opuD* was only significantly upregulated at 30 min and expression of *opuC* also peaked at 30 min and was only moderately upregulated later. In contrast, *opuA* and *opuE* exhibited continuous high expression at all-time points. With regard to previous studies, the observed differential temporal expression patterns could be interpreted as follows.

During vegetative growth, *opuA* expression is elaborately balanced with the extent of the cell’s internal solute pool, as sufficient intracellular amounts of osmoprotectants repress *opuA* transcription (Hoffmann et al., 2013). Thus, steady upregulation of the *opuA* operon during outgrowth at high salinity indicates that the outgrowing spores were not able to accumulate sufficient amounts of compatible solutes throughout the whole experiment (**Figure 4A**). Moreover, steady expression of *opuE*, which has a σ^A- as well as a σ^B-dependent promoter, is mediated by σ^A during sustained salt stress (Spiegelhalter and Bremer, 1998). Therefore, the observed steady upregulation of *opuE* in our study suggests that the osmospecific stress response governed by σ^A is important for the salt stress adaptation during outgrowth. While the early, transient upregulation of *opuD*, which is also controlled by both σ^A and σ^B promoters, would rather resemble σ^B-dependent transcription, a similar pattern was detected for

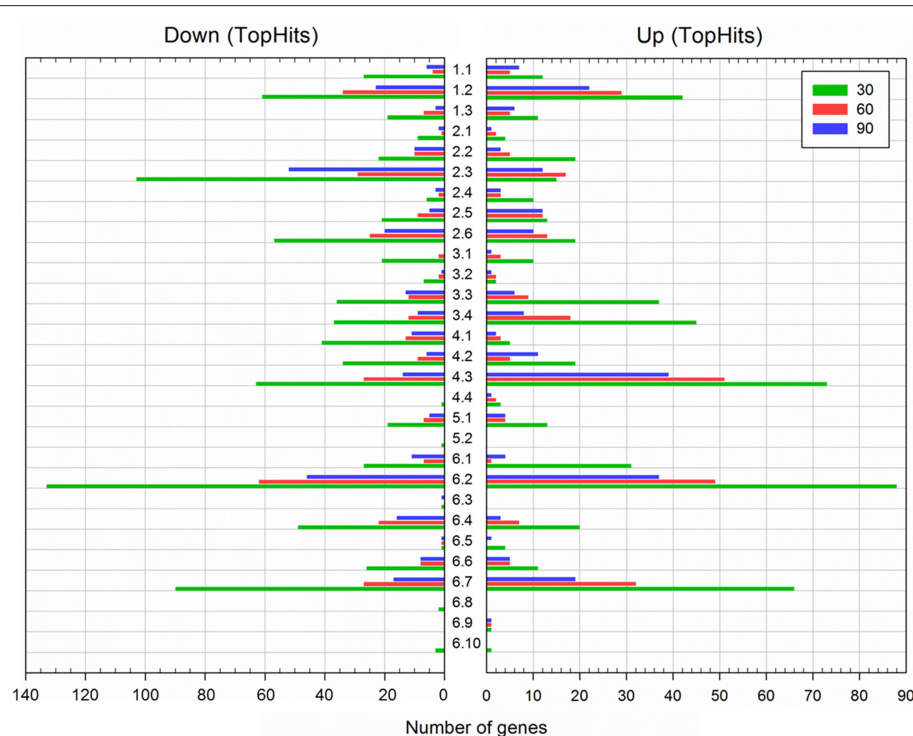


FIGURE 3 | Functional classification of differentially expressed genes during spore outgrowth in the presence of 1.2 M NaCl (TopHits). Genes were categorized according to SubtWiki (<http://subtwiki.uni-goettingen.de>). Sample time points: 30 min (green), 60 min (red), and 90 min (blue).

the *opuC* operon that is not a member of the σ^B -regulon (Spiegelhalter and Bremer, 1998; Hoffmann and Bremer, 2011; Young et al., 2013). At least in part, the transient upregulation of *opuD* and the *opuC* operon was due to an incremental transcription in non-stressed outgrowing spores (GSE81238). Furthermore, *opuC* transcription might have been affected by its repressor *opcR*: although the biological function of this *gbsR*-type repressor is still unknown (Lee et al., 2013), its expression pattern was strikingly similar to that of the *opuC* operon (Figure 4A).

Compared to the other *opu* genes, upregulation of the *opuB* genes was more variable; the overall expression levels, however, were comparably low (Figure 4A; GSE81238). Nevertheless, *opuB* transcription may likewise have been modulated by the repressor GbsR, which regulates choline uptake (via OpuB) and processing to GB (via GbsA and GbsB), and expression of which was upregulated as well during outgrowth at high salinity (Figure 4A; Nau-Wagner et al., 2012). GbsR can directly bind choline, which leads to derepression of the *opuB* and *gbsAB* operons, allowing efficient accumulation of GB (Boch et al., 1996; Nau-Wagner et al., 2012). Strikingly, despite *gbsR* upregulation and the absence of choline, *gbsAB* was upregulated in our experiment. The reason for this *gbsAB* upregulation remains to be determined.

Further evidence for the importance of compatible solutes during outgrowth under salt stress was the strong upregulation of the osmoadaptive proline synthesis genes *proH* and *proj*. In vegetative cells, osmotic induction of the *proHJ* operon can

be observed after a salt shock as well as during sustained high salinity and is mediated by an osmotically controlled σ^A -type promoter (Steil et al., 2003; Hahne et al., 2010; Brill et al., 2011a). Although osmoadaptive proline synthesis requires ProA (encoded in the not osmotically inducible *proBA* operon), *proA* was found to be repressed during outgrowth in high salt conditions (Figure 4A), which is in agreement with previous findings (Hahne et al., 2010; Brill et al., 2011a). Transcription of the *proBA* operon is regulated by a tRNA-responsive riboswitch, allowing *proBA* derepression only upon proline starvation (Brill et al., 2011b). Thus, the downregulation of *proA* in salt-stressed outgrowing spores may in fact signify derepression of *proBA* in non-stressed outgrowing spores, as these likely have a higher anabolic proline turnover due to a higher protein biosynthesis rate.

While most genes involved in the accumulation of osmoprotectants were upregulated during outgrowth at high salinity, the not osmotically inducible *ktrAB* operon was found to be downregulated at all-time points (Figure 4A). Since the KtrAB transporter system plays an important role in K^+ uptake as a first defense against high osmolality (Holtmann et al., 2003) it is possible that the K^+ accumulation phase had already ended within the first 30 min of outgrowth and *ktrAB* expression was downregulated at ≥ 30 min to prevent detrimental effects of further K^+ uptake. As *ktrAB* is regulated by *ydaO*-type riboswitch causing increased transcription termination in the presence of c-di-AMP (Nelson et al., 2013) and transcript

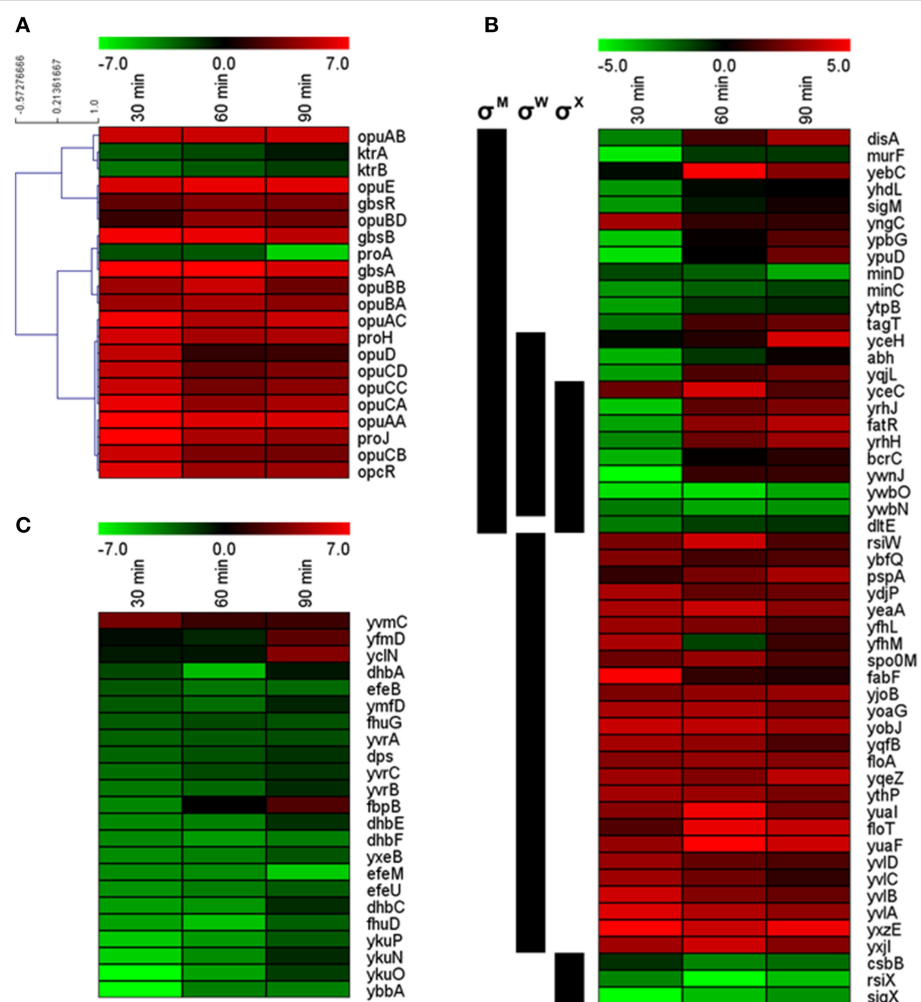


FIGURE 4 | Expression profiles of (A) genes associated with the hyperosmotic stress response, (B) differentially expressed members of the σ^M , σ^W , and σ^X regulons (regulon affiliations are indicated by black bars on the left), and (C) genes associated with iron homeostasis. Only significantly differentially expressed genes are shown. Cutoff-values ($\log_2\text{FC}$) of the color scale are indicated at the top of each figure.

levels of *ktrAB* were very low in salt-stressed outgrowing spores (GSE81238), it would be intriguing to investigate the role of c-di-AMP signaling in salt stress responses and outgrowth in more detail in future studies.

General Stress Response

Numerous previous studies on osmotically stressed vegetative cells of *B. subtilis* have indicated an induction of the σ^B -dependent general stress response upon sudden osmotic increases (e.g., Spiegelhalter and Bremer, 1998; Petersohn et al., 2001; Höper et al., 2006; Hecker et al., 2007; Nannapaneni et al., 2012; Nicolas et al., 2012; Young et al., 2013). As spores germinated in high-salinity media were also suddenly confronted with salt stress, an involvement of the general stress response would seem plausible. The *sigB* gene itself was not differentially expressed at any sample time point (Dataset S1), which was not surprising as σ^B is only transiently active after a salt shock (Spiegelhalter and Bremer, 1998; Young et al., 2013). Yet, in total, almost one-third of the σ^B regulon was differentially

expressed at one or several sample time points: 14 genes were significantly upregulated, whereas 31 genes were downregulated (Table 3; Figure S3A). Importantly, all upregulated genes except for the uncharacterized *ydeC* have additional regulators aside from σ^B (e.g., σ^W), which were likely responsible for the increased expression (see below). Moreover, only one of the 37 general stress response genes whose absence causes a salt-sensitive phenotype (i.e., *yflH*; Höper et al., 2005) was upregulated, whereas seven others were downregulated (Figure S3A). Indeed, σ^B was previously reported to be dispensable for colony formation from spores at high salinity (Tovar-Rojo et al., 2003). Altogether, our data suggest that the σ^B -dependent general stress response is not of major significance during outgrowth in the presence of 1.2 M NaCl.

Sigma Factors and Regulons

Aside from σ^B , the alternative sigma factors σ^M , σ^W , and σ^X have repeatedly been implicated with cell envelope and salt stress (Horsburgh et al., 2001; Petersohn et al., 2001; Steil et al., 2003;

TABLE 3 | Involvement of alternative sigma factors in the salt stress response of outgrowing spores^a.

Regulon	Description	Number of genes ^b	Differentially expressed ^c		
			%	#up	#down
<i>sigB</i>	General stress response	151	30	14	31
<i>sigD</i>	Regulation of flagella, motility, chemotaxis, and autolysis	24	33	0	27
<i>sigE</i>	Sporulation (early mother cell-specific)	176	9	8	7
<i>sigF</i>	Sporulation (early forespore-specific)	63	11	2	5
<i>sigG</i>	Sporulation (late forespore-specific)	108	10	3	8
<i>sigH</i>	Transcription of early stationary phase genes (sporulation, competence)	37	43	1	14
<i>sigI</i>	Control of a class of heat shock genes	6	50	0	3
<i>sigK</i>	Sporulation (late mother cell-specific)	103	7	2	4
<i>sigL</i>	Utilization of arginine, acetoin, and fructose; required for cold adaptation	23	52	0	12
<i>sigM</i>	ECF-type sigma factor responsible for intrinsic resistance against beta-lactam antibiotics	69	35	4	13
<i>sigO-rsoA</i>	Two-subunit sigma factor	5	20	1	0
<i>sigV</i>	ECF-type sigma factor; response to lysozyme	4	0	0	0
<i>sigW</i>	ECF-type sigma factor; activated by alkaline shock, polymyxin B, vancomycin, cephalosporin C, D-cycloserine, and triton X-100	65	54	28	4
<i>sigX</i>	ECF-type sigma factor; cell surface properties	29	45	1	9
<i>sigY</i>	ECF-type sigma factor; maintenance of the SPβ prophage	7	0	0	0
<i>ylaC</i>	ECF-type sigma factor; response to oxidative stress	4	0	0	0
<i>xpf</i>	PBSX phage RNA polymerase sigma factor	10	50	0	5

^aClassification and description according to SubtiWiki and (Souza et al., 2014).^bNumber of genes within the regulon.^cThe numbers of up- (#up) and downregulated (#down) genes only include genes that have the same expression direction (up/downregulated) at all three time points. The percentage of differentially expressed genes includes all genes.

Höper et al., 2006; Hahne et al., 2010). Hence, we analyzed the role of the different alternative sigma factors and major regulons in the salt stress response of outgrowing spores.

Among the genes encoding alternative sigma factors, only three significant changes were observed: downregulation of *sigM* at 30 min outgrowth, upregulation of *sigO* at 60 min outgrowth, and downregulation of *sigX* throughout the whole experiment (Dataset S1). It should be noted that upregulation of *sigO*, which forms a two-subunit sigma factor with RsoA, is almost certainly an artifact, because this gene was barely expressed at all and *rsoA* was not differentially expressed (GSE81238). While the repression of *sigX* under salt stress has previously been reported (Steil et al., 2003; Hahne et al., 2010; Nicolas et al., 2012), the lack of differential *sigW* expression was in contrast to the study by Hahne et al. (2010), in which a significant *sigW* upregulation 30 and 60 min after the osmotic upshift has been shown.

Nevertheless, more than half of the genes in the σ^W regulon were differentially expressed, most of them being upregulated (Table 3; Figure 4B), indicating importance of σ^W for the salt stress response during outgrowth. Interestingly, while Hahne et al. (2010) reported a maximum induction of the σ^W regulon at 30 min after NaCl addition, we observed three different expression patterns within this regulon: (i) 27 genes were upregulated at all-time points, (ii) four genes were downregulated at all-time points, and (iii) four genes were downregulated at 30 min and upregulated subsequently (Figure 4B). Most likely the distinct expression patterns of the latter two gene groups were

caused by their simultaneous control by σ^M and σ^X (Figure 4B). The constant upregulation of the σ^W regulon also supports the notion that the salt stress response of outgrowing spores is rather similar to that of cells growing at sustained high salinity and not to that of salt-shocked cells, as salt-shocked cells shut down the σ^W regulon about 20 min after the osmotic upshift (Steil et al., 2003).

Additionally, one-third of the σ^M regulon was differentially expressed, although 10 out of these 24 genes were also members of the σ^W regulon (Table 3; Figure 4B). While Hahne et al. (2010) have reported maximum upregulation of the σ^M regulon 60 min after NaCl addition, σ^M -dependent genes tended to be repressed in our study (Figure 4B). Downregulation was predominant at 30 min of outgrowth, which is consistent with the repression of the *sigM* gene at this time point. However, at the later time points, most genes became less repressed or were even upregulated (Figure 4B). Altogether, an involvement of σ^M in salt stress adaptation during outgrowth is possible, but the tendency for downregulation—in context with the salt-sensitive phenotype of *sigM* mutants (Horsburgh et al., 2001)—suggests that σ^M -dependent genes may be dispensable during the early outgrowth phase under salt stress. In consistence with previous reports (Steil et al., 2003; Hahne et al., 2010), the σ^X regulon was largely repressed during outgrowth at high salinity (Table 3). Notably, all differentially expressed σ^X genes (except *sigX* and the anti- σ^X factor *rsiX*) were also members of the σ^W and/or σ^M regulon (Figure 4B).

As summarized in **Table 3**, various genes belonging to the regulons of other alternative sigma factors were differentially expressed during outgrowth at high salinity as well. Most notably, many σ^D -dependent genes involved in motility and chemotaxis were repressed throughout the entire experiment (Figure S3B), which is in excellent agreement with previous findings from salt-stressed vegetative cells (Steil et al., 2003; Höper et al., 2006; Hahne et al., 2010; Nicolas et al., 2012). Furthermore, all differentially expressed genes of the σ^I , σ^L , and Xpf regulons were downregulated in our experiment (**Table 3**; Dataset S1). Some differential expression was also detected within the sporulation-related σ^E , σ^F , σ^G , σ^K , and σ^H regulons (**Table 3**). However, the portion of differential expression within the σ^E , σ^F , σ^G , and σ^K regulons was relatively low and can be explained by very low expression levels, non-sporulation-related gene functions, and/or different degradation rate of dormant spore transcripts in stressed vs. non-stressed outgrowing spores (Dataset S1). All differentially expressed σ^H -genes except the σ^W -dependent *spo0M* were downregulated (**Table 3**), consistent with the role of σ^H in sporulation initiation that is blocked at high salinity (Ruzal et al., 1998; Widderich et al., 2016).

Alignment of all *SubtiWiki*-annotated regulons with our data exhibited additional overlaps. While some regulators seemed to be active during outgrowth at high salinity (e.g., BirA, PyrR, LutR), genes in many other regulons behaved exactly opposite to their regulators' functions as repressors or activators (e.g., AzlB, PucR, RocR, Zur; Table S3). The latter observation suggests that these regulons were actively regulated in the non-stressed outgrowing spores. Consistently, *azlB* and *zur* have been reported to be overexpressed during outgrowth under non-stress conditions (Keijser et al., 2007).

While the DegS/DegU two-component system has previously been implicated in salt stress sensing and response (Ruzal and Sánchez-Rivas, 1998; Mäder et al., 2002; Steil et al., 2003), only five genes (19%) of the DegU regulon were differentially expressed in our study (Table S3; Dataset S1). Moreover, there was only a limited overlap (38%, mostly motility genes) with the DegS/DegU regulated genes that were reported to be differentially expressed in salt-stressed vegetative cells (Steil et al., 2003). Perhaps, the lack of major changes in the DegU regulon can be explained by the upregulation of *rapG*, which encodes a DegU-inhibiting response regulator aspartate phosphatase (Ogura et al., 2003). Nevertheless, the role of DegS/DegU in salt stress adaption during spore outgrowth remains questionable.

Induction of the PerR regulon in vegetative, salt-stressed cells has previously been hypothesized to indicate increased oxidative stress caused by high salinity (Höper et al., 2006). However, in our study, the PerR-dependent catalase gene *kata* was repressed while the other members of the regulon were not differentially expressed (Table S3; Dataset S1).

Overlap with Other Stress Responses

As many survival strategies of *B. subtilis* are closely interlinked (Höper et al., 2005; Lopez et al., 2009; Schultz et al., 2009), the transcriptional profile of genes known to be involved in other stress responses was analyzed as well (summarized in Table S4). Our data indicate a large overlap (about 40%) of

differential gene expression during outgrowth at high salinity and cell envelope stress, largely reflecting the changes in the σ^M , σ^W , and σ^X regulons described above (Table S4; **Figure 4B**). Notably, more than half of the 35 cell envelope stress-related genes that exhibited significant upregulation at one or more sample time points encoded hypothetical and poorly characterized proteins, whose role may be interesting to investigate in the future (Dataset S1). In addition, several genes encoding heat shock proteins, chaperones (e.g., *groEL*, *groES*, *dnaK*), and proteases (e.g., *clpE*, *clpX*) were upregulated in our experiment (Dataset S1). Protein quality control is important during outgrowth (Sinai et al., 2015) and likely even more so during outgrowth at high salinity, since osmotic upshifts have been proposed to cause protein denaturation and misfolding (Hahne et al., 2010). Additional overlaps between our data and genes involved in other stress responses are of unknown functional relevance and include the categories "Resistance against toxins/antibiotics" (27% overlap, 17 upregulated, 11 downregulated), "Resistance against oxidative and electrophile stress" (22% overlap, four upregulated, nine downregulated), and "Biosynthesis of antibacterial compounds" (27% overlap, four upregulated, 11 downregulated; Table S4; Dataset S1).

Cell Envelope

Vegetative *B. subtilis* cells growing under hyperosmotic conditions exhibit alterations of their cell envelope, i.e., changes in cell wall structure and membrane composition (López et al., 1998, 2006; Palomino et al., 2009; Hahne et al., 2010). During outgrowth at high salinity, cell envelope stress also seems to be apparent (see above). In total, 44 genes (ca. 23%) of the category "Cell wall" were differentially expressed (Dataset S1). Among these, especially the genes involved in cell wall turnover (8 genes) and cell wall synthesis (10 genes) were repressed, although *tagA* and *tagD* involved in early steps of teichoic acid biosynthesis were upregulated (**Figure 5A**). PBP4* (encoded by *pbpE*) has previously been proposed to play a role in peptidoglycan modification at high salinity (Palomino et al., 2009; Hahne et al., 2010), but the gene was not differentially expressed in our study (Dataset S1).

High-salinity-induced changes in the membrane composition of vegetative cells include an increase in saturated straight-chain fatty acids, unsaturated fatty acids, and cardiolipin, and a decrease in branched fatty acids (López et al., 1998, 2006). During outgrowth at high salinity, 21 out of 109 genes involved in lipid metabolism were differentially expressed (Dataset S1). Genes encoding enzymes for fatty acid utilization tended to be upregulated (**Figure 5B**), consistent with a previously reported global upregulation of genes involved in degradation of free fatty acids via β -oxidation (Hahne et al., 2010). In contrast, genes important for fatty acid and lipid biosynthesis exhibited expression changes in both directions. Since only little is known about membrane remodeling during spore outgrowth, the relevance of the observed transcriptomic differences and their actual impact on membrane composition is unclear. Nevertheless, in agreement with a possible increase in unsaturated fatty acids (López et al., 1998), the *des* gene encoding a fatty acid desaturase was upregulated (**Figure 5B**).

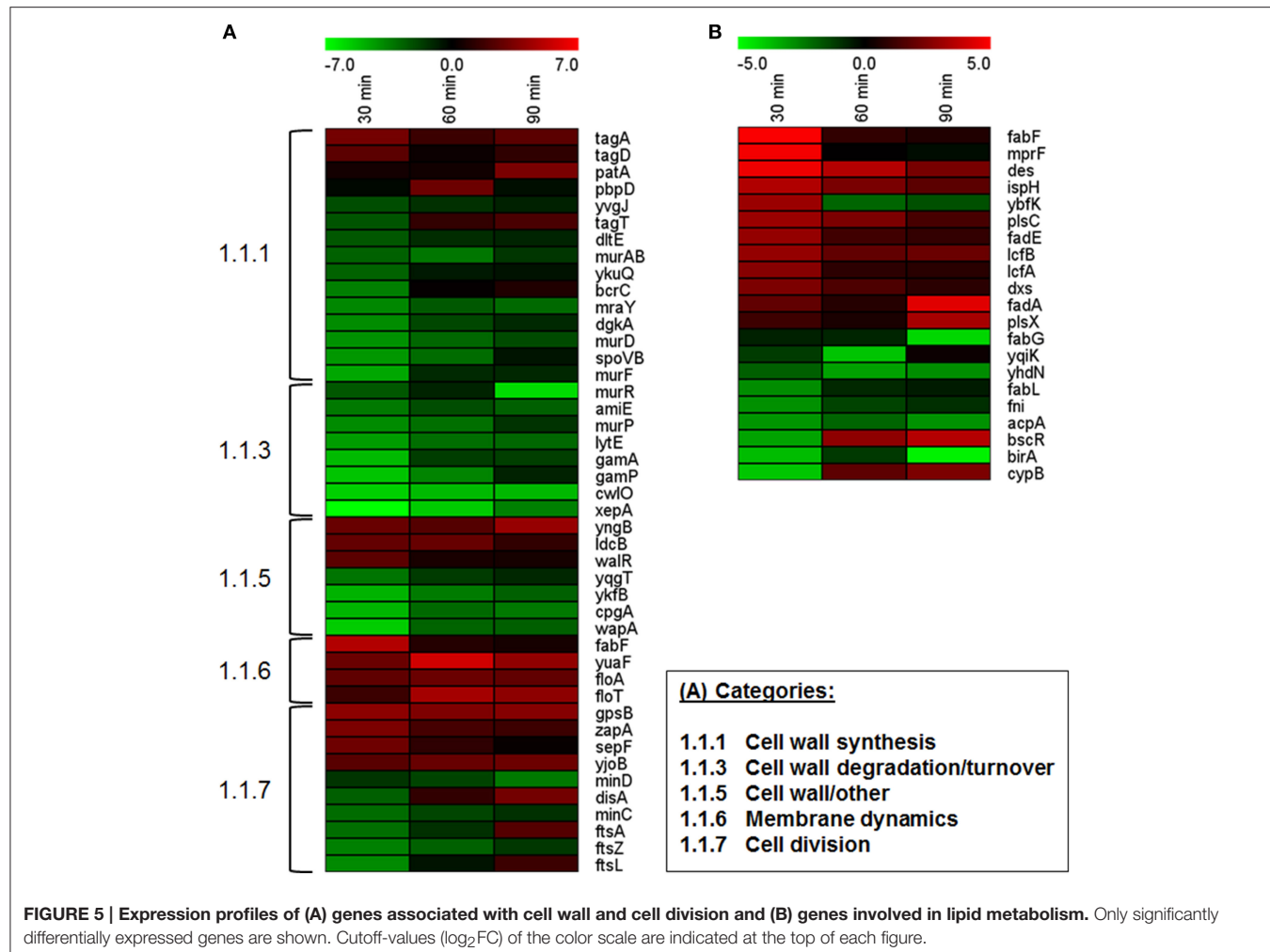


FIGURE 5 | Expression profiles of (A) genes associated with cell wall and cell division and (B) genes involved in lipid metabolism. Only significantly differentially expressed genes are shown. Cutoff-values ($\log_2\text{FC}$) of the color scale are indicated at the top of each figure.

Interestingly, although anionic phospholipids (in particular cardiolipin) play a role in osmoadaptation, possibly by changing biophysical membrane properties such as fluidity (Poolman et al., 2004; López et al., 2006; Romantsov et al., 2009; Unsav et al., 2013), neither the genes encoding cardiolipin synthases (*clsA*, *ywiE*, *ywjE*) nor *pgsA* (encoding a phosphatidylglycerophosphate synthase) were differentially expressed (Dataset S1). However, σ^W -dependent upregulation of *fabF* as well as *yuaF* and the flotillin-homologs *floT* and *floA* (Figure 4B, Dataset S1) suggests that changes of the cytoplasmic membrane (e.g., *fabF*-induced fluidity decrease) may play a role in osmoadaptation of outgrowing spores (Kingston et al., 2011).

Membrane Proteins and Transporters

The membrane protein and transporter transcriptome of outgrowing spores was severely altered by the presence of 1.2 M NaCl (Figure 3). In total, 54 ABC transporter genes (i.e., 26% of genes in this category), six phosphotransferase system genes (21%), and 65 other transporter genes (33%) were differentially expressed (Dataset S1). With regard to the importance of solute pool adjustments during osmotic stress adaptation on the one hand, and major molecular reorganization during outgrowth

on the other hand, this is not surprising and in agreement with previous transcriptomic and proteomic studies (Steil et al., 2003; Keijser et al., 2007; Hahne et al., 2010; Segev et al., 2013; Hoffmann and Bremer, 2016).

Overall, 44% of differentially expressed transporter genes exhibited upregulation (Dataset S1) and included (aside from *opu* transporter genes) many genes encoding cation efflux transporters: the *khtSTU* operon involved in K⁺ efflux, *mrpABC* of the *mrpABCDEFG* operon encoding *B. subtilis*' major Na⁺ extrusion system, as well as *nhaC* and *nhaK* involved in Na⁺ and monovalent cation efflux, respectively (Fujisawa et al., 2004, 2005; Gorecki et al., 2014). Upregulation of K⁺ efflux systems, which likewise occurs in salt-stressed cells (Steil et al., 2003; Hahne et al., 2010), is in agreement with the observed downregulation of the KtrAB K⁺ importer (see above; Figure 4A). Both transcriptional changes might constitute consequences of the initial K⁺ uptake phase of osmoadaptation (Whatmore et al., 1990) that may have ended before 30 min into outgrowth. Transcriptomic changes toward increased Na⁺ efflux most likely represent countermeasures against high intracellular Na⁺ concentrations that are toxic for *B. subtilis*, but may for instance build up due to the Na⁺-coupled activity of the OpuD and OpuE

transporters (**Figure 4A**; Gorecki et al., 2014; Hoffmann and Bremer, 2016). This would not only be in agreement with observations from vegetative cells (Hahne et al., 2010), but also with the downregulation of Na^+ symporter genes (*yocR*, *yrbD*, *yocS*, *putP*, *yodF*) in our study (Dataset S1).

Further upregulated transporter genes are functionally involved (i) in the uptake of zinc, phosphate, sulfonate, sulfate, glucose, gluconate, uracil, and cysteine; (ii) in branched-chain amino acid transport; and (iii) in the export of toxic peptides and antibiotics (Dataset S1). Although we detected upregulation of two genes for iron uptake (only at 90 min) and *sufC* involved in the synthesis of Fe-S clusters that were implicated in the salt stress response of vegetative cells (Höper et al., 2006), unexpectedly many iron and iron siderophore uptake systems were downregulated (see below; **Figure 4C**). While the di- and tripeptide importer *dtpT*, which can contribute to osmoprotection by taking up proline-containing peptides, was upregulated, genes encoding Dpp and Opp implicated in the same osmoprotective function (Zaprasis et al., 2013) were downregulated (Dataset S1). As it is possible that non-stressed outgrowing spores utilize these uptake systems to gain access to a broader nutrient spectrum, the relevance of extracellular peptides in outgrowth and salt-stress adaptation of outgrowing spores remains to be determined. Generally it is plausible that downregulation of many transporter genes in our study was in fact a consequence of higher metabolic and/or biosynthetic activity in non-stressed cells, as these genes are involved in the uptake of common metabolites including purines, nitrate, lactate, and various amino acids (Dataset S1).

In total, transporter genes constituted 42% of the differentially expressed membrane protein genes, emphasizing the importance of transport processes during outgrowth and osmoadaptation within this phase (**Figure 3**; Table S1). The functions of the membrane proteins encoded by the residual 58% of differentially expressed genes in this category were very diverse and included genes for regulatory proteins, flagellum, and chemotaxis, kinases, dehydrogenases, cell division proteins, and many poorly characterized proteins (Dataset S1). Moreover, about 30% of the differentially expressed non-transporter membrane protein genes encoded hypothetical proteins, some of which may be interesting to investigate in more detail with regard to their role in outgrowth and osmoadaptation.

Iron Homeostasis

Iron homeostasis is governed by the central iron regulatory protein Fur, which upon binding of excess iron becomes an active repressor (Hoffmann et al., 2002; Helmann, 2014). Previous studies showed that vegetative *B. subtilis* cells grown in SMM containing 1.2 M NaCl experience iron limitation, with genes involved in the synthesis of the iron siderophore bacillibactin (*dhbACEBF* operon) and other members of the Fur regulon becoming derepressed (Hoffmann et al., 2002; Steil et al., 2003). In contrast, in our study, *dhbA*, *dhbC*, *dhbE*, and *dhbF* and 15 other genes of the category “Acquisition of iron” (1.3.3) were repressed in the presence of 1.2 M NaCl (**Figure 4C**; Dataset S1). Although the downregulation of only 17 genes (34%) of the Fur regulon was significant, all residual genes in this regulon were also downregulated (albeit below the significance

threshold), possibly due to *fur* overexpression during outgrowth under non-stress conditions (Keijser et al., 2007). Overall, the downregulation of the Fur regulon in salt-stressed outgrowing spores may indicate a lower iron requirement, sparing a larger amount of iron to keep Fur active and its regulon repressed, thereby leading to lower iron acquisition. Possibly, the iron depot of spores of around 40 μg Fe/g (dry weight) (Granger et al., 2011) is sufficient for the potentially slower spore ripening processes at high salinity.

Metabolism

As the outgrowing spores in our study simultaneously had to cope with molecular rearrangements for metabolic initiation and osmoadaptation, it is not surprising that 372 genes involved in metabolism were differentially expressed. High salinity affected all aspects of metabolism, but various processes were influenced to different extents: genes in the categories “Electron transport and ATP synthesis” (2.1) and “Lipid metabolism” (2.4) were affected the least; genes of “Carbon metabolism” (2.2) and “Nucleotide metabolism” (2.5) exhibited intermediate alterations; and genes involved in “Amino acid/nitrogen metabolism” (2.3) and “Additional metabolic pathways” (2.6) were affected the most (**Figure 3**; Tables S1, S2).

In total, 70% of the differentially expressed metabolic genes were downregulated, reflecting the detrimental effects of salt stress and suggesting a metabolic decline comparable to the reduced growth rate or growth arrest that can be observed in vegetative salt-stressed cells (Boch et al., 1994; Hahne et al., 2010). Especially the genes related to amino acid metabolism (i.e., biosynthesis, acquisition, and utilization) experienced strong repression (**Figure 3**; Dataset S1), which is likely to result in generally slower adaptation and ripening processes, both requiring protein biosynthesis (Segev et al., 2013; Sinai et al., 2015; Hoffmann and Bremer, 2016). Moreover, global downregulation of the amino acid metabolism may further impede synthesis of osmoprotective proline from other amino acid precursors (Zaprasis et al., 2015). Although the acquisition of adequate osmoprotectant pools seems *per se* unlikely given the extremely nutrient-poor conditions of our experiment, amino acids that the outgrowing spores may acquire from SASP degradation or from peptides liberated from the spore coat seem to have low chances to be converted to proline based on our transcriptomic data (Tovar-Rojo et al., 2003; Zaprasis et al., 2013).

Despite the apparently restrained metabolism during outgrowth at high salinity, only 12 genes involved in carbon core metabolism were downregulated in our study (Dataset S1). Previous studies on salt-stressed vegetative cells indicated that the enzymes of the tricarboxylic acid cycle canalized toward 2-oxoglutarate synthesis and thus ultimately toward glutamate and subsequent proline synthesis (Höper et al., 2006; Hahne et al., 2010). However, we could not detect such an adaptation in our experiment, as most of the tricarboxylic acid cycle genes were either not differentially expressed or even downregulated (Dataset S1).

Next to numerous downregulated metabolic routes, the only pathway that was uniformly, significantly upregulated was the uridine-5-phosphate synthesis pathway, with all eight *pyr* genes

(*pyrABCDEFK*) involved in conversion of hydrogen carbonate to UMP showing strong upregulation (average $\log_2\text{FC} = 7.6$) at all investigated time points (Dataset S1). In contrast, six out of seven differentially expressed purine biosynthesis and acquisition genes as well as all 12 nucleotide utilization genes were downregulated. Unfortunately, the relevance of this difference in pyrimidine and purine assimilation is not clear.

Taken together, our data indicate that high salinity exerted manifold detrimental effects on the metabolism of outgrowing spores, which are especially grave given the low nutrient availability in our outgrowth medium.

CONCLUSIONS

In its natural habitats, *B. subtilis* is frequently exposed to increases in environmental salinity, which has profound influences on cellular physiology and triggers adaptive responses (Bremer, 2002; Hoffmann and Bremer, 2016). High salinity exerts detrimental effects on *B. subtilis* spore formation (Ruzal et al., 1998; Widderich et al., 2016), spore germination (Nagler et al., 2014, 2015, 2016; Nagler and Moeller, 2015), and, as shown here and previously, spore outgrowth (Tovar-Rojo et al., 2003; Nagler et al., 2014, 2016). Although it seems counter-intuitive that high salinity inhibits the formation of desiccation resistant spores, blocking this costly cellular differentiation program most likely reflects the inability of starving cells to gather sufficient resources (e.g., for the massive production of osmoprotective proline) required for sporulation during simultaneous salt stress (Brill et al., 2011a; Widderich et al., 2016). In contrast, spore germination and outgrowth can be initiated under non-growth-permissive salt conditions, likely resulting in a survival disadvantage and indicating the lack of a counteracting sensory and regulatory response system (Boch et al., 1994; Nagler et al., 2014, 2016).

Although we exposed spores to a severe salt shock simultaneously to the germination stimulus, the σ^B -directed stress response system surprisingly did not seem to be of major significance during this treatment. This suggests that (i) the stressosome controlling σ^B activity subsequent to a salt shock is either not (sufficiently) present in outgrowing spores, or (ii) that the cellular signal(s) controlling the release of the alternative transcription factor σ^B from its anti-sigma factor RsbW cannot be generated in outgrowing spores (Hecker et al., 2007; Marles-Wright and Lewis, 2010; Young et al., 2013; Hoffmann and Bremer, 2016).

The transcriptional profile of salt-stressed outgrowing spores resembled that of *B. subtilis* cells actively growing under continuous high-salinity conditions in many aspects (Steil et al., 2003; Hahne et al., 2010). Hence, the signals that trigger adaptive responses of *B. subtilis* to counteract sustained high salinity can apparently be perceived by outgrowing spores as well. At all investigated time points, salt-stressed outgrowing spores induced their complete genetic repertoire of osmoprotectant uptake and compatible solute synthesis, emphasizing the pivotal role of these substances also during outgrowth (**Figure 4A**). Unfortunately, the nature of the signal allowing osmotic induction of compatible

solute uptake and biosynthesis systems in *B. subtilis* remains to be determined (Bremer, 2002; Hoffmann and Bremer, 2016).

In outgrowing spores, the σ^D regulon was strongly downregulated in response to high salt concentrations (Figure S3), indicating that flagellar biosynthesis, assembly and swimming will be impaired in the emerging vegetative cells. This is surprising as one may have predicted that chemotaxis and the ability to swim would be useful traits to escape from osmotically unfavorable to nutritionally favorable conditions (Wong et al., 1995). Perhaps, the requirement to synthesize 20,000 flagellin subunits (Hag) for the production of a single filament is too resource-consuming for salt-stressed outgrowing spores (Mukherjee and Kearns, 2014). However, the strong down-regulation of flagellar genes and the concomitant abrogation of swimming have also been observed in *B. subtilis* cells exposed to prolonged high salinity (Steil et al., 2003).

In conclusion, our study provided new insights on the transcriptomic adaptations of outgrowing spores to the presence of high salt concentrations and points out another facet of the perturbing effects that osmotic stress can exert on the life cycle of spore-forming soil bacteria.

AUTHOR CONTRIBUTIONS

KN designed, performed, and evaluated the transcriptomics and spectrophotometric germination experiments, and prepared the text and figures of the manuscript. AK supported experimental design, gave scientific input, and edited the manuscript text. AD supported evaluation and handling of the transcriptomic data. OK arranged RNA sequencing and edited the manuscript text. KM and ML performed and evaluated the live cell imaging and scanning electron microscopy experiments, and edited the manuscript text. EB and TH supported evaluation of transcriptomic data and edited the manuscript text. RM gave scientific input and edited the manuscript text. All authors read and approved the final manuscript.

FUNDING

This work was supported by the Helmholtz Space Life Sciences Research School (SpaceLife) and the German Aerospace Center of the Helmholtz Association (Ph.D. fellowship of KN). RM and KN were supported by DLR grant DLR-FuE-Projekt ISS LIFE, Programm RF-FuW, Teilprogramm 475.

ACKNOWLEDGMENTS

We would like to acknowledge Dr. Christine Hellweg for her continuous support. The results of this study are part of the Ph.D. thesis of the first author KN.

SUPPLEMENTARY MATERIAL

The Supplementary Material for this article can be found online at: <http://journal.frontiersin.org/article/10.3389/fmicb.2016.01564>

REFERENCES

- Atluri, S., Ragkousi, K., Cortezzo, D. E., and Setlow, P. (2006). Cooperativity between different nutrient receptors in germination of spores of *Bacillus subtilis* and reduction of this cooperativity by alterations in the GerB receptor. *J. Bacteriol.* 188, 28–36. doi: 10.1128/JB.188.1.28-36.2006
- Bassi, D., Colla, F., Gazzola, S., Puglisi, E., Delledonne, M., and Cocconcelli, P. S. (2016). Transcriptome analysis of *Bacillus thuringiensis* spore life, germination and cell outgrowth in a vegetable-based food model. *Food Microbiol.* 55, 73–85. doi: 10.1016/j.fm.2015.11.006
- Boch, J., Kempf, B., and Bremer, E. (1994). Osmoregulation in *Bacillus subtilis*: synthesis of the osmoprotectant glycine betaine from exogenously provided choline. *J. Bacteriol.* 176, 5364–5371.
- Boch, J., Kempf, B., Schmid, R., and Bremer, E. (1996). Synthesis of the osmoprotectant glycine betaine in *Bacillus subtilis*: characterization of the *gbsAB* genes. *J. Bacteriol.* 178, 5121–5129.
- Bremer, E. (2002). “Adaptation to changing osmolarity,” in *Bacillus Subtilis and its Closest Relatives: From Genes to Cells*, eds A. L. Sonnenschein, R. M. Losick, and J. A. Hoch (Washington, DC: ASM Press), 385–391.
- Brill, J., Hoffmann, T., Bleisteiner, M., and Bremer, E. (2011a). Osmotically controlled synthesis of the compatible solute proline is critical for cellular defense of *Bacillus subtilis* against high osmolarity. *J. Bacteriol.* 193, 5335–5346. doi: 10.1128/JB.05490-11
- Brill, J., Hoffmann, T., Putzer, H., and Bremer, E. (2011b). T-box-mediated control of the anabolic proline biosynthetic genes of *Bacillus subtilis*. *Microbiology* 157, 977–987. doi: 10.1099/mic.0.047357-0
- De Jong, A., van der Meulen, S., Kuipers, O. P., and Kok, J. (2015). T-REX: transcriptome analysis webserver for RNA-seq expression data. *BMC Genomics* 16:663. doi: 10.1186/s12864-015-1834-4
- Fujisawa, M., Kusumoto, A., Wada, Y., Tsuchiya, T., and Ito, M. (2005). NhaK, a novel monovalent cation/H⁺ antiporter of *Bacillus subtilis*. *Arch. Microbiol.* 183, 411–420. doi: 10.1007/s00203-005-0011-6
- Fujisawa, M., Wada, Y., and Ito, M. (2004). Modulation of the K⁺ efflux activity of *Bacillus subtilis* YhaT by YhaT and the C-terminal region of YhaS. *FEMS Microbiol. Lett.* 231, 211–217. doi: 10.1016/S0378-1097(03)00959-5
- Gorecki, K., Hägerhäll, C., and Drakenberg, T. (2014). The Na⁺ transport in gram-positive bacteria defect in Mrp antiporter complex measured with ²³Na nuclear magnetic resonance. *Anal. Biochem.* 445, 80–86. doi: 10.1016/j.ab.2013.10.003
- Granger, A. C., Gaidamakova, E. K., Matrosova, V. Y., Daly, M. J., and Setlow, P. (2011). Effects of Mn and Fe levels on *Bacillus subtilis* spore resistance and effects of Mn²⁺, other divalent cations, orthophosphate, and dipicolinic acid on protein resistance to ionizing radiation. *Appl. Environ. Microbiol.* 77, 32–40. doi: 10.1128/AEM.01965-10
- Hahne, H., Mäder, U., Otto, A., Bonn, F., Steil, L., Bremer, E., et al. (2010). A comprehensive proteomics and transcriptomics analysis of *Bacillus subtilis* salt stress adaptation. *J. Bacteriol.* 192, 870–882. doi: 10.1128/JB.01106-09
- Hecker, M., Pané-Farré, J., and Völker, U. (2007). SigB-dependent general stress response in *Bacillus subtilis* and related gram-positive bacteria. *Annu. Rev. Microbiol.* 61, 215–236. doi: 10.1146/annurev.micro.61.080706.093445
- Helmann, J. D. (2014). Specificity of metal sensing: iron and manganese homeostasis in *Bacillus subtilis*. *J. Biol. Chem.* 289, 28112–28120. doi: 10.1074/jbc.R114.587071
- Hoffmann, T., and Bremer, E. (2011). Protection of *Bacillus subtilis* cold stress via compatible-solute acquisition. *J. Bacteriol.* 193, 1552–1562. doi: 10.1128/JB.01319-10
- Hoffmann, T., and Bremer, E. (2016). “Management of osmotic stress by *Bacillus subtilis*: genetics and physiology,” in *Stress and Environmental Regulation of Gene Expression and Adaptation in Bacteria*, ed F. de Bruijn (Hoboken, NJ: Wiley/Blackwell), 657–676.
- Hoffmann, T., Schütz, A., Brosius, M., Völker, U., and Bremer, E. (2002). High-salinity-induced iron limitation in *Bacillus subtilis*. *J. Bacteriol.* 184, 718–727. doi: 10.1128/JB.184.3.718-727.2002
- Hoffmann, T., Wensing, A., Brosius, M., Steil, L., Völker, U., and Bremer, E. (2013). Osmotic control of *opuA* expression in *Bacillus subtilis* and its modulation in response to intracellular glycine betaine and proline pools. *J. Bacteriol.* 195, 510–522. doi: 10.1128/JB.01505-12
- Holtmann, G., Bakker, E. P., Uozumi, N., and Bremer, E. (2003). KtrAB and KtrCD: two K⁺ uptake systems in *Bacillus subtilis* and their role in adaptation to hypertonicity. *J. Bacteriol.* 185, 1289–1298. doi: 10.1128/JB.185.4.1289-1298.2003
- Höper, D., Bernhardt, J., and Hecker, M. (2006). Salt stress adaptation of *Bacillus subtilis*: a physiological proteomics approach. *Proteomics* 6, 1550–1562. doi: 10.1002/pmic.200500197
- Höper, D., Völker, U., and Hecker, M. (2005). Comprehensive characterization of the contribution of individual SigB-dependent general stress genes to stress resistance of *Bacillus subtilis*. *J. Bacteriol.* 187, 2810–2826. doi: 10.1128/JB.187.8.2810-2826.2005
- Horsburgh, M. J., Thackray, P. D., and Moir, A. (2001). Transcriptional responses during outgrowth of *Bacillus subtilis* endospores. *Microbiology* 147, 2933–2941. doi: 10.1099/00221287-147-11-2933
- Keijser, B. J. F., Ter Beek, A., Rauwerda, H., Schuren, F., Montijn, R., van der Spek, H., et al. (2007). Analysis of temporal gene expression during *Bacillus subtilis* spore germination and outgrowth. *J. Bacteriol.* 189, 3624–3634. doi: 10.1128/JB.01736-06
- Kempf, B., and Bremer, E. (1998). Uptake and synthesis of compatible solutes as microbial stress responses to high-osmolality environments. *Arch. Microbiol.* 170, 319–330. doi: 10.1007/s002030050649
- Kingston, A. W., Subramanian, C., Rock, C. O., and Helmann, J. D. (2011). A σ^W-dependent stress response in *Bacillus subtilis* that reduces membrane fluidity. *Mol. Microbiol.* 81, 69–79. doi: 10.1111/j.1365-2958.2011.07679.x
- Lee, C. H., Wu, T. Y., and Shaw, G. C. (2013). Involvement of OpcR, a GbsR-type transcriptional regulator, in negative regulation of two evolutionarily closely related choline uptake genes in *Bacillus subtilis*. *Microbiology* 159, 2087–2096. doi: 10.1099/mic.0.067074-0
- López, C. S., Alice, A. F., Heras, H., Rivas, E. A., and Sánchez-Rivas, C. (2006). Role of anionic phospholipids in the adaptation of *Bacillus subtilis* to high salinity. *Microbiology* 152, 605–616. doi: 10.1099/mic.0.28345-0
- López, C. S., Heras, H., Ruzal, S. M., Sánchez-Rivas, C., and Rivas, E. A. (1998). Variations of the envelope composition of *Bacillus subtilis* during growth in hyperosmotic medium. *Curr. Microbiol.* 36, 55–61. doi: 10.1007/s002849900279
- Lopez, D., Vlamakis, H., and Kolter, R. (2009). Generation of multiple cell types in *Bacillus subtilis*. *FEMS Microbiol. Rev.* 33, 152–163. doi: 10.1111/j.1574-6976.2008.00148.x
- Mäder, U., Antelmann, H., Buder, T., Dahl, M. K., Hecker, M., and Homuth, G. (2002). *Bacillus subtilis* functional genomics: genome-wide analysis of the DegS-DegU regulon by transcriptomics and proteomics. *Mol. Genet. Genomics* 286, 455–467. doi: 10.1007/s00438-002-0774-2
- Mäder, U., Schmeisky, A. G., Flórez, L. A., and Stülpke, J. (2012). SubtiWiki - a comprehensive community resource for the model organism *Bacillus subtilis*. *Nucleic Acids Res.* 40, D1278–D1287. doi: 10.1093/nar/gkr923
- Marles-Wright, J., and Lewis, R. J. (2007). Stress responses of bacteria. *Curr. Opin. Struct. Biol.* 17, 755–760. doi: 10.1016/j.sbi.2007.08.004
- Marles-Wright, J., and Lewis, R. J. (2010). The stressosome: molecular architecture of a signaling hub. *Biochem. Soc. Trans.* 38, 928–933. doi: 10.1042/BST0380928
- Michna, R. H., Zhu, B., Mäder, U., and Stülpke, J. (2016). SubtiWiki 2.0 – an integrated database for the model organism *Bacillus subtilis*. *Nucleic Acids Res.* 44, D654–D662. doi: 10.1093/nar/gkv1006
- Mukherjee, S., and Kearns, D. B. (2014). The structure and regulation of flagella in *Bacillus subtilis*. *Annu. Rev. Genet.* 48, 319–340. doi: 10.1146/annurev-genet-120213-092406
- Nagler, K. (2012). *Investigation of Bacillus subtilis Spore Germination at High Salinity*. Master’s thesis, University of Cologne, Cologne.
- Nagler, K., Julius, C., and Moeller, R. (2016). Germination of spores of astrobiologically relevant *Bacillus* species in high-salinity environments. *Astrobiology* 16, 500–512. doi: 10.1089/ast.2015.1419
- Nagler, K., and Moeller, R. (2015). Systematic investigation of germination responses of *Bacillus subtilis* spores in different high-salinity environments. *FEMS Microbiol. Ecol.* 91:fiv023. doi: 10.1093/femsec/fiv023
- Nagler, K., Setlow, P., Li, Y. Q., and Moeller, R. (2014). High salinity alters the germination behavior of *Bacillus subtilis* with nutrient and nonnutritive germinants. *Appl. Environ. Microbiol.* 80, 1314–1321. doi: 10.1128/AEM.03293-13
- Nagler, K., Setlow, P., Reineke, K., Driks, A., and Moeller, R. (2015). Involvement of coat proteins in *Bacillus subtilis* spore germination in high-salinity environments. *Appl. Environ. Microbiol.* 81, 6725–6735. doi: 10.1128/AEM.01817-15

- Nannapaneni, P., Hertwig, F., Depke, M., Hecker, M., Mäder, U., Völker, U., et al. (2012). Defining the structure of the general stress regulon of *Bacillus subtilis* using targeted microarray analysis and random forest classification. *Microbiology* 158, 696–707. doi: 10.1099/mic.0.055434-0
- Nau-Wagner, G., Opper, D., Rolbetzki, A., Boch, J., Kempf, B., Hoffmann, T., et al. (2012). Genetic control of osmoadaptive glycine betaine synthesis in *Bacillus subtilis* through the choline-sensing and glycine betaine-responsive GbsR repressor. *J. Bacteriol.* 194, 2703–2714. doi: 10.1128/JB.0642-11
- Nelson, J. W., Sudarsan, N., Furukawa, K., Weinberg, Z., Wang, J. X., and Breaker, R. R. (2013). Riboswitches in eubacteria sense the second messenger c-di-AMP. *Nat. Chem. Biol.* 9, 834–839. doi: 10.1038/nchembio.1363
- Nicholson, W. L. (2002). Roles of *Bacillus* endospores in the environment. *Cell. Mol. Life Sci.* 59, 410–416. doi: 10.1007/s00018-002-8433-7
- Nicholson, W. L., Munakata, N., Horneck, G., Melosh, H. J., and Setlow, P. (2000). Resistance of *Bacillus* endospores to extreme terrestrial and extraterrestrial environments. *Microbiol. Mol. Biol. Rev.* 64, 548–572. doi: 10.1128/MMBR.64.3.548-572.2000
- Nicholson, W. L., and Setlow, P. (1990). “Sporulation, germination and outgrowth,” in *Molecular Biological Methods for Bacillus*, eds C. R. Harwood and S. M. Cutting (West Sussex: John Wiley & Sons Ltd.), 391–429.
- Nicolas, P., Mäder, U., Dervyn, E., Rochat, T., Leduc, A., Pigeonneau, N., et al. (2012). Condition-dependent transcriptome reveals high-level regulatory architecture in *Bacillus subtilis*. *Science* 335, 1103–1106. doi: 10.1126/science.1206848
- Ogura, M., Shimane, K., Asai, K., Ogasawara, N., and Tanaka, T. (2003). Binding of response regulator DegU to the *aprE* promoter is inhibited by RapG, which is counteracted by extracellular PhrG in *Bacillus subtilis*. *Mol. Microbiol.* 49, 1685–1697. doi: 10.1046/j.1365-2958.2003.03665.x
- Paidhungat, M., and Setlow, P. (2002). “Spore germination and outgrowth,” in *Bacillus Subtilis and Its Closest Relatives: From Genes to Cells*, eds A. L. Sonnenschein, R. M. Losick, and J. A. Hoch (Washington, DC: ASM Press), 537–548.
- Palomino, M. M., Sánchez-Rivas, C., and Ruzal, S. M. (2009). High salt stress in *Bacillus subtilis*: involvement of PBP4* as a peptidoglycan hydrolase. *Res. Microbiol.* 160, 117–124. doi: 10.1016/j.resmic.2008.10.011
- Petersohn, A., Brigulla, M., Haas, S., Hoheisel, J. D., Völker, U., and Hecker, M. (2001). Global analysis of the general stress response of *Bacillus subtilis*. *J. Bacteriol.* 183, 5617–5631. doi: 10.1128/JB.183.19.5617-5631.2001
- Poolman, B., Spitzer, J. J., and Wood, J. M. (2004). Bacterial osmosensing: roles of membrane structure and electrostatics in lipid-protein and protein-protein interactions. *Biochim. Biophys. Acta* 1666, 88–104. doi: 10.1016/j.bbamem.2004.06.013
- Rasband, W. (1997–2015). *ImageJ*. Bethesda, MD: National Institutes of Health. Available online at: <http://imagej.nih.gov/ij/>
- Record, M. T. Jr., Courtenay, E. S., Cayley, S., and Guttman, H. J. (1998). Biophysical compensation mechanisms buffering *E. coli* protein-nucleic acid interactions against changing environments. *Trends Biochem. Sci.* 23, 190–194. doi: 10.1016/S0968-0004(98)01207-9
- Romantsov, T., Guan, Z., and Wood, J. M. (2009). Cardiolipin and the osmotic stress response of bacteria. *Biochim. Biophys. Acta* 1788, 2092–2100. doi: 10.1016/j.bbamem.2009.06.010
- Ruzal, S. M., Lopez, C., Rivas, E., and Sánchez-Rivas, C. (1998). Osmotic strength blocks sporulation at stage II by impeding activation of early sigma factors in *Bacillus subtilis*. *Curr. Microbiol.* 36, 75–79. doi: 10.1007/s002849900282
- Ruzal, S. M., and Sánchez-Rivas, C. (1998). In *Bacillus subtilis* DegU-P is a positive regulator of the osmotic response. *Curr. Microbiol.* 37, 368–372. doi: 10.1007/s002849900395
- Schultz, D., Wolynes, P. G., Jacob, E. B., and Onuchuc, J. N. (2009). Deciding fate in adverse times: sporulation and competence in *Bacillus subtilis*. *Proc. Natl. Acad. Sci. U.S.A.* 106, 21027–21034. doi: 10.1073/pnas.0912185106
- Segev, E., Rosenberg, A., Mamou, G., and Ben-Yehuda, S. (2013). Molecular kinetics of reviving bacterial spores. *J. Bacteriol.* 195, 1875–1882. doi: 10.1128/JB.00093-13
- Segev, E., Smith, Y., and Ben-Yehuda, S. (2012). RNA dynamics in aging bacterial spores. *Cell* 148, 139–149. doi: 10.1016/j.cell.2011.11.059
- Setlow, P. (2003). Spore germination. *Curr. Opin. Microbiol.* 6, 550–556. doi: 10.1016/j.mib.2003.10.001
- Setlow, P. (2006). Spores of *Bacillus subtilis*: their resistance to and killing by radiation, heat and chemicals. *J. Appl. Microbiol.* 101, 514–525. doi: 10.1111/j.1365-2672.2005.02736.x
- Setlow, P. (2013). Summer meeting 2013 – when the sleepers wake: the germination of spores of *Bacillus* species. *J. Appl. Microbiol.* 115, 1251–1268. doi: 10.1111/jam.12343
- Setlow, P., and Kornberg, A. (1970). Biochemical studies of bacterial sporulation and germination. XXIII. Nucleotide metabolism during spore germination. *J. Biol. Chem.* 245, 3645–3652.
- Sinai, L., Rosenberg, A., Smith, Y., Segev, E., and Ben-Yehuda, S. (2015). The molecular timeline of a reviving bacterial spore. *Mol. Cell* 57, 685–707. doi: 10.1016/j.molcel.2014.12.019
- Skinner, M. E., Uzilov, A. V., Stein, L. D., Mungall, C. J., and Holmes, I. H. (2009). JBrowse: a next-generation genome browser. *Genome Res.* 19, 1630–1638. doi: 10.1101/gr.094607.109
- Souza, B. M., Castro, T. L., Carvalho, R. D., Seyffert, N., Silva, A., Miyoshi, A., et al. (2014). σ^{ECF} factors of gram-positive bacteria: a focus on *Bacillus subtilis* and the CMNR group. *Virulence* 5, 587–600. doi: 10.4161/viru.29514
- Spiegelhalter, F., and Bremer, E. (1998). Osmoregulation of the *opuE* proline transport gene from *Bacillus subtilis*: contributions of the sigma A- and sigma B-dependent stress-responsive promoters. *Mol. Microbiol.* 29, 285–296. doi: 10.1046/j.1365-2958.1998.00929.x
- Steil, L., Hoffmann, T., Budde, I., Völker, U., and Bremer, E. (2003). Genome-wide transcriptional profiling analysis of adaptation of *Bacillus subtilis* to high salinity. *J. Bacteriol.* 185, 6358–6370. doi: 10.1128/JB.185.21.6358-6370.2003
- Tovar-Rojo, F., Cabrera-Martinez, R. M., Setlow, B., and Setlow, P. (2003). Studies on the mechanism of the osmoresistance of spores of *Bacillus subtilis*. *J. Appl. Microbiol.* 95, 167–179. doi: 10.1046/j.1365-2672.2003.01958.x
- Unsay, J. D., Cosentino, K., Subburaj, Y., and García-Sáez, A. J. (2013). Cardiolipin effects on membrane structure and dynamics. *Langmuir* 29, 15878–15887. doi: 10.1021/la402669z
- Whatmore, A. M., Chudek, J. A., and Reed, R. H. (1990). The effects of osmotic upshock on the intracellular solute pools of *Bacillus subtilis*. *J. Gen. Microbiol.* 136, 2527–2535. doi: 10.1099/00221287-136-12-2527
- Widderich, N., Rodrigues, C. D. A., Commichau, F. M., Fischer, K. E., Ramirez-Guardiana, F. H., Rudner, D. Z., et al. (2016). Salt-sensitivity of SigH and SpoOA prevents sporulation of *Bacillus subtilis* at high osmolarity avoiding death during cellular differentiation. *Mol. Microbiol.* 100, 108–124. doi: 10.1111/mmi.13304
- Wong, L. S., Johnson, M. S., Sandberg, L. B., and Taylor, B. L. (1995). Amino acid efflux in response to chemotactic and osmotic signals in *Bacillus subtilis*. *J. Bacteriol.* 177, 4342–4349.
- Wood, J. M., Bremer, E., Csonka, L. N., Kraemer, R., Poolman, B., van der Heide, T., et al. (2001). Osmosensing and osmoregulatory compatible solute accumulation by bacteria. *Comp. Biochem. Phys. A* 130, 437–460. doi: 10.1016/S1095-6433(01)00442-1
- Young, J. W., Locke, J. C. W., and Elowitz, M. B. (2013). Rate of environmental change determines stress response specificity. *Proc. Natl. Acad. Sci. U.S.A.* 110, 4140–4145. doi: 10.1073/pnas.1213060110
- Zaprasis, A., Bleisteiner, M., Kerres, A., Hoffmann, T., and Bremer, E. (2015). Uptake of amino acids and their metabolic conversion into the compatible solute proline confers osmoprotection to *Bacillus subtilis*. *Appl. Environ. Microbiol.* 81, 250–259. doi: 10.1128/AEM.02797-14
- Zaprasis, A., Brill, J., Thüring, M., Wünsche, G., Heun, M., Barzantny, H., et al. (2013). Osmoprotection of *Bacillus subtilis* through import and proteolysis of proline-containing peptides. *Appl. Environ. Microbiol.* 79, 576–587. doi: 10.1128/AEM.01934-12
- Conflict of Interest Statement:** The authors declare that the research was conducted in the absence of any commercial or financial relationships that could be construed as a potential conflict of interest.
- Copyright © 2016 Nagler, Krawczyk, De Jong, Madela, Hoffmann, Laue, Kuipers, Bremer and Moeller. This is an open-access article distributed under the terms of the Creative Commons Attribution License (CC BY). The use, distribution or reproduction in other forums is permitted, provided the original author(s) or licensor are credited and that the original publication in this journal is cited, in accordance with accepted academic practice. No use, distribution or reproduction is permitted which does not comply with these terms.



FlhF Is Required for Swarming Motility and Full Pathogenicity of *Bacillus cereus*

Diletta Mazzantini¹, Francesco Celandroni¹, Sara Salvetti^{1†}, Sokhna A. Gueye¹, Antonella Lupetti¹, Sonia Senesi² and Emilia Ghelardi^{1,3*}

¹ Department of Translational Research and New Technologies in Medicine and Surgery, University of Pisa, Pisa, Italy,

² Department of Biology, University of Pisa, Pisa, Italy, ³ Research Center Nutraceuticals and Food for Health-Nutrafood, University of Pisa, Pisa, Italy

OPEN ACCESS

Edited by:

Ivan Mijakovic,
Chalmers University of Technology,
Sweden

Reviewed by:

Monika Ehling-Schulz,
University of Veterinary Medicine,
Austria

Michel Gohar,
Institut National de la Recherche
Agronomique, France

*Correspondence:

Emilia Ghelardi
emilia.ghelardi@med.unipi.it

†Present address:

Sara Salvetti,
San Giuseppe Hospital-USL 11,
Empoli, Italy

Specialty section:

This article was submitted to
Microbial Physiology and Metabolism,
a section of the journal
Frontiers in Microbiology

Received: 24 June 2016

Accepted: 03 October 2016

Published: 19 October 2016

Citation:

Mazzantini D, Celandroni F, Salvetti S, Gueye SA, Lupetti A, Senesi S and Ghelardi E (2016) FlhF Is Required for Swarming Motility and Full Pathogenicity of *Bacillus cereus*. *Front. Microbiol.* 7:1644.
doi: 10.3389/fmicb.2016.01644

Besides sporulation, *Bacillus cereus* can undergo a differentiation process in which short swimmer cells become elongated and hyperflagellated swarmer cells that favor migration of the bacterial community on a surface. The functionally enigmatic flagellar protein FlhF, which is the third paralog of the signal recognition particle (SRP) GTPases Ffh and FtsY, is required for swarming in many bacteria. Previous data showed that FlhF is involved in the control of the number and positioning of flagella in *B. cereus*. In this study, *in silico* analysis of *B. cereus* FlhF revealed that this protein presents conserved domains that are typical of SRPs in many organisms and a peculiar N-terminal basic domain. By proteomic analysis, a significant effect of FlhF depletion on the amount of secreted proteins was found with some proteins increased (e.g., B component of the non-hemolytic enterotoxin, cereolysin O, enolase) and others reduced (e.g., flagellin, L₂ component of hemolysin BL, bacillolysin, sphingomyelinase, PC-PLC, PI-PLC, cytotoxin K) in the extracellular proteome of a $\Delta flhF$ mutant. Deprivation of FlhF also resulted in significant attenuation in the pathogenicity of this strain in an experimental model of infection in *Galleria mellonella* larvae. Our work highlights the multifunctional role of FlhF in *B. cereus*, being this protein involved in bacterial flagellation, swarming, protein secretion, and pathogenicity.

Keywords: FlhF, *Bacillus cereus*, swarming, protein secretion, virulence

INTRODUCTION

Bacillus cereus is a Gram-positive, motile, spore-bearing rod, frequently isolated from the soil, where the spore ensures its persistence under adverse conditions. Long known as agent of food-borne diseases, this organism is now recognized to be able to cause local and systemic infections in humans (Bottone, 2010; Logan, 2012; Celandroni et al., 2016). The pathogenic potential of this bacterium is related to the secretion of several virulence proteins, e.g., hemolysins, phospholipases, trimeric toxins (hemolysin BL, HBL; non-hemolytic enterotoxin, NHE), cytotoxin K (CytK), proteases (Senesi and Ghelardi, 2010; Ramarao and Sanchis, 2013; Jeßberger et al., 2015), and to motility modes, such as swimming and swarming (Senesi et al., 2010; Celandroni et al., 2016). Bacterial swarming is a flagellum-driven social form of locomotion in which cells undergo a periodical differentiation process leading to the production of long and hyperflagellated elements, the swarmer cells, which coordinately migrate across surfaces (Kearns, 2010;

Partridge and Harshey, 2013). Swarming confers an advantage for the colonization of natural and host surfaces and can contribute to bacterial virulence. Notably, swarming increases HBL secretion by *B. cereus* (Ghelardi et al., 2007) and enhances the pathogenicity of this bacterium in an experimental endophthalmitis model (Callegan et al., 2006).

In a previous study, we demonstrated that the protein FlhF plays a major role in controlling the arrangement of flagella in *B. cereus* (Salvetti et al., 2007). The proteins FlhF and FlhG are essential for establishing correct place and quantity of flagella in many but not all bacterial species (Schniederberend et al., 2013). In *Bacillus subtilis*, FlhF and FlhG behave as two antagonistic proteins regulating the pattern of flagellar basal body formation to control flagella localization, but they do not influence the number of flagella on the cell surface (Guttenplan et al., 2013). In *B. cereus*, no FlhG homologue was found and the lack of FlhF, other than leading to mislocalization of flagella, causes a reduction in the number of flagella and reduces swimming migration (Salvetti et al., 2007).

FlhF belongs to the GTP-binding signal recognition particle (SRP) family, which also includes Ffh and FtsY (Bange et al., 2007; Schuhmacher et al., 2015). SRP-GTPases are required for the cotranslational targeting of many proteins to the membrane through the recognition and binding of their N-terminus signal peptide during protein synthesis. Nevertheless, FlhF appeared not to be involved in protein secretion mechanisms in *B. subtilis* (Zanen et al., 2004). Differently, in *Pseudomonas putida* and *B. cereus*, the FlhF depletion altered the profile of secreted proteins (Pandza et al., 2000; Salvetti et al., 2007). In particular, a $\Delta flhF$ mutant of *B. cereus* showed an increase in the extracellular levels of NHE and a decrease in HBL and phosphatidyl-choline specific phospholipase C (PC-PLC) (Salvetti et al., 2007). Thus, the aim of the present study was to gain more insight into the function of FlhF in *B. cereus* by evaluating the effects of FlhF depletion on interconnected cellular functions such as swarming, protein secretion, and virulence, which may all depend from protein targeting to the membrane.

MATERIALS AND METHODS

Bacterial Strains and Growth Conditions

Bacillus cereus ATCC 14579 wild type (wt), its *flhF* (GeneBank ID: *Bc1670*) mutant derivative ($\Delta flhF$, MP06), and complemented strain ($\Delta flhF$ -comp, MP07) (Salvetti et al., 2007) stocks from -80° C were streaked on brain heart infusion supplemented with 0.1% (w/v) glucose (BHIG; Becton Dickinson, Cockeysville, NJ, USA) plates and incubated at 37° C. BHIG was also used for liquid cultures. When required, 5 μ g/ml erythromycin for strain MP06 or 30 μ g/ml kanamycin for strain MP07 were added to the media. MP07 cultures were also supplemented with 4 mM isopropyl- β -D-1-tiogalattopyranoside (IPTG; Sigma-Aldrich, St. Louis, MO, USA) in order to induce *pspac* dependent gene expression.

In silico Analysis

BLAST¹ was used for comparative analysis of nucleotide and protein sequences. Protein sequences in the FASTA format were retrieved from the UniProt database² (The UniProt Consortium, 2015). Functional domain analysis was performed using the ProDom Server³ (Bru et al., 2005). The presumptive secondary and tridimensional structure of proteins were generated using the Phyre2 web portal for protein modeling, prediction and analysis⁴ (Kelley et al., 2015) and the Raptor X Structure Prediction Server⁵ (Källberg et al., 2012), respectively.

Swarming Motility

For each experiment, swarm plates (TrA plates; 1% tryptone, 0.5% NaCl, 0.7% granulated agar) were prepared fresh daily and allowed to sit at room temperature overnight before use (Salvetti et al., 2011). Swarming was initiated by spotting 50 μ l of a culture containing approximately 2×10^4 cells/ml onto the center of TrA plates, and incubating cultures at 37° C. Swarming migration was evaluated by measuring colony diameters after 8 h. Since *B. cereus* flagella are very fragile, bacterial samples were taken by slide overlay of single agar blocks (5 mm \times 5 mm) that contained different colony portions. Bacterial cells were stained with tannic acid and silver nitrate (Harshey and Matsuyama, 1994) for microscopy. Several samples were analyzed at 1000 \times magnification using an optical microscope (BH-2; Olympus, Tokyo, Japan). All experiments were performed in duplicate in three separate days.

Preparation of Culture Supernatants

Protein samples were prepared by growing bacterial cells to the late exponential growth phase in BHIG at 200 rpm for 6 h at 37° C. Culture supernatants were collected by high-speed centrifugation (10000 \times g), added with the serine protease inhibitor phenylmethylsulfonyl fluoride 1 mM (PMSF; Sigma-Aldrich), and stored at -80° C until use. Protein concentration in supernatants was determined by the bicinchoninic acid (BCA) assay (Smith et al., 1985), using bovine serum albumin as a standard. The activity of fructose-1,6-bisphosphate aldolase in culture supernatants was spectrophotometrically measured at 30° C by following the rate of NADH oxidation at 340 nm according to the method described by Warth (1980).

Two-Dimensional Electrophoresis (2-DE)

Proteins contained in supernatants were precipitated using the TCA method (trichloroacetic acid, Sigma-Aldrich). Precipitated proteins were washed eight-times with cold 96% (v/v) ethanol, air-dried and suspended in sample rehydration buffer (7 M urea, 2 M thiourea, 4% CHAPS, 2.4% aminosulfobetaine-14; Invitrogen, Carlsbad, CA, USA). ZOOM[®] IPG strips with a linear pH range of 4–7 (Invitrogen) were rehydrated for

¹<http://blast.ncbi.nlm.nih.gov/Blast.cgi>

²<http://www.uniprot.org/>

³<http://prodom.prabi.fr/prodom/current/html/home.php>

⁴<http://www.sbg.bio.ic.ac.uk/phyre2>

⁵<http://raptord.uchicago.edu/StructurePrediction/predict/>

16 h in 400 μ l of sample rehydration buffer and 10 μ g of protein samples were subsequently added by cup loading. Focusing was carried out at 200 V for 20 min, 450 V for 15 min, 750 V for 15 min, and 2000 V for 30 min using the Xcell SureLockTM Mini-Cell system (Invitrogen). The IPG strips were then equilibrated for 10 min in 5 ml of equilibration solution (LDS 1X; DTT 0.5 mM). For the second dimension, samples were run at 200 V for 35 min on 4–12% gradient SDS-PAGE gel (Bis-Tris ZOOMTM Gel, 1.0 mm IPG-well; Invitrogen). Three independent biological experiments were performed in separate days. Gels were silver or Coomassie Blue (Sigma–Aldrich) stained, according to standard procedures. Gels were scanned at 300 dpi and 8 bits depth on an Image Scanner equipped with a film-scanning unit and analyzed with the Image-Master 2D Platinum v.6 software (GE Healthcare, Little Chalfont, UK). The spots were quantified after normalization and spot volumes (pixel intensity \times area) were expressed as percentage of the total volume of the spots on the gel. Presumptive analysis of protein gels was performed by comparison of silver stained 2-DE gels with gels available in the literature (Gohar et al., 2002, 2005) and then protein spots were identified by spot excision from Coomassie-Blue stained gels and subsequent identification. To this purpose, excised spots were digested with 0.1–0.5 μ g of trypsin at 37° C for 6 h (Shevchenko et al., 1996). Digested proteins were analyzed by liquid chromatography coupled with tandem mass spectrometry (LC-MS/MS) at Université de Genève, Proteomics Core Facility (Genève, CH). Database searches were performed with the Mascot Server (Matrix Science Ltd; version 04_2014⁶) and results were analyzed and validated using the Scaffold software (Proteome Software Inc.). Searches were performed using trypsin for the fragments cleavage, allowing up to one trypsin miscleavage and without restriction on protein mass or isoelectric point (pI). Fixed modifications included carbamidomethylation of cysteine, while variable modifications comprised oxidation of methionine. Peptide masses ranged from 849.0 m/z to 4001.0 m/z with a charge (z) of 1 +. The mass tolerance was set to \pm 25 ppm. Significance was established according to expectancy (e) value transformed into MS score (with significance at a P-value <0.05 at scores over 70), percentage coverage and theoretical pI and molecular weight (Mw) compared to the approximate experimental values observed on 2-DE gels.

Identified proteins were classified based on their biological functions using the Kyoto Encyclopedia of Genes and Genomes (KEGG) database resource⁷. Protein sequences were analyzed using the SIGNALIP 4.1 Server⁸, TATP 1.0⁹, SecretomeP 2.0 Server¹⁰ and TMpred program¹¹ in order to evaluate the presence of Sec-type signals, Tat-type signals, non-classically secretion signals or transmembrane domains, respectively.

⁶<http://www.matrixscience.com>

⁷<http://www.genome.jp/kegg/>

⁸<http://www.cbs.dtu.dk/services/SignalP/>

⁹<http://www.cbs.dtu.dk/services/TatP/>

¹⁰<http://www.cbs.dtu.dk/services/SecretomeP/>

¹¹http://www.ch.embnet.org/software/TMPRED_form.html

Insects and Infection Experiments

Galleria mellonella larvae, obtained from Mous Live Bait (Balk, Netherland), were selected by weight (0.2–0.3 g) and absence of dark spots on the cuticle. Bacteria were grown to the late exponential growth phase in BHIG at 37° C for 6 h and harvested by centrifugation at 5000 \times g for 10 min. Bacterial suspensions were prepared in phosphate buffered saline (PBS: 1 M KH₂PO₄, 1 M K₂HPO₄, 5 M NaCl, pH 7.2) and bacteria counted using a hemocytometer. Three infectious doses (about 10³, 10², and 10¹ CFU per larva) were used to infect three groups of 20 larvae. Larva abdomen was accurately cleaned with 70% ethanol and 10 μ l of bacterial suspension was injected into the hemocoel through the last right pro-leg, with a sterile Hamilton syringe (Sigma–Aldrich) via a 26-gage needle. A control group of larvae was injected with PBS only. Infectious doses were checked by CFU count after plating appropriate dilutions and incubating 16 h at 37° C. Infected larvae were kept at 37° C and mortality was recorded after 24 h. Each experiment was performed three times in separate days.

To assess bacterial ability to multiply *in vivo*, groups of 20 animals were infected with 10⁴ CFU/larva of *B. cereus* wt, Δ flhF, or Δ flhF-comp. Groups of three insects were collected at different times post infection (2, 4, 6, 8, and 24 h) and their surfaces were disinfected with 70% ethanol. Larvae were homogenized in 2 ml of PBS using a Stomacher 400 Circulator (Seward, Worthing, UK). Serial dilutions of the homogenates were plated on LB agar and colonies were counted after incubation at 37° C for 24 h. Non-infected larvae were used as negative control. Three independent biological replicates were performed.

Statistical Analysis

Data were expressed as the mean \pm SD. A P-value <0.05 was considered significant. For 2-DE experiments, the One-way Anova analysis and the two-tailored Student's t-test for equal or unequal variance were applied. For *G. mellonella* experiments, the 50% lethal dose (LD₅₀) values were estimated by probit analysis (Finney, 1971). Differences in mortality rates obtained for each infectious dose and in the CFU number for each time tested were evaluated by the One-way Anova analysis.

RESULTS

In silico Analysis of *B. cereus* FlhF

By BLAST alignments, the flhF nucleotide sequence resulted to be highly conserved (from 90 to 100%; Score \geq 200) among different *B. cereus* strains. In a previous work (Salvetti et al., 2007), we showed that *B. cereus* FlhF possesses a C-terminal G domain, that is strongly conserved among SRP-GTPases (Zanen et al., 2004; Bange et al., 2007; Salvetti et al., 2007; Balaban et al., 2009; Green et al., 2009; Schniederberend et al., 2013; Schuhmacher et al., 2015), and a less conserved N-terminal B domain. Herein, revisited analysis with the ProDom program reveals a nucleoside-triphosphatase (amino acids 176–219), an SRP receptor (amino acids 220–302), an SRP54-type protein GTPase (amino acids 303–353), and an SRP-dependent cotranslational protein-membrane targeting (amino acids 354–439) subdomain

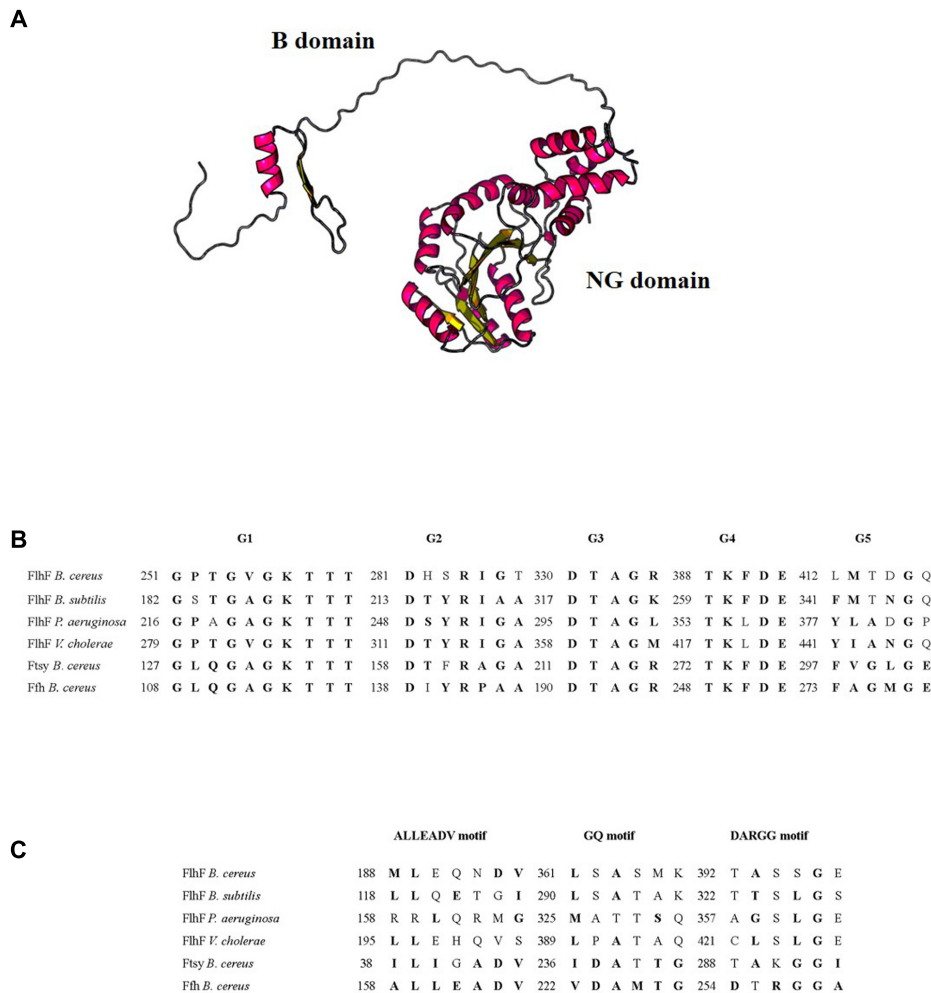


FIGURE 1 | In silico analysis of *B. cereus* FlhF. (A) Model of the three-dimensional structure of *B. cereus* FlhF. **(B)** Alignment of the amino acid sequences of the G1–G5 signatures of the G domain and their respective positions. **(C)** Alignment of the amino acid sequences of the ALLEADV, GQ and DARGG motifs and their respective positions. Conserved amino acids belonging to the same chemical class are marked in bold.

inside the NG domain of *B. cereus* FlhF. Unlike the FlhF proteins of *Vibrio cholerae*, *P. aeruginosa*, and *B. subtilis* in which the N-terminus comprises a GTPase activity subdomain, the N-terminus (B domain) of *B. cereus* FlhF is unique and functionally unknown.

We used the Phyre2 program (Kelley et al., 2015) and the Raptor X Structure Prediction Server (Källberg et al., 2012) in order to define the putative secondary and three-dimensional structure of *B. cereus* FlhF. The protein appeared to be constituted by 45% α -helices and 30% β -sheets and to consist of two distinct portions connected by an unstructured peptide linker (Figure 1A). The B domain was predicted by the Raptor X Structure Prediction Server only, with a *P*-value of 2.5×10^{-2} , while the NG domain was predicted by both programs with a good *P*-value (7.43×10^{-7} for Raptor X Structure Prediction Server and 100.0% confidence by the single highest scoring template with Phyre2) and it is 100% similar in structure to *B. subtilis* FlhF.

In all described SRP-GTPases, five signature elements (G1–G5) interacting with the GDP/GTP-Mg²⁺ complex have been identified in the G domain (Anand et al., 2006; Bange et al., 2007). These elements have never been described in *B. cereus* SRPs. As shown in Figure 1B, the alignment between the FlhF G1–G5 signatures of *B. subtilis*, *P. aeruginosa*, and *V. cholerae* with the amino acid sequence of *B. cereus* FlhF, FtsY, and Ffh revealed that all these signatures are also present inside the G domain of *B. cereus* SRP-GTPases. In particular, G3 and G4 signatures are identical among FlhF, Ffh, and FtsY of *B. cereus* and G1 is highly conserved in all the analyzed bacterial species. The G2 signature of *B. cereus* SRP-GTPases are less conserved compared to the same sequence of *B. subtilis*, *P. aeruginosa*, and *V. cholerae*, while G5 is generally less conserved among all the species analyzed.

Ffh and FtsY of many organisms contain additional sequence motifs (ALLEADV in the N domain; GQ and DARGG in the G domain) that are essential for the communication between functional domains (Bange et al., 2007). Since these motifs have

never been described in *B. cereus* SRPs, we first identified them in Ffh and FtsY of *B. cereus*, through amino acid alignments with the *Escherichia coli* and *B. subtilis* orthologs (data not shown). **Figure 1C** shows the alignment between the ALLEADV, GQ and DARGG motifs in *B. cereus* SRPs and the putative corresponding regions of FlhF in *B. subtilis*, *P. aeruginosa*, and *V. cholerae*.

FlhF and Swarming Motility

Previous data indicated absence of swarm cells in the $\Delta flhF$ mutant of *B. cereus* grown on swarming-supporting media (Salvetti et al., 2007). In the same experimental conditions, we show that FlhF depletion also impairs cell migration. Indeed, as shown in **Figure 2A**, the $\Delta flhF$ mutant gave rise to colonies (4.2 ± 0.32 mm of diameter) that were significantly smaller than those produced by the swarming proficient wt (18.4 ± 1.28 mm of diameter; $P = 0.0039$) or $\Delta flhF$ -comp strain (14.2 ± 1.8 mm of diameter; $P = 0.015$). As expected, long and hyperflagellated swarmer cells were visualized in the colonies produced by the wt and the $\Delta flhF$ -comp strain only (**Figure 2B**).

Effect of FlhF Depletion on Extracellular Proteins

To better characterize the effect of FlhF depletion on protein secretion by *B. cereus*, we performed comparative proteome analyses of the $\Delta flhF$ mutant, the wt, and the $\Delta flhF$ -comp strain grown in BHIG. There were no obvious growth differences between these strains in this medium, as already described (Salvetti et al., 2007). Additionally, as previously described (Salvetti et al., 2007), we again evaluated the activity of the cytosolic marker fructose-1,6-bisphosphate aldolase, a cytoplasmic enzyme that is not released by intact cells, in culture supernatants. No enzyme activity was detected. The bacterial supernatants were precipitated with TCA and analyzed using 2-DE. On average, 539 ± 103 spots were detected in the supernatant of the parental strain and 531 ± 99 spots in that derived from the $\Delta flhF$ -comp strain. This was not significantly different from the 430 ± 119 spots found in the mutant strain on average ($P > 0.05$). In the 2-DE gel analysis, 19 protein spots showed a different abundance of >1.5 -fold (≥ 1.5 for

upregulated proteins and ≤ 0.667 for downregulated proteins) in the $\Delta flhF$ mutant, compared to the wt (**Table 1**). These spots were identified by comparison with available gels (Gohar et al., 2002, 2005) and LC-MS/MS analysis. Three proteins were represented as multiple spots in the gel, having either similar mass but different isoelectric points or slight differences in the molecular mass due to putative post-translational modifications. No appreciable difference emerged between the wt and the $\Delta flhF$ -comp extracellular proteomes.

In the $\Delta flhF$ mutant, the amount of six proteins increased and 12 proteins decreased in abundance compared to the parental strain (**Table 1**). The extracellular protein products significantly more abundant in the $\Delta flhF$ mutant included three predicted secretory proteins, cereolysin O (Clo; $P = 0.007$), the B component of NHE (NHE_B; $P = 0.041$), both contributing to *B. cereus* pathogenicity (Lund and Granum, 1997; Alouf, 2000), and a protein with unknown function ($P = 0.017$). Three other proteins that do not exhibit a conventional signal peptide, the SodA superoxide-dismutase ($P = 0.048$), enolase (Eno; $P = 0.007$), and the chaperone GroEL ($P = 0.01$), were also present at higher levels in the supernatant of the $\Delta flhF$ mutant. Despite these proteins are cytosolic in nature, their orthologs are commonly detected in an extracellular form in many bacteria, *B. cereus* and other *Bacillus* species included (Nouwens et al., 2002; Braunstein et al., 2003; Lenz et al., 2003; Gohar et al., 2005).

Six predicted secretory proteins playing a role in *B. cereus* pathogenicity, since they are able to degrade phospholipids (PC-PLC; $P = 0.017$. PI-PLC; $P = 0.0034$. Smase; $P = 0.0072$), proteins (bacillolysin, NprP2; $P = 0.032$ and $P = 0.007$. Collagenase, ColA; $P = 0.0002$), and to form pores in planar lipid bilayers (cytotoxin K; $P = 0.034$), were significantly less abundant in the extracellular proteome of the $\Delta flhF$ mutant. The membrane-anchored substrate-binding protein OppA_1 of the oligopeptide permease transporter (Slamti et al., 2015) was also significantly reduced ($P = 0.01$) in the mutant secretome. In agreement with our previous results (Salvetti et al., 2007), the flagellin proteins BC1657 ($P = 0.0091$) and BC1658 ($P = 0.016$), classified as non-conventionally secreted proteins by the SecretomeP 2.0 server, were found significantly less abundant in the $\Delta flhF$ strain. In addition, a significant reduction of the L₂ component of HBL (HBL-L₂; $P = 0.023$), apparently lacking a signal peptide by the SIGNALIP 4.1 but herein classified as secretory accordingly to Fagerlund et al. (2010), was demonstrated for the mutant strain. The mutant also displayed a reduction in the spots corresponding to aconitate hydratase (BC3616; $P = 0.0048$) and elongation factor-Tu (EF-Tu; $P = 0.002$), commonly found in the cytoplasm.

Contribution of FlhF to *B. cereus* Pathogenicity

Based on the observation that several virulence proteins were less abundant in the supernatant of the $\Delta flhF$ mutant and that this strain was unable to swarm, we wondered whether the deficiency in FlhF would affect *B. cereus* pathogenicity in an *in vivo* model of infection. To this aim, larvae of the greater wax moth *G. mellonella*, which have been shown to provide useful insights into the pathogenesis of a wide range of microbial

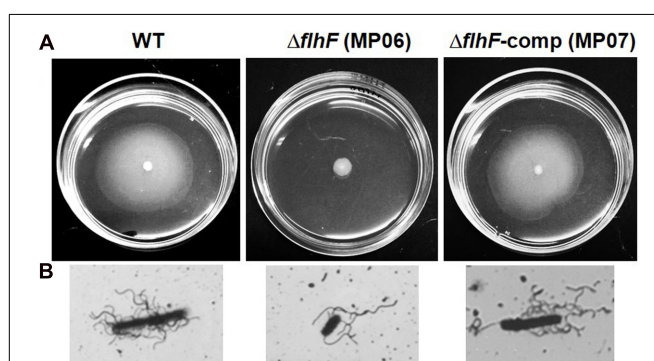


FIGURE 2 | Analysis of swarming motility. (A) Colonies produced on swarming TrA plates. **(B)** Representative cells obtained from swarming TrA plates and stained with tannic acid and silver nitrate.

TABLE 1 | *Bacillus cereus* ATCC 14579 supernatant proteins appreciably increased, reduced or absent in the supernatant of the $\Delta flhF$ (MP06) mutant following growth in BHIG broth.

Accession number	Functional annotation and designation ^a	Function category	MS score ^b	No of peptides ^c	Putative secretion or retention signals ^d	Ratio ^e MP06/wt	Ratio ^e MP07/wt
BC5101	Hemolysin, cereolysin O, Clo	Bacterial toxin	82	13	S	2.56	1.00
BC5445	Superoxide-dismutase, manganese-dependent SodA	Enzyme	77	4	NCS	2.44	1.00
BC5135	Enolase, Eno	Metabolism	80	10	TM	2.22	0.95
BC3874	Unknown (lipoprotein), Unk_3*	Unknown	75; 73	15; 12	S	2.05; 1.39	1.00; 1.09
BC0295	60 kDa chaperone, GroEL	Folding, sorting and degradation	89	14	TM	1.85	1.00
BC1810	Enterotoxin Nhe, component B, NHE_B	Bacterial toxin	84	9	S	1.82	1.00
BC0670	Phosphatidylcholine-specific phospholipase C, PC-PLC*	Bacterial toxin, Enzyme	81; 78	8; 7	S	0.76; 0.36	0.95; 1.00
BC2735	Neutral protease, bacillolysin, NPrP2*	Bacterial toxin, Enzyme	76; 82	16; 14	S	0.51; 0.21	1.10; 0.98
BC3761	Phosphatidylinositol-specific phospholipase C, PI-PLC	Bacterial toxin, Enzyme	76	9	S	0.47	0.91
BC1658	Flagellin, Fla	Cell motility	86	7	NCS	0.40	0.83
BC0671	Sphingomyelinase, Smase	Bacterial toxin, Enzyme	75	8	S	0.39	1.10
BC3104	Enterotoxin HBL, lytic component L ₂ , HBL-L₂	Bacterial toxin	83	14	S ^f	0.38	1.00
BC1179	Oligopeptide binding protein, OppA_1	Transporters	80	20	S, TM	0.32	1.25
BC1110	Hemolysin, cytotoxin K, CytK	Bacterial toxin	77	7	S	0.23	0.92
BC3616	Aconitate hydratase	Metabolism	79	21	TM	0.22	1.00
BC1657	Flagellin, Fla	Cell motility	86	7	NCS	0.22	1.11
BC0129	Elongation factor-Tu, EF-Tu	Translation factor	78	9	—	0	1.00
BC3161	Collagenase, ColA	Enzyme	80	12	S	0	1.00

^aThe designations (short names) used for the various proteins are included. ^bMS score is the score obtained by MASCOT. Protein scores greater than 70 are significant ($P < 0.05$). ^cThe number of peptides used to identify a protein. ^dS: export signal peptide (SignalP 4.1 Server); TM transmembrane domain (TM pred); NCS: non-classically secreted protein (SecretomeP 2.0 Server). ^eRatio between the intensity of protein spots. *Proteins represented as multiple spots in the gels. ^fNo signal peptide was evidenced by the 4.1 version of SignalP Server. However, this protein has been reported as Sec-dependent (Fagerlund et al., 2010).

infections (Jander et al., 2000; Purves et al., 2010), were used to evaluate the pathogenicity of the wt, $\Delta flhF$, and $\Delta flhF$ -comp strains. Larvae were intra-hemocoelically injected with three doses of mid-log phase bacteria and the number of dead larvae was recorded. As shown in Figure 3, a significant reduction in larvae mortality compared to the wt was observed when the $\Delta flhF$ mutant was inoculated at the three doses ($P < 0.01$ for the highest dose, and $P < 0.05$ for the other doses). No significant difference was observed in the mortality rates after injection of the wt or the $\Delta flhF$ -comp strain at different doses. As resulted from Probit analysis, the LD₅₀ of the $\Delta flhF$ mutant was higher ($3.16 \pm 0.83 \times 10^3$ CFU per larva) than the value obtained for the wt (9.10 ± 6.73 CFU per larva). The LD₅₀ of the $\Delta flhF$ -comp strain was $6.27 \pm 4.63 \times 10^1$ CFU per larva.

To test whether differences in larvae mortality could be attributed to a defect in bacterial growth *in vivo*, the bacterial load in infected larvae was quantified over time. Larvae were infected with 10^4 CFU of wt, $\Delta flhF$, or $\Delta flhF$ -comp. At selected time points, the number of CFU per larva was determined. Infection of *G. mellonella* with all *B. cereus* strains resulted in

an initial 10-fold reduction compared to the infectious dose in the CFU recovered from infected larvae at 2-h post infection (wt: 1755 ± 214.6 CFU/larva; $\Delta flhF$: 1673 ± 350.4 CFU/larva; $\Delta flhF$ -comp: 1780 ± 280.2 CFU/larva). Bacterial recovery progressively increased over time up to 10000-fold the infectious dose at 24-h post infection (wt: $3.45 \pm 0.102 \times 10^8$ CFU/larva; $\Delta flhF$: $3.48 \pm 0.856 \times 10^8$ CFU/larva; $\Delta flhF$ -comp: $3.46 \pm 0.103 \times 10^8$ CFU/larva). No significant difference in the CFU recovery of different strains was observed at each time point considered (data not shown). *B. cereus* was never recovered from non-infected larvae. Our data demonstrate that *B. cereus* wt, $\Delta flhF$, and $\Delta flhF$ -comp are able to replicate at the same rate in *G. mellonella*.

DISCUSSION

Most of the information on the physiological role of FlhF comes from studies on polarly flagellated, monotrichous bacteria, in which the deletion of *flhF* results in the absence or mislocalization of flagella leading to swimming/swarming

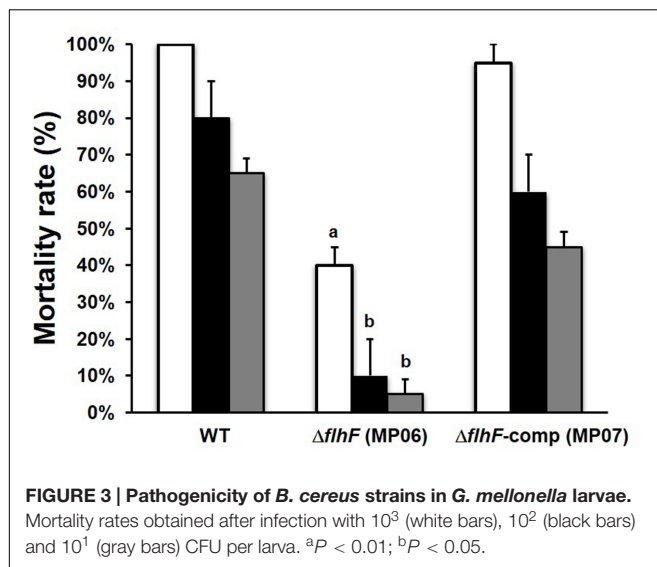


FIGURE 3 | Pathogenicity of *B. cereus* strains in *G. mellonella* larvae. Mortality rates obtained after infection with 10^3 (white bars), 10^2 (black bars) and 10^1 (gray bars) CFU per larva. ^a $P < 0.01$; ^b $P < 0.05$.

defects (Schuhmacher et al., 2015). In peritrichously flagellates, *flhF* orthologs are found in *Bacillus* and *Clostridium* species and data on FlhF function have been produced for *B. subtilis* and *B. cereus* (Carpenter et al., 1992; Zanen et al., 2004; Bange et al., 2007; Salvetti et al., 2007; Guttenplan et al., 2013). In both species, deletion of *flhF* leads to mislocalization of flagella and, in *B. cereus*, flagellar number as well as swimming motility are also reduced (Salvetti et al., 2007). FlhF has been suggested to target the first building block to the future flagellar assembly site by an unclear mechanism (Schuhmacher et al., 2015). The B-domain of FlhF seems to play an important role and differences within this domain might be important criteria to define different flagellation patterns in different species.

In this study, *in silico* analysis shows that, similar to Ffh and FtsY, *B. cereus* FlhF contains a conserved NG domain that includes the GTPase (G-domain) and the regulatory domain (N-domain). Besides the NG domain, FlhF contains an N-terminal domain of basic character (B-domain) that seems to be natively unfolded (Figure 1A), as already demonstrated for *B. subtilis* FlhF (Bange et al., 2007), but displays no homology with the same domain of other bacteria. This result is in line with the significant variations in size and conservation found in the B-domain among species, which suggested that this domain might exert species-specific functions (Schuhmacher et al., 2015).

SRP-GTPases are known to form dimers depending on the GTP load (Leipe et al., 2002; Gasper et al., 2006). While Ffh and FtsY aggregate to form a heterodimeric complex, FlhF act as a stable homodimer that bound GTP/GDP-Mg²⁺ in many organisms (Bange et al., 2007; Green et al., 2009; Schniederberend et al., 2013). SRPs dimerization capacity requires specific amino acid motifs that are typical of eukaryotic and bacterial SRP-GTPases (Anand et al., 2006) and constitute the active site. The presence of typical sequence motifs in

B. cereus FlhF (Figures 1B,C) suggests that the protein forms a stable homodimer bound to GTP also in this organism.

By analyzing migration on TrA, an ideal medium for evaluating swarming migration by *B. cereus* ATCC 14579 (wt; Salvetti et al., 2011), we show that swarming motility is completely abolished in the $\Delta flhF$ mutant of *B. cereus*. This finding together with the previous demonstration that the mutant swimming motility was only reduced (Salvetti et al., 2007) suggests that other factors than flagella may be affected by the FlhF depletion. In fact, while swimming motility of cells primarily depends on flagella, additional factors are required for swarming. Perturbations in the flagellar motor, outer polysaccharides, osmotic agents, surfactants, as well as quorum-sensing signals have been shown to alter swarming in several bacteria (Kearns, 2010; Partridge and Harshey, 2013). Future studies will be required for defining the effects of FlhF deprivation on these factors.

Comparative proteomic analysis of culture supernatants indicated that the $\Delta flhF$ mutant of *B. cereus* displays an alteration in the quantity of certain extracellular proteins (Table 1). The amount of the major part of these proteins was lower in the proteome of the mutant compared to the wt and $\Delta flhF$ -comp strain, suggesting that FlhF can be involved in protein secretion, as already reported for *P. putida* (Pandza et al., 2000). In the SRP system, the SRP (Ffh)/4.5S RNA complex, in its GTP-bound form, attaches to the N-terminal sequence of the newly formed protein as it comes off the ribosome, and then docks with its receptor (FtsY) on the membrane, thus resulting in the insertion of the protein into the membrane (Akopian et al., 2013). *B. cereus* FlhF is homologous to both the SRP and the membrane receptor of this pathway and, as already suggested for other bacteria (Bange et al., 2007; Balaban et al., 2009), could play a role in either activities. FlhF has been shown to recruit the earliest flagellar component FliF and to insert itself in the cytoplasmic membrane in *V. cholerae* (Green et al., 2009). *B. cereus* FlhF could perform a similar function for flagellar proteins, but also for other proteins (PC-PLC, NPrP2, PI-PLC, Smase, HBL-L₂, CytK) that need to be directed to Sec translocase to be exported outside the cell. Nevertheless, although less pronouncedly, these proteins are still present in the secretome of the $\Delta flhF$ mutant, suggesting that, if FlhF acts as SRP, protein targeting to the membrane can still occur even in the absence of functional FlhF and that other systems may act in the export of these proteins. Although the secretion defects observed in the absence of functional FlhF might be due to its role as SRP-like protein, an effect of FlhF deprivation on regulatory pathways shared between the genes encoding the altered proteins cannot be excluded.

Galleria mellonella was previously shown to be a good alternative to the mouse model for evaluating the virulence of *B. cereus* (Salamitou et al., 2000). The virulence potential of *B. cereus* is due to the secretion of a plethora of virulence proteins, but also to the presence of flagella, which play a crucial role in swimming and swarming motility and in bacterial adhesion to surfaces. Infection of *G. mellonella* with a *B. cereus* mutant in

the Smase gene was previously shown to cause a reduction in larvae mortality, while mutations in *nheBC* had a little impact on *G. mellonella* survival (Doll et al., 2013). Infection with a *B. cereus* mutant in *codY*, encoding a positive regulator of the PC-PLC gene and many other virulence genes (Frenzel et al., 2012; Slamti et al., 2015), as well as with swimming defective mutant (Frenzel et al., 2015), drastically reduced larvae mortality. *G. mellonella* infection with a *B. thuringiensis* strain unable to swarm and to secrete of HBL-L₂ resulted in a strong reduction of larvae mortality (Bouillaut et al., 2005). In this study, we demonstrate that lack of FlhF substantially reduces *B. cereus* pathogenicity in *G. mellonella*. Since no difference with the wt in the replication of the $\Delta flhF$ mutant in *G. mellonella* was found, we can assume that the reduced pathogenicity of the mutant is due to the different virulence potential this strain shows. Other than being less flagellated and unable to swarm, the mutant strain shows a reduction in the secretion of PC-PLC, Smase, HBL-L₂, and many other virulence proteins (PI-PLC, CytK and ColA) (Beecher et al., 2000; Bottone, 2010; Ramarao and Sanchis, 2013). Despite the amount of some virulence proteins (NHE_B and Clo) is increased in the secretome of the $\Delta flhF$ mutant, we can speculate that these factors have a minor impact on *B. cereus* pathogenicity in *G. mellonella*. Therefore, the reduced production of some virulence proteins, of swimming, and the lack of swarming motility appear responsible of the scarce pathogenicity exerted by the $\Delta flhF$ mutant in *G. mellonella*.

REFERENCES

- Akopian, D., Shen, K., Zhang, X., and Shan, S. O. (2013). Signal recognition particle: an essential protein targeting machine. *Annu. Rev. Biochem.* 82, 693–721. doi: 10.1146/annurev-biochem-072711-164732
- Alouf, J. E. (2000). Cholesterol-binding cytolytic protein toxins. *Int. J. Med. Microbiol.* 290, 351–356. doi: 10.1016/S1438-4221(00)80039-9
- Anand, B., Verma, S. K., and Prakash, B. (2006). Structural stabilization of GTP-binding domains in circularly permuted GTPases: implications for RNA binding. *Nucleic Acids Res.* 34, 2196–2205. doi: 10.1093/nar/gkl178
- Balaban, M., Joslin, S. N., and Hendrixson, D. R. (2009). FlhF and its GTPase activity are required for distinct processes in flagellar gene regulation and biosynthesis in *Campylobacter jejuni*. *J. Bacteriol.* 191, 6602–6611. doi: 10.1128/JB.00884-09
- Bange, G., Petzold, G., Wild, K., Parltz, R., and Sinning, I. (2007). The crystal structure of the third signal-recognition particle GTPase FlhF reveals a homodimer with bound GTP. *Proc. Natl. Acad. Sci. U.S.A.* 104, 13621–13625. doi: 10.1073/pnas.0702570104
- Beecher, D. J., Olsen, T. W., Somers, E. B., and Wong, A. C. (2000). Evidence for contribution of tripartite hemolysin BL, phosphatidylcholine-prefering phospholipase C, and collagenase to virulence of *Bacillus cereus* endophthalmitis. *Infect. Immun.* 68, 5269–5276. doi: 10.1128/IAI.68.9.5269-5276.2000
- Bottone, E. J. (2010). *Bacillus cereus*, a volatile human pathogen. *Clin. Microbiol. Rev.* 23, 382–398. doi: 10.1128/CMR.00073-09
- Bouillaut, L., Ramarao, N., Buisson, C., Gilois, N., Gohar, M., Lereclus, D., et al. (2005). FlhA influences *Bacillus thuringiensis* PlcR-regulated gene transcription, protein production, and virulence. *Appl. Environ. Microbiol.* 71, 8903–8910. doi: 10.1128/AEM.71.12.8903-8910.2005
- Braunstein, M., Espinosa, B. J., Chan, J., Belisle, J. T., and Jakobs, W. R. Jr. (2003). SecA2 functions in the secretion of the superoxide dismutase a and in the virulence of *Mycobacterium tuberculosis*. *Mol. Microbiol.* 48, 453–464. doi: 10.1046/j.1365-2958.2003.03438.x
- Bru, C., Courcelle, E., Carrère, S., Beausse, Y., Dalmar, S., and Kahn, D. (2005). The ProDom database of protein domain families: more emphasis on 3D. *Nucleic Acids Res.* 33, D212–D215. doi: 10.1093/nar/gki034
- Callegan, M. C., Novosad, B. D., Ramirez, R., Ghelardi, E., and Senesi, S. (2006). Role of swarming migration in the pathogenesis of *Bacillus* endophthalmitis. *Invest. Ophthalmol. Vis. Sci.* 47, 4461–4467. doi: 10.1167/iovs.06-0301
- Carpenter, P. B., Hanlon, D. W., and Ordal, G. W. (1992). *flhF*, a *Bacillus subtilis* flagellar gene that encodes a putative GTP-binding protein. *Mol. Microbiol.* 6, 2705–2713. doi: 10.1111/j.1365-2958.1992.tb01447.x
- Celandroni, F., Salvetti, S., Gueye, S. A., Mazzantini, D., Lupetti, A., Senesi, S., et al. (2016). Identification and pathogenic potential of clinical *Bacillus* and *Paenibacillus* isolates. *PLoS ONE* 11:e0152831. doi: 10.1371/journal.pone.0152831
- Doll, V. M., Ehling-Schulz, M., and Vogelmann, R. (2013). Concerted action of sphingomyelinase and non-hemolytic enterotoxin in pathogenic *Bacillus cereus*. *PLoS ONE* 8:e61404. doi: 10.1371/journal.pone.0061404
- Fagerlund, A., Lindbäck, T., and Granum, P. E. (2010). *Bacillus cereus* cytotoxins Hbl, Nhe and CytK are secreted via the Sec translocation pathway. *BMC Microbiol.* 10:304. doi: 10.1186/1471-2180-10-304
- Finney, D. J. (ed.) (1971). *Probit Analysis*, 3rd Edn. Cambridge: Cambridge University Press.
- Frenzel, E., Doll, V., Pauthner, M., Lücking, G., Scherer, S., and Ehling-Schulz, M. (2012). CodY orchestrates the expression of virulence determinants in emetic *Bacillus cereus* by impacting key regulatory circuits. *Mol. Microbiol.* 85, 67–88. doi: 10.1111/j.1365-2958.2012.08090.x
- Frenzel, E., Kranzler, M., Stark, T. D., Hofmann, T., and Ehling-Schulz, M. (2015). The endospore-forming pathogen *Bacillus cereus* exploits a small colony variant-based diversification strategy in response to aminoglycoside exposure. *MBio*, 6, e1172–e1115. doi: 10.1128/mBio.01172-15
- Gasper, R., Scrima, A., and Wittinghofer, A. (2006). Structural insights into HypB, a GTP-binding protein that regulates metal binding. *J. Biol. Chem.* 281, 27492–27502. doi: 10.1074/jbc.M600809200

CONCLUSION

The flagellar protein FlhF, which controls the number and localization of flagella in *B. cereus* (Salvetti et al., 2007), is essential for swarming motility and full virulence. FlhF might act directly or through regulatory mechanisms on protein secretion or synthesis. Protein-protein interaction studies and partial gene deletion mutants will help in clarifying the molecular mechanisms underlying its peculiar activity.

AUTHOR CONTRIBUTIONS

All authors listed, have made substantial, direct and intellectual contribution to the work, and approved it for publication.

FUNDING

This research received no specific grant from any funding agency in the public, commercial, or not-for-profit sectors.

ACKNOWLEDGMENTS

The authors pay tribute to the late Professor Mario Campa for his long-standing inspiration and support.

- Ghelardi, E., Celadroni, F., Salvetti, S., Ceragioli, M., Beecher, D. J., Senesi, S., et al. (2007). Swarming behavior and hemolysin BL secretion in *Bacillus cereus*. *Appl. Environ. Microbiol.* 73, 4089–4093. doi: 10.1128/AEM.02345-06
- Gohar, M., Gilois, N., Graveline, R., Garreau, C., Sanchis, V., and Lereclus, D. (2005). A comparative study of *Bacillus cereus*, *Bacillus thuringiensis* and *Bacillus anthracis* extracellular proteomes. *Proteomics* 5, 3696–3711. doi: 10.1002/pmic.200401225
- Gohar, M., Økstad, O. A., Gilois, N., Sanchis, V., Kolstø, A.-B., and Lereclus, D. (2002). Two-dimensional electrophoresis analysis of extracellular proteome of *Bacillus cereus* reveals the importance of the PlcR regulon. *Proteomics* 2, 784–791. doi: 10.1002/1615-9861(200206)2:6<784::AID-PROT784>3.0.CO;2-R
- Green, J. C. D., Kahramanoglou, C., Rahman, A., Pender, A. M. C., Charbonnel, N., and Fraser, G. (2009). Recruitment of the earliest component of the bacterial flagellum to the old cell division pole by a membrane-associated signal recognition particle family GTP-binding protein. *J. Mol. Biol.* 391, 679–690. doi: 10.1016/j.jmb.2009.05.075
- Guttenplan, S. B., Shaw, S., and Kearns, D. B. (2013). The cell biology of peritrichous flagella in *Bacillus subtilis*. *Mol. Microbiol.* 87, 211–229. doi: 10.1111/mmi.12103
- Harshey, R. M., and Matsuyama, T. (1994). Dimorphic transition in *Escherichia coli* and *Salmonella typhimurium*: surface-induced differentiation into hyperflagellate swarmer cells. *Proc. Natl. Acad. Sci.* 91, 8631–8635. doi: 10.1073/pnas.91.18.8631
- Jander, G., Rahme, L. G., and Ausubel, F. M. (2000). Positive correlation between virulence of *Pseudomonas aeruginosa* mutants in mice and insects. *J. Bacteriol.* 182, 3843–3845. doi: 10.1128/JB.182.13.3843-3845.2000
- Jeßberger, N., Krey, V. M., Rademacher, C., Böhm, M. E., Mohr, A. K., Ehling-Schulz, M., et al. (2015). From genome to toxicity: a combinatorial approach highlights the complexity of enterotoxin production in *Bacillus cereus*. *Front. Microbiol.* 10:560. doi: 10.3389/fmicb.2015.00560
- Källberg, M., Wang, H., Wang, S., Peng, J., Wang, Z., Lu, H., et al. (2012). Template-based protein structure modeling using the raptorX web server. *Nat. Protoc.* 7, 1511–1522. doi: 10.1038/nprot.2012.085
- Kearns, D. B. (2010). A field guide to bacterial swarming motility. *Nat. Rev. Microbiol.* 8, 634–644. doi: 10.1038/nrmicro2405
- Kelley, L. A., Mezulis, S., Yates, C. M., Wass, M. N., and Sternberg, M. J. E. (2015). The Phyre2 web portal for protein modeling, prediction and analysis. *Nat. Protoc.* 10, 845–858. doi: 10.1038/nprot.2015.053
- Leipe, D. D., Wolf, Y. I., Koonin, E. V., and Aravind, L. (2002). Classification and evolution of P-loop GTPases and related ATPases. *J. Mol. Biol.* 317, 41–72. doi: 10.1006/jmbi.2001.5378
- Lenz, L. L., Mohammadi, S., Geissler, A., and Portnoy, D. A. (2003). SecA2-dependent secretion of autolytic enzymes promotes *Listeria monocytogenes* pathogenesis. *Proc. Natl. Acad. Sci. U.S.A.* 100, 12432–12437. doi: 10.1073/pnas.2133653100
- Logan, N. A. (2012). *Bacillus* and relatives in foodborne illness. *J. Appl. Microbiol.* 112, 417–429. doi: 10.1111/j.1365-2672.2011.05204.x
- Lund, T., and Granum, P. E. (1997). Comparison of biological effect of the two different enterotoxin complexes isolated from three different strains of *Bacillus cereus*. *Microbiology* 143, 3329–3336. doi: 10.1099/00221287-143-10-3329
- Nouwens, A. S., Willcox, M. D. P., Walsh, B. J., and Cordwell, S. J. (2002). Proteomic comparison of membrane and extracellular proteins from invasive (PAO1) and cytotoxic (6206) strains of *Pseudomonas aeruginosa*. *Proteomics* 2, 1325–1346. doi: 10.1002/1615-9861(200209)2:9<1325::AID-PROT1325>3.0
- Pandza, S., Baetens, M., Park, C. H., Au, T., Keyan, M., and Matin, A. (2000). The G-protein FlhF has a role in polar flagellar placement and general stress response induction in *Pseudomonas putida*. *Mol. Microbiol.* 36, 414–423. doi: 10.1046/j.1365-2958.2000.01859.x
- Partridge, J. D., and Harshey, R. M. (2013). Swarming: flexible roaming plans. *J. Bacteriol.* 195, 909–918. doi: 10.1128/JB.02063-12
- Purves, J., Cockayne, A., Moody, P. C., and Morrissey, J. A. (2010). Comparison of the regulation, metabolic functions, and roles in virulence of the glyceraldehyde-3-phosphate dehydrogenase homologues gapA and gapB in *Staphylococcus aureus*. *Infect. Immun.* 78, 5223–5232. doi: 10.1128/IAI.00762-10
- Ramarao, N., and Sanchis, V. (2013). The pore-forming haemolysins of *Bacillus cereus*: a review. *Toxins* 5, 1119–1139. doi: 10.3390/toxins5061119
- Salamitou, S., Ramicé, F., Brehelin, M., Bourguet, D., Gilois, N., Gominet, M., et al. (2000). The plcR regulon is involved in the opportunistic properties of *Bacillus thuringiensis* and *Bacillus cereus* in mice and insects. *Microbiology* 146, 2825–2832. doi: 10.1099/00221287-146-11-2825
- Salvetti, S., Faegri, K., Ghelardi, E., Kolstø, A.-B., and Senesi, S. (2011). Global gene expression profile for swarming *Bacillus cereus* bacteria. *Appl. Environ. Microbiol.* 77, 5149–5156. doi: 10.1128/AEM.00245-11
- Salvetti, S., Ghelardi, E., Celadroni, F., Ceragioli, M., Giannessi, F., and Senesi, S. (2007). FlhF, a signal recognition particle-like GTPase, is involved in the regulation of flagellar arrangement, motility behavior and protein secretion in *Bacillus cereus*. *Microbiology* 153, 2541–2552. doi: 10.1099/mic.0.2006/005553-0
- Schniederberend, M., Abdurachim, K., Murray, T., and Kazmierczak, B. I. (2013). The GTPase activity of FlhF is dispensable for flagellar localization, but not motility, in *Pseudomonas aeruginosa*. *J. Bacteriol.* 195, 1051–1060. doi: 10.1128/JB.02013-12
- Schuhmacher, J. S., Thormann, K. M., and Bange, G. (2015). How bacteria maintain location and number of flagella? *FEMS Microbiol. Rev.* 39, 812–822. doi: 10.1093/femsre/fuv034
- Senesi, S., and Ghelardi, E. (2010). Production, secretion and biological activity of *Bacillus cereus* enterotoxins. *Toxins* 2, 1690–1703. doi: 10.3390/toxins2071690
- Senesi, S., Salvetti, S., Celadroni, F., and Ghelardi, E. (2010). Features of *Bacillus cereus* swarm cells. *Res. Microbiol.* 161, 743–749. doi: 10.1016/j.resmic.2010.10.007
- Shevchenko, A., Jensen, O. N., Podtelejnikov, A. V., Sagliocco, F., Wilm, M., Vorm, O., et al. (1996). Linking genome and proteome by mass spectrometry: large-scale identification of yeast proteins from two dimensional gels. *Proc. Natl. Acad. Sci. U.S.A.* 93, 14440–14445. doi: 10.1073/pnas.93.25.14440
- Slamti, L., Lemy, C., Henry, C., Guillot, A., Huillet, E., and Lereclus, D. (2015). CodY regulates the activity of the virulence quorum sensor PlcR by controlling the import of the signaling peptide PapR in *Bacillus thuringiensis*. *Front. Microbiol.* 6:1501. doi: 10.3389/fmicb.2015.01501
- Smith, P. K., Krohn, R. I., Hermanson, G. T., Mallia, A. K., Gartner, F. H., Provenzano, M. D., et al. (1985). Measurement of protein using bicinchoninic acid. *Anal. Biochem.* 150, 76–85. doi: 10.1016/0003-2697(85)90442-7
- The UniProt Consortium. (2015). UniProt: a hub for protein information. *Nucleic Acids Res.* 43, D204–D212. doi: 10.1093/nar/gku989
- WARTH, A. D. (1980). Heat stability of *Bacillus cereus* enzymes within spores and in extracts. *J. Bacteriol.* 143, 27–34.
- Zanen, G., Antelmann, H., Westers, H., Hecker, M., van Dijl, J. M., and Quax, W. (2004). FlhF, the third signal recognition particle-GTPase of *Bacillus subtilis*, is dispensable for protein secretion. *J. Bacteriol.* 186, 5956–5960. doi: 10.1128/JB.186.17.5956-5960.2004

Conflict of Interest Statement: The authors declare that the research was conducted in the absence of any commercial or financial relationships that could be construed as a potential conflict of interest.

Copyright © 2016 Mazzantini, Celadroni, Salvetti, Gueye, Lupetti, Senesi and Ghelardi. This is an open-access article distributed under the terms of the Creative Commons Attribution License (CC BY). The use, distribution or reproduction in other forums is permitted, provided the original author(s) or licensor are credited and that the original publication in this journal is cited, in accordance with accepted academic practice. No use, distribution or reproduction is permitted which does not comply with these terms.

